



DIPLOMARBEIT

Monte Carlo simulation of the activation of air at the MedAustron project

Ausgeführt am

Atominstitut der österreichischen Universitäten

der Technischen Universität Wien

unter Anleitung von:

O. Univ. Prof. DI Dr. Johannes Aiginger (ATI)

und

DI Dr. Helmut Vincke (CERN)

durch

Matthias Karacson

Schützengasse 1/10/50

2700 Wiener Neustadt

ACKNOWLEDGEMENTS

First of all, I wish to thank Univ. Prof. DI Dr. Johannes Aiginger and Doz. Dr. Michael Benedikt for giving me the opportunity to work on this thesis at CERN, and Ass. Prof. DI Dr. Karin Poljanc for her organizational help. These 14 months at one of the world's largest centres for scientific research became a great and rewarding experience, thanks to all the people providing support, to whom I am deeply indebted.

I really want to thank Helmut Vincke for supervising in the most helpful, competent and friendly manner, Edi for his efforts of teaching me in the ways of FLUKA, Chris and Stefan for always coming up with a useful hint or a better solution to every problem I encountered, as well as Christina, Heinz, Herta, Julia, Petra, Lilly, Julian and especially Lukas, Claus, Hannes, Eva, Steffi and Christine for being great colleagues and friends, and for making not only coffee breaks, but also my stay as a whole as enjoyable as possible.

And last but not least I of course wish to thank my parents for their continuous support.

ABSTRACT

The interdisciplinary MedAustron project, a national radio-oncological center for research and treatment of cancer patients, is being built in Austria in order to establish future oriented radiotherapeutical methods for cancer control via Ion therapy, and furthermore nonclinical research structures opening up a diverse panorama of many different applications. Radiation monitoring in treatment rooms and the areas housing particle accelerator components is essential for protecting patients, personnel and the environment. Considering the capability of the MedAustron accelerator of producing proton beams for experimental purposes with energies significantly higher than those needed for patient treatment, the topic of air activation gains importance as a part of a general radiation protection plan.

The FLUKA Monte Carlo Code allows for an accurate simulation of high-energy proton and ion beams and their effects on local air volumes in a detailed geometry of the MedAustron facility, enabling an estimation of airborne radioactivity and the related consequences that are to be expected during operation of the particle accelerator. The goal of this thesis is to give such an estimation with a focus on the radiological consequences for personnel and environment.

With the help of a generic study, two methods for the calculation of air activation are evaluated for their usefulness in the planned scenarios: A method using calculated fluence distributions of protons, neutrons and pions for folding them with production cross sections of relevant radioactive isotopes, and a direct simulation of isotope production incorporated in the FLUKA code.

The appropriate method is then applied to the different scenarios. These scenarios comprise the simulation of air activation during treatment and possible experimental procedures in the four irradiation rooms of the facility, as well as the simulation of the activation of air due to beam losses at specified points in the main machine hall. Scenarios considering the release of the activated air into the environment after a cooldown period are conceived while regarding radiation protection rules defined by Austrian law. Also, committed dose rates for personnel entering treatment rooms after various irradiation scenarios are estimated.

Calculations show that legal limits will be observed during foreseen operation procedures. Irradiation procedures in the experimental area of the facility with maximum energy particle beams can temporary result in a significant increase of radiation due to air activation in comparison with normal patient treatment operation, demanding for continuous surveillance and logging of air activation inside the facility.

KURZZUSAMMENFASSUNG

Mit dem interdisziplinären MedAustron Projekt soll in Österreich ein nationales radioonkologisches Zentrum für Forschung und die Behandlung von Krebspatienten etabliert werden, das zukunftsweisende radiotherapeutische Methoden zur Krebsbekämpfung mittels Ionentherapie zur Verfügung stellt, und darüber hinaus über den Aufbau nichtklinischer Forschungsstrukturen ein vielfältiges Panorama an verschiedensten Anwendungsmöglichkeiten eröffnet. Eine Überwachung der entstehenden Radioaktivität in den Behandlungsräumen sowie in den Bereichen, die Komponenten des Teilchenbeschleunigers beherbergen, ist notwendig für den Schutz von Patienten, Personal und der Umgebung. Aufgrund der Möglichkeit, mit dem MedAustron Teilchenbeschleuniger Strahlenergien für experimentelle Zwecke zu produzieren, die weit über die zur Patientenbehandlung benötigten Energien hinausgehen, erlangt auch die Problemstellung der Luftaktivierung größere Bedeutung innerhalb eines allgemeinen Strahlenschutzkonzepts.

Der FLUKA Monte Carlo Code ermöglicht eine genaue Simulation von hochenergetischen Protonen- und Ionenstrahlen und deren radiologischen Auswirkungen auf lokale Luftvolumina in einer detaillierten Geometrie der MedAustron Anlage, und damit eine Abschätzung des Grads der Luftaktivierung und der damit verbundenen Konsequenzen, die während des Beschleunigerbetriebs zu erwarten sind. Ziel dieser Arbeit ist eine ebensolche Abschätzung unter besonderer Beachtung der Konsequenzen für Personal und Umwelt.

Mithilfe einer generischen Studie werden zwei Methoden zur Berechnung der Luftaktivierung bezüglich ihrer Verwendbarkeit in den geplanten Szenarios untersucht: Eine Methode basierend auf der Berechnung von Fluenzen von Protonen, Neutronen und Pionen und deren Faltung mit Wirkungsquerschnitten für die Produktion relevanter radioaktiver Isotope, und eine im FLUKA Code integrierte direkte Simulation der Isotopenproduktion.

Die jeweils geeignetste Methode wird dann auf die verschiedenen Szenarios angewandt. Diese Szenarios beinhalten die Simulation der Luftaktivierung während der Behandlung von Patienten und möglichen Versuchsaufbauten in den Behandlungsräumen, sowie die Simulation der Luftaktivierung durch Strahlverluste an definierten Verlustpunkten in der Beschleunigerhalle. Szenarios bezüglich der Freigabe aktivierter Luft nach einer Abklingzeit werden unter der Beachtung des österreichischen Strahlenschutzgesetzes durchdacht. Ausserdem werden Folgedosisraten für Personal, welches die Behandlungsräume nach verschiedenen Bestrahlungsszenarien betritt, abgeschätzt.

Die Berechnungen zeigen, dass die gesetzlichen Vorgaben während des vorgesehenen Betriebs eingehalten werden. Bestrahlungsvorgänge mit maximal verfügbarer Strahlenergie im Experimentalraum der Anlage können kurzzeitig zu einer deutlichen Erhöhung der Strahlenbelastung durch Luftaktivierung führen im Vergleich zum Betrieb während der Behandlung von Patienten, was eine kontinuierliche Überwachung und Aufzeichnung der Luftaktivierung innerhalb der Anlage erfordert.

TABLE OF CONTENTS

MedAustron – An Introduction	1
Medical advantages of Ion therapy	1
Scientific master plan	2
Layout	3
Monte Carlo Simulation	4
Introduction	4
FLUKA: A multiparticle transport code	4
FLUKA tracking and scoring	5
Induced airborne radioactivity	6
Introduction	6
Neutron interactions	6
Radiation produced by particle accelerators	7
Air activation at accelerator facilities	8
Activation Monitoring	9
Regarding Austrian radiation protection law	9
Comparison of two methods to calculate the activation of air by means of a generic study	10
Introduction	10
Simulation Details	10
Geometry	10
Materials	11
Particle transport thresholds	12
Scoring approach	13
FLUKA method for production of nuclides	13
Folding method for the production of nuclides:	14
Results	15
800 MeV protons	15
400 MeV ions	18
Discussion	21

Detailed study of air activation within a FLUKA geometry of the MedAustron facility.....	25
Introduction.....	25
Simulation details	25
Geometry.....	25
Materials.....	26
Irradiation rooms 1-4.....	28
Synchrotron hall and Loss Points.....	34
Particle transport thresholds.....	39
Scoring approach	40
Results	50
Irradiation room 1 (IR1).....	50
Irradiation room 2 (IR2).....	60
Irradiation room 3 (IR3).....	61
Irradiation room 4 (IR4 - Proton Gantry).....	62
Summary tables for irradiation rooms 1-4	63
Radiological exposure of the MedAustron Personnel	72
Irradiation room 1	72
Irradiation room 2	76
Irradiation room 3	78
Irradiation room 4	80
Synchrotron room loss points.....	83
Horizontal beam dump (bdh)	83
Electrostatic septum (ese)	90
Magnetic septum (mse).....	97
Chopper dump (bdc).....	104
High energy line beam dump.....	111
Effective dose rates in the synchrotron hall caused by loss points	116
Conclusion	119
References	121

Appendix:.....	124
Part A: Generic study	124
Part B: MedAustron treatment rooms	141
Part C: MedAustron synchrotron hall loss points	169

MEDAUSTRON – AN INTRODUCTION

Founding on international collaboration efforts, the interdisciplinary MedAustron project, a national radio-oncological center for research and treatment of cancer patients, is being built in Austria in order to establish future oriented radiotherapeutical methods for cancer control via Ion therapy. Furthermore the development of nonclinical research structures will not only advance the knowledge about, and thus the Ion therapy itself, but it will also open up a rich and diverse panorama of many different applications.

MEDICAL ADVANTAGES OF ION THERAPY

When treating tumors in the vicinity of radiosensitive organs and tissue, the use of protons and carbon ions for treatment enables a distinct reduction of the radiation exposure of the healthy tissue in front of the tumor in comparison to the nowadays common methods using electrons and photons, and it is even able to almost totally spare the healthy tissue behind the tumor. As an illustration, Figure 1 shows a comparison of depth dose distributions of different beam types.

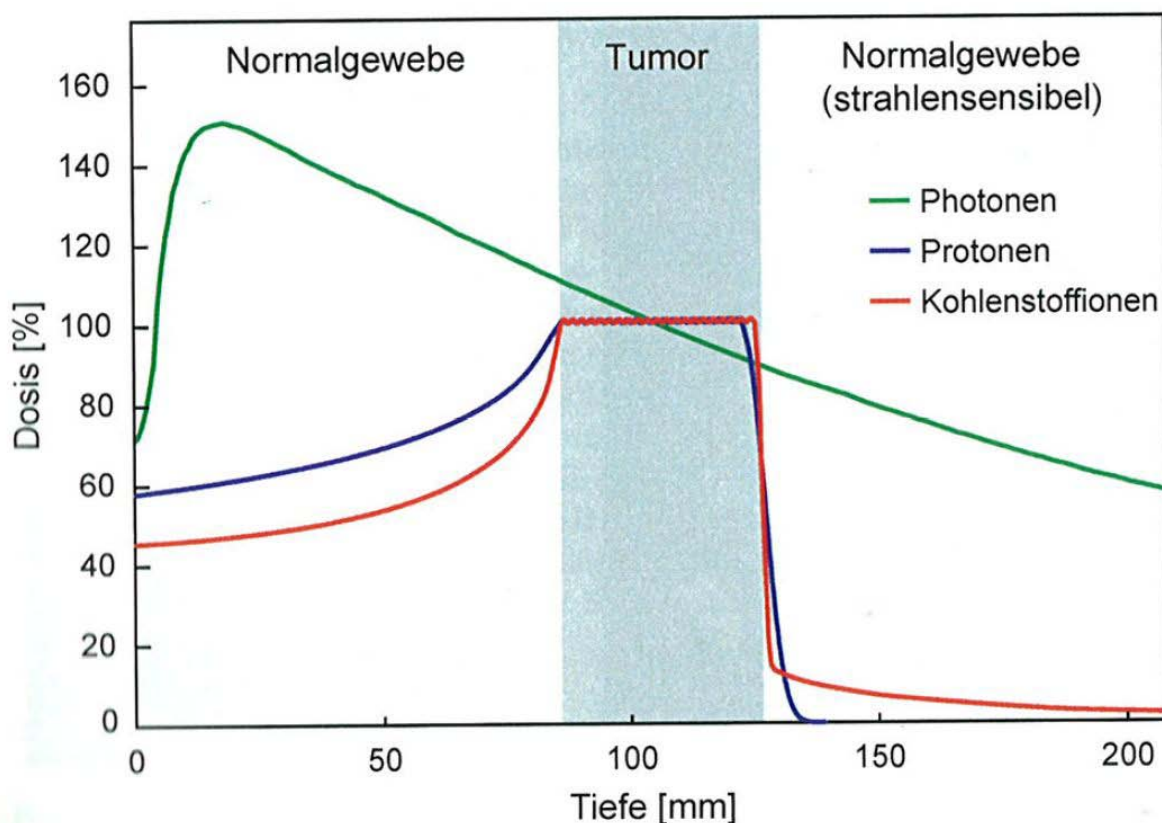


Figure 1: Depth dose distribution for treatment of photons (green), protons (blue) and carbon ions (red) assuming a 40 mm wide tumor in 85 to 125 mm tissue depth. The graph shows a dose distribution of a beam coming from the left side with increasing tissue depth. [1]

When moving through matter, a charged particle loses energy by constantly interacting with its environment. However while reducing the energy of a moving proton or ion, its interaction-cross section increases, which leads to the formation of a peak in terms of energy deposition at the end of its path. This so called Bragg Peak allows for a very precise deposition of dose within matter. By facilitating a variation of the beam energy, a broadening of the peak and therefore an efficient dose distribution can be attained.

Because of the exceptional conservation of healthy tissue, Ion therapy allows for the application of higher dose rates than actual methods, so that even tumors that are highly resistant against conventional radiation treatment are becoming treatable.

SCIENTIFIC MASTER PLAN

Medical operation and clinical research, concerning especially the efficiency and side effects of the ion therapy treatment, the optimization of treatment strategies and techniques and the further development of new therapy methods, will play a major role in the interdisciplinary project. In parallel, nonclinical research structures are to be established, which will enable a scientific substantiation of the clinical studies and also allow for participation on a broad spectrum of European research programs.

Some essential issues of clinical research will be approached, with just a few examples being:

- ❖ A statistically significant confirmation of worldwide findings concerning ion therapy treatment results by increasing the number of cases
- ❖ The expansion of treatment methods to include tumor types where the patient could theoretically profit from the new treatment form, but where there are not enough clinical results available yet to confirm this
- ❖ An investigation concerning the achievable reduction of acute or late side effects for the cancer patients and of the required expenditure for concomitant and follow-up treatment
- ❖ The replacement of other oncologic therapies (operation, chemotherapy)

The concept of nonclinical research for MedAustron generally encompasses: Biomedical research, medical-physical research and technical-physical research.

In the area of biomedical research, the focus will be on radiobiological and tumorphysiological fundamental research, for example the clarification of the correlation between energy adjusted Ion radiation and various cell specific, genetic and physiological parameters.

Medical-physical achievements during the last few years brought proof that a reduction of the irradiation of normal tissue during treatment does in fact reduce unwelcome side effects. During the course of the implementation of three-dimensional radiotherapy, the limitations of conventional Photon- and Electron-therapy, as well as the problematic nature of a patient that is subject to physical changes during the treatment, became obvious. These posed challenges open up a whole lot of new areas for future research approaches, for example Ion ray dosimetry and its many intertwined applications.

From a technical-physical point of view, a broad spectrum of supplementary research programs, in addition to the naturally applicable area of accelerator physics, will profit from the project. Detector development and the accompanying material science research will be just one of many potential beneficiaries. Research places funded by industrial interest groups, for instance in the areas of space research or experimental physics, are also envisaged. [1]

On the 26th of November 2007, a general agreement between the European Organization for Nuclear Research **CERN** (Conseil Européen pour la Recherche Nucléaire) and the government of Lower Austria was signed in order to establish a collaboration to exchange expertise in the fields of hadron therapy and non clinical particle beam research. [20]

LAYOUT

The whole accelerator facility, pictured in Figure 2, can be divided into three sections:

1. The injector, which consists of particle sources and the linear accelerator that is responsible for the pre-acceleration of protons and ions;
2. The synchrotron, that further accelerates particles over several cycles until they reach the requested energy;
3. The High Energy Beam Transport line (HEBT) that starts with the beam extraction equipment and includes beam guiding equipment to feed the beam into each of the four irradiation rooms.

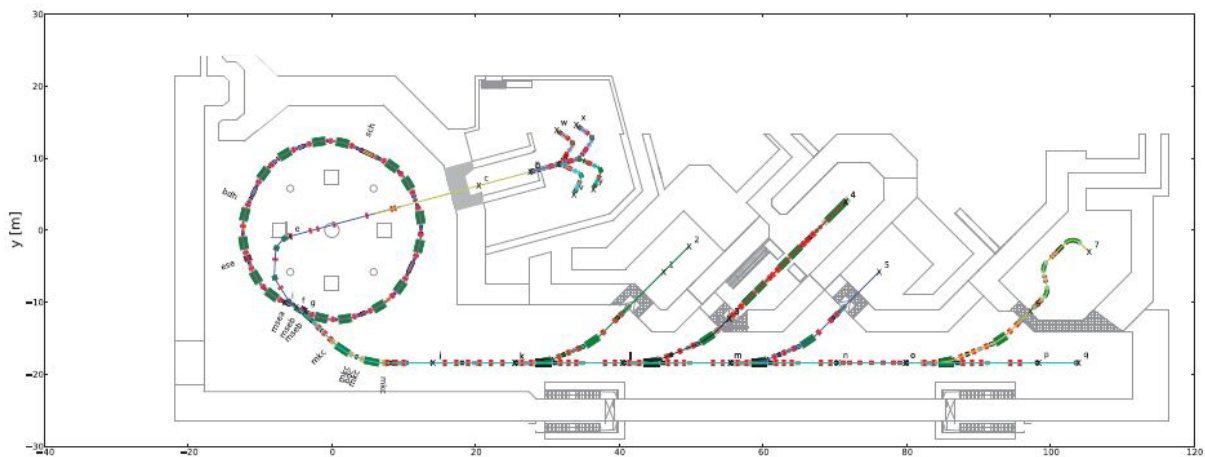


Figure 2: Schematic layout of the accelerator part of the MedAustron facility, including the three main systems: Injector, Synchrotron and the High Energy Beam Transport line (HEBT), which starts at the beam extraction point from the synchrotron ring and ends at the HEBT beam dump. Green boxes signify dipole bending magnets, orange boxes stand for quadrupole focusing magnets. [4]

Studies concerned with air activation consider the four irradiation rooms as well as designated relevant beam loss points in the synchrotron hall and along the HEBT. The injection room is not covered by these studies, since particles at the injector will only reach a maximum kinetic energy of 7 MeV per nucleon, which is not enough to cause relevant levels of activation of the air inside, especially when considering implemented self-shielding of the machinery and low radiation caused by losses. [4]

The accelerator facility will be operated during 24 hours per day and 7 days per week all year, in order to enable an optimum of utilization. Operation will only be halted for maintenance and repair services. [4]

MONTE CARLO SIMULATION

INTRODUCTION

The Monte Carlo method is based on the use of random sampling to obtain results. It is one of the most useful methods for evaluating radiation hazards for realistic geometries, which are generally difficult to characterize using analytic techniques. Calculation via random sampling is done by constructing a series of trajectories from primary particles with each segment chosen at random from a distribution of applicable processes. The results of these applicable interactions may be a number of particles of varying types, energies and directions, each of which will be followed in turn.

Results reached by using the Monte Carlo method are based on the number of times that an event of interest occurred per primary particle. Being a counting process, it has a counting uncertainty and the variance will decrease with the square root of the number of calculations done. Thus, processes with high probability can be simulated with more accuracy than low probability processes such as the passage of particles through thick shielding attenuating radiation levels by many orders of magnitude. [12]

FLUKA: A MULTIPARTICLE TRANSPORT CODE

FLUKA is a general purpose tool for calculations of particle transport and interactions with matter, covering an extended range of applications. The prediction of radiation damage for example has always been a traditional field of application of FLUKA, however earlier versions were restricted to calculations of hadron damage to accelerator components. Progressive implementation of new capabilities, e.g. to deal with the low-energy neutron component of the cascade, has extended the field of interest to include electronics and other sensitive detector parts. In addition, radiation damage calculations and simulations for shielding design are not limited to proton accelerators any longer, but include electron accelerators of any energy, photon factories, and any kind of radiation source, be it artificial or natural.

The present version of FLUKA has been used successfully in diverse domains, such as background studies for underground detectors, cosmic ray physics, shielding of synchrotron radiation hutch, calculation of dose received by aircraft crews, evaluation of organ dose in a phantom due to external radiation, detector design for radiation protection as well as for high energy physics, electron and proton radiotherapy, neutrino physics, shielding of free-electron lasers, maze design for medical accelerators, etc. The addition of the simulation of heavy ion interactions also opens the field for applications concerning hadrotherapy. [3]

Physical models implemented in FLUKA build on consistency among all reaction steps and types, conservation laws are enforced at each step, and results are checked against experimental data at single interaction level. Also, microscopic models are adopted whenever possible. As a consequence, final predictions are obtained with a minimal set of free parameters fixed for all energy/target/projectile combinations. Therefore results in complex cases, as well as properties and scaling laws, arise naturally from the underlying physical models, predictivity is provided where no experimental data are directly available, and correlations within interactions and among shower components are preserved. [3]

FLUKA can simulate with high accuracy the interaction and propagation in matter of about 60 different particles, including photons and electrons from 1 keV to thousands of TeV, neutrinos, muons of any energy,

hadrons of energies up to 20 TeV (up to 10 PeV by linking FLUKA with the DPMJET code) and all the corresponding antiparticles, neutrons down to thermal energies and heavy ions. Time evolution and tracking of emitted radiation from unstable residual nuclei can be performed on line.

For most applications, no programming is required from the user. Input files are assembled of so called “cards”, which stands for lines of code that follow a defined pattern, where each number or string at a certain position defines the parameters of the simulation. In addition, a number of user interface routines (in Fortran 77) are available for users with special requirements. [3]

Based on the Combinatorial Geometry (CG) package [17], geometry input enables the user to combine several basic convex shapes, called bodies, into more complex shapes, called regions, by using the Boolean operations union, intersection and subtraction. During the development of FLUKA, several new body shapes including infinite cylinders and planes, which are in principle half-spaces, have been introduced, increasing accuracy, speed and making input preparation easier. [3]

Considering the complexity of a Boolean built geometry that is based on the actual MedAustron construction plan, SimpleGeo 4.1 [14] has been used to view and modify models for simulations as well as visualize results. SimpleGeo is an interactive solid modeler available for Windows operating systems, which allows for flexible and easy creation of models. Existing geometries can be imported for viewing and modifying, or geometries can be built from scratch. Geometry inputs can be exported into various formats including FLUKA. By using the plugin DaVis 3D, visualization of 3-dimensional USBINs via display of up to 3 planes, that can be interactively moved through the data set and superimposed on top of the geometry, is possible. Also, integrated volume calculation using a quasi-Monte Carlo algorithm provides for an accurate tool when working with complex structures.

FLUKA outputs of scoring results can be given in commonly accessible ASCII format, as well as in the form of binary files. Scoring into readable ASCII formatted output files has the advantage of providing greater flexibility concerning postprocessing of data. FLUKA inherent routines like the later mentioned usrsuvev routine, and graphical interface / visualization tools like FLAIR [18] only work with binary scoring files.

A more detailed description of FLUKA can be found in [3].

FLUKA TRACKING AND SCORING

To obtain the total fluence, every particle appearing in the simulation has to be followed in terms of location, energy, angle and direction at any given time.

Fluence scoring, used in fluence USRTRACK or fluence USBIN detectors in FLUKA, is done by recording the track-length of particles as a function of energy and angle. The fluence is then estimated as **volume density of particle trajectory length**.

Three main types of scoring methods are used in the following studies:

The **USRTRACK** scoring card defines a detector for a track-length fluence estimator of either single particle types or groups of particles, allowing for linear or logarithmic binning in energy with a maximum of 400 bins. When scoring neutron fluence, 260 low energy neutron bins placed between energies of 1E-14 GeV and 20

MeV are always scored separately, with requested bins above 20 MeV being allocated based on the requested total energy range.

USRBIN scoring cards yield distributions of one of several quantities in a regular spatial structure, that is independent from the geometry. Available mesh structures range from spatial cylindrical R- ϕ -Z, over Cartesian X-Y-Z to region-based binning possibilities. Most of the offered scoring quantities are based on track-length density (fluence), which, if requested as for several figures in the following chapters, results in fluence maps given in cm/cm³ per primary particle.

RESNUCLEi cards can score residual nuclei produced in inelastic interactions on a region basis during simulation. Results are totally dependent on FLUKA internal models and libraries for elements and materials. Information about the FLUKA neutron cross-section library can be gathered at [3].

INDUCED AIRBORNE RADIOACTIVITY

INTRODUCTION

The following paragraphs contain an overlook regarding dominant types of radiation and induced radioactivity generally found at particle accelerator facilities, including a short introduction to the measuring of the activation of air at a proton beam facility.

Charged particles directly accelerated, and otherwise manipulated by the electromagnetic fields within the accelerator, are referred to as **primary particles** or **beam**. All other particles that are produced from this beam, either due to interactions of primary particles with matter, their decay or due to synchrotron radiation, are referred to as **secondary particles**.

NEUTRON INTERACTIONS

Neutrons carry no charge and therefore cannot interact in matter by means of the Coulomb force, which dominates the energy loss mechanisms for charged particles and electrons. Interaction takes place with nuclei of the absorbing material, resulting in the disappearance of the neutron with a replacement in form of secondary radiation, or at least in a significant change of energy or direction of the incident neutron.

Secondary radiation resulting from neutron interactions is almost always comprised of heavy charged particles, which may be produced either as a result of neutron-induced nuclear reactions or they may be the nuclei of the absorbing material itself, which have gained energy by collision.

Relative probabilities of various types of neutron interactions change dramatically with neutron energy:

For slow neutrons, with a kinetic energy of less than 0.5 eV, significant interactions include elastic scattering with absorber nuclei and a large set of neutron-induced nuclear reactions. Due to the small kinetic energy of the neutrons, only small amounts of energy can be transferred to the nucleus by elastic scattering, which often serves to bring slow neutrons into thermal equilibrium with the absorber medium before a different type of

interaction takes place. Many of the slow neutrons will therefore be found in the energy range of the so called thermal neutrons, which have an average energy of 0.025 eV at room temperature.

Slow neutron interactions of real importance are neutron-induced reactions that create secondary radiations in the form of gamma rays, charged particles like protons, alpha particles or even fission products. In most materials, the radiative capture reaction (n, γ) is the most probable and plays an important part in the attenuation or shielding of neutrons.

With increasing neutron energy (above 0.5 eV), the probability of most neutron-induced reactions rapidly decreases. However, the importance of scattering becomes greater, because the neutron can transfer an appreciable amount of energy in one collision, being moderated or slowed to lower energies. Secondary radiation in this case consists of recoil nuclei, which have picked up energy from collisions. The most efficient moderator is hydrogen, because the neutron can lose up to all of its energy in a single collision with a hydrogen nucleus, while only a partial energy transfer is possible for heavier nuclei.

Inelastic scattering with nuclei can occur, if the energy of the fast neutron is sufficiently high. In this case, the recoil nucleus is elevated to one of its excited states during the collision, and de-exciting quickly afterwards by emitting a gamma ray. By inelastic scattering, a neutron can lose a greater fraction of its energy than it would in an equivalent elastic collision. [13]

RADIATION PRODUCED BY PARTICLE ACCELERATORS

From a dosimetric standpoint, direct beams at proton accelerators nearly always dominate over any type of secondary phenomena in terms of the level of hazard, since the beam current is generally confined to small dimensions. Below an energy of about 200 MeV per primary particle, the proton range in tissue is less than the typical thickness of the human body, so a high fraction of the proton's energy is absorbed by tissue. At increasing energies above 200 MeV, an increasing fraction of the proton's energy escapes from the body, requiring a far larger fluence of protons to deliver the same absorbed dose or dose equivalent. [12]

For protons having energies in the ranges above 10 MeV up to 200 MeV and higher, neutrons are usually the dominant feature of the radiation field resulting from interactions of primary particles. In this region of energy, neutron yields are smoother functions of energy due to the lack of resonances, but are also more forward-peaked. At the lower energies of this region, some of the neutrons produced are so-called evaporation neutrons, which have an isotropic distribution due to their production mechanism, which can be essentially viewed as "boiling" off of a nucleus that has been "heated" by the absorption of energy of an incident particle. Other neutrons produced are cascade neutrons that result directly from individual nuclear reactions, which do exhibit a preferred directionality. [12]

In the energy region up to 1 GeV per primary particle, more possible reaction channels open up, and the number of emitted protons becomes approximately equal to the number of neutrons. Also, at these energies, cascade neutrons become much more important than evaporation neutrons, which results in a more sharply forward-peaked radiation field with increasing primary particle energy. [12]

A hadronic cascade is initiated at proton accelerators when the beam interacts with targets, beam absorbers and accelerator components to produce neutrons and other particles.

The collision between a nucleon with high kinetic energy and a nucleus produces a large number of particles including other nucleons, pions, kaons as well as fragments of the struck nucleus. Notably pions are becoming more important at higher energies of primary protons, when their production becomes energetically possible. They are absorbed with absorption lengths that are comparable in magnitude with proton absorption lengths. Also, pions decay into muons, which lack nuclear interactions and therefore have long ionization ranges, providing a pathway for energy to escape a hadronic cascade. One important reaction channel of high energy hadrons can be found in the production of neutral pions. Neutral pions decay after $8.4 \cdot 10^{-17}$ seconds mostly into 2 photons, which are the production origin of electromagnetic cascades. At very high energies, meaning tens of GeV per primary particle, most of the initial particle energy is transformed into electromagnetic cascades via this process.

Cascade neutrons are emitted by direct impact with a spectrum extending up to the incident energy with diminishing probability. [12]

General considerations made above for radiation fields regarding proton accelerators are also appropriate for accelerated ions. Because the ionization range for ions of a given kinetic energy decreases as a function of ion mass, targets become effectively "thicker" as the ion mass increases. Neutron yield and dose equivalent data as well as calculations become very sparse at higher energies and especially at higher masses of the accelerated ions. Data is usually normalized in terms of kinetic energy per atomic mass unit, or kinetic energy per nucleon, because reaction parameters generally scale to that parameter. [12]

Regarding radiological consequences, implications caused by accelerated protons differ greatly from the ones faced in more commonly found electron irradiation facilities. At electron accelerators, significant air activation will not occur without bremsstrahlung, because nuclear cross sections of electrons are about two orders of magnitude smaller than those of photons. In general, the resulting airborne radioactivity is short lived, and the concentrations are usually quickly reduced to levels where exposure rates are small compared to those caused by activated accelerator components. [12]

AIR ACTIVATION AT ACCELERATOR FACILITIES

Air is a medium suitable to keep conditions for accelerator components acceptable for them to function. The accelerator housing, where beam losses are bound to take place, may be ventilated and the air is recycled or released into the environment, or a combination of the two. As a consequence of interactions of hadronic and electromagnetic cascades with airborne nuclei, the air inside the accelerator housing may become activated. Based on the assumption of pure air, which consists mainly of Nitrogen, Oxygen, Argon and CO_2 , about 39 relevant radionuclides with half lives longer than a few seconds can be produced. Activities of these released isotopes depend on their half lives, with longer half-life generally implying a lower activity. Lighter radionuclides, including H-3, Be-7, C-11, N-13, O-14 or O-15, are produced from light and abundant nuclei of Nitrogen and Oxygen. Ar-41 is produced mainly by thermal neutron capture on the stable Ar-40. C-14 is also produced through the (n, p) reaction on N, although its activity is low. Isotopes created from Nitrogen and Oxygen are predominantly in their gaseous form, as is Ar-41. C-11 occurs as ^{11}CO and $^{11}\text{CO}_2$, which are also gases at room temperature. Tritium occurs as HT and HTO. Other radionuclides, e.g. Be-7, attach to aerosol particles. Air also contains a variety of aerosol particles that are susceptible to activation, with the most important being Na-24 and Na-22. [15]

ACTIVATION MONITORING

An example of a ventilation monitoring station, which was also considered for use at CERN, can be found at [16]. Such a station is equipped with a monitor for short-lived radioactive gases, capable of recording their released activity online, as well as with an aerosol sampler. The station mentioned in [16] is optimized for an air flow of 5 m^3 per hour, if aerosol filters are installed, enabling continuous monitoring of radioactive gases. Prior filtration of the air can help to reduce perturbing outside influences on measurements, including effects due to moisture or smoke.

A suitable detector for the gas monitor is a compensated double semiconductor detector that is sensitive to beta radiation. Compensation is necessary in order to distinguish the actual measurements from background gamma radiation, which is likely to come from filtered radionuclides attached to aerosols which are caught in the main filtering units of the ventilation systems that are most probably close by. A simple subtraction of the signal that is recorded by a twin detector that only measures pure air can eliminate and therefore compensate this background.

The aerosol sampler filter is exposed to the air for one or two weeks and then analyzed in a laboratory for general beta- and gamma activity. Beta counting is performed in order to quantify pure beta emitters like P-32, P-33 and S-35, which may be important for the exposure of agricultural plants in the area of concern. Very short-lived radionuclides are impossible to analyze correctly via long exposure and lengthy analysis procedures of the aerosol filter. However, studies have shown that their contribution to the total effective doses to members of the public is negligible compared with other radionuclide categories. [15], [6]

REGARDING AUSTRIAN RADIATION PROTECTION LAW

The release of radioactive air from radiation facilities is regulated by the *Allgemeine Strahlenschutzverordnung (Anlage 12)*. [19]

For the release of radioactive substance in the form of aerosol, gas or vapour together with exhaust air, at a total release quantity between 10^4 and 10^5 cubic metres per hour, Ci values given in [19] apply. At a release volume of 10^4 m^3 at maximum, the tenfold of the Ci values applies. These Ci values are defined as upper limits of specific activity, given in $[\text{Bq}/\text{m}^3]$ for a range of different radioactive isotopes, that must not be overstepped.

In addition, if several different radioactive nuclei are subject to a simultaneous release, a sum value $\Sigma(\text{activities} / \text{Ci clearance levels})$ of the quotients of actual activities and their respective Ci values has to be calculated. If this sum value does not exceed 1, limits are observed. [19]

COMPARISON OF TWO METHODS TO CALCULATE THE ACTIVATION OF AIR BY MEANS OF A GENERIC STUDY

INTRODUCTION

In order to simulate the activation of air in a given volume, 2 different methods are considered. One method comprises the calculation of the fluences of protons, neutrons and pions with FLUKA in order to fold these with the appropriate cross sections for nuclide productions after the simulation is completed. On the other hand, FLUKA is able to calculate nuclide production by itself. The results of both methods are being compared by means of a generic study, to assess advantages and disadvantages of both concerning their suitability to the MedAustron geometry.

SIMULATION DETAILS

GEOMETRY

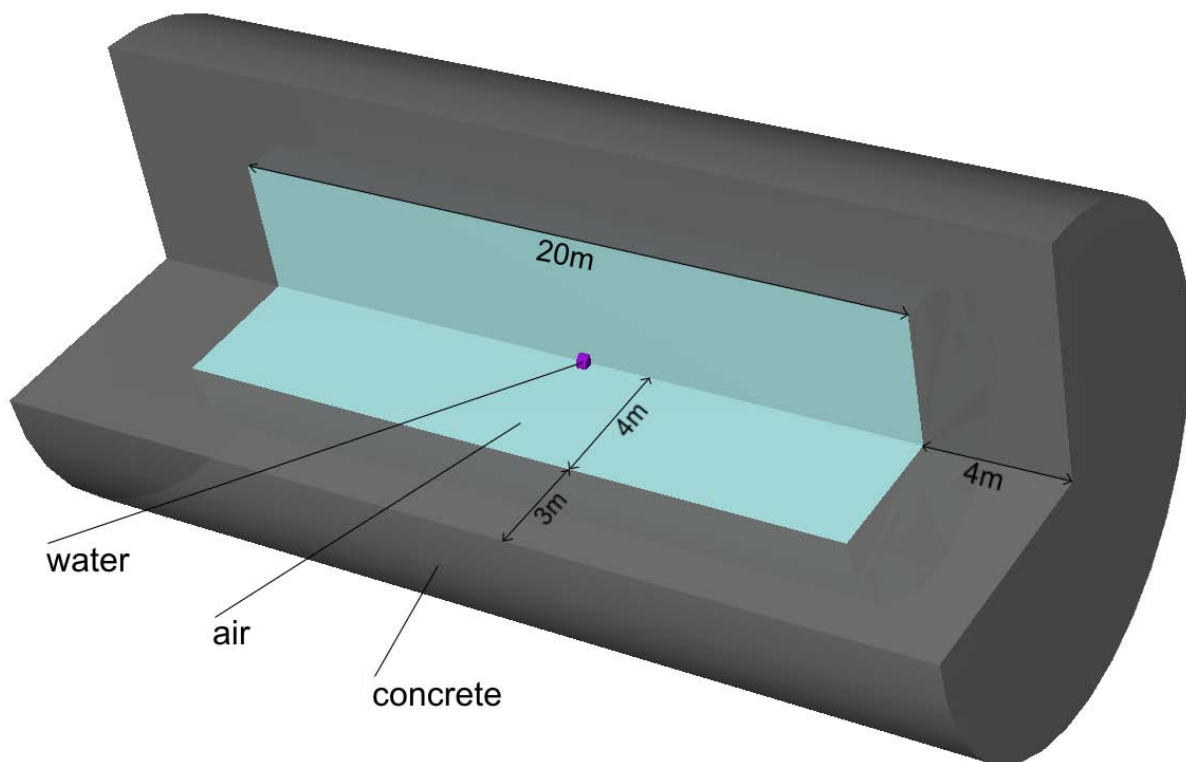


Figure 3: Cutaway view of the geometry

The actual geometry, displayed via cutaway view in Figure 3, lies inside a 40 m long cylindrical vacuum region with a 20 m radius, which is surrounded by an 80 m long cylindrical blackhole with a 40 m radius.

A hollow concrete 28 m long cylinder with a radius of 7 m, a 3 m thick outside wall and 4 m thick top and bottom wall contains an air volume with a 30cm long water target with a 30 cm radius at its center. The bottom area of the target is centered at the geometrical zero point, while the surrounding cylindrical air and concrete cylinders are centered symmetrically on zero.

The volume of the air inside the cylinder is 1005 m³.

The air volume surrounding the target is used as USRTRACK **detector**, to score **neutrons**, **protons**, as well as positive and negative **pions**.

The pencil beam propagates along the positive z-axis, starting 10cm in front of the target.

MATERIALS

The used compounds, described in the following Tables 1, 2 and 3, were directly taken from the library included in FLAIR, but without the optional MAT-PROP and STERNHEIMER parameters.

CONCRETE-COMPOUND:

FLUKA: CONCRETE

(Density = 2.34 g/cm³)

Table 1: Material composition of the concrete compound. The mass fraction of each element is represented in percentage of total mass.

Component	Amount (%)
Carbon	23.16
Oxygen	40.16
Silicon	12.16
Calcium	12.16
Hydrogen	10.16
Magnesium	2.16

AIR-COMPOUND:

FLUKA: AIR

(Density = 0.00120484 g/cm³)

Table 2: Material composition of the air compound. The mass fraction of each element is represented in percentage of total mass.

Component	Amount (%)
Carbon	0.01248
Nitrogen	75.5267
Oxygen	23.1781
Argon	1.2827

WATER-COMPOUND:

FLUKA: WATER

(Density = 1g/cm³)

Table 3: Material composition of the water compound. The atomic fraction of each element is represented in percentage of the total number of atoms.

Component	Amount (%)
Hydrogen	66.6
Oxygen	33.3

PARTICLE TRANSPORT THRESHOLDS

The lower threshold for particle transport of hadrons was set to 0.1 MeV for all hadrons except neutrons which were followed down to thermal energies.

Besides the hadron cascade simulation, also the EMF (ElectroMagneticFLUKA), a FLUKA function that enables the transport of electrons, positrons and photons, was activated during the simulation. Although the air activation contribution is considered very small compared to the hadronic part, this option was activated in order to account for photon-hadron production (mainly γ , n) to get a more precise value for comparison. Also, due to the simple setup of the simulation, computational time with EMF on was still very short. EMFCUT was utilized to set the energy production threshold for electron-, positron- and photon energies to 10 keV. The upper measuring limit of all USRTRACK detectors was set to 1 GeV.

SCORING APPROACH

To illustrate the behavior of the beam inside the geometry, cylindrical R- ϕ -Z **USRBIN**s using particle 201 (FLUKA/FLAIR: ALL-PART) for scoring the fluence of all particles are placed along the central beam axis in Z-direction. The cylindrical USRBINs spanning 30 m in Z-direction with a radius of 10 m provide 100 bins along the radius and 200 along the Z-axis. Due to the cylinder-symmetry of the geometry, no angle based bins are created, so all figures based on these USRBINs show symmetrical results around the beam axis.

In addition, a **RESNUCLEi** detector for scoring residual nuclei inside the air volume, as well as a **USRTRACK** track-length detector, are used to calculate airborne radioactivity.

FLUKA METHOD FOR PRODUCTION OF NUCLIDES

RESNUCLEi cards can score residual nuclei produced in inelastic interactions on a region basis during simulation. When providing the correct volume for the region in the input, yields will be listed per primary particle per cm³ in the result file.

FLUKA is able to calculate the radionuclide production per primary proton and their respective decay during irradiation and after a given set of cooling times during simulation, by using a combination of input cards (RADDECAY, IRRPROFI, DCYSCORE). However, results of detectors linked with these cards concur 100% with results received by the applicable offline user routine **usrsuwev**. The offline calculation with said routine allows for time savings during the actual simulation.

Two additional **PHYSICS** cards are activated during the simulations in order to score reasonable results in connection with the RESNUCLEi detectors:

SDUM = COALESCE (“on”) card as well as SDUM = EVAPORAT (“new evap with heavy frag”) activate special physics models needed for the generation and evaporation of heavy fragments, which is not activated by default because of the associated CPU penalty. [3]

Binary result files of the RESNUCLEi scoring are interpreted via the FLUKA user routine **usrsuwev**, providing the user with an output file of the scored yield as well as an evolution file containing the calculated activity of the different scored residual nuclei after several user-defined cooling times.

FLUKA also handles isomers, for example Na24 and Cl34. The usually produced yield of the isotope in question is split equally into each type of isomer and the ground state. During simulation of the irradiation time, nuclide production continues normally, while created isotopes begin to decay, according to their half-life. Regarding isotopes with short lived isomers as found in the simulation, equilibrium between parent and daughter nuclide establishes itself after a long enough irradiation time at a ratio of 2:1 in the case of one considered isomer.

FOLDING METHOD FOR THE PRODUCTION OF NUCLIDES:

In order to score particle track length $\Lambda(E)$ in the air volume as a function of energy, **USRTRACK** detectors were attached to the volume. Each detector for protons and positively as well as negatively charged pions was assigned 100 bins within an energy range between 0.01 MeV and 1 GeV. To accomplish this for the neutron detector, the requested number of bins in the FLUKA card had to be set to 823 bins, to get exactly 100 bins for the energy range between 20 MeV and 1 GeV, besides getting the standard 260 low-energy bins between 1E-14 GeV and 20 MeV. This is a consequence of FLUKA-inherent scaling of the low-energy neutron bins with respect to the selected total energy range.

To calculate the nuclide production in a given volume, the produced energy-dependent path lengths $\Lambda_k(E)$ of protons, neutrons, positive and negative charged pions per primary particle in the observed volume are simulated by FLUKA. Conversion of path lengths into associated production rates P_i of the Radionuclide i is conducted after the following rule:

$$P_i = \sum_{j,k} n_j \int dE \sigma_{i,j,k}(E) \Lambda_k(E) \quad (1)$$

P_i production rate P_i of radionuclide i

n_j atomic density of element j in air

$\Lambda_k(E)$ energy dependent path length of particle type k

$\sigma_{i,j,k}(E)$... energy dependent cross section for production of radionuclide i from reaction of particle type k with isotope j

Cross sections of the different elements consider their natural isotope composition. [7]

The executable **airactiv5-260** ([6], [7]) converts the individual track-length spectra obtained by the USRTRACK detectors by folding them with respective residual nuclei production cross sections into radionuclides produced in the regarded air volume via formula (1).

An important difference between the two methods is reflected in the indication of the respective uncertainty values and the arising consequences. The folding of particle fluences, which can be gained in a comparably short time showing small uncertainty values, with corresponding cross sections, which are pre-calculated and provided with negligible uncertainty, results in a value with impressively small uncertainty, after a very acceptable computing time. Direct statistical computation of the residual nuclei done by FLUKA itself on the other hand requires a lot of computing time to achieve reasonable uncertainty values, due to the sometimes very low probabilities of producing some isotopes. Very low uncertainty values that are comparable to the folding method require unreasonable amounts of computational power.

All calculations are made under the assumption that **no air exchange** will take place.

RESULTS

800 MEV PROTONS

FLUENCE (*800 MeV proton beam*)

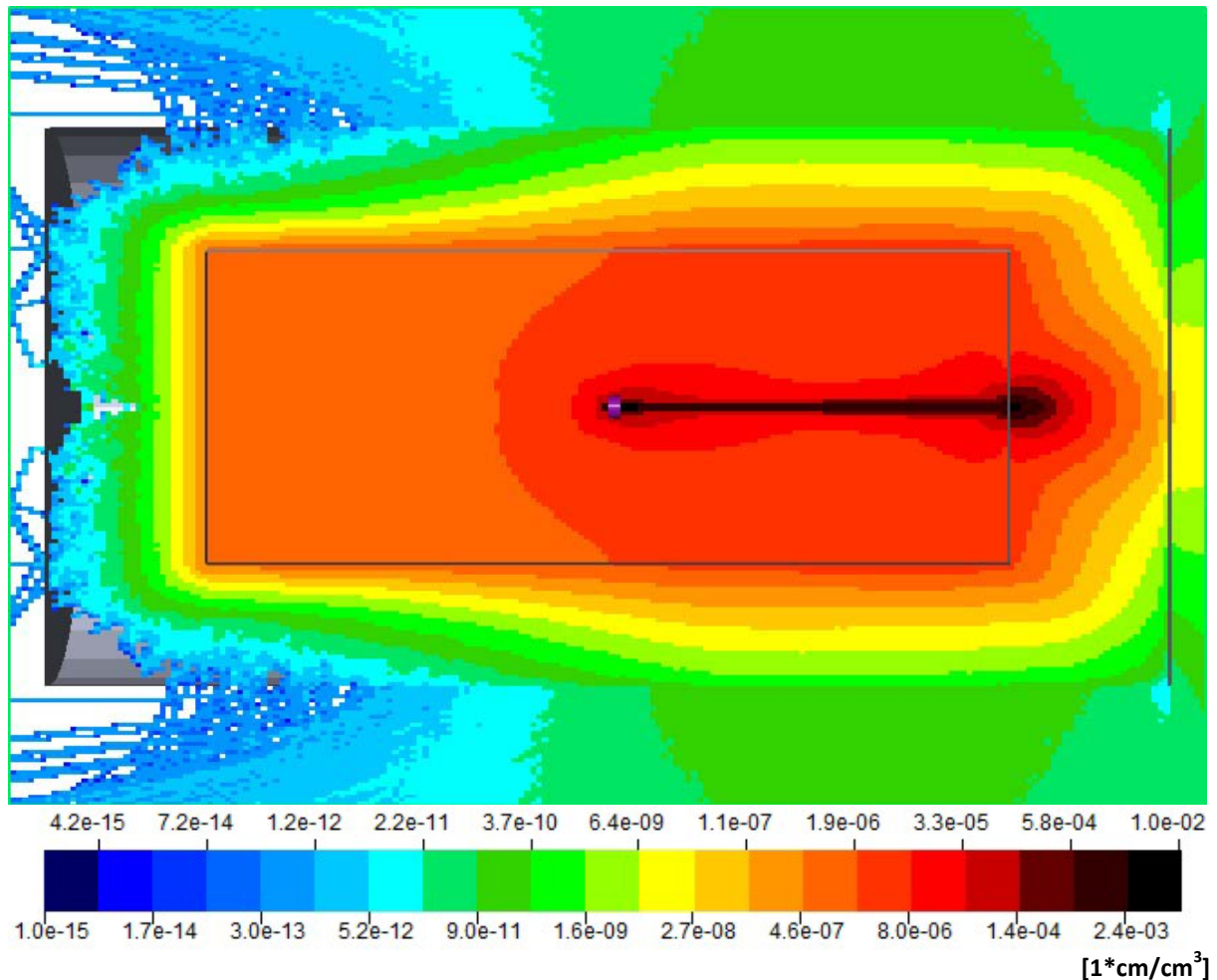


Figure 4: Fluence of all particles caused by 800 MeV protons [$1 \cdot \text{cm}/\text{cm}^3/\text{primary particle}$]

Figure 4 shows a map of the fluence inside the structure caused by an 800 MeV proton beam. The beam is started 10 cm in front of the 30 cm thick water target and is not fully attenuated inside the target because of the high energy of its particles. Therefore it crosses a big portion of the air volume before it hits the wall at the end of the cylinder. This is a possible scenario for experiments at the MedAustron facility, where thin samples are placed in the way of a high energy beam, which results in the majority of high energy particles not being stopped until they hit the wall at the end of the room.

The energy spectra of the 4 types of hadrons used for calculating activation via folding them with cross sections are depicted in Figure 5 by lethargy style, which means multiplying the fluence value with its corresponding energy. As there are only energy ranges given when scoring USRTRACKs, the mean value of ranges was taken for the abscissa to form the graph seen below.

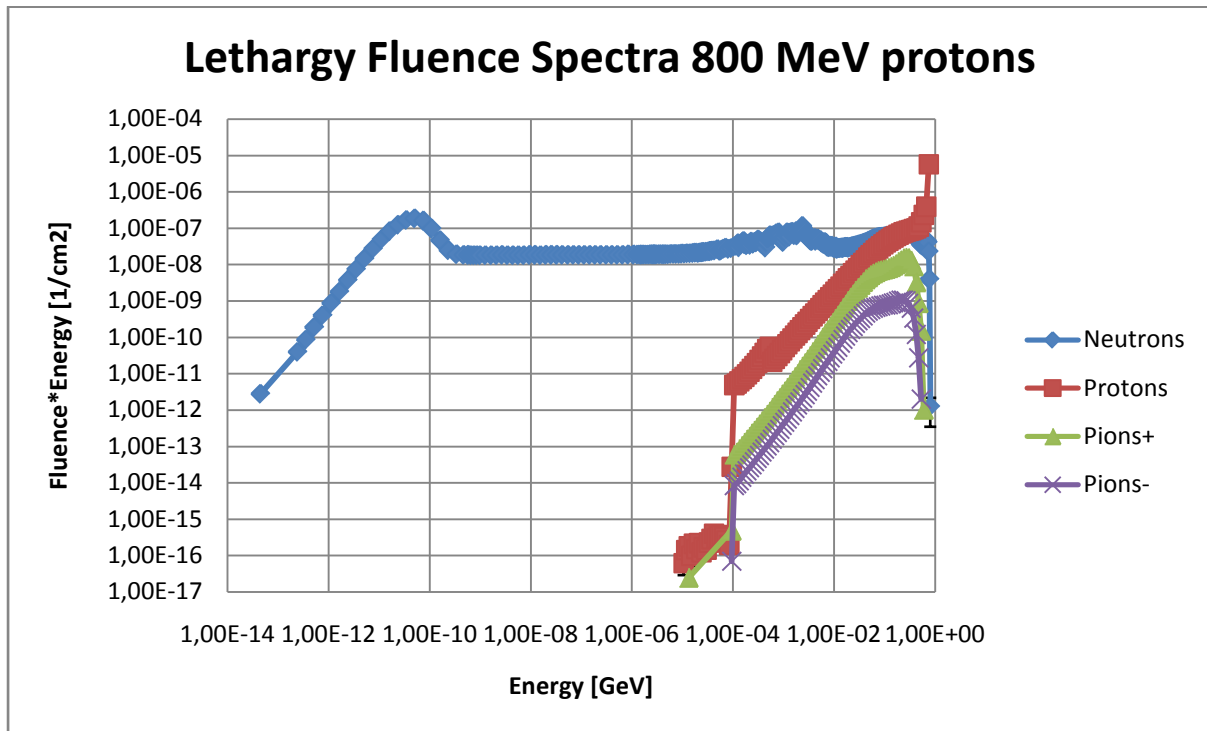


Figure 5: Lethargy fluence spectra of neutrons, protons, negative and positive pions scored in the air volume surrounding the target during 1h of irradiation with an 800 MeV proton beam, which are used to calculate the production of isotopes via folding method

The peak energy of the beam at 800 MeV is very recognizable when regarding the proton spectrum. This is due to the fact that the target is not thick enough to harbor the Bragg peak of the high energy beam inside, and therefore many primary protons are scored crossing the air volume behind it over several meters until they hit the wall.

The large skip in fluence values that is displayed for protons and pions at an energy of 0.1 MeV is caused by the fact that the chosen hadron transport thresholds are cut off below 0.1 MeV, while the detector scores protons and pions down to an energy of 0.01 MeV.

COMPARISON OF RESULTS 800 MEV PROTONS

Detailed tables showing the results and comparisons for each nuclide are listed in Appendix A. The relative error of yields given by the folding method is not mentioned in the tables, because it is never exceeding 0.1%.

To compare differences in activation calculations, yields given by both methods are checked against each other for every given isotope appearing in both calculations. Since FLUKA results yield more mostly short lived isotopes directly after stopping the beam, also sum values adding up all calculated activities are compared in Table 4 directly after the beam stop as well as after 1 hour and after 1 day cooling time. FLUKA results are marked by the affix *RESNUC*, while folding method results are called *airactiv*.

Calculations needed for the estimation of environmental exposure through air released from the MedAustron facility, which are explained later in the according chapters, involve simulations where every isotope created requires a given time until it is released into the environment. This means that decay during continuous irradiation is completely ignored, because only the time to decay that each particle gets counts in regard to calculating the overall activity. Table 4 incorporates additional columns ("*airactiv ref.*") showing results calculated via folding method, but ignoring decay during the 1h irradiation procedure, which give an idea of the influence that short lived isotopes have on the overall activation during irradiation procedures.

Table 4: Total activity of the air directly after 1h of irradiation with an 800 MeV proton beam, and after two cooling times (1h, 1d), according to FLUKA ("RESNUC"), the folding method including decay during irradiation ("airactiv") and the reference folding method ignoring decay during irradiation ("airactiv ref."), as well as the ratio between the FLUKA results and the results of the folding method

Cooling times	Bq/cm3 RESNUC	Bq/cm3 airactiv	Bq/cm3 airactiv ref.	RESNUC/airactiv	RESNUC/airactiv ref.
0s	5.28E-02	3.50E-02	3.64E-01	1.51E+00	1.45E-01
3600s (1h)	1.77E-03	1.61E-03	3.81E-03	1.10E+00	4.65E-01
86400s (1d)	4.88E-06	4.57E-06	4.59E-06	1.07E+00	1.06E+00

FLUKA scoring via RESNUCLEi card lists simulated isomers in a different table (Table 5). Isomers are generated by splitting the generated yields of an isotope equally into ground state and isomer state(s). Yields of the isomers are not included in the original list of isotopes found in Appendix A, but are still considered for the sum of activities in Table 4, because many of them already decay during irradiation, adding to the overall activity of the original isotope.

Table 5: List of isomers produced by FLUKA and scored in the RESNUCLEi card, along with their calculated activities directly after 1h of irradiation with an 800 MeV proton beam, and their corresponding error values.

Isomer	T 1/2 [s]	Bq/cm3	rel.err. %
24 Na	0.0202	7.96E-06	15.3
26 Al	6.345	5.14E-06	18
34 Cl	1920	3.38E-06	15.6
38 Cl	0.715	5.44E-05	5.9
38 K	0.9239	4.98E-07	72.4

The sum values of the activity of all isomers combined is 7.14E-5 Bq/cm3 directly after the irradiation, which does not have any significant influence on the total sum of activities shown above.

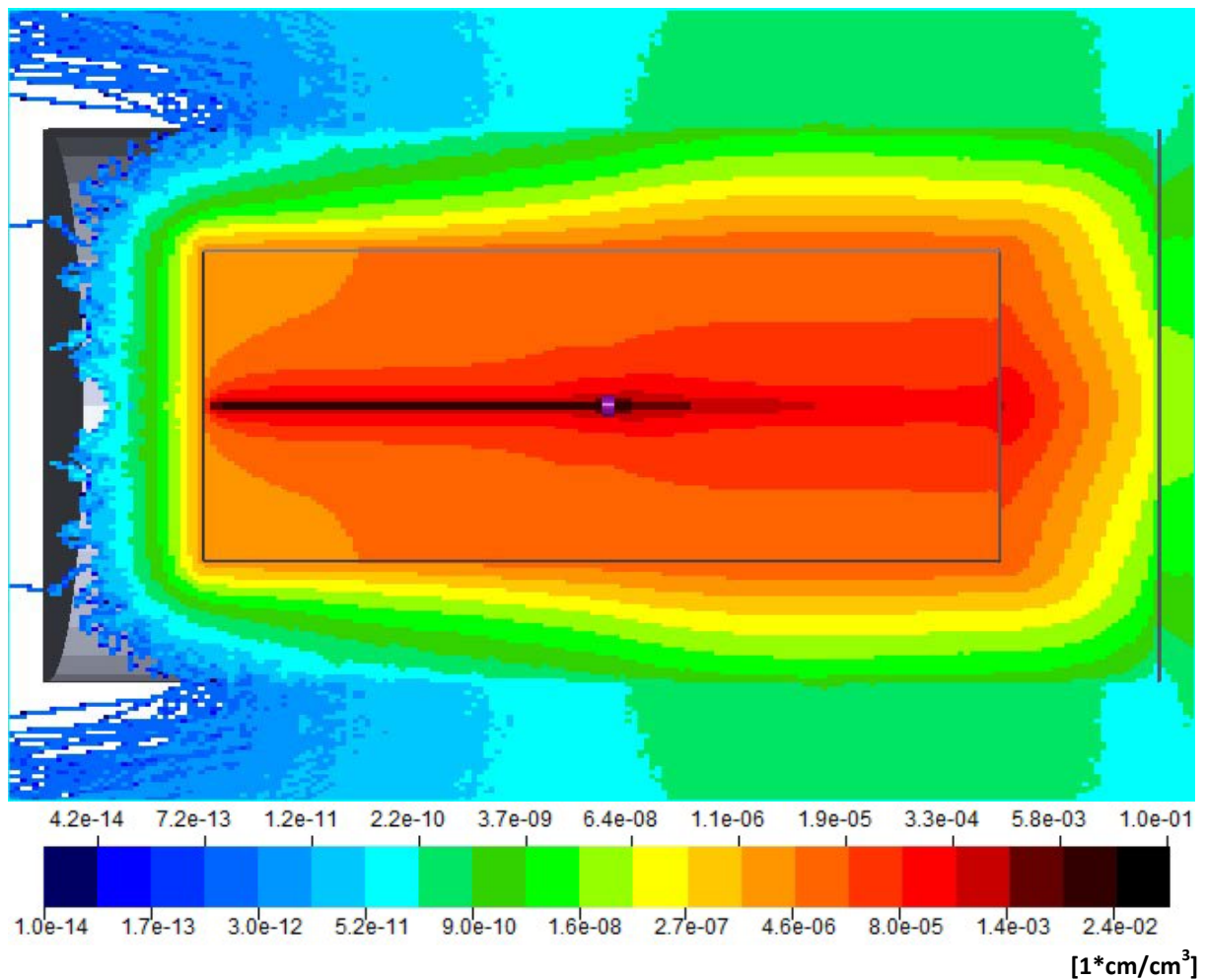
FLUENCE (*400 MeV C12 ion beam*)

Figure 6: Fluence of all particles caused by 400 MeV ions [$1 \cdot \text{cm}/\text{cm}^3/\text{primary particle}$]

Figure 6 shows a map of the fluence inside the structure caused by a 400 MeV ion beam. To incorporate a distinguishing characteristic into the simulation, the beam was started almost 10 m away from the centred target, in order to see a difference caused by the absence of cross sections describing the interactions between the main ion beam and the air when using the folding method. 30 cm of water as a target already suffice to attenuate the ion beam enough so that only secondary particles make it through.

The energy spectra of the 4 types of hadrons used for calculating activation via folding them with cross sections is depicted in Figure 7 by lethargy style, which means multiplying the fluence value with its corresponding energy. As there are only energy ranges given when scoring USRTRACKs, the mean value of ranges was taken for the abscissa to form the graph seen below.

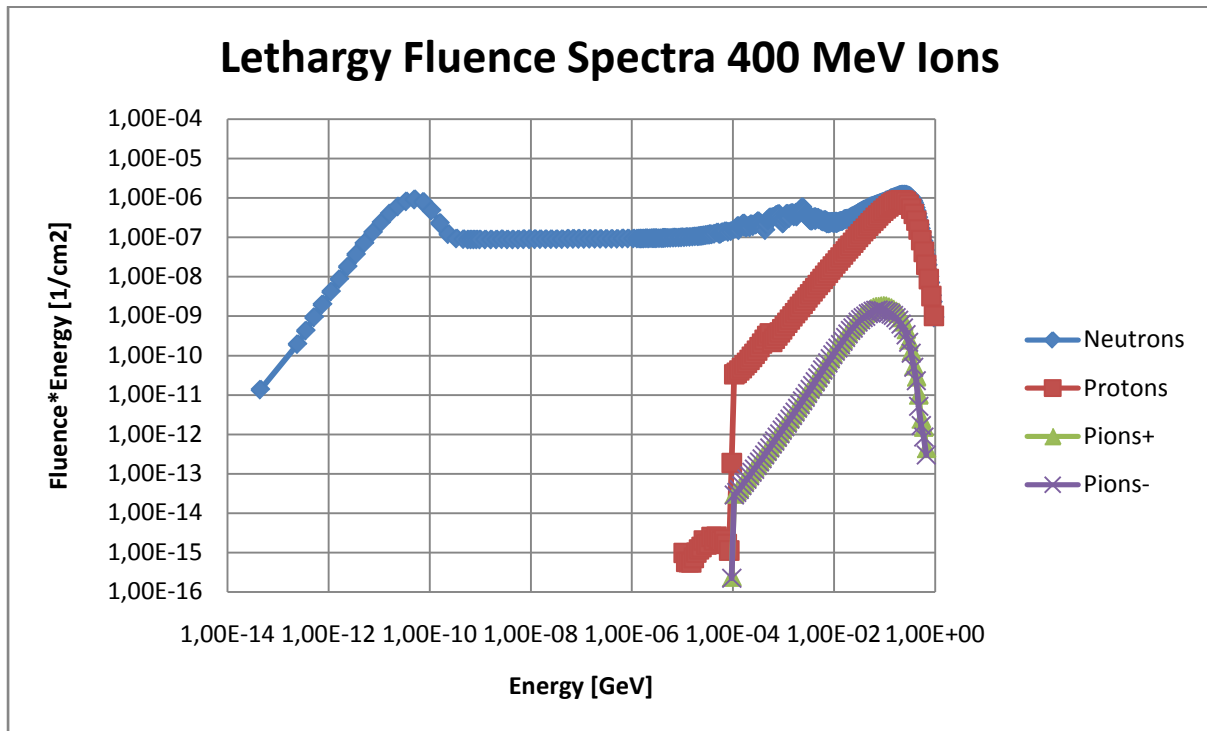


Figure 7: Lethargy fluence spectra of neutrons, protons, negative and positive pions scored in the air volume surrounding the target during 1h of irradiation with an 400 MeV ion beam, which are used to calculate the production of isotopes via folding method

Although the main ion beam cannot be seen in this depiction, the broad peaks of all scored particles gather clearly around the 400 MeV mark, with secondary particles sometimes even absorbing more energy than the 400 MeV per nucleon of the main beam..

COMPARISON OF RESULTS 400 MEV IONS

Detailed tables showing the results and comparisons for each nuclide are listed in Appendix A. The relative error of yields given by the folding method is not mentioned in the tables, because it is never exceeding 0.1%

To compare differences in activation calculations, yields given by both methods are checked against each other for every given isotope appearing in both calculations. Since FLUKA results yield more mostly short lived isotopes directly after stopping the beam, also sum values adding up all calculated activities are compared in Table 6 directly after the beam stop as well as after 1 hour and after 1 day cooling time. FLUKA results are marked by the affix *RESNUC*, while folding method results are called *airactiv*.

Calculations needed for the estimation of environmental exposure through air released from the MedAustron facility, which are explained later in the according chapters, involve simulations where every isotope created leaves the room immediately and has the same time to decay until release into the environment. This means that decay during continuous irradiation is completely ignored, because only the time to decay that each particle gets while being transported outside counts in regard to calculating the overall activity. Table 6 incorporates additional columns ("*airactiv ref.*") showing results calculated via folding method, but ignoring decay during the 1h irradiation procedure, which give an idea of the influence that short lived isotopes have on the overall activation during irradiation procedures.

Table 6: Total activity of the air directly after 1h of irradiation with a 400 MeV carbon ion beam, and after two cooling times (1h, 1d), according to FLUKA ("*RESNUC*"), the folding method including decay during irradiation ("*airactiv*") and the reference folding method ignoring decay during irradiation ("*airactiv ref.*"), as well as the ratio between the FLUKA results and the results of the folding method

Cooling times	Bq/cm3 RESNUC	Bq/cm3 airactiv	Bq/cm3 airactiv ref.	RESNUC/airactiv	RESNUC/airactiv ref.
0s	2.98E-01	1.22E-01	1.24E+00	2.44E+00	2.41E-01
3600s (1h)	1.01E-02	5.47E-03	1.28E-02	1.85E+00	7.93E-01
86400s (1d)	5.14E-05	1.05E-05	1.06E-05	4.88E+00	4.85E+00

The list of isomers produced by FLUKA is scored separately from the list of isotopes. Their calculated activities directly after 1h of irradiation with the ion beam are listed in Table 7.

Table 7: List of isomers produced by FLUKA and scored in the RESNUCLEi card, along with their calculated activities directly after 1h of irradiation with an 800 MeV proton beam, and their corresponding error values.

Isomer	T 1/2 [s]	Bq/cm3	rel.err. %
24 Na	0.0202	3.07E-05	15.4
26 Al	6.345	2.53E-05	12.8
34 Cl	1920	1.88E-05	14.3
38 Cl	0.715	3.95E-04	3.6
38 K	0.9239	2.69E-06	42.2

The sum values of the activity of all isomers combined is 4.73E-4 Bq/cm3 directly after the irradiation, which does not have any significant influence on the total sum of activities shown above.

DISCUSSION

Processing the BINARY as well as the ASCII output of the RESNUCLEi detectors results in exactly the same amount of residual nuclei per cm^3 per primary particle. An examination of the expected activity in Bq/cm^3 also leads to the same results using both methods.

Some isotopes with negligible contribution to the total activity are ignored by the folding method, which uses a given list of cross sections that is already comprised of the main contributors for airborne radiation.

All isotopes appearing in the direct FLUKA simulation that are not listed by the results of the airactiv5-260 routine do either turn up in negligible tiny amounts, which is also indicated by their corresponding relative error values given by FLUKA which can be as high as 99%, or disappear very quickly due to their very short half-life.

In conclusion, the direct simulation of the production of isotopes via FLUKA yields more conservative results of the total activity when comparing the results considering the decay during one hour of irradiation.

A detailed view of the 800 MeV proton simulation shows the total activity calculated by FLUKA directly after the stop of the beam (0s) being higher by a factor of about 1.5 compared to the folding method directly after the stop of the beam.

This conservative factor of 1.5 is mainly caused by the circumstance that the specific cross sections for N-13 used by FLUKA differ from the ones used by the airactiv5-260 routine, with the latter ones resembling experimental values with more accuracy. Figures 8, 9, 10 and 11 show comparisons between the different cross sections of protons, neutrons and pions in the respective routines, which are used to simulate the production of N-13 and the cross sections gained by experiments. The routine airactiv5-260 that is used with the folding method utilizes the cross sections evaluated by Huhtinen, marked red in the figures below. [6]

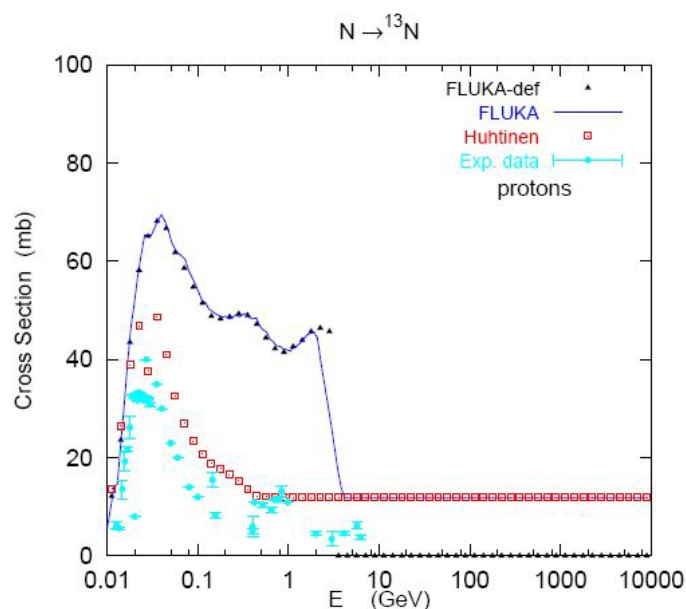


Figure 8: Red dots indicate N-13 production cross sections by protons on nitrogen evaluated by Huhtinen [7], which are compared with experimental data (light blue dots) [8] and to predictions of the available FLUKA version (dark blue line). [6]

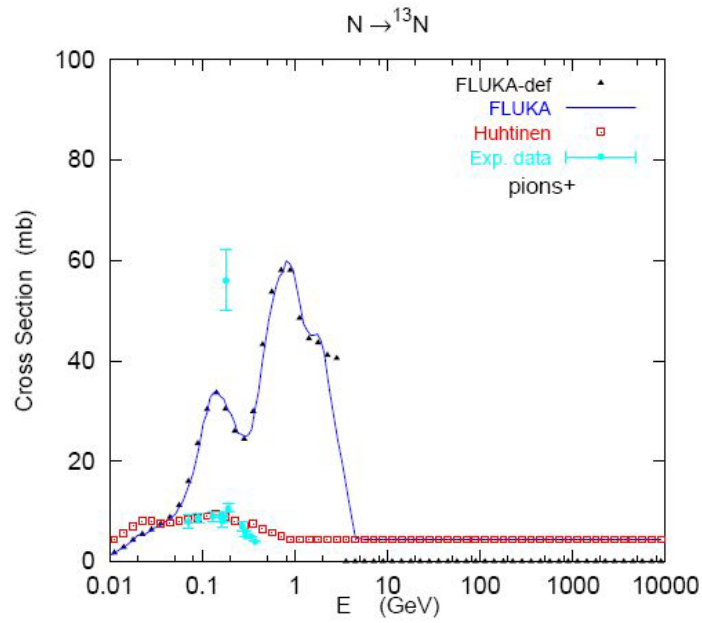


Figure 9: Red dots indicate N-13 production cross sections by positively charged pions on nitrogen evaluated by Huhtinen [7], which are compared with experimental data (light blue dots) [8] and to predictions of the available FLUKA version (dark blue line). [6]

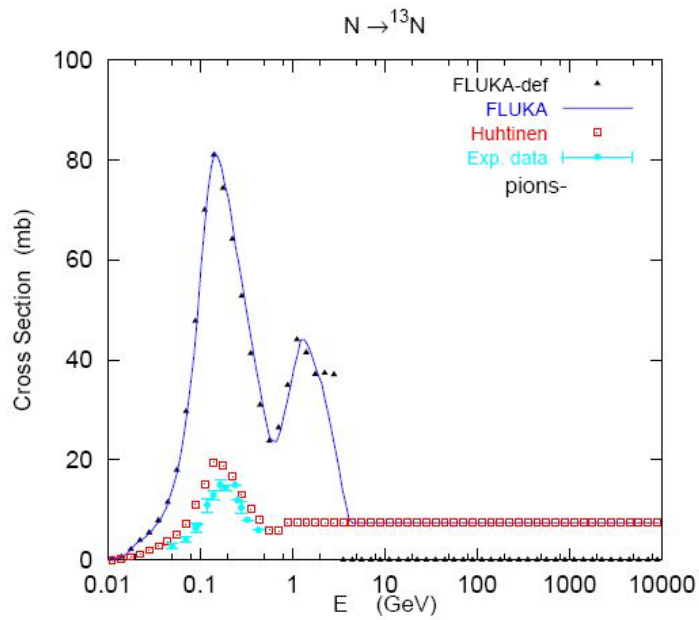


Figure 10: Red dots indicate N-13 production cross sections by negatively charged pions on nitrogen evaluated by Huhtinen [7], which are compared with experimental data (light blue dots) [8] and to predictions of the available FLUKA version (dark blue line). [6]

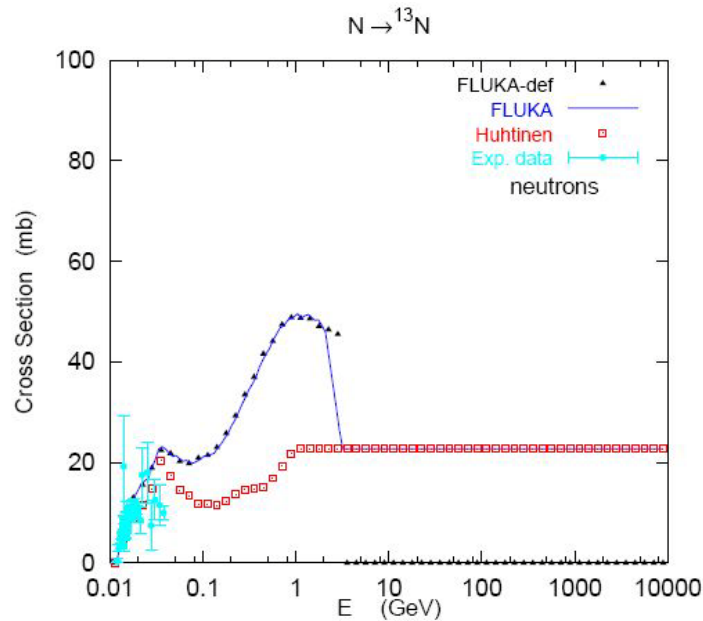


Figure 11: Red dots indicate N-13 production cross sections by neutrons on nitrogen evaluated by Huhtinen [7], which are compared with experimental data (light blue dots) [8] and to predictions of the available FLUKA version (dark blue line). [6]

As can be seen especially in Figure 8 and Figure 11, cross sections for the production of N-13 by neutrons and protons between 0.25 and 0.8 GeV are significantly overestimated by FLUKA, explaining the difference in yield production between the two methods.

A detailed view of the 400 MeV ion beam simulation shows the total activity of FLUKA results directly after the stop of the beam (0s) being higher by a factor of 2.44, which is caused by a combination of using the cross sections of N-13, responsible for the factor of 1.5 discussed with the proton beam simulations, and of course the fact that the ion beam crosses half of the inner air volume before hitting the target. The folding method used for these simulations does not include cross sections for ion beams, which means that any isotopes produced by the main beam will not show up in the results of the folding method.

The greater activity of the FLUKA results compared to both calculations by folding methods at longer cooling times are caused by the fact that FLUKA is creating more long lived isotopes during the simulation than what the folding methods yield. After about one day of cooldown, only long lived isotopes like H-3 and Be-7 are left to be the main source of radiation and their bigger yield given by FLUKA, due to the consideration of the radionuclide production caused by ions, is responsible for the difference.

Regarding the sum values gained by using the folding method while ignoring decay during irradiation (*airactiv ref.*), it can be seen that the short-lived isotopes really dominate airborne radioactivity results. N-13 for example, being responsible for most of the radiation created, due to the high percentage of nitrogen that the air consists of, has a half-life of about 10 minutes, which enables a lot of decay processes going on during 1 hour of continuous irradiation, explaining in parts the huge differences between *airactiv* and *airactiv ref.* results in calculated activation via folding method seen in Table 4 and Table 6.

For the simulation of air activation caused by proton beams, the folding method utilizing airactiv5-260 will be used, because the cross sections for the production of N-13 yield results that are closer to experimental data. Also, it proved to be the more efficient and time saving approach in this specific case.

When using an ion beam, the processing of particle fluences with the folding method proves difficult, because activation production events caused by the ion particles in the main beam will not be counted towards total activation of the air. Therefore, the activation of air in ion-beam scenarios where the beam is to be expected to traverse a significant length (>1m) of airspace will be calculated by using FLUKA itself, namely scoring with the RESNUCLEi card and evaluating the yields by using the usrsuvev user routine.

DETAILED STUDY OF AIR ACTIVATION WITHIN A FLUKA GEOMETRY OF THE MEDAUSTRON FACILITY

INTRODUCTION

Taking the insights gained from the generic study, simulations inside a realistic geometry are conducted in order to obtain detailed results for specific irradiation scenarios inside the MedAustron facility. Irradiation scenarios concerned with air activation, taking into account beams with the highest energies available for the respective scenarios, are considered for all irradiation rooms as well as for beam losses inside the synchrotron hall to conservatively estimate implications for personnel working at MedAustron as well as for the air released from the facility.

SIMULATION DETAILS

GEOMETRY

An early build of the MedAustron geometry modeled by Lukas Jägerhofer was adopted and modified in order to create single volumes of air for each particular treatment room and the synchrotron hall to enable region based scoring of fluences and activation. Featuring accurate proportions of the different treatment rooms as well as appropriate targets and target positions for the assumed beam directions, simulations inside the treatment rooms should provide for a conservative but useful estimation of the activation of air during various scenarios of irradiation.

Losses scheduled for different designated loss points inside the synchrotron hall are simulated in a very conservative manner by building only the bare minimum of necessary collision points. As the exact dimensions of the final machine parts to be implemented in the hall could only be estimated at the time of simulation, an extremely conservative approach was chosen to estimate an absolute worst case of particles scattered around the hall, triggering activation of isotopes.

MATERIALS

All single elements including lead, iron and carbon are standard elements integrated by FLUKA. [3]

The compounds used for air and water, described in Table 8 and Table 9, were directly taken from the library included in FLAIR, but without the optional MAT-PROP and STERNHEIMER parameters.

AIR-COMPOUND:

FLUKA: AIR

(Density = 0.00120484 g/cm³)

Table 8: Material composition of the air compound. The mass fraction of each element is represented in percentage of total mass.

Component	Amount (%)
Carbon	0.01248
Nitrogen	75.5267
Oxygen	23.1781
Argon	1.2827

WATER-COMPOUND:

FLUKA: WATER

(Density = 1g/cm³)

Table 9: Material composition of the water compound. The atomic fraction of each element is represented in percentage of the total number of atoms.

Component	Amount (%)
Hydrogen	66.6
Oxygen	33.3

The normal concrete used for simulation is a concrete used at CERN with the element composition listed in Table 10 and a density of 2.4 g/cm³.

CONCRETE-COMPOUND

FLUKA: CONCRETE

(Density = 2.4 g/cm³)

Table 10: Material composition of the concrete compound. The mass fraction of each element is represented in percentage of total mass.

Component	Amount (%)
Hydrogen	0.561
Carbon	4.377
Oxygen	48.204
Magnesium	1.512
Aluminum	2.113
Iron	1.263
Silicon	16.175
Sodium	0.446
Calcium	23.929
Titan	0.173
Potassium	0.833
Sulfur	0.414

The compound **heavy concrete (HEAVCONC)** is made of exactly the same composition as normal concrete, listed in Table 10, but has the double density, at 4.8 g/cm³.

IRRADIATION ROOMS 1-4

Figure 12 and Figure 13 display 3D illustrations of the geometry used for simulating irradiation scenarios in the treatment rooms. Grey areas indicate structures made of concrete, while dark grey means that a heavy concrete with double density is used. Heavy concrete has to be applied, when space constraints do not allow for very thick walls to be erected, which is the case at wall breakthroughs conducting the beam from the High Energy Beam Transfer line (HEBT) into the treatment rooms where heavy grapping machinery has to be installed, or at walls required for heavy shielding, which is in this case the maze connecting irradiation room 1, where high energy beam experiments will be conducted, to the rest of the facility.

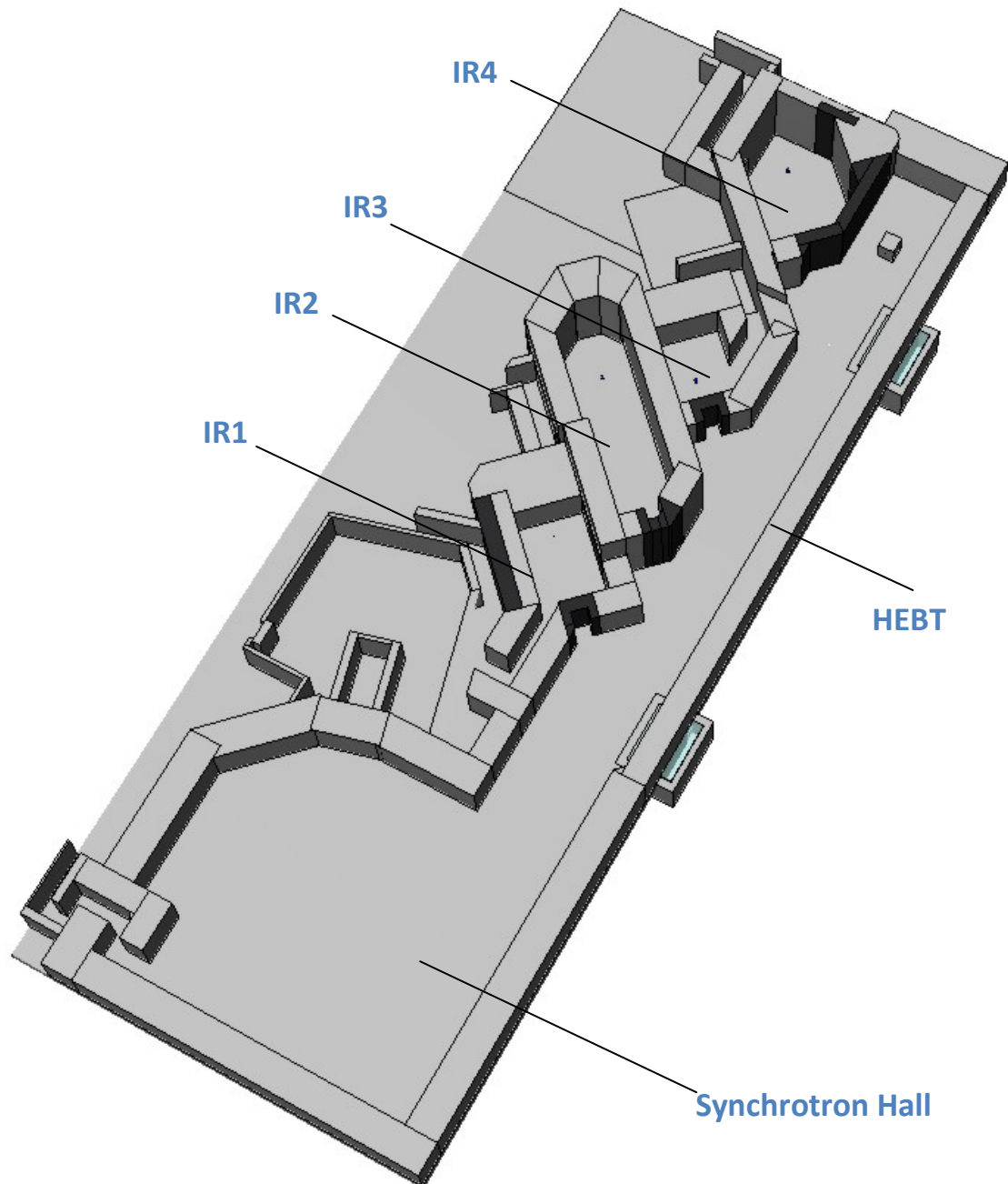


Figure 12: Bird view of the insides of the geometry used for simulations inside the treatment rooms. Grey areas are made of concrete, dark grey means heavy concrete which has double density of normal concrete. The ceiling was made transparent for a better view.

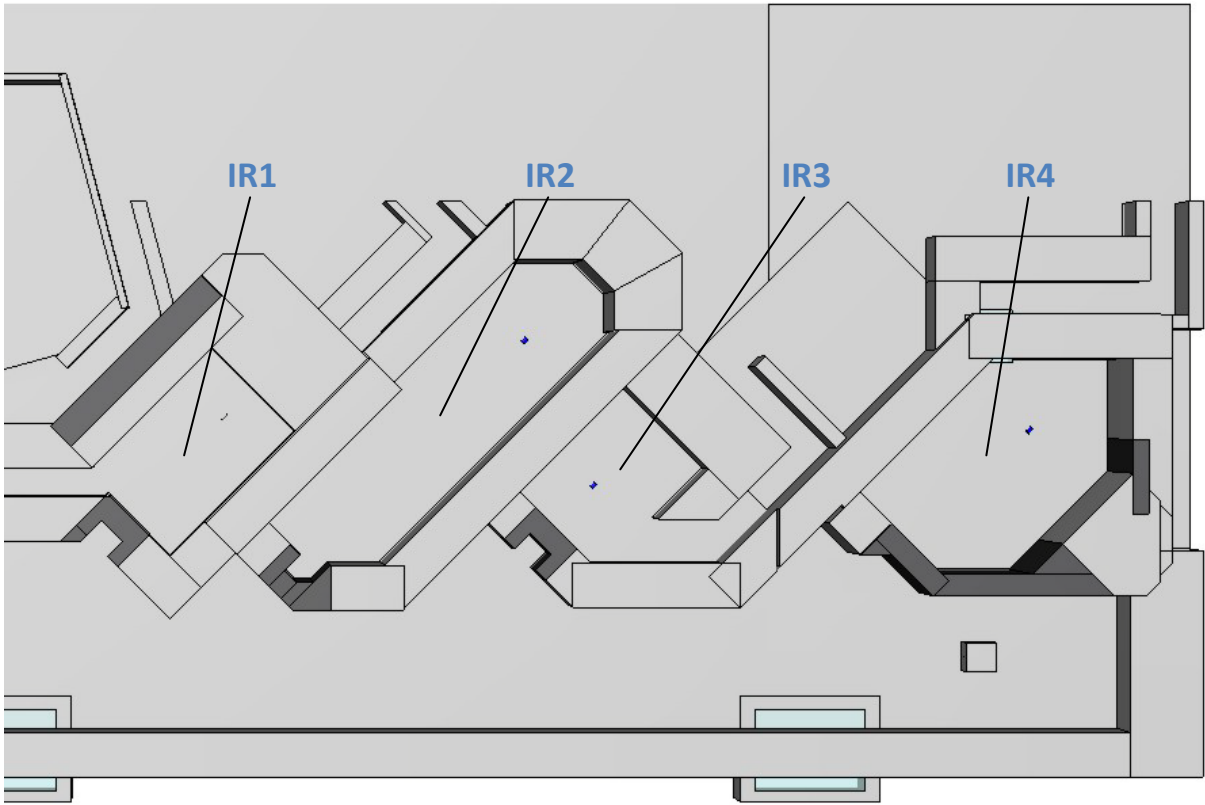


Figure 13: Top view of the 4 irradiation rooms with targets inside. Grey areas are made of concrete, dark grey means heavy concrete which has double density of normal concrete. The ceiling was made transparent for a better view.

Irradiation room 1 (IR1) is a non-clinical area designed especially for experiments conducted with the high energy 800 MeV proton beam provided by the accelerator. Although also proton beams with lower energy and carbon ion beams will be used for experiments, the room is equipped with heavy shielding to compensate for the maximum irradiation scheduled to happen in the facility.

To comply with the experimental nature of irradiation scenarios in this room, a 50 cm long lead cylinder with a diameter of 5 cm serves as a heavy target designated to stop the beam and produce as many secondaries as possible. The target cylinder is located at beam height, which is 125 cm from the floor, in the rear part of the room to leave enough space for the beam, which is started at the wall breakthrough, to cross a big air volume.

The air volume, i.e. scoring region, as pictured in Figure 14, contains only a small part of the directly connected maze leading to the exit. Ventilation in this room will be designed in a way, so that no air from irradiation rooms will escape into non classified areas, meaning that it will be channeled from the entrance into the room and from there through ventilation channels into the synchrotron area. So irradiation of the defined volume will provide for an adequate estimation of activation in this room.

SimpleGeo 4.1 [14] was used to calculate the volume of the region by using a quasi-Monte-Carlo algorithm, with the result being 515 m³.

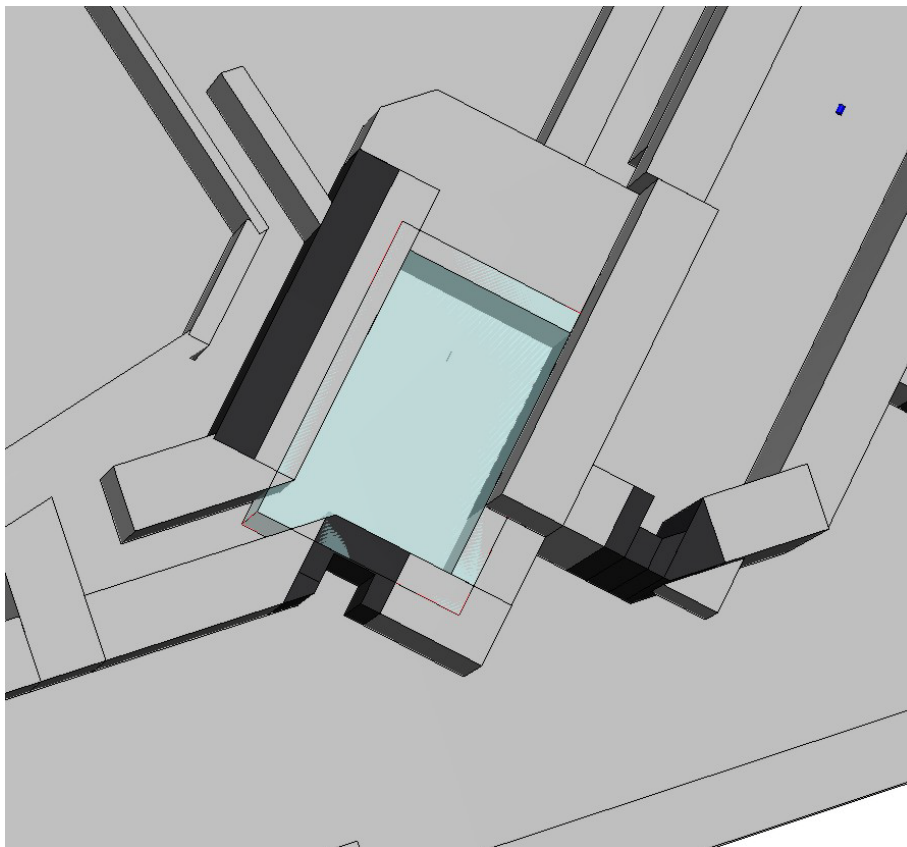


Figure 14: Sketch outline in blue of the air volume used as scoring region in irradiation room 1. The ceiling was made transparent for a better view of the structure.

Irradiation room 2 (IR2) is a very long and big treatment room designed for treatment of patients by using a carbon ion beam at 400 MeV per nucleon maximum. Its ceiling is elevated to enable a second beam line to shoot vertically from top to bottom. Figure 15 shows a top down view of the room with the target positioned in the upper half.

Being a treatment room for human patients, a water target has been placed at a height of 125 cm from the ground with its base always turned to face the beam to simulate appropriate conditions. The target has a length of 40 cm and a diameter of 30 cm to make sure that the Bragg peak of a 400 MeV carbon ion beam is establishing itself fully inside the water volume.

The volume of the room, according to SimpleGeo 4.1 is 2000 m³.

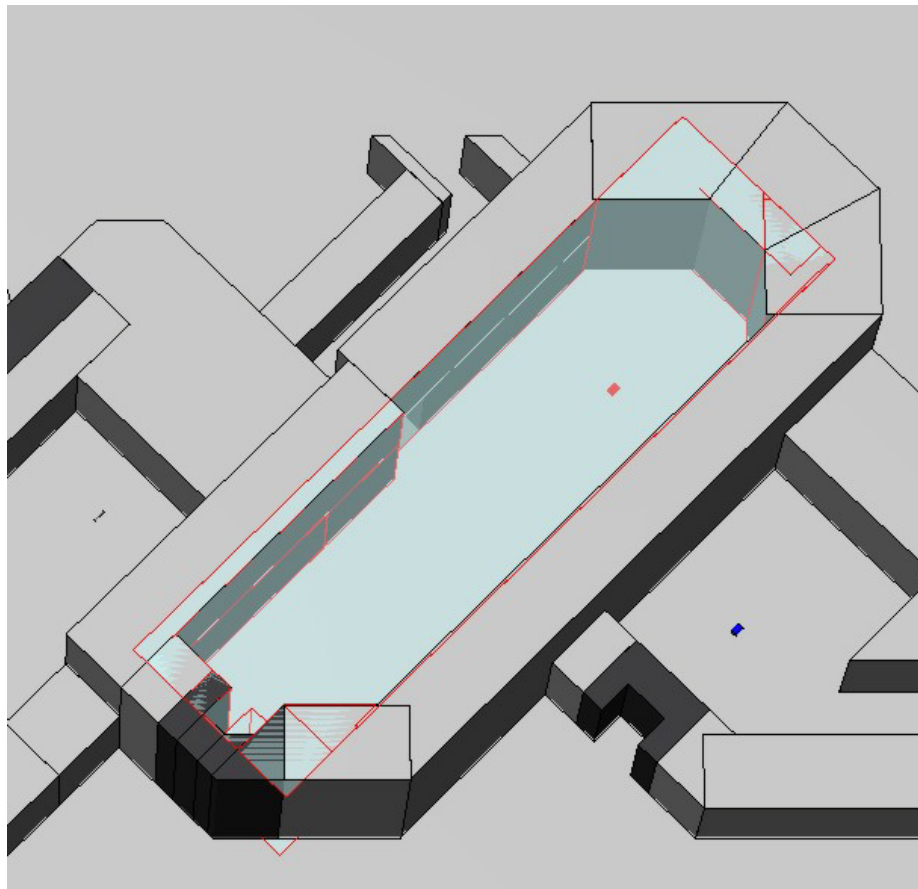


Figure 15: Sketch outline in blue of the air volume used as scoring region in irradiation room 2. Due to difficulties with the graphical engine, red outlines of cut away objects are still displayed. The water target in the upper half of the room is also marked red. The ceiling was made transparent for a better view of the structure.

Irradiation room 3 (IR3) is the smallest of the irradiation rooms featuring only one possible direction for the beam, coming directly horizontal from the wall break. Like in IR2, the focus of operation will be the treatment of patients with a 400 MeV carbon ion beam. As can be seen in Figure 16, the maze connecting the room to the rest of the facility is not considered in the simulations, which renders this part of the simulations especially conservative, considering the small volume of the room.

Again, a water cylinder with a length of 40 cm and a diameter of 30 cm placed in the lower half of the room serves as a target for simulations.

SimpleGeo 4.1 calculation of the volume results in 287 m³.

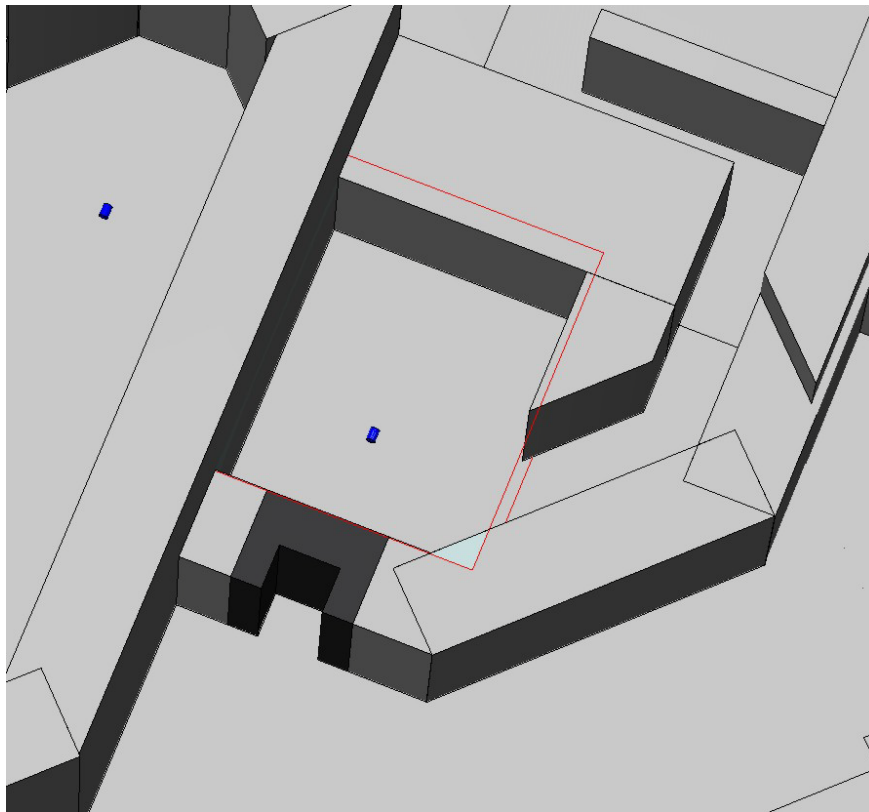


Figure 16: Sketch outline (red lines) of the air volume used as scoring region in irradiation room 3. The ceiling was made transparent for a better view of the structure.

Irradiation room 4 (IR4) is a specially designed room accommodating a proton gantry, featuring a maximum energy of 250 MeV per proton. The installation of the mounting suspension of a gantry entails a lowering of the floor to allow for ground level entry, as well as an elevated ceiling to permit free overhead movement of the gantry. Figure 17 shows an outline of the volume used as scoring region.

A water cylinder with a length of 40 cm and a diameter of 30 cm whose base is always turned to face the beam serves again as a target.

The volume of the room according to SimpleGeo 4.1 is 1970 m³.

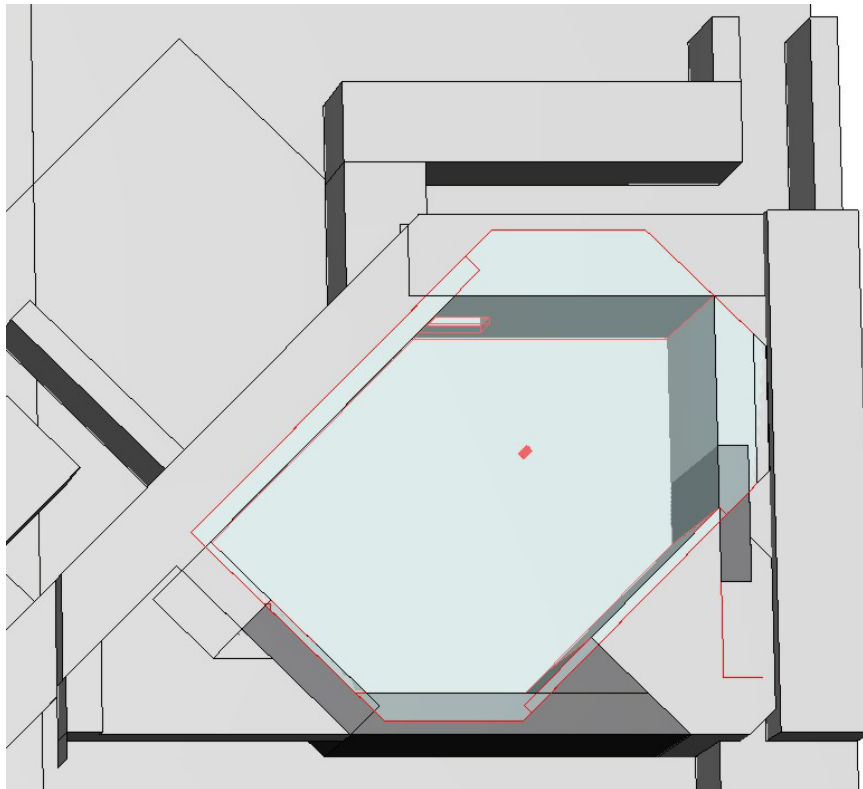


Figure 17: Sketch outline in blue of the air volume used as scoring region in irradiation room 4. Due to display errors, red outlines of cut away objects are still displayed. The ceiling was made transparent for a better view of the structure.

SYNCHROTRON HALL AND LOSS POINTS

In order to conduct proper simulations of air activation by synchrotron hall loss points, the MedAustron geometry had to be modified in a way so that the whole synchrotron hall plus the high energy beam transfer (HEBT) form one huge defined volume including the formerly cut-out parts that came from the construction of special wall formations around the treatment rooms.

The resulting volume was measured by SimpleGeo 4.1 with a quasi-Monte-Carlo algorithm to be 11883 m^3 which is already taking into account the added objects for simulating dipoles, beam dumps and the loss points themselves.

The geometry used for simulating the beam losses is illustrated in Figure 18, Figure 19 and Figure 20. In addition to the geometry used for simulating inside the irradiation rooms, several structures for sketching the loss points and a more realistic beam dump at the end of HEBT have been added. The irradiation rooms themselves have been in parts changed for the simulations in order to arrange for a combination of formerly separate air volumes into a single volume encompassing the synchrotron hall and the HEBT. This does have absolutely no negative influence on air activation simulations inside the synchrotron hall.

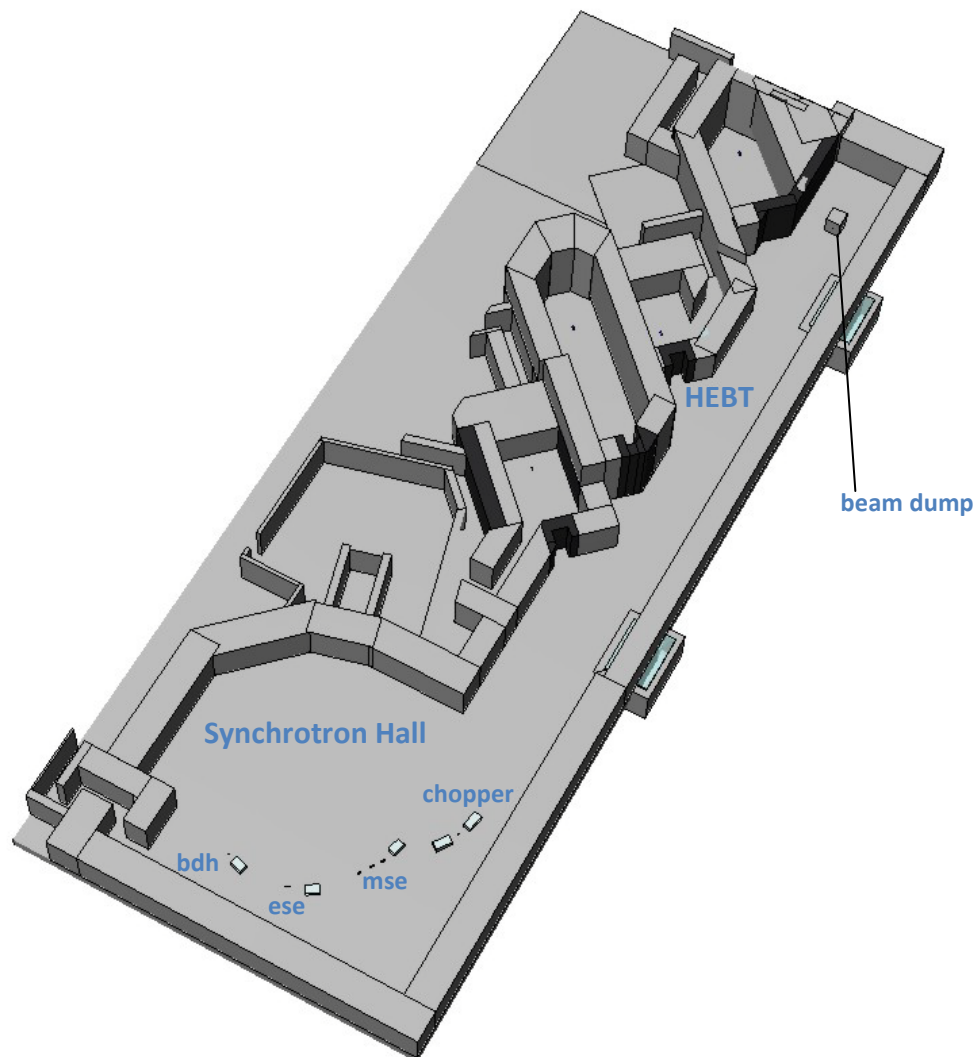


Figure 18: Bird view of the insides of the geometry used for simulations in the synchrotron hall, with representations of the loss points. Grey areas are made of concrete, dark grey means heavy concrete which has double density of normal concrete. The ceiling was made transparent for a better view.

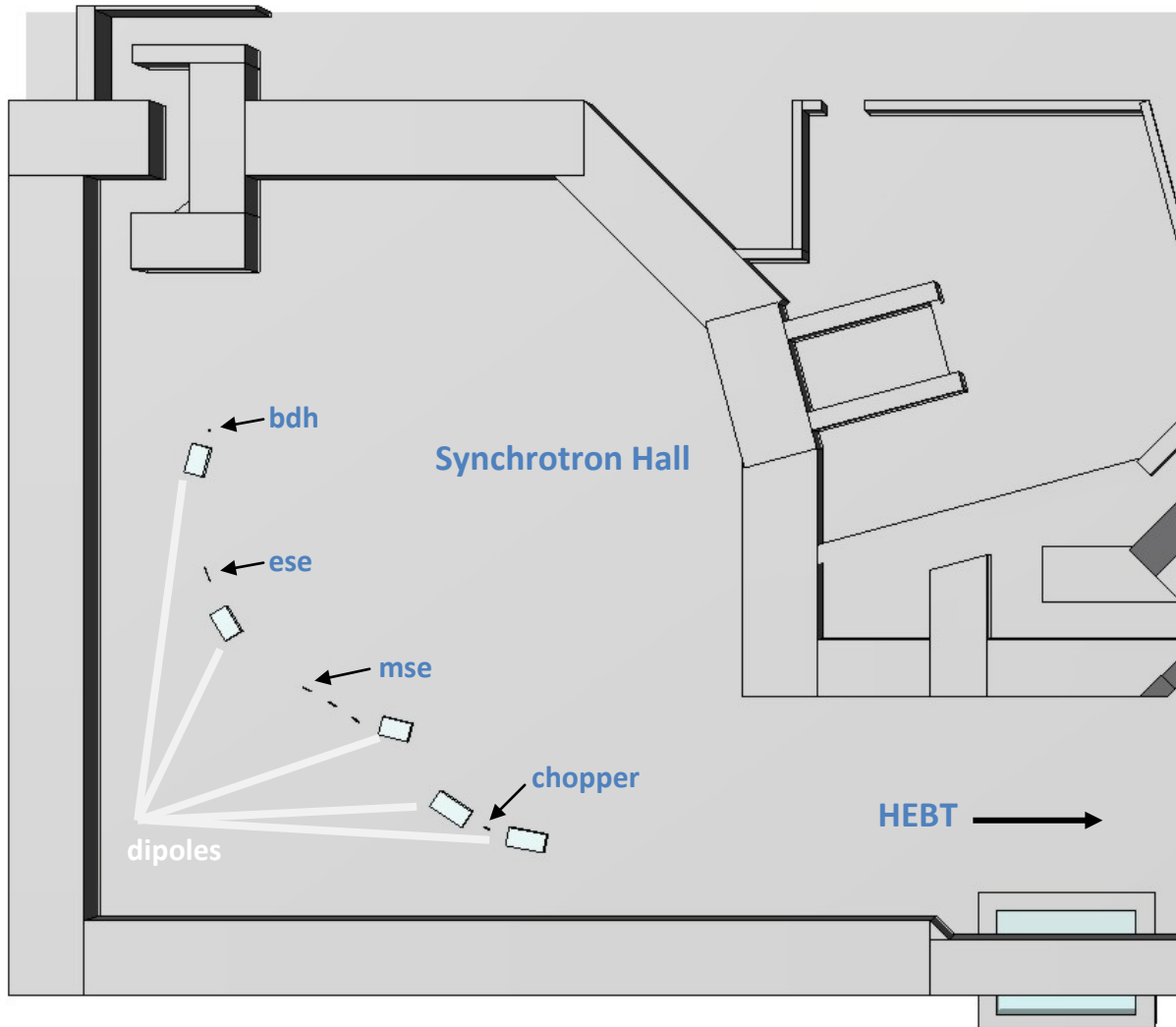


Figure 19: Top view of the synchrotron hall with representations of loss points and some dipoles, represented by iron blocks in light grey. Grey areas are made of concrete, dark grey means heavy concrete which has double density of normal concrete. The ceiling was made transparent for a better view.

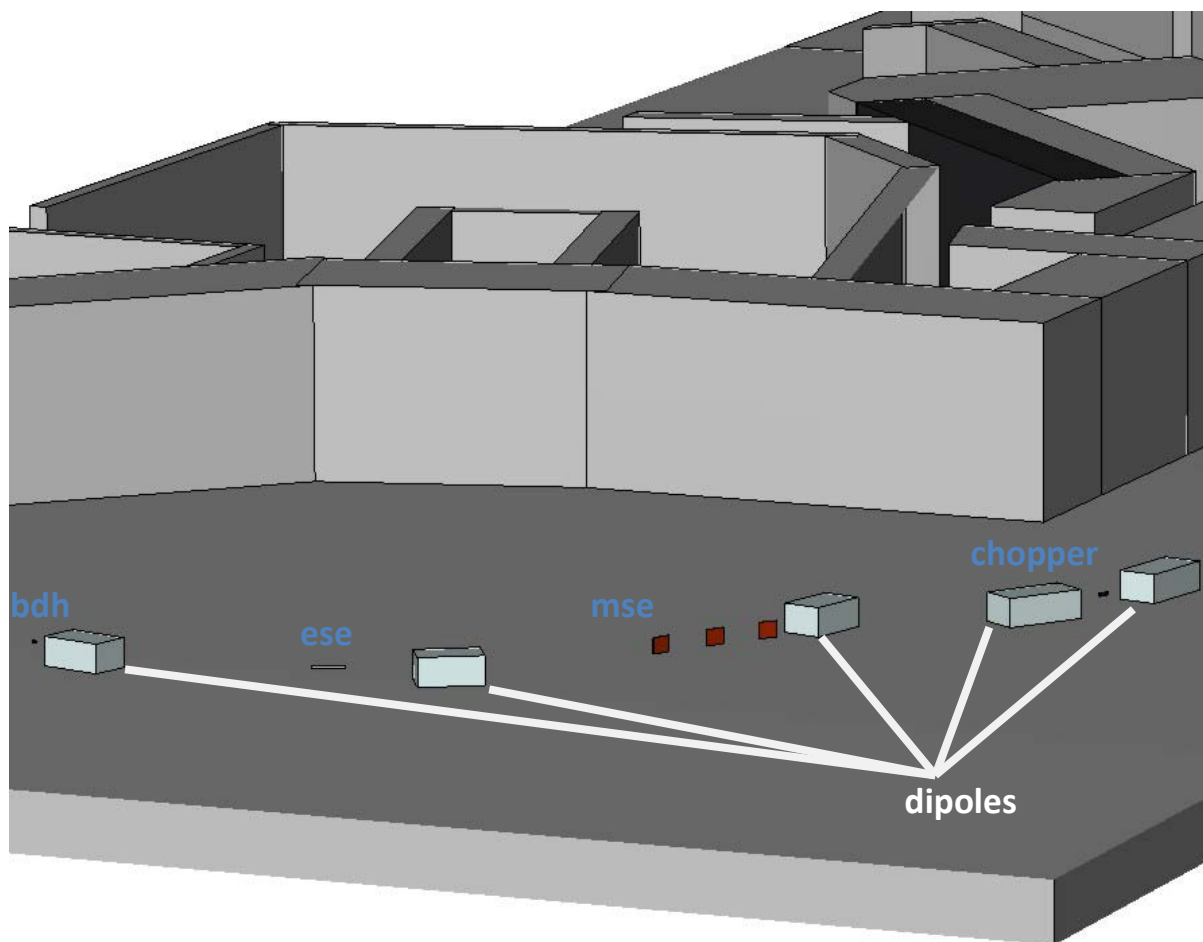


Figure 20: Side view of the synchrotron hall with representations of loss points and some dipoles, represented by iron blocks in light grey. Grey areas are made of concrete, dark grey means heavy concrete which has double density of normal concrete. The ceiling was made transparent for a better view.

HORIZONTAL BEAM DUMP (BDH)

The horizontal beam dump is an 8 cm long tungsten block vertically centred at beam height with a cross section in beam direction of $6 \times 6 \text{ cm}^2$. The beam is set to start about 1 cm in front of the target, parallel to the edges, but at a distance of only 5 mm from the side facing the synchrotron centre. In the final design of the machine, the beam will be moved slightly horizontally out of its usual path to hit the tungsten block, so 5 mm is a conservative estimation, considering that the only machine part that can shield scattered particles in the vicinity is a dipole block, which is essentially an iron block further down the beam path, centred at beam height and measuring 72 cm height, 160 cm width and 100 cm length. These generic dipole resembling blocks are also used with the following loss points.

ELECTROSTATIC SEPTUM (ESE)

The original molybdenum foil used for splitting the beam in half by adding an electrostatic field is only about 0.1 mm thick. However, due to the fact that by hitting the foil on its edge and shooting along its axis with a pencil beam, it cannot be made sure, because of the scattering of particles that would normally be guided back into the beam path and return for interaction after another few rounds, that all beam particles are “lost” by interacting with the foil. Therefore the foil was made thicker in the simulation to make enough space for the beam to interact with it.

The foil used in the simulation is 1 cm wide (“thick”), 7.40 cm high and 80 cm long. Higher self shielding caused by the greater thickness of the foil is countered by the fact that any other shielding around the foil except for a dipole along the further beam path is left out.

MAGNETIC SEPTUM (MSE)

The design of the magnetic extraction septum is made of several parts. Three rectangular copper coils are set along the extraction path to take on a split beam and move the bunches further apart. Only the part of the coil placed in the middle of the split beam is implemented for the first coil, which is represented by a 48 cm long, 40 cm high and 1 cm wide copper plate. Also all losses at the mse are simulated to happen on the first coil. To put at least a minimum of shielding elements in the vicinity of the loss point, the other 2 coils of the extraction septum are represented by similar copper plates that are double as thick (2 cm), and also a dipole is placed along the further beam path.

CHOPPER DUMP

The chopper dump is represented by a tungsten block similar to the horizontal beam dump, but with a length of 30 cm instead of 8 cm. In the simulation, the beam hits the block also similar to the bdh along its axis, but about 1 cm away from its side wall instead of 5 mm. The most remarkable differences are 2 dipoles in the direct vicinity, shielding any directly forward- and backscattered secondary particles, although there are not many that make it through the 30 cm long tungsten block. In the plans for the accelerator components, these two extraction line dipoles differ slightly in length from their counterparts used inside the synchrotron ring, so the length of the generic iron blocks in the geometry is adjusted to 205 cm.

BEAM DUMP (HEBT)

The high energy beam dump has the most sophisticated and realistic design of all the implemented loss points, as the design this part of the beam line was already described in detail for the UVP. [4]

The 2 m wide, 2.10 m long and 2.50 m high beam absorber is pictured in Figure 21 with measurements displayed in Figure 22. Inside a concrete shell lies an iron block, centred at beam height, with a length of 100 cm and a surface facing the beam of $80 \times 80 \text{ cm}^2$. At the beam entrance point, the iron block features a 30 cm long carbon cylinder with a diameter of 10 cm directed along the beam for attenuation of backscattered secondary particles.

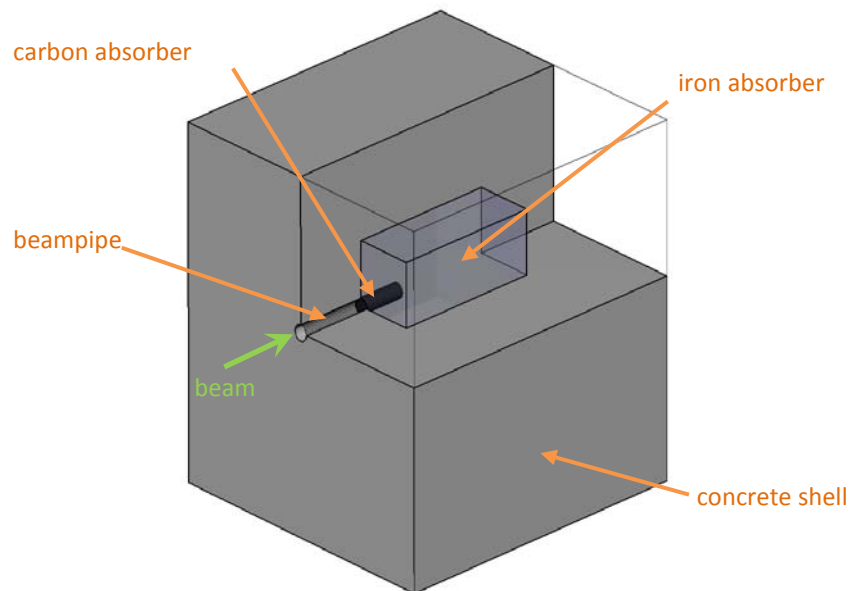


Figure 21: Sketch of the beam dump at the end of the High Energy Beam Transfer line

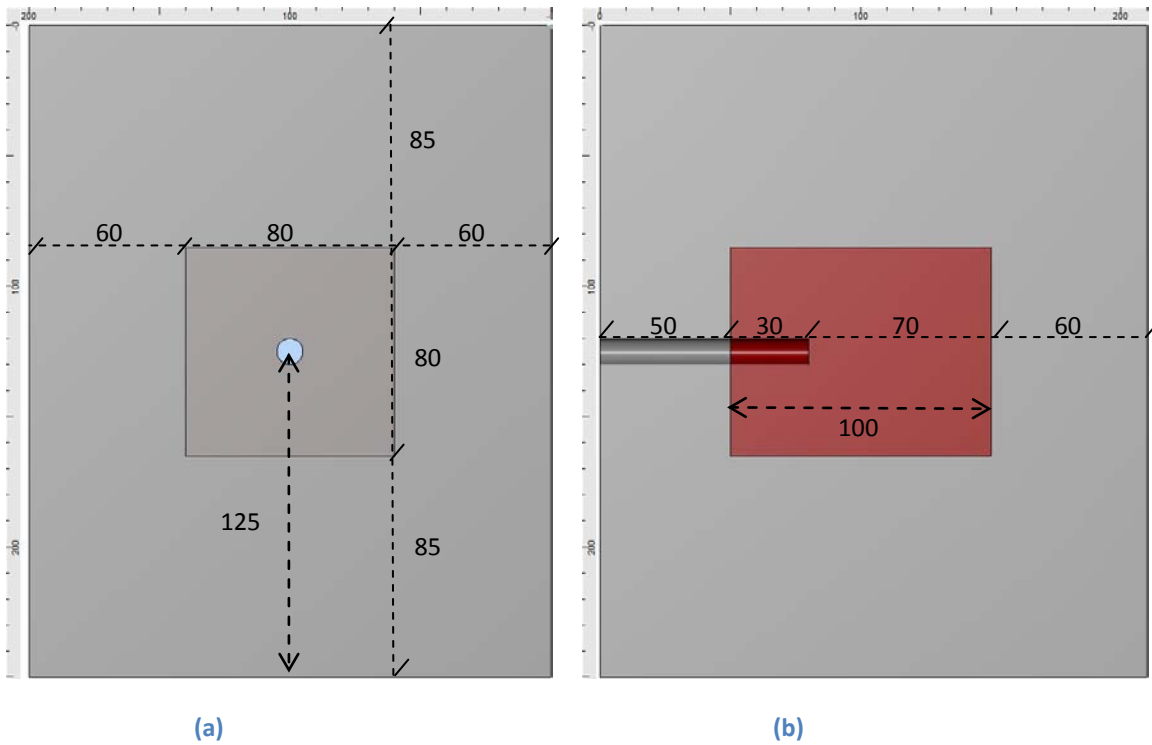


Figure 22: Front view of the beam dump in beam direction (a) and cut view from the side in the beam plane (b), with measurements in cm. Grey areas are made of concrete, red areas of iron, dark red stands for carbon, light blue marks air inside the entrance pipe

Situated at the end of the HEBT, its back wall is placed at a distance of 820 cm from the inner wall of the hall, and its centre is located 435 cm away from the wall to the Gantry room as well as 5 m away from the wall on the other side.

PARTICLE TRANSPORT THRESHOLDS

The lower threshold for particle transport of hadrons was set to 0.1 MeV for all hadrons except neutrons which were followed down to thermal energies.

EMF (ElectroMagneticFLUKA), a FLUKA function that enables the transport of electrons, positrons and photons, was turned OFF to significantly save CPU time. Omitting the electromagnetic showers has almost no effect on the measurement of air activation, due to the fact that only hadrons, neutrons, positive and negative pions are used to calculate air activation by folding fluences with cross sections.

SCORING APPROACH

The beam is usually started on a horizontal plane lying 125 cm above the floor level of the main part of the facility, which is referred to as “beam height” in the descriptions. The horizontal beam scenario in IR4 also has a beam starting on this plane, but above a lowered floor. During vertical irradiation scenarios, the base of the target cylinders that is hit by the beam also lies at beam height, meaning exactly 125 cm above floor level.

The volumes of the different USRTRACK detectors were calculated with a quasi Monte-Carlo method provided by SimpleGeo 4.1 and then filled in the correspondent space in the respective cards, so results were given as per cm³.

For illustrating purposes, X-Y-Z **USBIN** detectors using particle 201 (FLUKA/FLAIR: ALL-PART) for scoring the fluence of all particles are placed inside the MedAustron geometry. Bin sizes vary between 50x50x50 cm³ for general overviews inside the treatment rooms and the synchrotron hall, down to 0.5x0.5x0.5 cm³ to indicate finer details on smaller structures, for example points of beam impacts at loss points in the synchrotron hall.

RADIOLOGICAL EXPOSURE OF THE ENVIRONMENT THROUGH MEDAUSTRON

In order to conservatively estimate the environmental exposure caused by irradiation in one of the treatment rooms, calculations based on yield results from the simulations have been made. Assuming that every produced nuclide has, due to ventilation design, at least one full hour to decay before leaving the facility, activities have been calculated directly by multiplying yield with their respective decay constants without incorporating decay during a given irradiation time. Also, the activated isotopes from the treatment rooms will be diluted into the air of the synchrotron room before being able to leave the facility. For the calculations, it was assumed that 14.000 m³ of air per hour will be released to the environment, which is also the volume that activated air will be diluted in.

The specific activities of the radionuclides emitted from the MedAustron facility are calculated with formula (2)

$$A_i(t_{cool}) = \frac{P_i I}{V} e^{-\lambda_i t_{cool}} \quad (2)$$

$A_i(t_{cool})$ specific activity of radionuclide i that is released into the environment after a defined cooling time t_{cool}

P_i ... total activity of isotope i produced in air by a proton respectively a carbon ion

t_{cool} ... cooling time between isotope production and release into the environment

I ... intensity of proton / carbon ion beam per hour

V ... Volume containing the produced radioactivity

In addition to the yearly averaged values for air activation, also the respective peak values, reached through short term irradiation with the maximum of the available intensity are being calculated.

The calculation of specific air activation ($\text{Bq}/(\text{m}^3)$) released per hour into the environment is based on the following scheduled beam intensities per year listed in Table 11 and Table 12, as well as the maximum available intensities that the machine is capable of providing. Abbreviations for the different types of beams will be used:

p800 ... proton beam with 800 MeV

p250 ... proton beam with 250 MeV

i400 ... C12 ion beam with 400 MeV per nucleon

The **maximum available intensities** per second, that the accelerator at MedAustron can provide, are

- 2E+10 protons per second at 800 MeV per proton
- 1E+9 ions per second at 400 MeV per nucleon
- 2E+10 protons per second at 250 MeV per proton

Intensities per second, listed in the following tables, are calculated by dividing the scheduled intensity per year by 365/24/3600, aiming for an average distribution of irradiation procedures over the course of a year.

Table 11: Intensities per beam type per year listed for the four irradiation rooms on the left hand side, with values divided by 365/24/3600 on the right hand side representing average intensities per second over the course of a year

Intensities of IR1-4 per year			
	p800	i400	p250
IR1	1.80E+16	7.80E+14	7.80E+15
IR2		4.70E+14	
IR3		4.70E+14	
IR4			6.70E+15

Intensities of IR1-4 per second			
	p800	i400	p250
IR1	5.71E+08	2.47E+07	2.47E+08
IR2		1.49E+07	
IR3		1.49E+07	
IR4			2.12E+08

Table 12 lists the beam loss intensities expected for each designated loss point in the synchrotron hall. The chopper dump is not expected to be hit by protons with an energy of 800 MeV. **Bdump** is an abbreviation for the beam dump installed at the end of the HEBT.

Table 12: Intensities per beam type per year listed for each designated loss point in the synchrotron hall on the left hand side, with values divided by 365/24/3600 on the right hand side representing average intensities per second over the course of a year

Int. at loss points per year			
	p800	i400	p250
chopper		1.90E+14	1.60E+15
mse	2.90E+14	3.00E+13	2.50E+14
ese	2.90E+14	3.00E+13	2.50E+14
bdh	2.40E+14	1.80E+14	1.50E+15
Bdump	4.90E+14	2.10E+13	2.10E+14

Int. at loss points per second			
	p800	i400	p250
chopper		6.02E+06	5.07E+07
mse	9.20E+06	9.51E+05	7.93E+06
ese	9.20E+06	9.51E+05	7.93E+06
bdh	7.61E+06	5.71E+06	4.76E+07
Bdump	1.55E+07	6.66E+05	6.66E+06

The effect of losses along the high energy beam transfer line (HEBT) concerning the activation of air will be less than 1% compared to the estimated losses in the synchrotron hall, due to their lower intensity, which is a factor 100 smaller than the intensities of the loss points in the synchrotron hall. [5] No simulation are conducted concerning these points along the HEBT. The beam dump at the end of the HEBT is expected to see higher intensities and is therefore included in the simulations.

Not all isotopes that appear in the results of the simulations due to the high beam energy inside the MedAustron facility are covered by the documentation of clearance levels in Austrian law (Anhang 6, Tabelle 1 allgemeine Strahlenschutzverordnung). [19]

In order to be able to give a conservative estimation of radiation exposure of the environment, an evaluation of the Ci values of isotopes in question is performed, using the following guidelines:

To determine an appropriate Ci value for an isotope in question, a reference isotope is used that shares chemical attributes, and provides a reference Ci value to base further estimations on. For isotopes of oxygen, sodium, magnesium, sulfur and chloride, reference isotopes of the same element have been used, which guarantee the same biological half-life in the human body. Present isotopes of neon, aluminum, phosphorus and potassium were not as easy to compare.

Ne-23 and Ne-24 are compared to the known Ci value of Argon 41, while using the biological half live assigned to radon, lacking reliable sources for neon and argon. To aluminum, oxygen in form of O-15 was assigned as reference isotope, mainly because physical half-lives of the isotopes are similar and no isotope with a known Ci value and similar chemical properties could be found. Up to this time, no biological function has been attributed to this metal, and, more importantly, aluminum accumulation in tissues and organs result in their dysfunction and toxicity. Biological half-life of aluminum is based on its half-life in the human brain, which is assumed to be 7 years [11], or in other words the conservative choice, since accumulation in the human body would lead to no contribution to the effective half-life of the isotope. Nitrogen serves as reference for phosphorus, and sodium as reference for potassium, since their respective references are in the same element group of the periodic table and therefore show similar chemical properties.

All other biological half-lives were taken from [10].

The effective half-life of an isotope then follows the formula (3).

$$\frac{1}{T_{effective}} = \frac{1}{T_{physical}} + \frac{1}{T_{biological}} \quad (3)$$

This also means that, considering the rather short physical half-lives of the isotopes missing Ci values, the rather long but hard to determine biological half-lives of elements do not have a very strong influence on the effective half-life of the isotope. One exception here are the biological half-lives of the noble gases neon and argon, which were conservatively assumed to have a half-life of 30 minutes, taking into account that many sources point to a biological half-life between 30-70 minutes of the radioactive noble gas radon. [9] This is due to the fact that noble gases diffuse well in liquids and therefore enter and exit the bloodstream continuously through the pulmonary alveoli without giving in to any chemical reaction.

If there is a selection of various isotopes available for reference, an isotope with the most similarities considering radiation characteristics is chosen. To evaluate these similarities, the Q-value of decays as well as the average beta energy (\bar{E}_{Beta}) of emitted positrons or electrons is considered.

After choosing an appropriate reference isotope (*Iso1*), the Ci value of the isotope in question (*Iso2*) is calculated with the following formula (4):

$$C_i(Iso_2) = C_i(Iso_1) \times \frac{1}{\frac{T_{1/2 \text{ effective}}(Iso_2)}{T_{1/2 \text{ effective}}(Iso_1)} \times \text{Max} \left[\frac{Q - \text{value}(Iso_2)}{Q - \text{value}(Iso_1)}, \frac{\bar{E}_{\text{Beta}}(Iso_2)}{\bar{E}_{\text{Beta}}(Iso_1)} \right]}$$

(4)

The data of isotopes used for the calculation of the Ci values is summarized in Table 13, whereas the actual results of the calculation together with the values given by Austrian law form the complete list of Ci values in Table 14, which are the base values for all conducted calculations in the following chapters concerning Ci values and committed dose rates.

The Q-value Q_v used in formula (3) above is the energy released by a nuclear reaction, defined in terms of the rest masses m_i of the participants. Assuming a nuclear reaction $m_1+m_2 \Rightarrow m_3+m_4$, Q_v is given by formula (5) :

$$Q_v = [(m_1+m_2) - (m_3+m_4)]c^2$$

(5)

This Q_v is positive for exothermal and negative for endothermal reactions. [12]

This list of limit values also includes radio nuclides that are contributing to the received dose by immersion (e.g. Ar-41) or ingestion. Although the calculated committed dose rates for these isotopes in closed spaces can be considered too high for most cases, they were still used to conservatively cover all conceivable scenarios. Also, these values are to be applied to the general population, and not to occupationally radiation-exposed personnel.

Table 13: Data of isotopes used for the calculation of Ci values not mentioned by Austrian law. Effective half time ($t_{1/2 \text{ eff}}$) is calculated via formula (3) using the physical and biological half times of the isotopes.

Isotope	$t_{1/2 \text{ ph}}$ [s]	$t_{1/2 \text{ bio}}$ [s]	$t_{1/2 \text{ eff}}$ [s]	av. β Energy [keV]	Q-value [keV]
H-3	3.89E+08				
Be-7	4.61E+06				
Be-10	5.05E+13				
C-11	1.22E+03				
C-14	1.81E+11				
N-13	5.98E+02	9.98E+07	597.90	492.1	2220.49
O-14	70.606	7.78E+06	70.61	777.4	5143.04
O-15	1.22E+02	7.78E+06	122.24	735.28	2754.05
O-19	26.91	7.78E+06	26.91	1743.2	4821
F-18	6.59E+03				
Ne-23	37.24	1.80E+03	36.49	1903.4	4375.84
Ne-24	202.8	1.80E+03	182.26	804.6	2470
Na-22	8.21E+07	9.50E+05	939517.86	194.9	2842.2
Na-24	5.39E+04	9.50E+05	50964.60	556.2	5515.78
Na-25	59.1	9.50E+05	59.10	1506.9	3835.3
Mg-27	567.48	1.56E+09	567.48	703.4	2610.33
Mg-28	7.53E+04	1.56E+09	75272.36	153.2	1831.8
Al-26	2.26E+13				
Al-28	134.484	2.21E+08	134.48	1243.2	4642.24
Al-29	393.6	2.21E+08	393.60	978	3679.5
Si-31	9.44E+03				
Si-32	5.46E+09				
P-30	149.88	9.98E+07	149.88	1439.3	4232.3
P-32	1.23E+06				
P-33	2.19E+06				
P-35	47.3	9.98E+07	47.30	1024.1	3988.8
S-35	7.54E+06	7.78E+06	3828791.88	49	167.14
S-37	303	7.78E+06	302.99	801.9	4865.3
S-38	10320	7.78E+06	10306.32	490	2937
Cl-34	1920	2.51E+06	1918.53	418	5491.28
Cl-36	9.46E+12	2.51E+06	2505599.34	247	708
Cl-38	2.23E+03				
Cl-39	3.34E+03				
Cl-40	81	2.51E+06	81.00	1547.8	7482
Ar-37	3.03E+06				
Ar-39	8.49E+09				
Ar-41	6.56E+03	1.80E+03	1412.46	465.3	2491.61
K-38	458.16	9.50E+05	457.94	1205.3	5713.1
K-40	4.027E+16	9.50E+05	950400.00	615.7	1311.09

Table 14: Law-defined Ci values and calculated Ci values for isotopes not mentioned by Austrian law. Calculation was done using formula (4) with a reference isotope that should resemble the chemical properties, and therefore the behavior in the human body of the isotope in question.

Isotope	t 1/2 eff [s]	Ci a.StSV	reference Isotope	Ci (defined and calculated)
H-3		100		100
Be-7		600		600
Be-10		1		1
C-11		600		600
C-14		6		6
N-13	5.98E+02	2000		2000
O-14	7.06E+01		O-15	927.09
O-15	1.22E+02	1000		1000
O-19	2.69E+01		O-15	1916.02
F-18		500		500
Ne-23	3.65E+01		Ar-41	1892.75
Ne-24	1.82E+02		Ar-41	896.31
Na-22	9.40E+05	1		1
Na-24	5.10E+04	90		90
Na-25	5.91E+01		Na-24	28648.19
Mg-27	5.67E+02		Mg-28	577.79
Mg-28	7.53E+04	20		20
Al-26		0.5		0.5
Al-28	1.34E+02		O-15	537.59
Al-29	3.94E+02		O-15	232.45
Si-31		300		300
Si-32		0.32		0.32
P-30	1.50E+02		N-13	2727.82
P-32		1		1
P-33		20		20
P-35	4.73E+01		N-13	12148.03
S-35	3.83E+06	20		20
S-37	3.03E+02		S-35	8682.34
S-38	1.03E+04		S-35	422.83
Cl-34	1.92E+03		Cl-36	16.84
Cl-36	2.51E+06	0.1		0.1
Cl-38		500		500
Cl-39		600		600
Cl-40	8.10E+01		Cl-36	292.72
Ar-37		2.00E+08		200000000
Ar-39		6000		6000
Ar-41	1.41E+03	200		200
K-38	4.58E+02		Na-24	4622.10
K-40	9.50E+05		Na-22	0.31

CALCULATION OF ACCUMULATED COMMITTED DOSE RATE THROUGH DIRECT PRESENCE IN THE RADIOACTIVE AIR ENVIRONMENT OF THE TREATMENT ROOMS

To calculate the accumulated committed dose rate through exposure to radioactive air, the following parameters are considered:

1. production of airborne radioactivity per proton, respectively carbon ion computed for every room
2. beam intensity, duration of irradiation and cooling time before access
3. volume of the rooms
4. air exchange rate of the rooms
5. conversion factor from specific airborne radioactivity (Bq/m³) into accumulated committed dose per hour (Table 15)

With the help of formulas (1) and (2), the specific air activation after irradiation plus cooling time can be calculated through formula (6):

$$A_i(t_{irr} + t_{cool}) = \frac{P_i I}{V} (1 - e^{-\lambda_i t_{irr}}) e^{-\lambda_i t_{cool}} \quad (6)$$

P_i ... produced total activity of isotope i in air per proton respectively carbon ion

t_{irr} ... duration of irradiation

T_{cool} ... cooling time

I ... protons / carbon ions per second

V ... volume of the room

To calculate the accumulated committed dose, the conversion factor (Table 15) has to be used on all computed isotopes. The sum of all individual contributions from isotopes yields the overall accumulated committed dose per hour received through exposure to radioactive air.

Formula (6) does not take into account air exchange through ventilation. The air exchange rate will be factored in by considering the average duration of stay of air molecules.

The graph showing the decay of the committed dose rate adds up the single sums of the activity concentrations of every nuclide after converting them into committed dose rates via conversion factors. According to formula (7)

$$A_{(t)} = A_0 * 2^{-\frac{t}{t_{1/2}}} \quad (7)$$

t ...time [s]

A(t) ...activity at time t [Bq]

A₀ ...initial activity [Bq]

t_{1/2} ...half-life period [s]

the activity of every measured nuclide is calculated for a decay time of 24 hours, in intervals of 1 minute (1440 intervals). Subsequently the single activities are converted via formula (10) into [μSv/h] via manually determined conversion coefficients emerging from Ci values given by Austrian radiation protection law as well as estimated ones given in Table 15, and added up to give a committed dose rate value.

In order to calculate the integral dose over the course of a day, a simple trapezoidal rule shown in formula (8) was applied to the dose rate values, meaning the **SUMMATION** over the subareas Q, which stand for the 1 minute intervals

$$Q(f) = \frac{b - a}{2} (f(a) + f(b)). \quad (8)$$

where a, b indicate consecutive points, in this case time indices, on the abscissa, and f(a, b) their respective committed dose rate values on the ordinate.

CALCULATION OF CONVERSION FACTORS OF ACTIVITY INTO COMMITTED DOSE RATES

In order to calculate the exposure to radiation of a person residing in radioactive air, the legal limits for unrestricted release of air into the environment, i.e. the C_i values listed in *allgemeine Strahlenschutzverordnung (StSV) Anlage 12, Tabelle 1*, are consulted. This list of limit values also includes radio nuclides that are contributing to the received dose by immersion (e.g. Ar-41) or ingestion. Although the calculated committed dose rates for these isotopes in closed spaces can be considered too high for most cases, they were still used to conservatively cover all conceivable scenarios. Also, these values are to be applied to the general population, and not to occupationally radiation-exposed personnel.

According to the StSV, it can be assumed that the yearly committed dose of a single person residing in undiluted radioactive air is not exceeding 300 μSv , if C_i limits are observed. Hence formula (9) can be used to calculate the maximum exposure per hour and per radioisotope that results from a stay in an atmosphere with a radionuclide concentration yielding 1 Bq/m^3 .

$$\frac{\text{committed dose rate}}{\text{specific air activation}} \text{ as } \frac{\left(\frac{\mu\text{Sv}}{\text{h}}\right)}{\left(\frac{\text{Bq}}{\text{m}^3}\right)} = \frac{\frac{300}{(24 \times 365)}}{C_i} \quad (9)$$

The conversion factors resulting from filling C_i values into formula (9) in Table 15 are further used to calculate the radiation exposure of personnel who are staying in radioactive air with a given radionuclide content. This is done by including them in formula (10), where the committed dose rate that a person gets is calculated by summing up the converted activities for each isotope at the specified cooling time.

$$\dot{D}(t_{cool}) = \sum_k \frac{dA_k(t_{cool})}{dV} \frac{300}{(24 \times 365) C_{i_k}} \quad (10)$$

The conversion factors are considered conservative and incorporate not only the committed dose through inhalation but also through immersion and ingestion.

Table 15: List of legal limits for unrestricted release into the environment (Ci values) and committed dose rate conversion factors calculated by formula (9) in $[(\mu\text{Sv/h})/(\text{Bq/m}^3)]$ for each relevant isotope.

Isotope	Ci [Bq/m ³]	($\mu\text{Sv/h})/(\text{Bq/m}^3)$
H-3	100.00	3.425E-04
Be-7	600.00	5.708E-05
Be-10	1.00	3.425E-02
C-11	600.00	5.708E-05
C-14	6.00	5.708E-03
N-13	2000.00	1.712E-05
O-14	927.09	3.694E-05
O-15	1000.00	3.425E-05
O-19	1916.02	1.787E-05
F-18	500.00	6.849E-05
Ne-23	1892.75	1.809E-05
Ne-24	896.31	3.821E-05
Na-22	1.00	3.425E-02
Na-24	90.00	3.805E-04
Na-25	28648.19	1.195E-06
Mg-27	577.79	5.927E-05
Mg-28	20.00	1.712E-03
Al-26	0.50	6.849E-02
Al-28	537.59	6.370E-05
Al-29	232.45	1.473E-04

Isotope	Ci [Bq/m ³]	($\mu\text{Sv/h})/(\text{Bq/m}^3)$
Si-31	300.00	1.142E-04
Si-32	0.32	1.070E-01
P-30	2727.82	1.255E-05
P-32	1.00	3.425E-02
P-33	20.00	1.712E-03
P-35	12148.03	2.819E-06
S-35	20.00	1.712E-03
S-37	8682.34	3.944E-06
S-38	422.83	8.099E-05
Cl-34	16.84	2.034E-03
Cl-36	0.10	3.425E-01
Cl-38	500.00	6.849E-05
Cl-39	600.00	5.708E-05
Cl-40	292.72	1.170E-04
Ar-37	200000000.00	1.712E-10
Ar-39	6000.00	5.708E-06
Ar-41	200.00	1.712E-04
K-38	4622.10	7.409E-06
K-40	0.31	1.094E-01

RESULTS

IRRADIATION ROOM 1 (IR1)

800 MEV PROTON BEAM

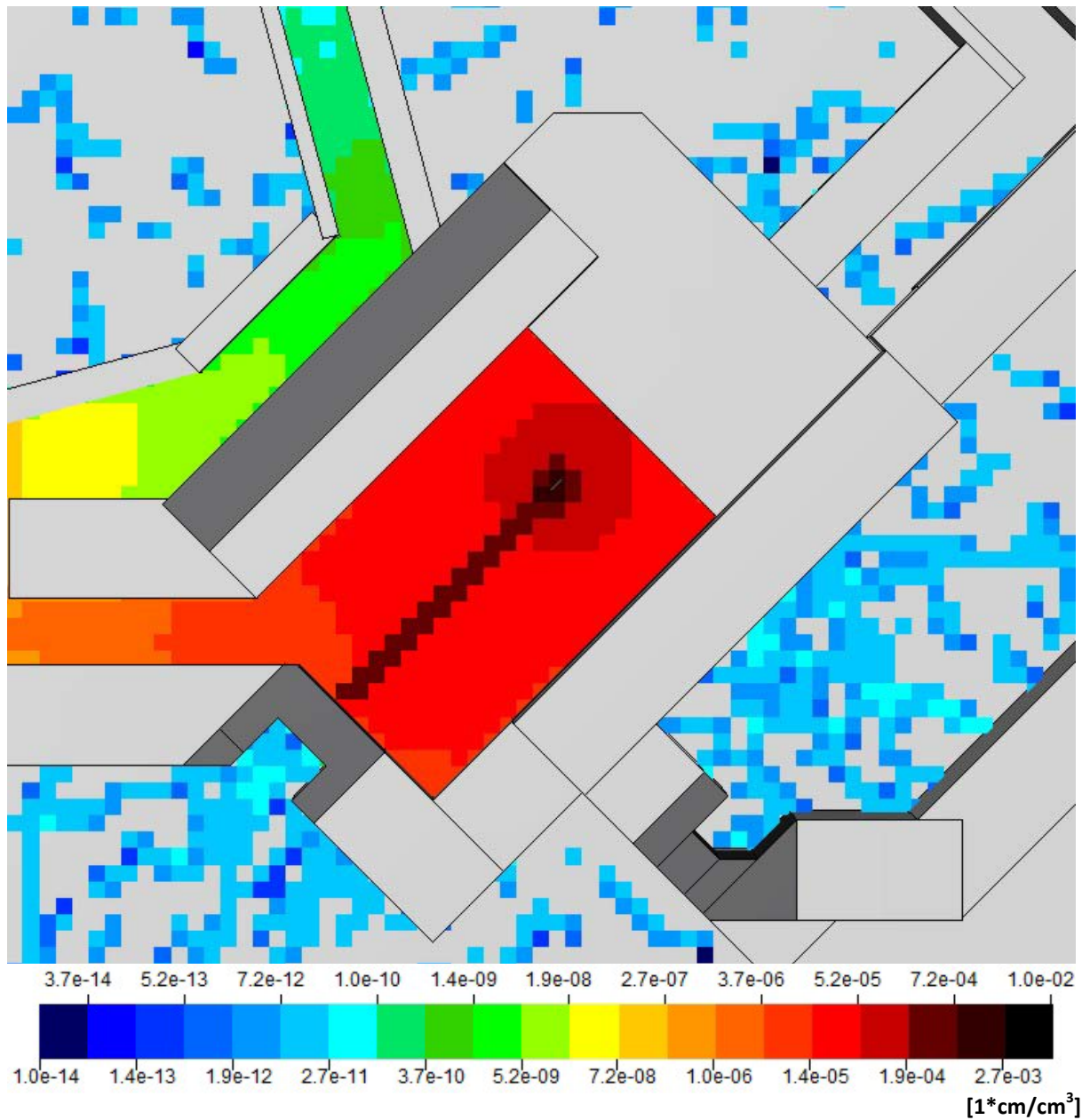


Figure 23: Fluence per primary particle of all particles in the treatment room 1 on beam height, when a horizontal proton beam with 800 MeV hits the lead target, viewed from above

DIRECT RELEASE SCENARIO

Because this is an irradiation room destined for conducting experiments on a range of different targets, an absolute worst case scenario is brought up to simulate the impact of possible experimental setups on air activation in this room. As can be seen in Figure 23 in a top down view of the USBIN scoring fluence at beam height, the 800 MeV proton beam starts directly at the wall where the opening for the beam pipe is to be expected, and hits a lead cylinder with a diameter of 5 cm at the far side of the room, so air activation by the main beam itself as well as by secondary particles created by hitting a heavy target are taken into this conservative estimation.

An example of tables showing the values for each isotope the simulation produced with a maximum intensity of $2E+10$ protons per second (Table 16), as well as the comparisons with Ci values (Table 17) follow to outline the routine of calculating sum values. Subsequent tables for all other performed simulations will be listed in the appendix, only the sum values will be listed in their respective chapters.

In this scenario, isotopes are produced constantly for a direct release into the environment, respectively a release incorporating a cooling time that is equally applied to each produced isotope. Each cooling time stands for an amount of time that every isotope would get for decay from the moment of production until its release.

Table 16 lists from left to right: Name and mass number of the isotope created by folding fluences from the simulation with cross sections via the `airactiv5-260` executable, physical half live of the isotope, yield per primary particle per cm^3 (the direct result given by the executable), the relative error of the folding results (which is usually very low, because the cross sections in the executable are provided with an already very low error), and the calculated activity in Bq/m^3 in the air of the room after cooling times of 0 seconds, 1 minute, 10 minutes, 3600/3.1 seconds (which corresponds to the 3.1 full air exchanges foreseen for this irradiation room), and 1 hour.

All results in Table 16 and Table 17 were calculated based on irradiation with a total intensity of $2.32E+13$ protons, corresponding to an irradiation time of 1161.29 seconds with an intensity of $2E+10$ protons per second, with an 800 MeV proton beam impinging on a 50 cm long lead cylinder with a diameter of 5 cm. By using the actual volume of the room, which is $515 m^3$ for specific air activation calculations, this corresponds to a total air volume of 1545 m^3 being released from the room per hour, respectively $515 m^3$ per 1161.29 seconds, during continuous irradiation with maximum intensity.

Table 17 lists from left to right: The isotopes with mass number, their respective physical half-lives, the correspondent Ci values including the estimated ones underlined in blue, and the comparison value resulting from dividing the activation values after several cooling times from Table 16 by their respective Ci values.

Table 16: Yield results (per primary particle per cm³) and relative errors, as well as specific activities (in Bq/m³) for each isotope after several cooling times (in seconds) after irradiation with a total intensity of 2.32E+13 protons, which corresponds to 3.1 air exchanges per hour during continuous irradiation with an 800 MeV proton beam and an intensity of 2E+10 protons per second

Isotope	t 1/2 [s]	yield/pp/cm ³	rel.err.	0s	60s	600s	1191.29s	3600s
H-3	3.89E+08	2.54E-12	0.01%	1.05E-01	1.05E-01	1.05E-01	1.05E-01	1.05E-01
Be-7	4.61E+06	8.55E-13	0.00%	2.99E+00	2.99E+00	2.99E+00	2.99E+00	2.99E+00
Be-10	5.05E+13	4.74E-13	0.01%	1.51E-07	1.51E-07	1.51E-07	1.51E-07	1.51E-07
C-11	1.22E+03	1.13E-12	0.01%	1.49E+04	1.44E+04	1.06E+04	7.70E+03	1.93E+03
C-14	1.81E+11	5.00E-10	0.02%	4.45E-02	4.45E-02	4.45E-02	4.45E-02	4.45E-02
N-13	5.98E+02	1.79E-12	0.01%	4.82E+04	4.50E+04	2.40E+04	1.25E+04	7.42E+02
O-14	7.10E+01	1.14E-13	0.02%	2.58E+04	1.44E+04	7.39E+01	3.08E-01	1.41E-11
O-15	1.22E+02	1.45E-12	0.00%	1.91E+05	1.36E+05	6.36E+03	2.64E+02	2.60E-04
O-19	2.71E+01	1.53E-16	0.00%	9.09E+01	1.96E+01	1.97E-05	1.14E-11	9.32E-39
F-18	6.59E+03	4.21E-15	0.00%	1.03E+01	1.02E+01	9.66E+00	9.11E+00	7.05E+00
Ne-23	2.80E+01	3.94E-16	0.00%	2.27E+02	5.13E+01	8.03E-05	7.41E-11	4.48E-37
Ne-24	2.03E+02	8.23E-17	0.00%	6.53E+00	5.32E+00	8.40E-01	1.23E-01	2.96E-05
Na-22	8.21E+07	1.14E-15	0.00%	2.24E-04	2.24E-04	2.24E-04	2.24E-04	2.23E-04
Na-24	5.40E+04	1.79E-15	0.00%	5.34E-01	5.33E-01	5.30E-01	5.26E-01	5.10E-01
Na-25	6.00E+01	7.03E-16	0.00%	1.89E+02	9.43E+01	1.84E-01	2.81E-04	1.64E-16
Mg-27	5.70E+02	1.02E-15	0.00%	2.88E+01	2.68E+01	1.39E+01	7.02E+00	3.62E-01
Mg-28	7.53E+04	3.03E-16	0.00%	6.48E-02	6.48E-02	6.44E-02	6.41E-02	6.27E-02
Al-26	2.26E+13	1.44E-15	0.00%	1.03E-09	1.03E-09	1.03E-09	1.03E-09	1.03E-09
Al-28	1.34E+02	3.30E-15	0.00%	3.95E+02	2.90E+02	1.79E+01	9.90E-01	3.42E-06
Al-29	3.96E+02	1.83E-15	0.00%	7.44E+01	6.70E+01	2.60E+01	9.74E+00	1.36E-01
Si-31	9.44E+03	1.94E-15	0.00%	3.31E+00	3.29E+00	3.17E+00	3.04E+00	2.54E+00
Si-32	5.46E+09	1.02E-15	0.00%	3.01E-06	3.01E-06	3.01E-06	3.01E-06	3.01E-06
P-30	1.50E+02	1.07E-15	0.00%	1.15E+02	8.71E+01	7.17E+00	5.36E-01	6.80E-06
P-32	1.23E+06	1.10E-14	0.00%	1.43E-01	1.43E-01	1.43E-01	1.43E-01	1.43E-01
P-33	2.19E+06	7.74E-15	0.00%	5.68E-02	5.68E-02	5.68E-02	5.68E-02	5.67E-02
P-35	4.74E+01	8.69E-16	0.00%	2.95E+02	1.23E+02	4.57E-02	1.24E-05	4.05E-21
S-35	7.55E+06	9.91E-15	0.00%	2.11E-02	2.11E-02	2.11E-02	2.11E-02	2.11E-02
S-37	3.04E+02	4.40E-15	0.02%	2.33E+02	2.03E+02	5.93E+01	1.65E+01	6.29E-02
S-38	1.03E+04	2.12E-15	0.00%	3.30E+00	3.29E+00	3.17E+00	3.06E+00	2.59E+00
Cl-34	1.92E+03	4.72E-16	0.00%	3.96E+00	3.87E+00	3.19E+00	2.60E+00	1.08E+00
Cl-36	9.50E+12	2.49E-14	0.01%	4.22E-08	4.22E-08	4.22E-08	4.22E-08	4.22E-08
Cl-38	2.23E+03	1.72E-14	0.01%	1.24E+02	1.22E+02	1.03E+02	8.65E+01	4.06E+01
Cl-39	3.34E+03	3.47E-14	0.01%	1.67E+02	1.65E+02	1.48E+02	1.32E+02	7.93E+01
Cl-40	8.40E+01	3.46E-15	0.02%	6.63E+02	4.04E+02	4.69E+00	4.57E-02	8.32E-11
Ar-37	3.03E+06	4.43E-14	0.01%	2.36E-01	2.36E-01	2.36E-01	2.36E-01	2.36E-01
Ar-39	8.49E+09	1.26E-13	0.02%	2.39E-04	2.39E-04	2.39E-04	2.39E-04	2.39E-04
Ar-41	6.58E+03	1.04E-12	0.02%	2.55E+03	2.53E+03	2.39E+03	2.25E+03	1.74E+03
K-38	4.58E+02	3.09E-16	0.02%	1.09E+01	9.92E+00	4.38E+00	1.87E+00	4.68E-02
K-40	4.04E+16	8.56E-16	0.06%	3.41E-13	3.41E-13	3.41E-13	3.41E-13	3.41E-13

Table 17: Ci values for the isotopes gained by the simulation as well as the comparison of activities after several cooling times (0s, 60s, 600s, 1161.29s, 3600s), after irradiation with a total intensity of 2.32E+13 protons, which corresponds to 3.1 air exchanges per hour during continuous irradiation with an 800 MeV proton beam and an intensity of 2E+10 protons per second, to their respective Ci value. Calculated Ci values not mentioned in Austrian law are underlined in light blue. Sum values of the comparison values after the listed cooling times are listed at the bottom, underlined in dark blue.

Isotope	t 1/2 [s]	Ci	0s	60s	600s	1161.29s	3600s
H-3	3.89E+08	100.0	1.05E-03	1.05E-03	1.05E-03	1.05E-03	1.05E-03
Be-7	4.61E+06	600.0	4.98E-03	4.98E-03	4.98E-03	4.98E-03	4.98E-03
Be-10	5.05E+13	1.0	1.51E-07	1.51E-07	1.51E-07	1.51E-07	1.51E-07
C-11	1.22E+03	600.0	2.48E+01	2.40E+01	1.76E+01	1.28E+01	3.22E+00
C-14	1.81E+11	6.0	7.42E-03	7.42E-03	7.42E-03	7.42E-03	7.42E-03
N-13	5.98E+02	2000.0	2.41E+01	2.25E+01	1.20E+01	6.27E+00	3.71E-01
O-14	7.10E+01	927.1	2.79E+01	1.55E+01	7.97E-02	3.32E-04	1.52E-14
O-15	1.22E+02	1000.0	1.91E+02	1.36E+02	6.36E+00	2.64E-01	2.60E-07
O-19	2.71E+01	1916.0	4.74E-02	1.02E-02	1.03E-08	5.98E-15	4.86E-42
F-18	6.59E+03	500.0	2.06E-02	2.05E-02	1.93E-02	1.82E-02	1.41E-02
Ne-23	2.80E+01	1892.7	1.20E-01	2.71E-02	4.24E-08	3.92E-14	2.37E-40
Ne-24	2.03E+02	896.3	7.29E-03	5.94E-03	9.38E-04	1.38E-04	3.30E-08
Na-22	8.21E+07	1.0	2.24E-04	2.24E-04	2.24E-04	2.24E-04	2.23E-04
Na-24	5.40E+04	90.0	5.93E-03	5.92E-03	5.88E-03	5.84E-03	5.66E-03
Na-25	6.00E+01	28648.2	6.58E-03	3.29E-03	6.43E-06	9.82E-09	5.71E-21
Mg-27	5.70E+02	577.8	4.99E-02	4.64E-02	2.40E-02	1.21E-02	6.26E-04
Mg-28	7.53E+04	20.0	3.24E-03	3.24E-03	3.22E-03	3.21E-03	3.13E-03
Al-26	2.26E+13	0.5	2.05E-09	2.05E-09	2.05E-09	2.05E-09	2.05E-09
Al-28	1.34E+02	537.6	7.35E-01	5.40E-01	3.33E-02	1.84E-03	6.36E-09
Al-29	3.96E+02	232.5	3.20E-01	2.88E-01	1.12E-01	4.19E-02	5.87E-04
Si-31	9.44E+03	300.0	1.10E-02	1.10E-02	1.06E-02	1.01E-02	8.47E-03
Si-32	5.46E+09	0.3	9.41E-06	9.41E-06	9.41E-06	9.41E-06	9.41E-06
P-30	1.50E+02	2727.8	4.21E-02	3.19E-02	2.63E-03	1.96E-04	2.49E-09
P-32	1.23E+06	1.0	1.43E-01	1.43E-01	1.43E-01	1.43E-01	1.43E-01
P-33	2.19E+06	20.0	2.84E-03	2.84E-03	2.84E-03	2.84E-03	2.84E-03
P-35	4.74E+01	12148.0	2.43E-02	1.01E-02	3.76E-06	1.02E-09	3.33E-25
S-35	7.55E+06	20.0	1.06E-03	1.06E-03	1.06E-03	1.06E-03	1.06E-03
S-37	3.04E+02	8682.3	2.69E-02	2.34E-02	6.83E-03	1.90E-03	7.24E-06
S-38	1.03E+04	422.8	7.81E-03	7.78E-03	7.50E-03	7.23E-03	6.14E-03
Cl-34	1.92E+03	16.8	2.35E-01	2.30E-01	1.89E-01	1.55E-01	6.41E-02
Cl-36	9.50E+12	0.1	4.22E-07	4.22E-07	4.22E-07	4.22E-07	4.22E-07
Cl-38	2.23E+03	500.0	2.48E-01	2.43E-01	2.06E-01	1.73E-01	8.11E-02
Cl-39	3.34E+03	600.0	2.79E-01	2.76E-01	2.46E-01	2.19E-01	1.32E-01
Cl-40	8.40E+01	292.7	2.27E+00	1.38E+00	1.60E-02	1.56E-04	2.84E-13
Ar-37	3.03E+06	200000000.0	1.18E-09	1.18E-09	1.18E-09	1.18E-09	1.18E-09
Ar-39	8.49E+09	6000.0	3.98E-08	3.98E-08	3.98E-08	3.98E-08	3.98E-08
Ar-41	6.58E+03	200.0	1.27E+01	1.26E+01	1.19E+01	1.13E+01	8.71E+00
K-38	4.58E+02	4622.1	2.35E-03	2.15E-03	9.48E-04	4.05E-04	1.01E-05
K-40	4.04E+16	0.3	1.09E-12	1.09E-12	1.09E-12	1.09E-12	1.09E-12
Sum:			2.85E+02	2.14E+02	4.91E+01	3.14E+01	1.28E+01

On the bottom of the list of Table 17 the sum values of all Ci values after a specific cooling time are given. In the case of short time irradiation of heavy targets in irradiation room 1, these sum values can sometimes exceed the clearance levels for free release defined by Austrian law. Ventilation in all irradiation rooms is therefore designed to mix the irradiated air with roughly 14.000 m³ of air during its passage through the air of the synchrotron hall, and utilize this procedure to provide a cooling time for the air of at least one full hour.

Color scales indicate that immediately after irradiation, isotopes with a comparably short half-life like O-15 dominate the table of activation at first, but after a few minutes, the main bulk of radiation will be represented by radiation from the isotopes C-11, N-13 and Ar-41.

Comparison with legal limits and their sum values in Table 17 shows that it is necessary, in the worst case of possible irradiation procedures, to dilute the activated air and hold it inside the building to let the parameters fall below clearance levels defined by Austrian law.

REALISTIC DILUTION PLUS COOLDOWN SCENARIO

Ventilation design at the MedAustron facility will make sure that every produced nuclide has at least one full hour to decay before leaving the facility. Also, the activated isotopes from the treatment rooms will be diluted into the air of the synchrotron room before being able to leave the facility. For the calculations, it was assumed that 14.000 m³ of air per hour will be released to the environment, which is also the volume that activated air will be diluted in. The following calculations focus on specific activities produced during irradiation with different intensities compared to Ci values for release into the environment.

Based on the intended scenario of diluting the air during 1 hour inside the synchrotron hall with an air volume of 14.000 m³ are the results in Table 18, which lists from left to right: The isotope and its mass number, the total activity per year induced by a beam intensity of 1.80E+16 protons with 800 MeV, the average specific activity in [Bq/m³] (produced at an intensity of 5.71E+8 protons per second), the maximum specific activity in [Bq/m³] (produced at an intensity of 2E+10 protons per second), the Ci values as defined by Austrian law together with estimated ones, and the comparison value resulting from dividing the average and maximum activation values by their respective Ci values.

Table 18: Activity of the air after irradiation of a lead target with an 800 MeV proton beam, compared to Ci values, considering a cooling time of 1 hour and thinning the air to a volume of 14.000 m³ at average (5.71E+8) particles per second) and maximum (2E+10 particles per second) intensity

Isotope	Bq (total/y)	av. sp. act.	max. sp. act.	Ci [Bq/m ³]	av./Ci	max./Ci
H-3	4.19E+04	3.42E-04	1.20E-02	100.00	3.42E-06	1.20E-04
Be-7	1.19E+06	9.72E-03	3.41E-01	600.00	1.62E-05	5.68E-04
Be-10	6.04E-02	4.92E-10	1.72E-08	1.00	4.92E-10	1.72E-08
C-11	5.94E+09	6.29E+00	2.20E+02	600.00	1.05E-02	3.67E-01
C-14	1.78E+04	1.45E-04	5.08E-03	6.00	2.42E-05	8.47E-04
N-13	1.92E+10	2.42E+00	8.46E+01	2000.00	1.21E-03	4.23E-02
O-14	1.03E+10	4.59E-14	1.61E-12	927.09	4.95E-17	1.73E-15
O-15	7.62E+10	8.47E-07	2.97E-05	1000.00	8.47E-10	2.97E-08
O-19	3.63E+07	3.03E-41	1.06E-39	1916.02	1.58E-44	5.55E-43
F-18	4.11E+06	2.29E-02	8.03E-01	500.00	4.59E-05	1.61E-03
Ne-23	9.04E+07	1.46E-39	5.11E-38	1892.75	7.70E-43	2.70E-41
Ne-24	2.61E+06	9.64E-08	3.38E-06	896.31	1.08E-10	3.77E-09
Na-22	8.92E+01	7.27E-07	2.55E-05	1.00	7.27E-07	2.55E-05
Na-24	2.13E+05	1.66E-03	5.81E-02	90.00	1.84E-05	6.46E-04
Na-25	7.53E+07	5.32E-19	1.87E-17	28648.19	1.86E-23	6.51E-22
Mg-27	1.15E+07	1.18E-03	4.12E-02	577.79	2.04E-06	7.14E-05
Mg-28	2.59E+04	2.04E-04	7.15E-03	20.00	1.02E-05	3.57E-04
Al-26	4.09E-04	3.34E-12	1.17E-10	0.50	6.68E-12	2.34E-10
Al-28	1.58E+08	1.11E-08	3.90E-07	537.59	2.07E-11	7.25E-10
Al-29	2.97E+07	4.44E-04	1.56E-02	232.45	1.91E-06	6.69E-05
Si-31	1.32E+06	8.27E-03	2.90E-01	300.00	2.76E-05	9.66E-04
Si-32	1.20E+00	9.80E-09	3.43E-07	0.32	3.06E-08	1.07E-06
P-30	4.59E+07	2.21E-08	7.76E-07	2727.82	8.12E-12	2.84E-10
P-32	5.72E+04	4.66E-04	1.63E-02	1.00	4.66E-04	1.63E-02
P-33	2.27E+04	1.85E-04	6.47E-03	20.00	9.23E-06	3.23E-04
P-35	1.18E+08	1.32E-23	4.61E-22	12148.03	1.08E-27	3.80E-26
S-35	8.43E+03	6.87E-05	2.41E-03	20.00	3.44E-06	1.20E-04
S-37	9.31E+07	2.05E-04	7.17E-03	8682.34	2.36E-08	8.26E-07
S-38	1.32E+06	8.44E-03	2.96E-01	422.83	2.00E-05	7.00E-04
Cl-34	1.58E+06	3.51E-03	1.23E-01	16.84	2.09E-04	7.31E-03
Cl-36	1.68E-02	1.37E-10	4.81E-09	0.10	1.37E-09	4.81E-08
Cl-38	4.95E+07	1.32E-01	4.63E+00	500.00	2.64E-04	9.25E-03
Cl-39	6.68E+07	2.58E-01	9.04E+00	600.00	4.30E-04	1.51E-02
Cl-40	2.65E+08	2.71E-13	9.49E-12	292.72	9.25E-16	3.24E-14
Ar-37	9.41E+04	7.66E-04	2.69E-02	200000000.00	3.83E-12	1.34E-10
Ar-39	9.54E+01	7.78E-07	2.72E-05	6000.00	1.30E-10	4.54E-09
Ar-41	1.02E+09	5.67E+00	1.99E+02	200.00	2.83E-02	9.93E-01
K-38	4.33E+06	1.52E-04	5.34E-03	4622.10	3.30E-08	1.16E-06
K-40	1.36E-07	1.11E-15	3.89E-14	0.31	3.55E-15	1.24E-13
Sum:					4.16E-02	1.46E+00

Calculations with the intensity budgeted for a whole year ($1.8E+16$ protons with 800 MeV for irradiation room 1) and distributed over that year (equaling $5.71E+8$ protons per second) show that all calculated activities as well as their sum values are well below Ci clearance levels.

In the case of 1 hour of irradiation of a lead target with 800 MeV protons with the maximum available intensity of $2E+10$ protons per second in irradiation room 1, even after a cooling time of 1 hour and diluting the air from the room to 14.000 m³ of air from the synchrotron room, the sum value $\Sigma(\text{activities} / \text{Ci clearance levels})$ of all activities compared to their respective Ci values is still significantly above the allowed value of 1.0, although all single isotope values comply with the Ci values themselves. Therefore diligent measuring and logging of all activated air released from the facility is essential.

400 MEV ION BEAM

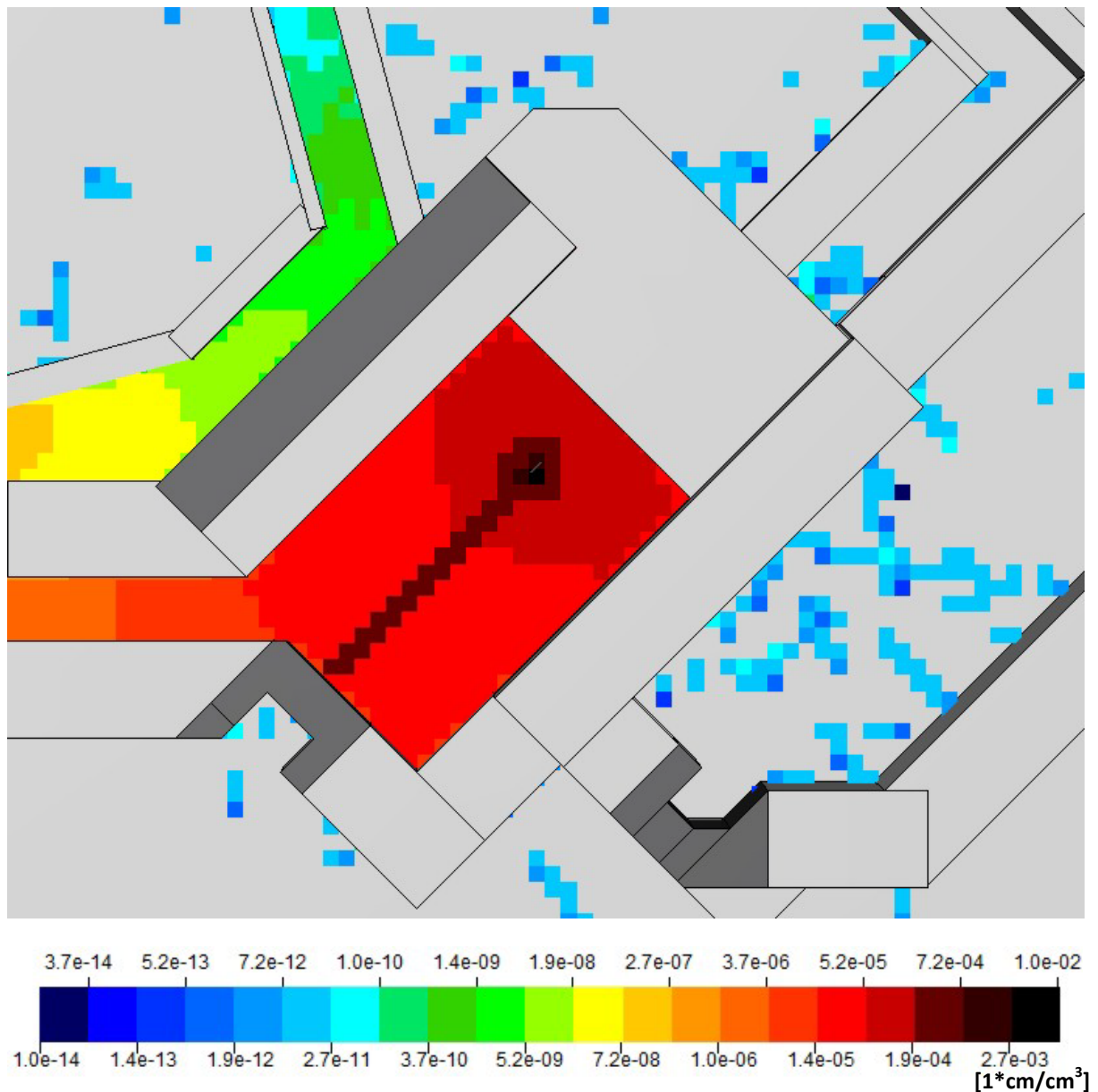


Figure 24: Fluence per primary particle of all particles in the treatment room 1 on beam height, when a horizontal ion beam with 400 MeV hits the lead target, viewed from above

Irradiation room 1 will be hosting various experimental setups, which will also make use of the high energy ion beams that the machine is capable of producing. To consider a scenario of high exposure of the air by the beam and eventually produced secondary particles, the setup for an 800 MeV proton beam starting at the wall and impinging on a 50 cm long lead cylinder with a diameter of 5 cm has been reused, changing the beam to a 400 MeV per nucleon carbon ion beam. The result is illustrated by a USBIN showing fluences of all particles at beam height in Figure 24.

Detailed tables of the environmental release scenario results are listed in Appendix B. Summary tables for all irradiation rooms are listed at the end of this chapter.

250 MEV PROTON BEAM

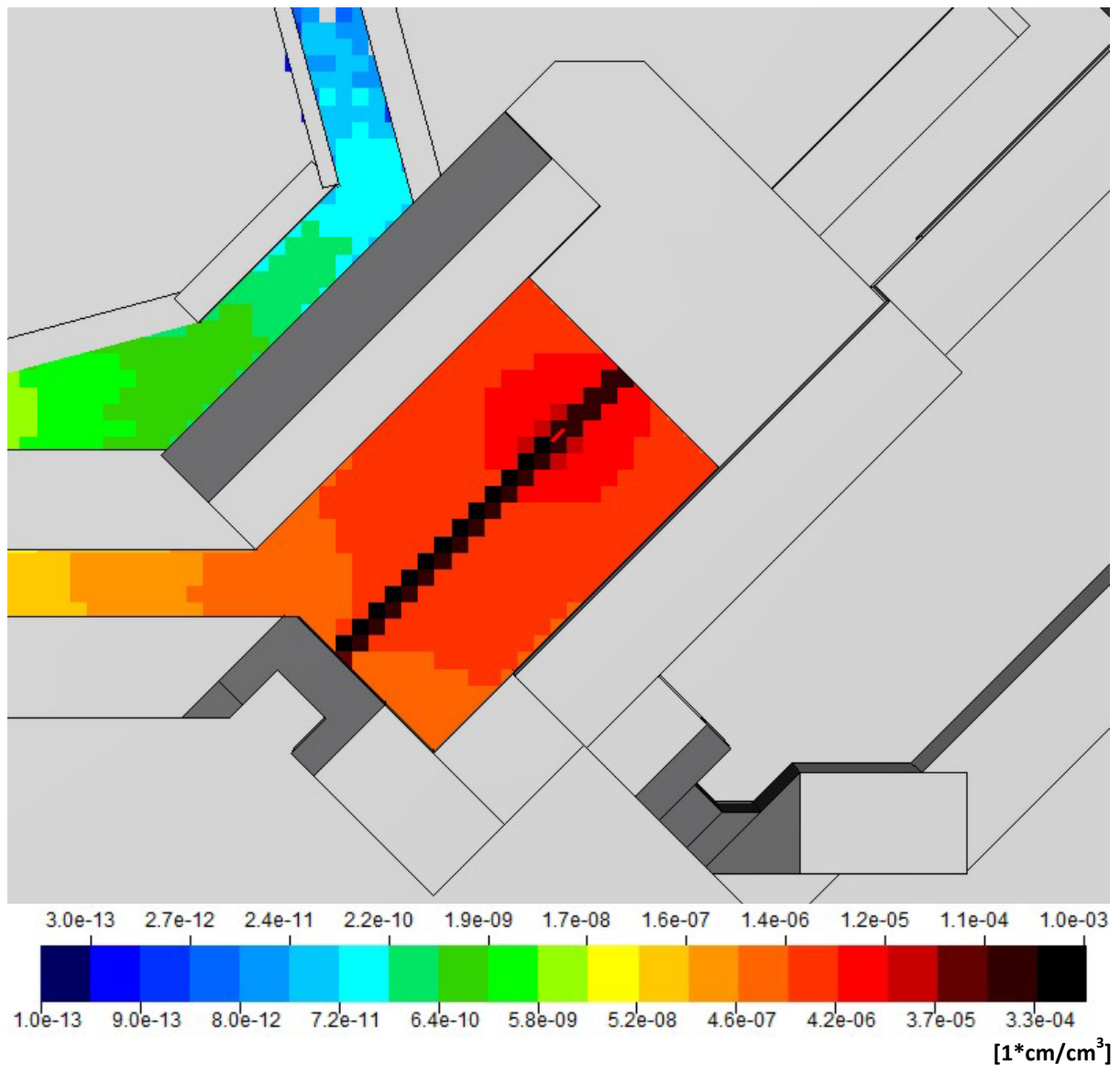


Figure 25: Fluence per primary particle of all particles in the treatment room 1 on beam height, when a horizontal proton beam with 250 MeV hits the lead target, viewed from above

In addition to the 800 MeV proton and 400 MeV ion beam scenarios, also simulations featuring a 250 MeV proton beam crossing the room and impinging on a 50 cm long lead cylinder with 5 cm diameter are carried out. Figure 25 displays a fluence of all particles at beam height showing the beam starting at the lower wall and hitting the lead target.

What looks like the beam missing the target in Figure 25, is correctly displayed by taking a closer look, taken in Figure 26. The 250 MeV proton beam is, because of its comparably lower energy than the other 2 regarded beams, much more susceptible to widening through scattering processes when passing through several meters of air on its way to the target. After about 9 meters transition through an air volume, the beam widens up enough to partially bypass the lead cylinder with 5 cm diameter, so that several high energy protons manage to get through the room unhindered until they hit the wall.



Figure 26: Fluence per primary particle of all particles showing the widening of the 250 MeV proton beam when it hits the target with 5 cm diameter

This scenario of a partially longer beam path, compared to the 800 MeV proton beam scenario, also explains the relatively high committed dose rates caused by the lower energy proton beam, also compared to 800 MeV protons, which are still responsible for the highest activation of air. By letting the primary beam cross the bigger portion of the room, production of N-13 with the 250 MeV proton beam for example is about 90% as high as N-13 production in the 800 MeV proton beam scenario, both of which can be found in the respective tables in Appendix B.

Detailed tables of the environmental release scenario results are listed in Appendix B. Summary tables for all irradiation rooms are listed at the end of this chapter.

IRRADIATION ROOM 2 (IR2)

400 MEV ION BEAM HORIZONTAL

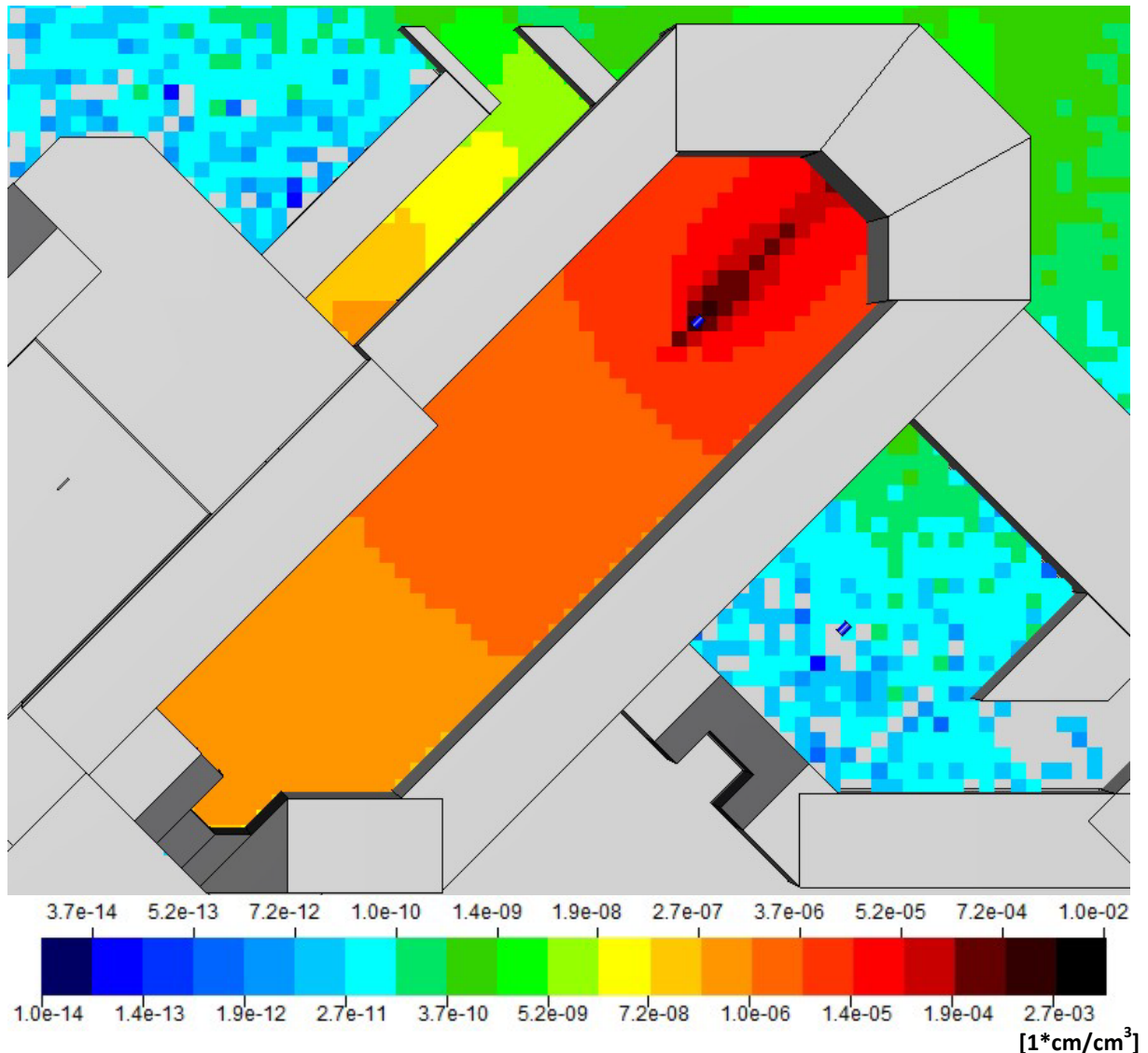


Figure 27: Fluence per primary particle of all particles in the treatment room 2 on beam height, when a horizontal ion beam with 400 MeV hits the water target, viewed from above

Irradiation room 2 will be used for the treatment of patients by applying carbon ion beams with a maximum energy of 400 MeV per nucleon. The beam can be sent from two different directions: Horizontal like pictured in the fluence USRBIN in Figure 27, or vertical from ceiling to floor. The ample room size is explained by the space needs of the equipment and machinery that needs to be installed, to be able to bend and focus the beam for a total of 270 degrees. The horizontal as well as the vertical beam scenario are simulated with the ion beam hitting a water cylinder from a distance of 1 m.

Detailed tables of the environmental release scenario results are listed in Appendix B. Summary tables for all irradiation rooms are listed at the end of this chapter.

IRRADIATION ROOM 3 (IR3)

400 MEV ION BEAM

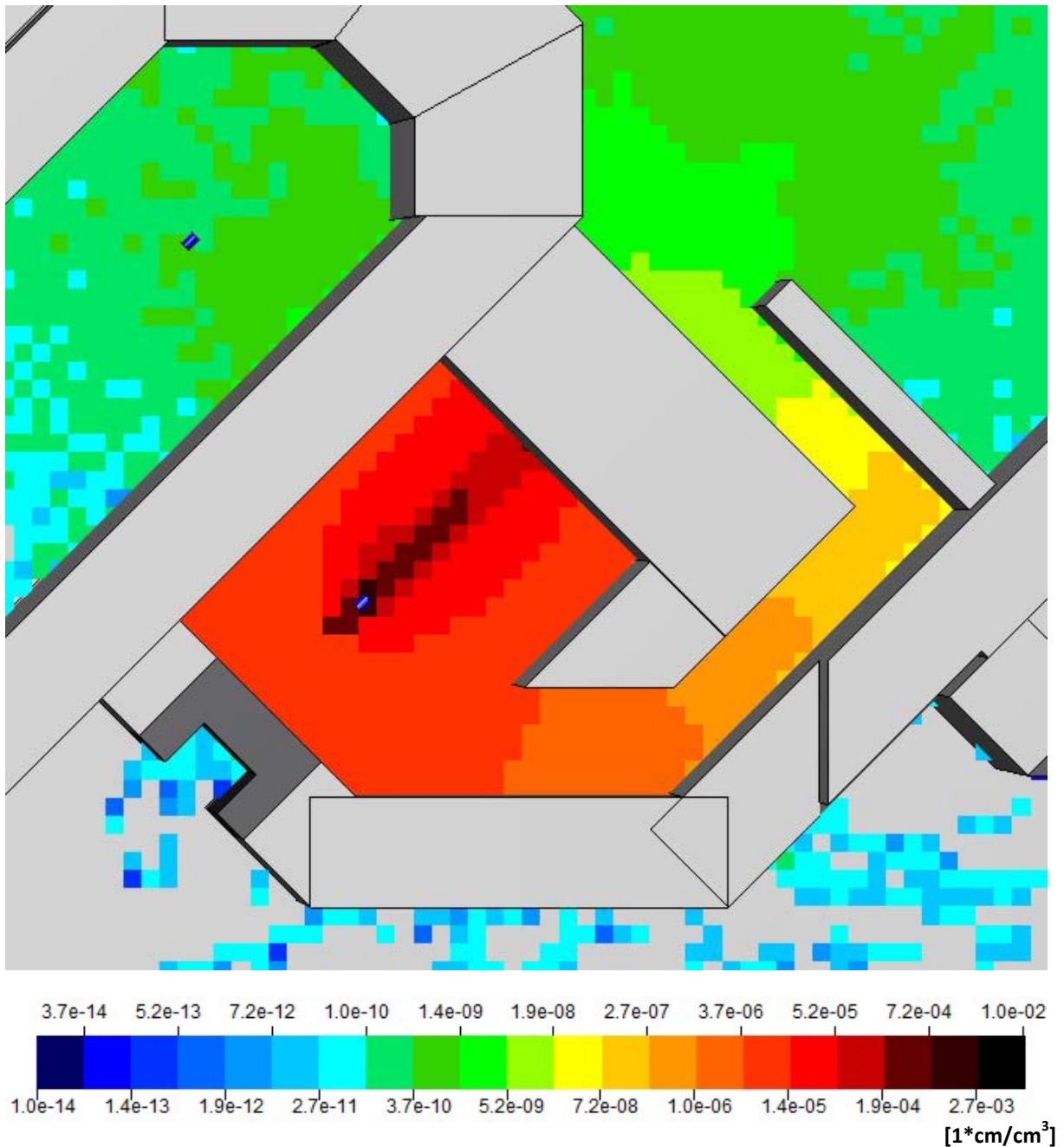


Figure 28: Fluence per primary particle of all particles in the treatment room 3 on beam height, when a horizontal ion beam with 400 MeV hits the water target, viewed from above

Like irradiation room 2, plans for irradiation room 3 focus on the treatment of patients by applying carbon ion beams with a maximum energy of 400 MeV per nucleon. The biggest difference between the two rooms comes from the fact that IR3 will only support one possible beam direction, coming directly out of the wall bordering to the HEPT, pictured in Figure 28, which calls for a lot less space being used for machinery, resulting in a smaller volume for IR3. Assuming that a beam nozzle will be installed to guide the beam as close as

possible to the patient, a very conservative distance of 1 m is chosen between the start of the beam and the base of the target cylinder in the simulation.

Detailed tables of the environmental release scenario results are listed in Appendix B. Summary tables for all irradiation rooms are listed at the end of this chapter.

IRRADIATION ROOM 4 (IR4 - PROTON GANTRY)

250 MEV PROTON BEAM HORIZONTAL

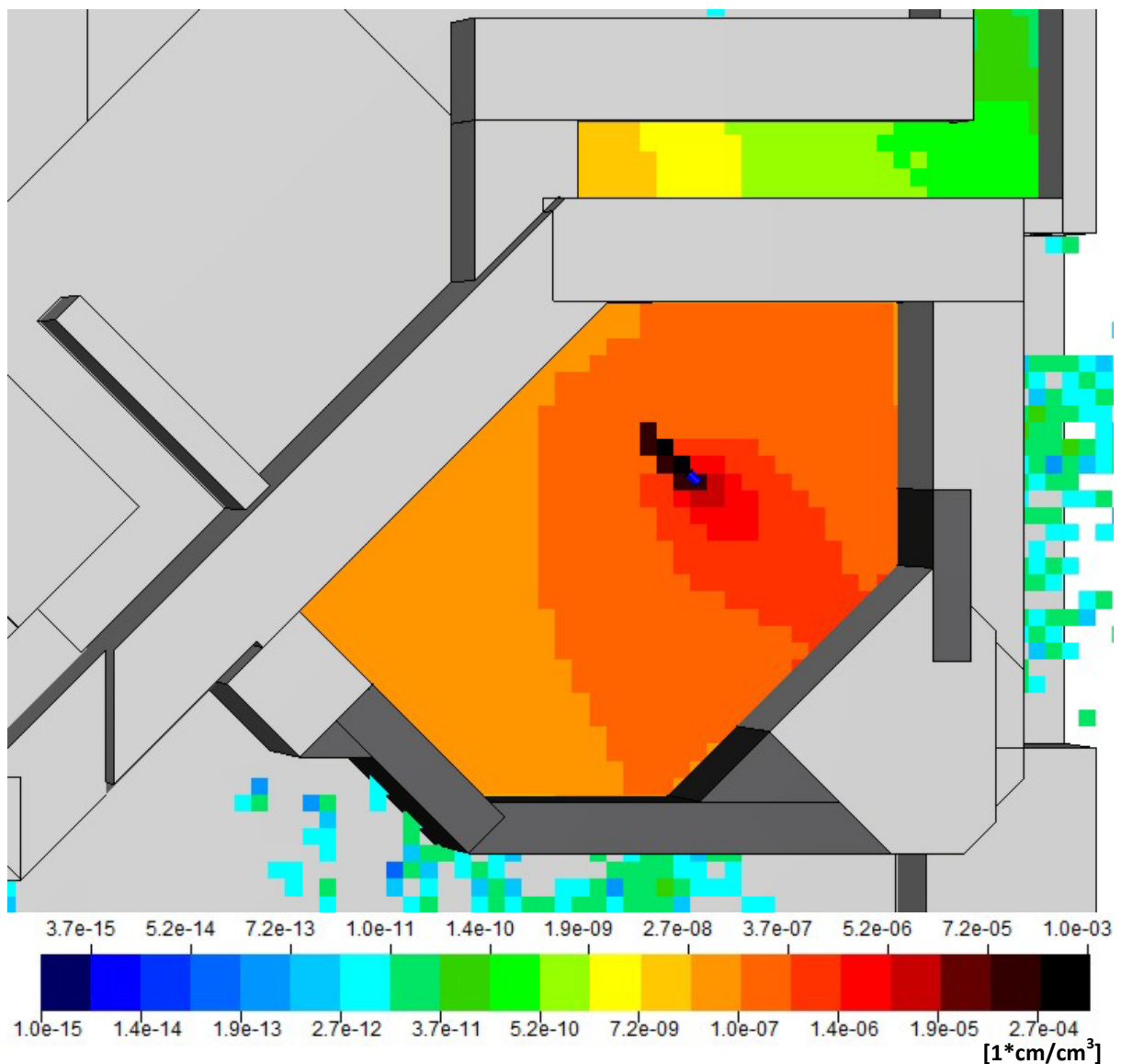


Figure 29: Fluence per primary particle of all particles in the treatment room 4 on beam height, when a horizontal proton beam with 250 MeV hits the water target, viewed from above

The proton gantry that will be installed in this room will be able to turn 180 degrees and guide a proton beam with a maximum energy of 250 MeV from top to bottom, bottom to top, or to any position lying on a half circle spanning in between those directions, that always points to the outer walls of the facility. [4] For simulations using FLUKA, a horizontal beam scenario, pictured by an all particle fluence USBIN at beam height in Figure 29, as well as two alternative vertical scenarios are regarded to estimate the activation of air during possible irradiation procedures.

In the horizontal as well as the vertical beam scenario that features a beam direction going from top to bottom, 1.5 m of distance between the start of the beam and the base of the water cylinder is chosen as a very conservative estimation. For the vertical beam scenario shooting from bottom to top, only 1 m of distance between beam start and target is applied, making for a still conservative approach assuming an intermediate floor being installed in the room.

Detailed tables of the environmental release scenario results are listed in Appendix B. Summary tables for all irradiation rooms are listed below.

SUMMARY TABLES FOR IRRADIATION ROOMS 1-4

Detailed tables showing the results and comparisons for each nuclide are listed in Appendix B. The following tables show summary values of the comparisons between the calculated activities and their respective Ci values.

Tables labeled “direct release” are only compiled to illustrate the necessity to dilute the air from the treatment rooms and let it cool down before it can be released into the environment, in order to comply to the legal limits given by Austrian law.

Conservative estimations for sum values of Ci comparisons for the cooled down and diluted air that will really be released into the environment are labeled “comparisons with limits for unrestricted release”.

Abbreviations for the different types of beams will be used:

p800 ... proton beam with 800 MeV

p250 ... proton beam with 250 MeV

i400 ... C12 ion beam with 400 MeV per nucleon

IRRADIATION ROOM 1

Activities and comparison values with Ci limits are calculated for a fictional direct release scenario, in which the activated isotopes in the air of the treatment room are measured against Ci values, taking into account ventilation but no dilution with the air of the synchrotron room. Since the exact points of air extraction inside the rooms are still unknown, the decrease of the activity at several cooling times is regarded, namely after 0 seconds, after 1 minute, 10 minutes, 1 hour, and after the time the ventilation should take to conduct one full air exchange in the room, which is 1161.29 seconds in the case of 3.1 exchanges per hour. An extraction point in the vicinity of the target means less cooling time for the activated isotope until its release to the outside air. The average time an isotope should take to get outside in this scenario should be 1161.29 seconds.

Table 19 shows the sums of comparison values of activation versus Ci limits after an irradiation with a total intensity of $2.32\text{E}+13$ protons, respectively $1.16\text{E}+12$ carbon ions, corresponding to an irradiation time of 1161.29 seconds using the maximum available intensity of $2\text{E}+10$ protons per second respectively $1\text{E}+9$ ions per second. Considering a full air exchange of the 515 m^3 air volume every 1161.29 seconds, meaning 3.1 exchanges and a total released air volume of 1545 m^3 per hour, this irradiation time, coupled with using the actual room volumes for calculations, corresponds to the actual exposure of the environment by extracted air during continuous beam operation following this fictional scenario. It is assumed that every isotope created needs the same average amount of time until release into the environment, which is directly correlated to the described cooling times. This means that the activity induced during irradiation is continuously released into the environment by means of ventilation, and the total amount of activation released has to be compared, per isotope as well as per sum values, to the legal limits, i.e. Ci values, defined by Austrian law.

Table 19: Comparison values of sums of activities divided by their respective Ci values in a direct release scenario after irradiation with a total intensity of $2.32\text{E}+13$ protons, respectively $1.16\text{E}+12$ carbon ions, which corresponds to 3.1 air exchanges per hour at full intensity of the beam, considering several cooling times

IR1	Intensity/air exch.	Sum act/Ci 0s	60s	600s	1161.29s	3600s
p800	$2.32\text{E}+13$	$2.85\text{E}+02$	$2.14\text{E}+02$	$4.91\text{E}+01$	$3.14\text{E}+01$	$1.28\text{E}+01$
i400	$1.16\text{E}+12$	$2.35\text{E}+01$	$1.80\text{E}+01$	$4.86\text{E}+00$	$3.09\text{E}+00$	$1.08\text{E}+00$
p250	$2.32\text{E}+13$	$2.90\text{E}+02$	$2.11\text{E}+02$	$3.64\text{E}+01$	$1.98\text{E}+01$	$4.52\text{E}+00$

Regarding a release of air between 10^4 and 10^5 m^3 per hour, the sum of comparison values of Table 19 based on calculated activities would be significantly higher than the legal limit of 1 even after an average cooling time. Although Austrian law allows for 10 times the activity outlined by Ci values, if the released air volume is less than 10^4 m^3 , which would be the case in this very special scenario, this would still not suffice.

For estimating a fictional direct release scenario considering average intensities expected per year, the results from Table 19 are divided by a factor calculated by comparing the average with the maximum available intensity, with results displayed in Table 20.

Table 20: Comparison values of sums of activities divided by their respective Ci values in a direct release scenario after irradiation with a total intensity of 6.63E+11 protons, respectively 2.87E+10 carbon ions, which corresponds to 3.1 air exchanges per hour at average intensity of the beam, considering several cooling times

IR1	Intensity/air exch.	Sum act/Ci	0s	60s	600s	1161.29s	3600s
p800	6.63E+11	8.14E+00	6.10E+00	1.40E+00	8.97E-01	3.65E-01	
i400	2.87E+10	5.81E-01	4.46E-01	1.20E-01	7.64E-02	2.68E-02	
p250	2.87E+11	3.58E+00	2.62E+00	4.50E-01	2.45E-01	5.60E-02	

The sums of comparison values in the fictional proton beam direct release scenarios, calculated by using average beam intensities, are still above legal limits, even after a considerable cooling time of over 10 minutes in the case of 800 MeV proton energy. As a consequence, plans for the MedAustron facility include a ventilation system that will provide for dilution and more time to decay for any activated isotopes in the treatment rooms.

Estimations for the activity of the air that is to be released, after dilution with the 14.000 m³ of the synchrotron hall and at least 1 hour of cooling, compared to limits defined by Austrian law are given in Table 21, which lists, besides the scheduled intensity per year for each type of beam, the sum values gained by comparing the calculated activity of each calculated isotope with their respective Ci value and summing up all of these comparison values. For an unrestricted release into the environment, this sum value must not exceed 1.

In this scenario, each Ci value of each isotope is not exceeded by their respective activity, which can be regarded in the tables in Appendix B.

Table 21: Sum values of specific activities compared to Ci values. Sum av/Ci compares specific activities generated considering average intensity, Sum max/Ci compares activities generated by consideration of maximum available intensity

IR1	Intensity/y	Sum av/Ci	Sum max/Ci
p800	1.80E+16	4.16E-02	1.46E+00
i400	7.80E+14	3.02E-03	1.22E-01
p250	7.80E+15	6.38E-03	5.16E-01

While the values for the proton beam scenarios are calculated by using the folding method, the values for the ion beam scenario are derived by using yields simulated by FLUKA and on the base of these yields calculating activities and comparing them to Ci values, using the same guidelines as with the folding method. This ion beam scenario is the only one where FLUKA RESNUCLEi-scored yields are believed to be more accurate, despite the overestimation of cross sections, because the folding method, lacking the necessary cross sections, does not take into account isotopes created by the main ion beam, which is in this case crossing about 2/3rds of the room, while direct simulation and scoring via RESNUCLEi card in FLUKA does.

Although FLUKA scores a lot more individual types of nuclides during simulations, for which no defined Ci values exist, none of them is of any relevance to the calculations, due to their either very short half-lives (less than 1 second on average) or the very small quantities they are scored in.

IRRADIATION ROOM 2

In this irradiation room, two possible scenarios for beam direction are considered. The 400 MeV ion beam can be sent horizontally to a target as well as vertically from the direction of the ceiling. Since all possible irradiation scenarios in this room are based on the assumption that the beam will start very close to the target, that the Bragg peak of the beam lies inside the target, and calculations have been conducted considering a beam starting 1m in front of the target in both directions, only the folding method is used to calculate activities, neglecting any activation caused by the main ion beam.

Using a fictional direct release scenario, Table 22 shows the sums of comparison values of activation versus Ci limits after an irradiation with a total intensity of 2.25E+12 ions per second, which corresponds to 1.6 full air exchanges of the 2000 m³ big room volume, meaning a full exchange every 2250 seconds, using the maximum available intensity of 1E+9 ions per second. Sum values are listed for several cooling times and for both possible beam directions.

Table 22: Comparison values of sums of activities divided by their respective Ci values in a direct release scenario after irradiation with a total intensity of 2.25E+12 protons, which corresponds to 1.6 air exchanges per hour at full intensity of the beam, considering several cooling times

IR2	Intensity/air exch.	Sum act/Ci 0s	60s	600s	2250s	3600s
i400 horizontal	2.25E+12	1.08E+01	7.97E+00	1.59E+00	4.73E-01	2.58E-01
Alternative:						
i400 vertical	2.25E+12	3.97E+00	2.98E+00	6.84E-01	2.53E-01	1.63E-01

For estimating a fictional direct release scenario considering average intensities expected per year, the results from Table 22 are divided by a factor calculated by comparing the average with the maximum available intensity, with results displayed in Table 23.

Table 23: Comparison values of sums of activities divided by their respective Ci values in a direct release scenario after irradiation with a total intensity of 3.35E+10 protons, which corresponds to 1.6 air exchanges per hour at average intensity of the beam, considering several cooling times

IR2	Intensity/air exch.	Sum act/Ci 0s	60s	600s	2250s	3600s
i400 horizontal	3.35E+10	1.61E-01	1.19E-01	2.37E-02	7.05E-03	3.85E-03
Alternative:						
i400 vertical	3.35E+10	5.92E-02	4.44E-02	1.02E-02	3.76E-03	2.44E-03

The vertical beam scenario shows less activation, because there is less space for forward-directed secondary particles behind the target in this direction, considering that the target centre lies only 1.25 metres above ground, whereas there are several metres between target and wall when shooting horizontally.

Estimations for the activity of the air that is to be released, after dilution with the 14.000 m³ of the synchrotron hall and at least 1 hour of cooling, compared to limits defined by Austrian law are given in Table 24, which lists, besides the scheduled intensity per year for each type of beam, the sum values gained by comparing the calculated activity of each calculated isotope with their respective Ci value and summing up all of these comparison values. For an unrestricted release into the environment, this sum value must not exceed 1.

In this scenario, each Ci value of each isotope is not exceeded by their respective activity, which can be regarded in the tables in Appendix B.

Table 24: Sum values of specific activities compared to Ci values. Sum av/Ci compares specific activities generated considering average intensity, Sum max/Ci compares activities generated by consideration of maximum available intensity

IR2	Intensity/y	Sum av/Ci	Sum max/Ci
i400 horizontal	4.70E+14	8.81E-04	5.91E-02
Alternative:			
i400 vertical	4.70E+14	5.57E-04	3.74E-02

Again, the vertical beam scenario shows less overall activation of the air being released to the environment. Considering the legal limit for the sum values being 1, almost two orders of magnitude above, it does not make much of a difference.

IRRADIATION ROOM 3

This small treatment room with a volume of 287 m³ will be equipped with a nozzle for ion beams up to 400 MeV per nucleon that goes in horizontal direction only. Table 25 shows comparison values after an irradiation with a total intensity of 1.16E+12 ions per second, which corresponds to 3.1 full air exchanges per hour, meaning a full exchange every 1161.29 seconds, and using the maximum available intensity of 1E+9 ions per second, in a fictional direct release scenario.

Table 25: Comparison values of sums of activities divided by their respective Ci values in a direct release scenario after irradiation with a total intensity of 1.16E+12 protons, which corresponds to 3.1 air exchanges per hour at full intensity of the beam, considering several cooling times

IR3	Intensity/air exch.	Sum act/Ci	0s	60s	600s	1161.29s	3600s
i400	1.16E+12	3.89E+01		2.87E+01	5.55E+00	3.12E+00	7.92E-01

For estimating a fictional direct release scenario considering average intensities expected per year, the results from Table 25 are divided by a factor calculated by comparing the average with the maximum available intensity, with results displayed in Table 26.

Table 26: Comparison values of sums of activities divided by their respective Ci values in a direct release scenario after irradiation with a total intensity of 1.73E+10 protons, which corresponds to 3.1 air exchanges per hour at average intensity of the beam, considering several cooling times

IR3	Intensity/air exch.	Sum act/Ci	0s	60s	600s	1161.29s	3600s
i400	1.73E+10	5.80E-01		4.28E-01	8.27E-02	4.65E-02	1.18E-02

The slightly higher sum values in a fictional direct release scenario, compared to the bigger irradiation room 2, come from the fact that the volume of room 3 is significantly smaller, whereas a larger portion of the air volume is exposed to radiation coming from secondary particles.

Estimations for the activity of the air that is to be released, after dilution with the 14.000 m³ of the synchrotron hall and at least 1 hour of cooling, compared to limits defined by Austrian law are given in Table 27, which lists, besides the scheduled intensity per year for each type of beam, the sum values gained by comparing the calculated activity of each calculated isotope with their respective Ci value and summing up all of these comparison values. For an unrestricted release into the environment, this sum value must not exceed 1.

In this scenario, each Ci value of each isotope is not exceeded by their respective activity, which can be regarded in the tables in Appendix B.

Table 27: Sum values of specific activities compared to Ci values. Sum av/Ci compares specific activities generated considering average intensity, Sum max/Ci compares activities generated by consideration of maximum available intensity

IR3	Intensity/y	Sum av/Ci	Sum max/Ci
i400	4.70E+14	7.51E-04	5.04E-02

Due to the limitation to ion beam therapy and the very small amount of scheduled intensity per year, air activation in this irradiation room only offers a minor contribution to the overall activity released from the facility.

IRRADIATION ROOM 4

Since this room will be equipped with a proton gantry, no definite beam direction for a proper simulation can be assumed. To estimate results, 3 different beam directions of which the gantry will be capable, including one horizontal and two vertical directions, are regarded. Table 28 shows comparison values after an irradiation with a total intensity of $3.43\text{E}+13$ protons, which corresponds to 2.1 full air exchanges per hour, meaning a full exchange every 1714.29 seconds, and using the maximum available intensity of $2\text{E}+10$ protons per second, in a fictional direct release scenario.

Table 28: Comparison values of sums of activities divided by their respective Ci values in a direct release scenario after irradiation with a total intensity of $3.43\text{E}+13$ protons, which corresponds to 2.1 air exchanges per hour at full intensity of the beam, considering several cooling times

IR4	Intensity/air exch.	Sum act/Ci 0s	60s	600s	1714.29s	3600s
p250 horizontal	3.43E+13	1.91E+01	1.40E+01	2.52E+00	9.41E-01	3.26E-01
Alternatives:						
p250 up	3.43E+13	1.86E+01	1.36E+01	2.46E+00	9.18E-01	3.19E-01
p250 down	3.43E+13	1.79E+01	1.32E+01	2.36E+00	8.84E-01	3.10E-01

For estimating a fictional direct release scenario considering average intensities expected per year, the results from Table 28 are divided by a factor calculated by comparing the average with the maximum available intensity, with results displayed in Table 29.

Table 29: Comparison values of sums of activities divided by their respective Ci values in a direct release scenario after irradiation with a total intensity of $3.64\text{E}+11$ protons, which corresponds to 2.1 air exchanges per hour at average intensity of the beam, considering several cooling times

IR4	Intensity/air exch.	Sum act/Ci 0s	60s	600s	1714.29s	3600s
p250 horizontal	3.64E+11	2.03E-01	1.49E-01	2.68E-02	9.99E-03	3.47E-03
Alternatives:						
p250 up	3.64E+11	1.97E-01	1.45E-01	2.61E-02	9.75E-03	3.39E-03
p250 down	3.64E+11	1.90E-01	1.40E-01	2.51E-02	9.39E-03	3.29E-03

In this case, all three directions show similar results, which is caused by the fact that the 1970 m^3 big room has a very special architecture, a deeper floor and a higher ceiling, where the forward-directed high energy secondary particles have enough space to irradiate similar portions of the room.

Estimations for the activity of the air that is to be released, after dilution with the 14.000 m³ of the synchrotron hall and at least 1 hour of cooling, compared to limits defined by Austrian law are given in Table 30, which lists, besides the scheduled intensity per year for each type of beam, the sum values gained by comparing the calculated activity of each calculated isotope with their respective Ci value and summing up all of these comparison values. For an unrestricted release into the environment, this sum value must not exceed 1.

In this scenario, each Ci value of each isotope is not exceeded by their respective activity, which can be regarded in the tables in Appendix B.

Table 30: Sum values of specific activities compared to Ci values. Sum av/Ci compares specific activities generated considering average intensity, Sum max/Ci compares activities generated by consideration of maximum available intensity

IR4	Intensity/y	Sum av/Ci	Sum max/Ci
p250 horizontal	6.70E+15	1.02E-03	9.64E-02
Alternatives:			
p250 upwards	6.70E+15	1.00E-03	9.43E-02
p250 downwards	6.70E+15	9.72E-04	9.15E-02

Again, simulation of three different beam directions leads to very similar results. Since this is a room designated to the treatment of patients, the maximum comparison value shown above will most likely never be reached. Average air activation is still small compared to the possible activation in the experimental irradiation room 1.

SUMMARY OF TREATMENT ROOM CALCULATIONS

Regarding comparison values of Ci values against specific activities gained by irradiating a target with the maximum available intensity, considering a direct release after several cooling times but without any dilution, which will not even be possible regarding the design of the MedAustron facility, shows that the concept of diluting and cooling the activated air from the irradiation rooms is a well chosen one which will make an unrestricted release in view of the limits given by Austrian law very feasible.

Considering that the calculations for all these values were done in a very conservative manner, almost all gained values for unrestricted release still comply to the maximum sum value $\Sigma(\text{activities} / \text{Ci clearance levels})$ of 1 defined by Austrian law, with the sole exception of the case of irradiation of a small lead target with a proton beam with 800 MeV at an intensity of 2E+10 particles per second in irradiation room 1. Although a short-lived transgression of activation limits given by Austrian law is allowed as long as limits are observed on average [19], it shows that diligent measuring and logging of all activities released from the treatment rooms is required.

RADIOLOGICAL EXPOSURE OF THE MEDAUSTRON PERSONNEL

The following figures are based on calculations that take the decay during irradiation already into account in order to illustrate the exposure of personnel entering the room directly after the stop of the beam. All scenarios are based on using the maximum available intensity and the maximum beam energy available in the respective rooms, resulting in very conservative estimations.

IRRADIATION ROOM 1

Figure 30 shows the rate of committed dose (blue curve) and the integral committed dose development (red curve) after 1 hour of irradiation of a lead target with an 800 MeV proton beam at maximum intensity of $2E+10$ protons per second without considering any ventilation of the room. This is a very conservative scenario depicting a case of maximum air activation with the highest radionuclide concentration. It shows how short lived isotopes dominate the exposure of a person inside the room, which means that there is no linear correlation between the duration of the irradiation and the activation of the air. Reducing the duration of the irradiation by half is not going to reduce the activation of air by the same factor.

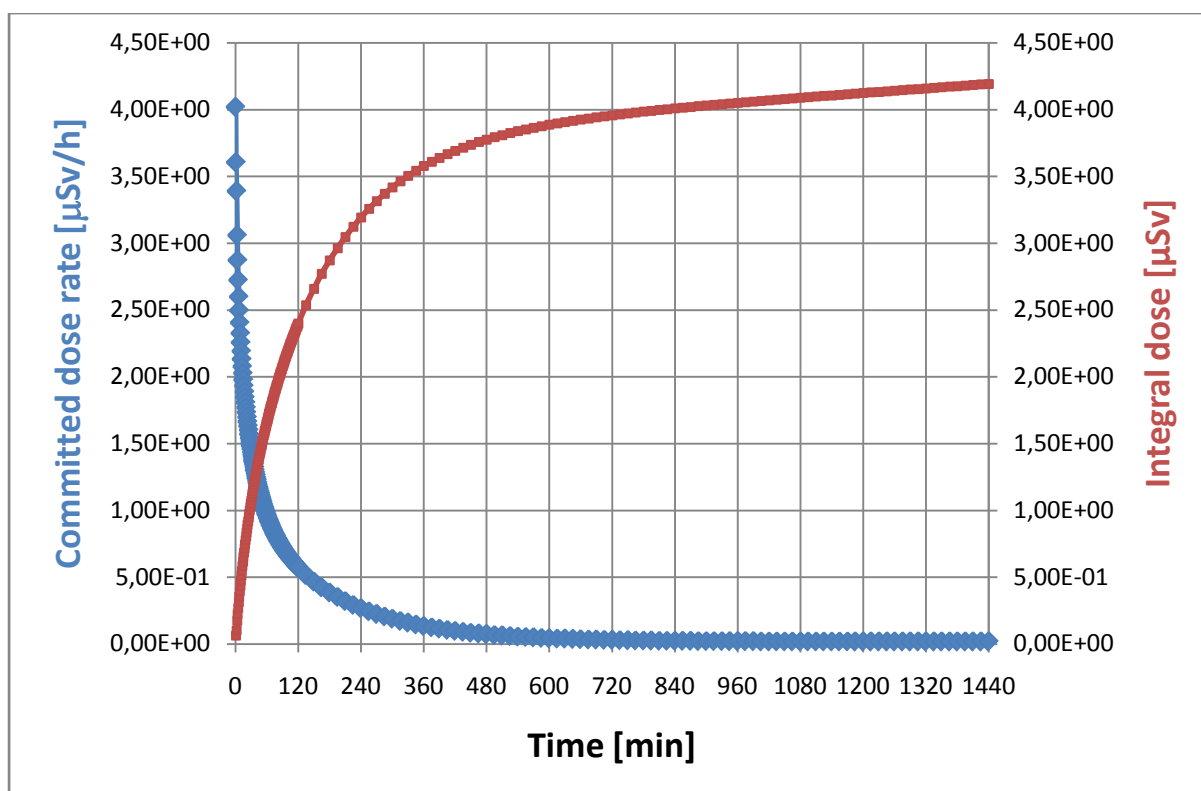


Figure 30: Rate of committed dose and integral committed dose development over time after the end of 1h beam operation with a 800 MeV proton beam at an intensity of $2E+10$ protons per second, not considering ventilation

Customarily, ventilation during beam operation should always be running, so Figure 30 already displays an absolute worst case of irradiation. To more realistically estimate the impact of the high energy proton beam activated, the following scenario was conceived:

The air exchange rate in irradiation room 1 is predefined to be 3.1 times per hour. When regarding an irradiation time of $3600/3.1 = 1161.29$ seconds at maximum intensity of $2E+10$ protons per second, this corresponds to a continuous operation with 3.1 air exchanges per hour. The irradiation time correlates to the average duration of stay of an air molecule in the non clinical room, if the air volume inside is renewed 3.1 times per hour.

Figure 31 displays the committed dose rate and the integral committed dose development as a function of time directly after the beam stop, ignoring ventilation after beam stop for the time of cooling and showing only natural decay as reason for the decrease of radiation in the air.

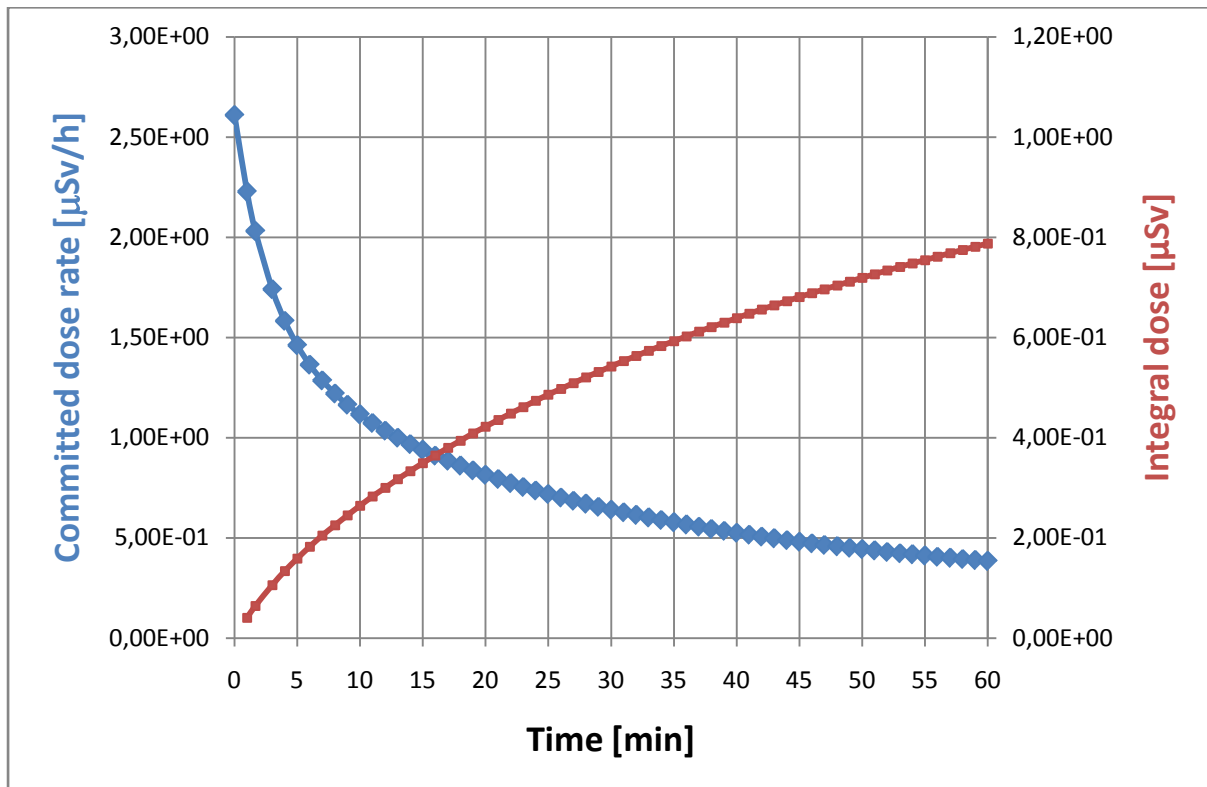


Figure 31: Rate of committed dose and integral committed dose development over time after the end of 1161.29s beam operation, which corresponds to a full exchange of the air volume in the room at a rate of 3.1 exchanges per hour, with a 800 MeV proton beam at an intensity of $2E+10$ protons per second

The exact manner of the dilution of the airborne radiation achieved through ventilation is not known as of now. Therefore the influence of ventilation was neglected after the stop of beam operation, leading to a conservative estimation of the situation.

After about 13 minutes of cooling time, the committed dose rate already falls below $1 \mu\text{Sv/h}$. Considering roughly 20 minutes for an exchange of the air volume, the reduction of radiation in the air is mainly caused by natural decay of the isotopes.

Before entering the room, the committed dose rate by inhalation should be lowered below 1 $\mu\text{Sv/h}$. This can be achieved by natural radioactive decay as well as by ventilating the room and exchanging the air inside. The effectiveness of the radioactive dilution has to be verified by measurements before access to the room can be granted. Also a homogenous distribution of airborne radioactivity has to be ensured by proper ventilation in order to coincide with calculations. There is also the possibility of designing the ventilation in the way that air from areas with increased radioactivity, like target or beam dump surroundings, will be evacuated first. Monitor(s) have to be installed at locations where the maximum of airborne radioactivity is expected.

Ventilation installations are also responsible for keeping irradiated air from leaking into non radiologically classified areas.

An estimation of committed dose rates caused by 1h operation of a 400 MeV carbon ion beam inside IR1 is depicted in Figure 32.

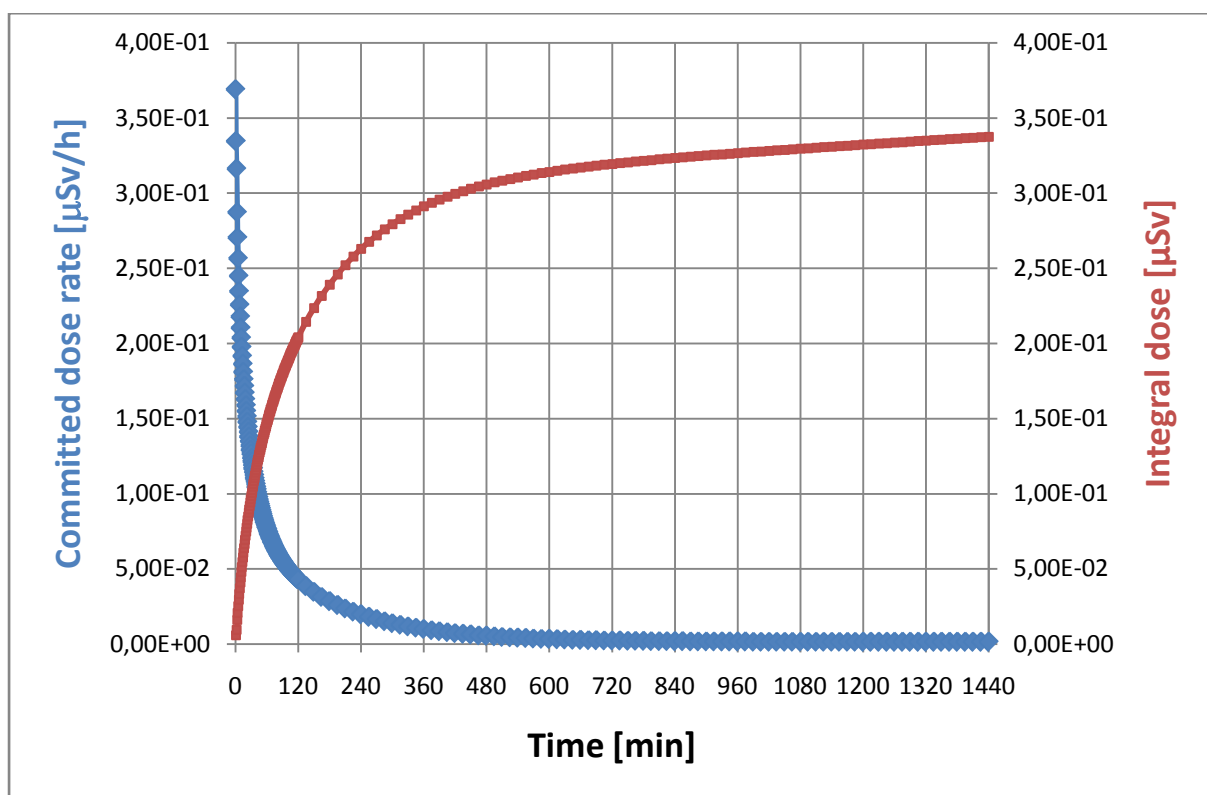


Figure 32: Rate of committed dose and integral committed dose development over time after the end of 1h beam operation with a 400 MeV ion beam at an intensity of $1\text{E}+9$ ions per second, not considering ventilation

The committed dose rate (blue curve) and integral committed dose rate development (red curve) displayed in Figure 32 are based on yield results of FLUKA RESNUCLEi scoring, because a significant part of radiation inside the air volume is induced by the main ion beam interacting with air molecules, which cannot be considered when using the folding method for the calculation of produced isotopes. When comparing results to the two proton beam scenarios, it becomes apparent, that the high energy carbon ions do have a relatively low influence on the total air activation.

The impact of the 250 MeV proton beam particles on the activation of air inside IR1 is emphasized by the results displayed in Figure 33, where the 250 MeV proton beam crosses a large portion of the room until it hits the lead target, with a few primary particles bypassing the target and hitting the back wall of the room and therefore crossing a larger volume of air than the main beam of 800 MeV protons.

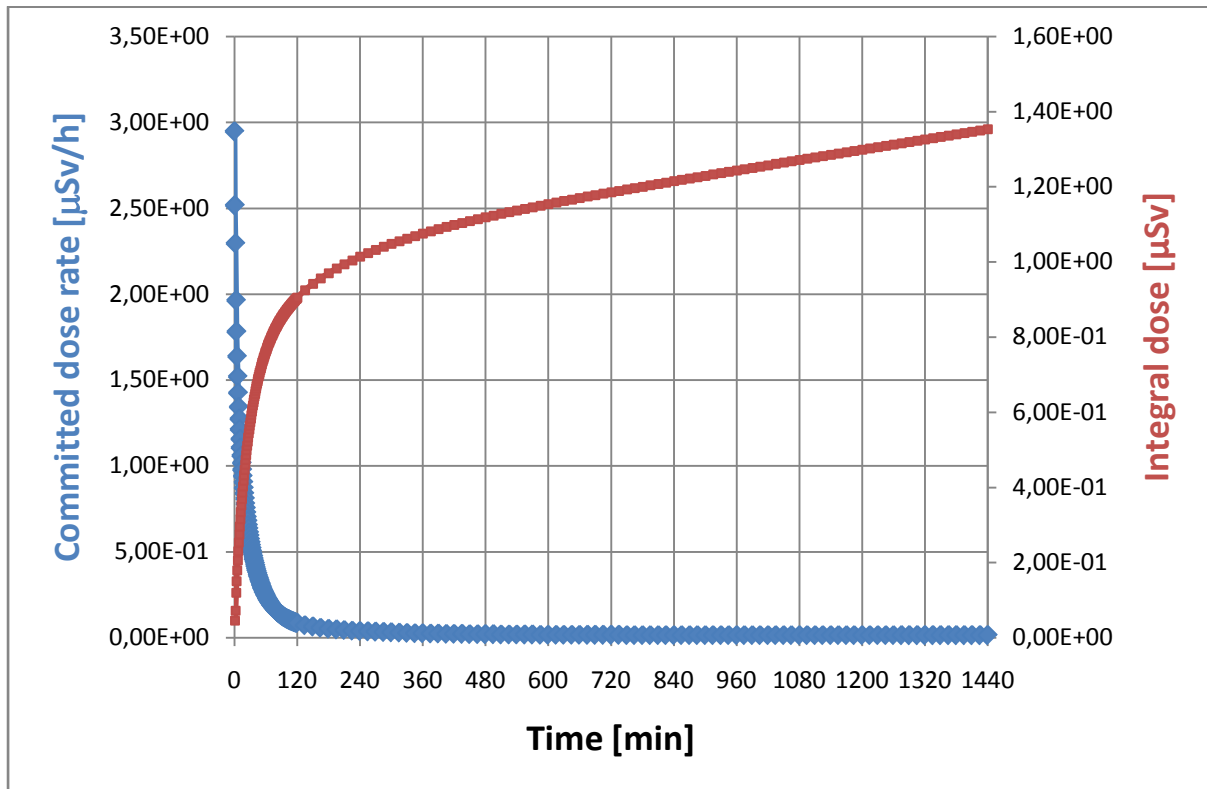


Figure 33: Rate of committed dose and integral committed dose development over time after the end of 1h beam operation with a 250 MeV proton beam at an intensity of $2E+10$ protons per second, not considering ventilation

With key isotope production being almost as high as in the 800 MeV proton beam scenario calculated above, committed dose rates upon direct entry after stopping the beam are relatively high too, which can be seen in Figure 33. Results of simulations done in the treatment rooms listed below show that the production of radioactive nuclides in the air is significantly reduced if the proton beam is started at a short distance from the target. The main reason for such relatively high results is the huge crossing area that the primary beam particles share with the air volume when being sent across the room. Seeing how strongly the main beam gets widened by scattering on air molecules during its passage through the room, as displayed in Figure 26, this is a very unlikely scenario for experiments where a straight beam will be expected.

Inhalation of the air should not expose the person entering the room to more than $1 \mu\text{Sv/h}$. A short waiting time gap between stopping the beam and entering the room should be considered to lower the committed dose rate by means of natural radioactive decay, regarding short lived isotopes, as well as by utilization of ventilation measurements.

IRRADIATION ROOM 2

Being a treatment room for patients, it can be assumed that the beam with a maximum energy of 400 MeV per nucleon will be started as near as possible to the area that is to be treated, negating activation caused by the primary beam going through air. In addition to a very large air volume considered for simulations in this irradiation room, committed dose rate calculations result in very low estimations for personnel entering the room directly after beam stop, even after very conservative assumptions concerning the irradiation time, which is in the case of a horizontal beam scenario displayed in Figure 34 about 1 hour.

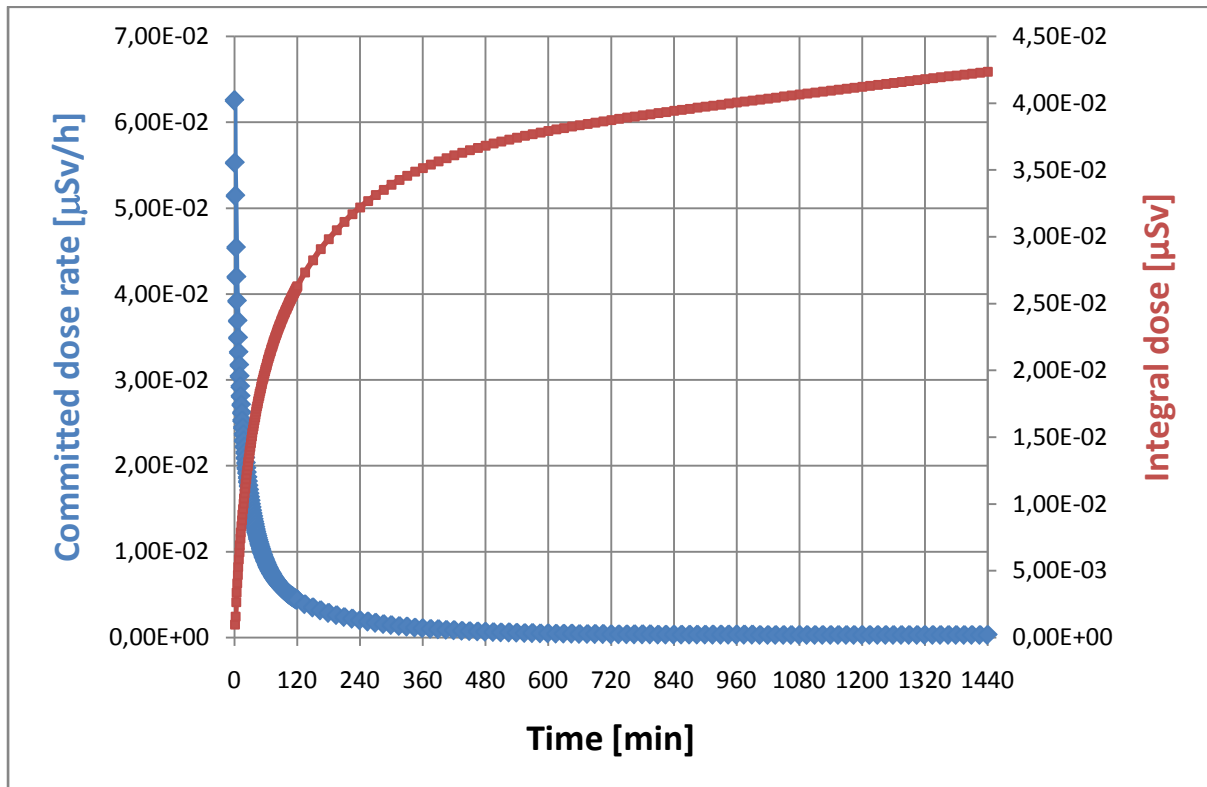


Figure 34: Rate of committed dose and integral committed dose development over time after the end of 1h beam operation with a 400 MeV ion beam at an intensity of $1\text{E}+9$ ions per second, not considering ventilation. Horizontal beam scenario.

The comparably large size of the room is explained by the fact that heavy machinery will be placed inside in order to bend and focus the beam to have it come down vertically on the target. A vertical 400 MeV ion beam scenario using a water target and 1 hour of irradiation without ventilation results in the committed dose rate pictured in Figure 35.

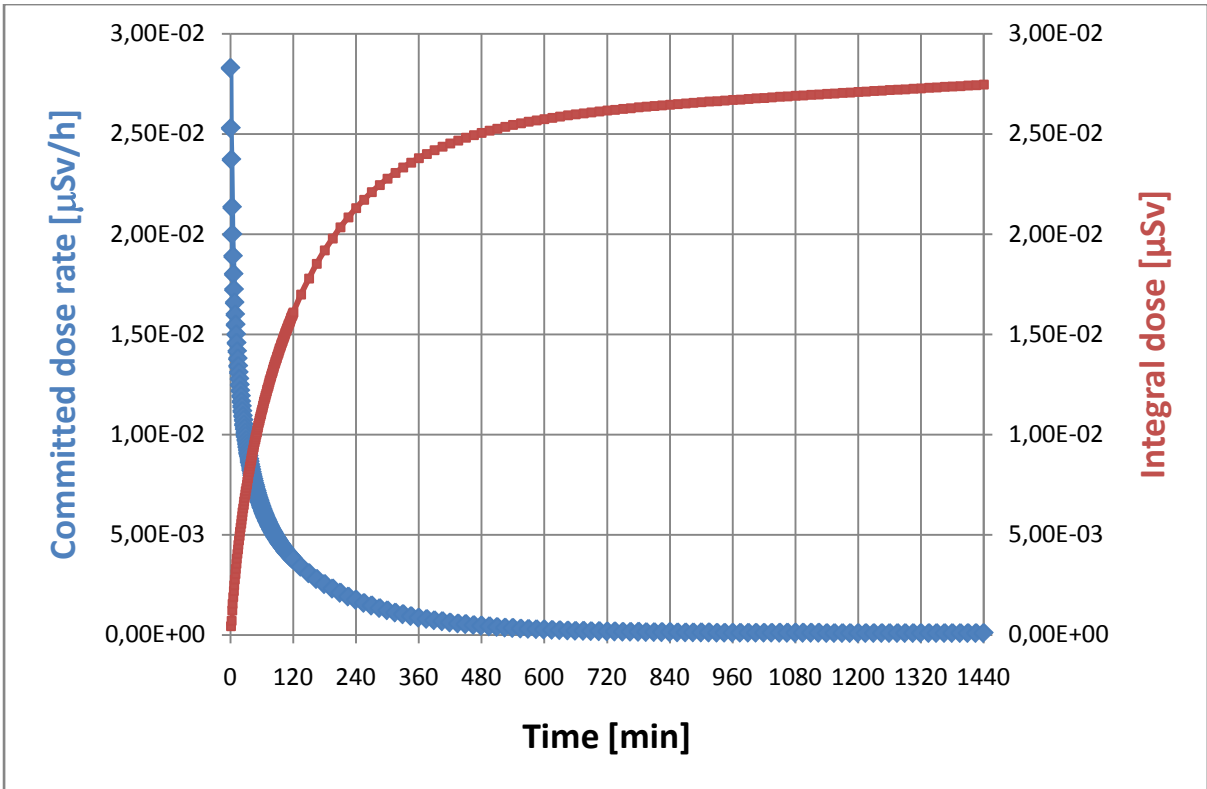


Figure 35: Rate of committed dose and integral committed dose development over time after the end of 1h beam operation with a 400 MeV ion beam at an intensity of 1E+9 ions per second, not considering ventilation. Vertical beam scenario.

The results of the vertical beam scenario that is pictured in Figure 35 show a lot less activation and therefore a lower committed dose rate than the horizontal one. The main reason for this can be explained by regarding the geometry of the scenario. As the target is placed only 125 cm above the floor, secondary particles generated inside the target have a lot less space to cross before hitting the floor, as opposed to the horizontal beam scenario, where several meters lie between the target and the next wall.

IRRADIATION ROOM 3

IR3 features only one possible beam direction for the 400 MeV ion beam, which results in a much smaller volume required for the room. Results of the simulations regarding 1 hour of irradiation with no ventilation are displayed in Figure 36.

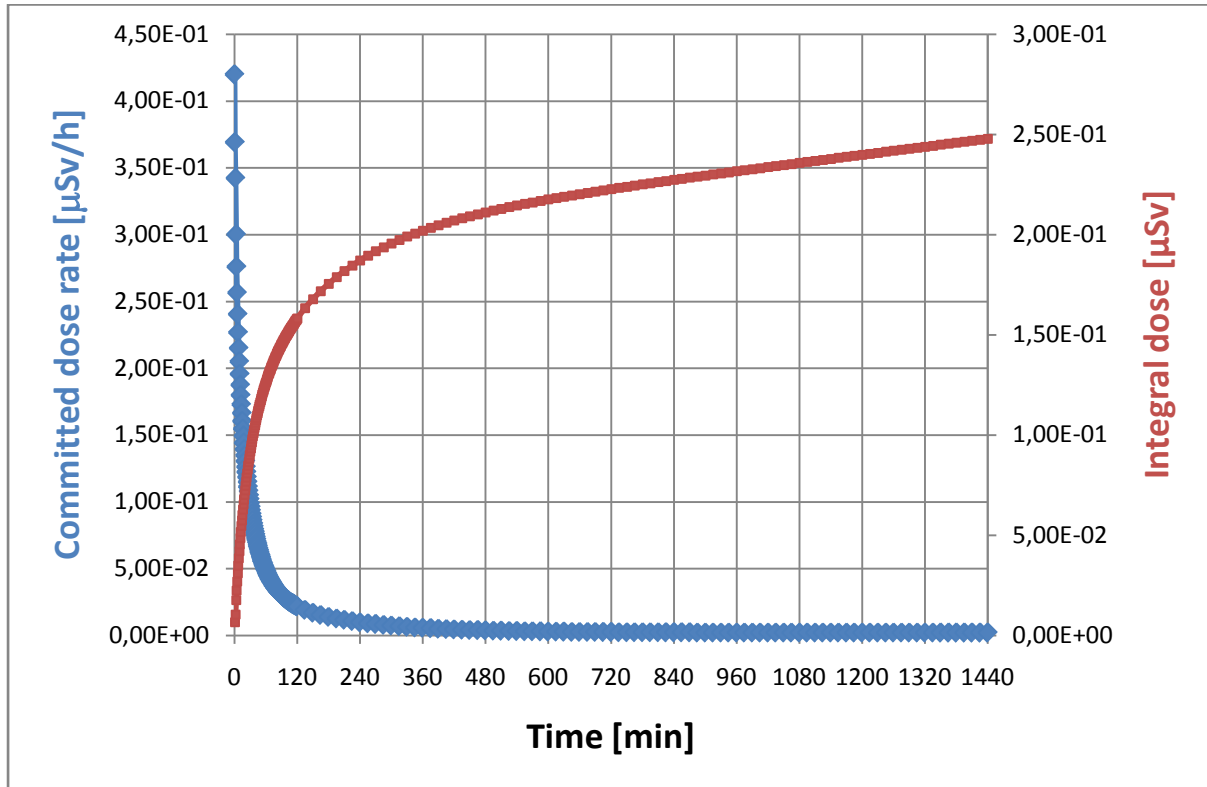


Figure 36: Rate of committed dose and integral committed dose development over time after the end of 1h beam operation with a 400 MeV ion beam at an intensity of $1\text{E}+9$ ions per second, not considering ventilation

Due to the volume of IR3 being significantly smaller than IR2, air activation per volume unit and resulting committed dose rates are evidently higher. While one hour of irradiation at the highest beam energy is a very conservatively chosen scenario for a treatment room meant to handle human patients, committed dose rate levels calculated directly after beam stop are not very high compared to a recommended maximum of $1 \mu\text{Sv/h}$.

Being the smallest room featuring the highest beam energy used for the treatment of patients, results of a conservative estimation of the average exposure of a person having to enter the room directly after the cessation of a treatment session are displayed in Figure 37.

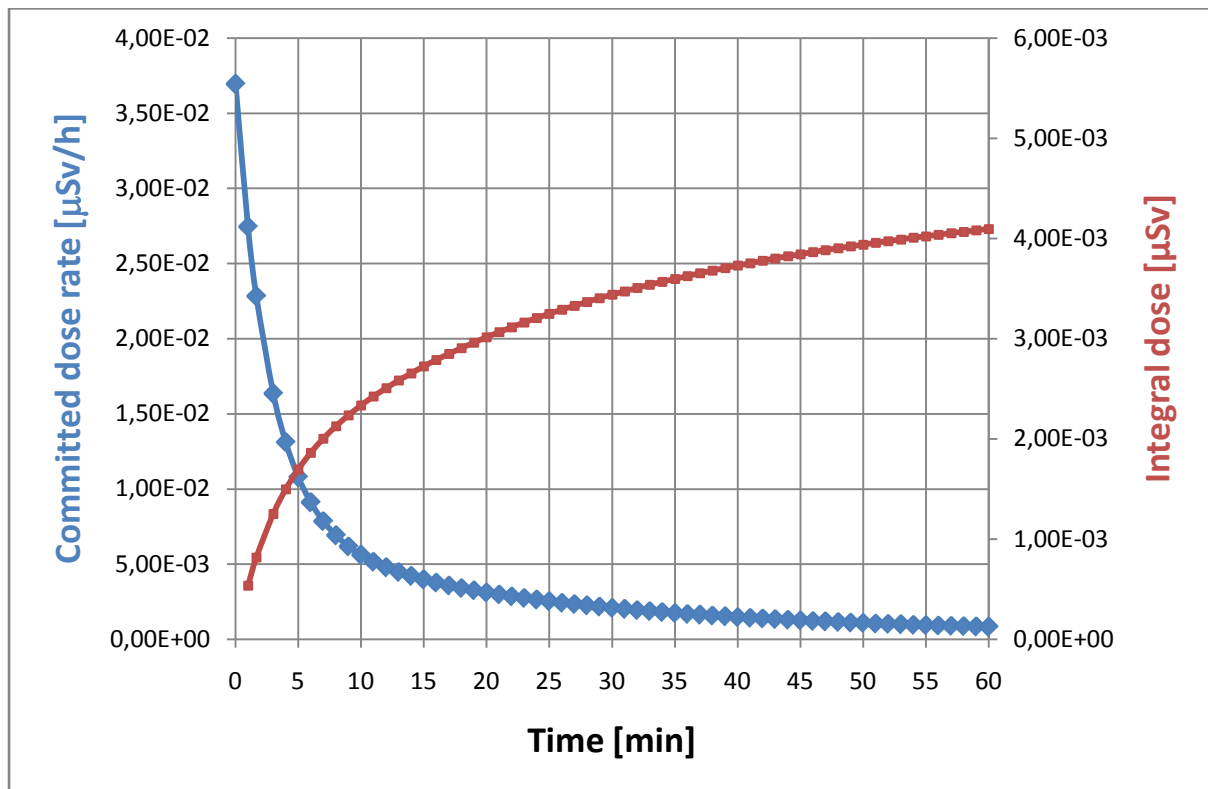


Figure 37: Rate of committed dose and integral committed dose development over time after the end of 35.2 seconds of beam operation with a 400 MeV ion beam at an intensity of 1E+9 ions per second, not considering ventilation

The integral intensity of 1E+9 carbon ions per second emitted over 35.2 seconds equals the average total delivered to a patient per treatment unit. [4] Figure 37 shows the committed dose rate and the integral committed dose development directly after the stop of the beam, ignoring ventilation.

Clinical operation requires about 20 minutes of time between two irradiation procedures, during which a complete exchange of the air inside this treatment room can be conducted. As a consequence, this scenario serves as a realistic estimation concerning air activation and its consequences for the MedAustron personnel.

IRRADIATION ROOM 4

IR4 features a gantry delivering proton beams at a maximum energy of 250 MeV, which needs a lot of space for mounting and manoeuvring, necessitating a special room geometry allowing for a very large airspace inside. Although the machine will be able to cover various possible beam directions on a 180 degree circle around the target, only three possible scenarios with an irradiation time of 1 hour and no ventilation with the gantry resting in place are regarded. Figure 38 displays the results gained from hitting the water target from a distance of 1.5 metres with a horizontal beam pointing to the outside wall of the facility, as pictured in Figure 29.

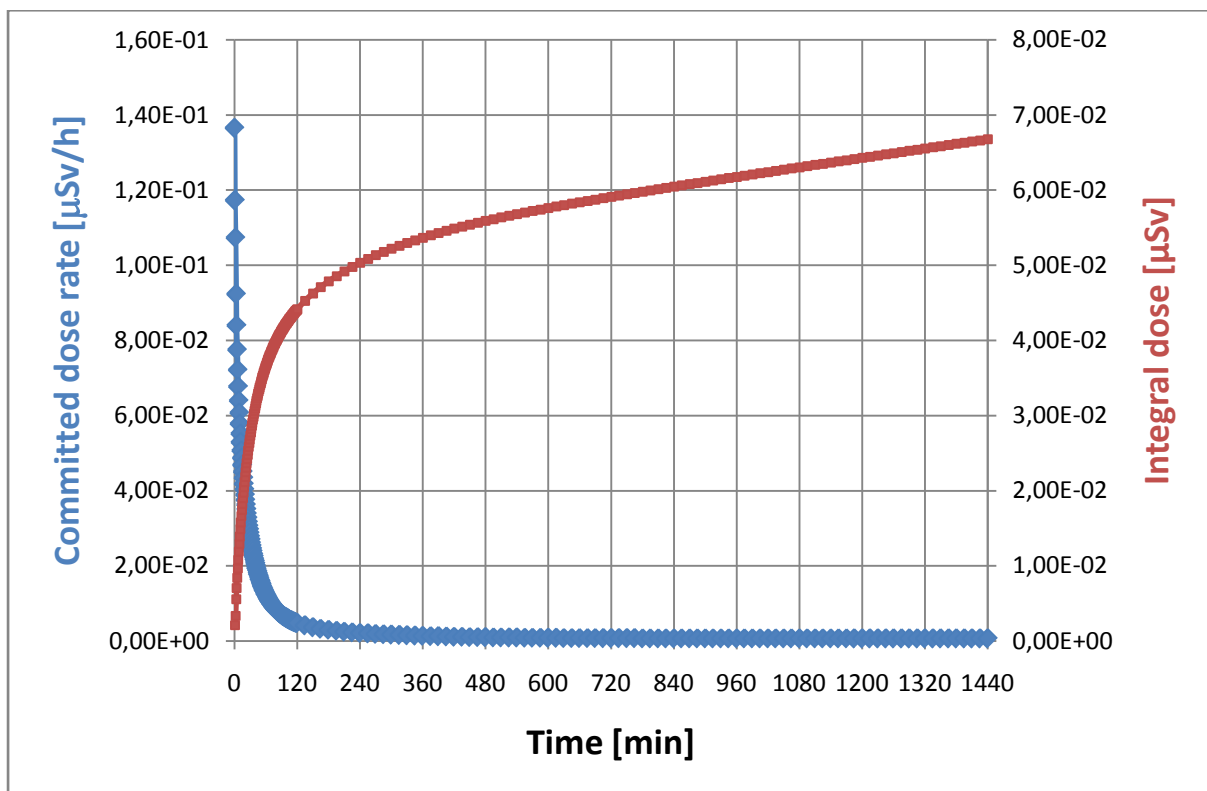


Figure 38: Rate of committed dose and integral committed dose development over time after the end of 1h beam operation with a 250 MeV proton beam at an intensity of $2E+10$ protons per second, not considering ventilation. Horizontal beam scenario.

Since the 250 MeV proton beam is started only 1.5 m in front of the target, where all primary beam particles and a lot of secondary particles are attenuated, committed dose rate calculations show very low results considering the conservative irradiation time of one hour at maximum energy.

Figure 39 displays the results when directing the beam from floor to ceiling. The beam is started 25 cm above the floor, assuming an intermediate floor being installed in the room, allowing for only 1 m distance to the target, which is still a conservative estimation of distance between gantry head and patient.

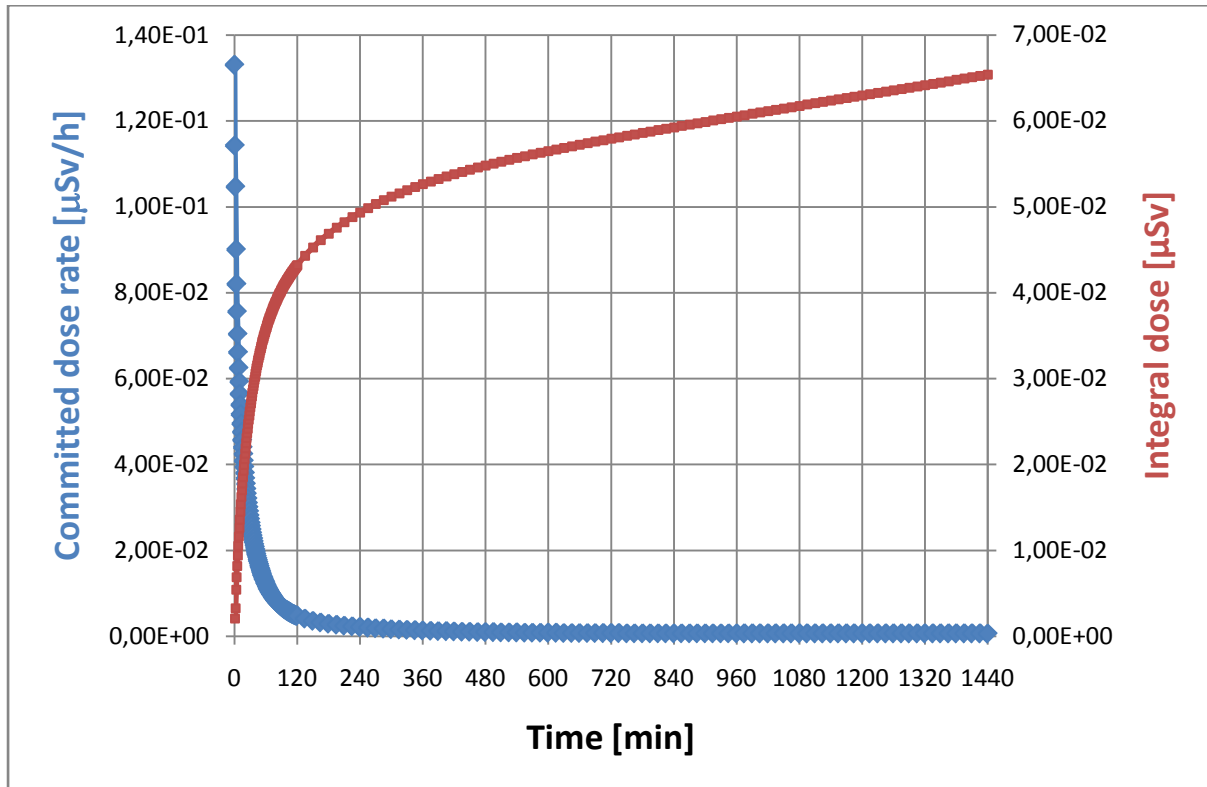


Figure 39: Rate of committed dose and integral committed dose development over time after the end of 1h beam operation with a 250 MeV proton beam at an intensity of $2\text{E}+10$ protons per second, not considering ventilation. Upward beam scenario.

In a top to bottom scenario, 1.5 metres of distance to the target is chosen again to allow for very conservative estimations, with the results pictured in Figure 40.

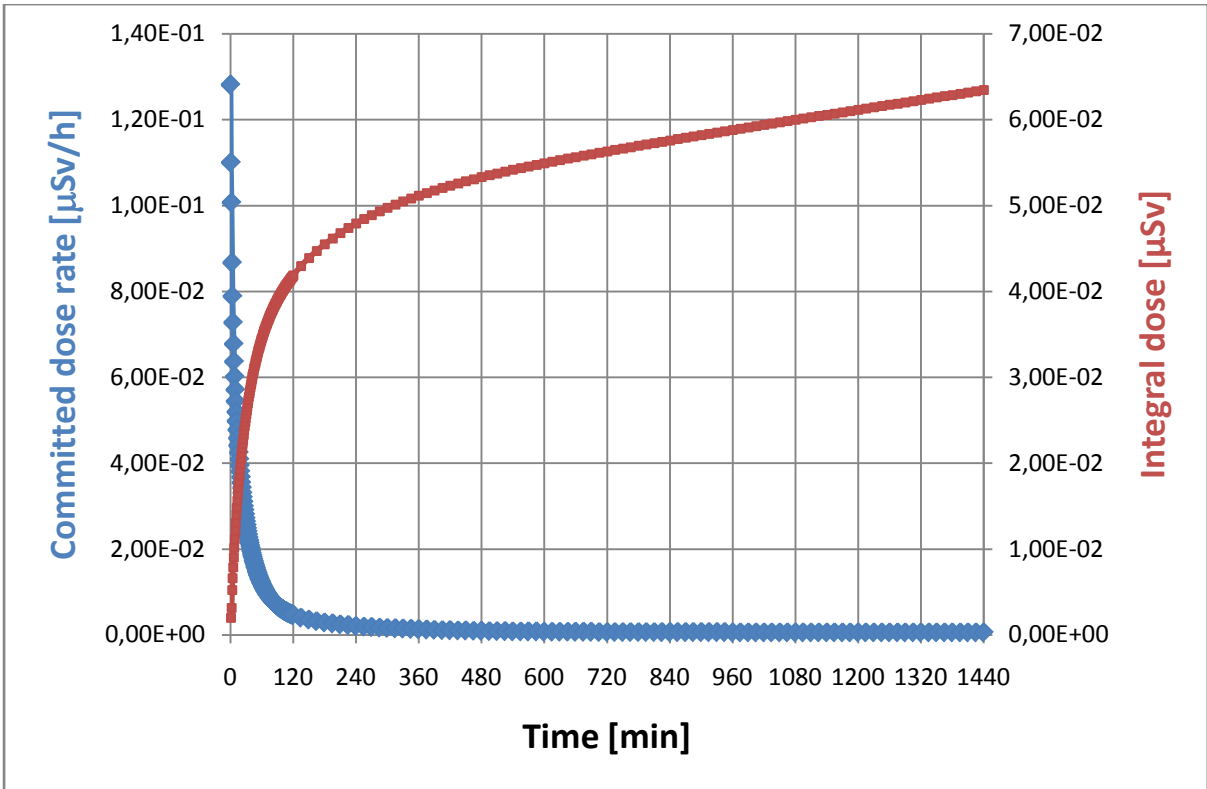


Figure 40: Rate of committed dose and integral committed dose development over time after the end of 1h beam operation with a 250 MeV proton beam at an intensity of $2E+10$ protons per second, not considering ventilation. Downward beam scenario.

Due to special geometry parameters, a higher ceiling and lower floor in regard to the assumed beam height, all 3 regarded beam scenarios show similar results.

Considering short irradiation procedures during the treatment of patients as well as the effects of ventilation on the decrease of airborne radioactivity, all conservative simulations for the treatment rooms exhibit very low estimated committed dose rates compared to the possible scenarios designed for the experimental-focused IR1.

SYNCHROTRON ROOM LOSS POINTS

During normal operation, the main part of activated air will be contributed by from the irradiation rooms, especially from irradiation room 1 for non clinical research, because the planned ventilation induces air from the irradiation rooms to the synchrotron hall in order to provide cooldown time for the isotopes before releasing them into the environment.

Activation of air in the synchrotron hall was on one hand calculated by using the expected intensities per year as an average value for constant irradiation of the air in the hall and on the other hand by separately simulating a beam loss at full intensity at each designated loss point in the hall. Designated loss points are a horizontal beam dump (bdh) integrated in the synchrotron ring, an electrostatic (ese) as well as a magnetic extraction septum (mse), a chopper dump at the beginning of the high energy beam line (HEBT) and the beam dump at the end of the HEBT.

As cooldown time for the comparisons with Ci values, 10 minutes was chosen as a conservative value for the average isotope to reach the outside air.

HORIZONTAL BEAM DUMP (BDH)

PROTON BEAM 800 MEV

In this simulation of the losses on the horizontal beam dump, all beams are impinging on the side of the tungsten target at a distance of about 5 mm from the side, as can be seen in Figure 41.

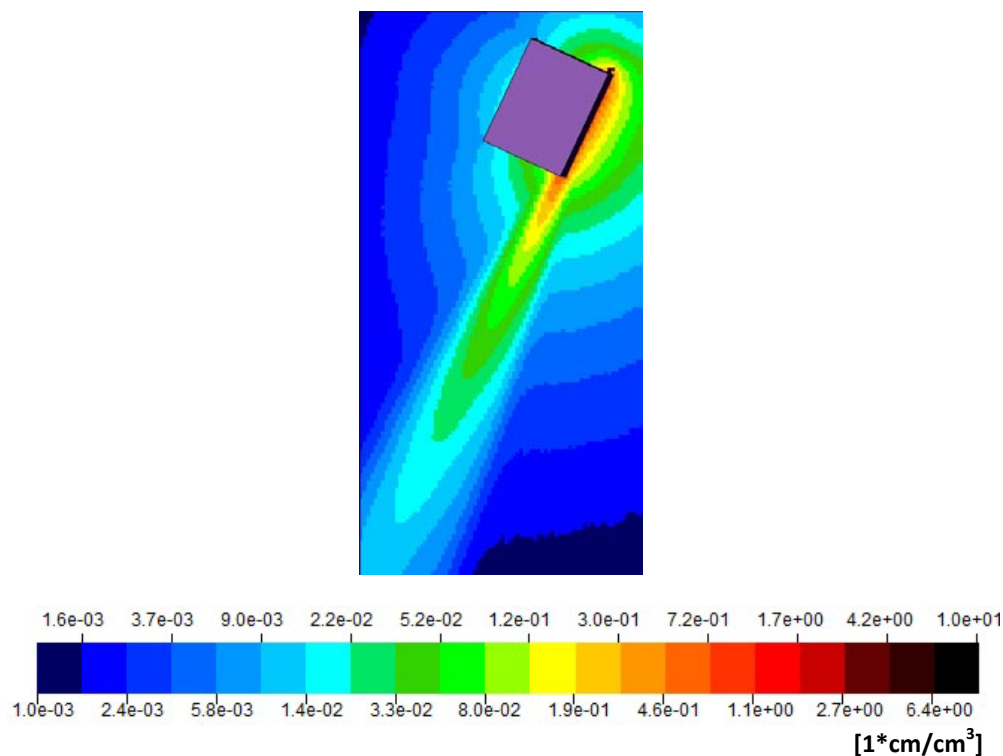


Figure 41: Fluence per primary particle of all particles on beam height when the 800 MeV proton beam hits the 8cm long Tungsten beam dump, viewed from above

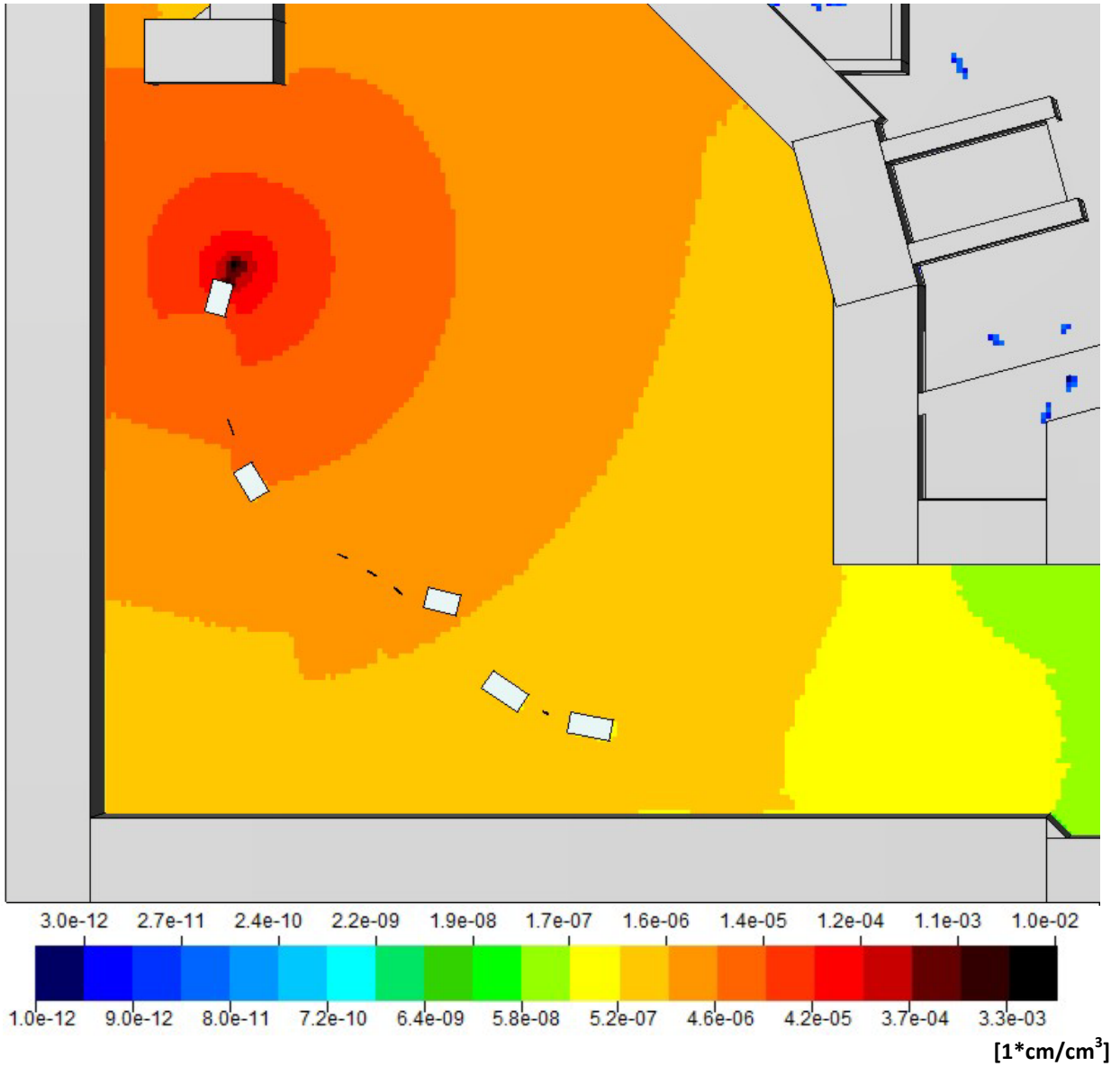


Figure 42: Fluence per primary particle of all particles in the synchrotron hall on beam height, when a proton beam with 800 MeV hits the horizontal beam dump, viewed from above

Figure 42 shows that most of the attenuated beam and its secondary particles that come out of the tungsten target are stopped at the next dipole magnet. Stronger scattered particles are crossing almost the whole synchrotron hall. In the built MedAustron facility, they will be shielded by massive amounts of machinery standing all around the hall, as well as the minor shielding mount holding the tungsten dump itself.

ION BEAM 400 MEV

Figure 43 shows the 400 MeV ion beam impinging on the side of the target and being strongly attenuated in comparison to the 800 MeV proton beam. Most secondary particles escape to the side.

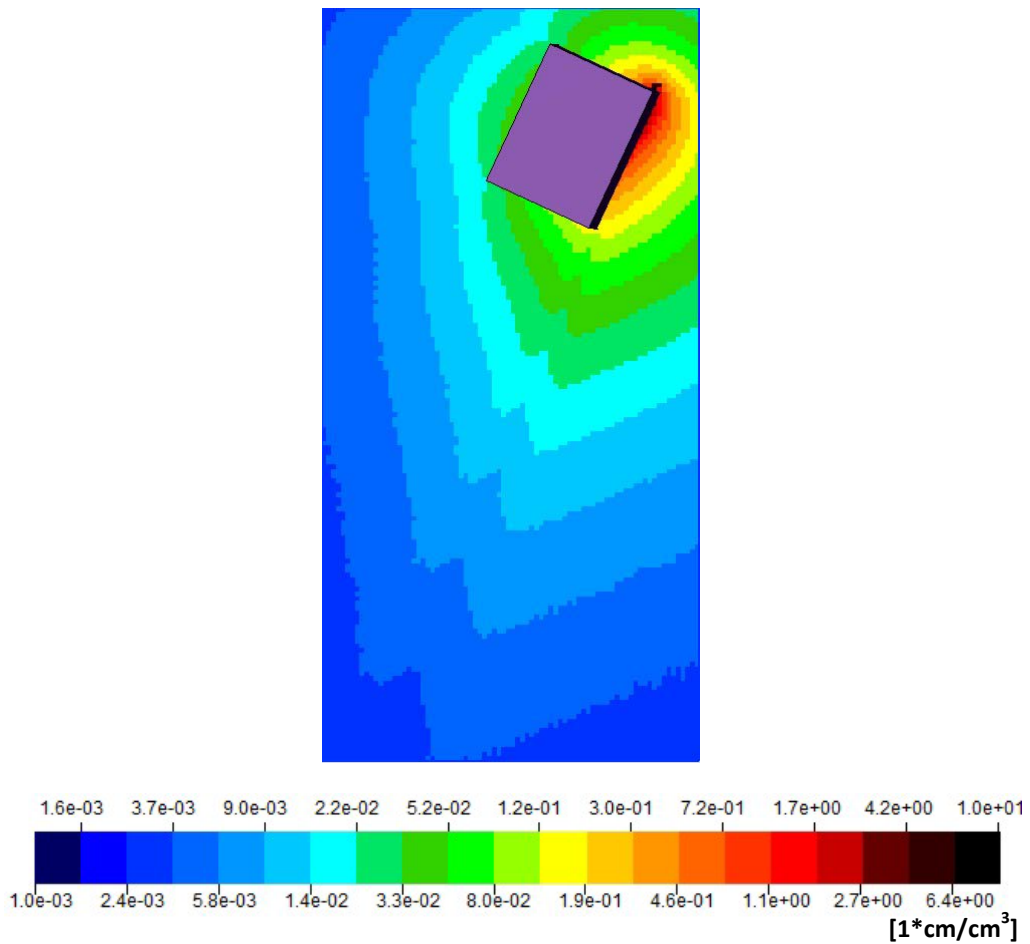


Figure 43: Fluence per primary particle of all particles on beam height when the 400 MeV ion beam hits the 8cm long Tungsten beam dump, viewed from above

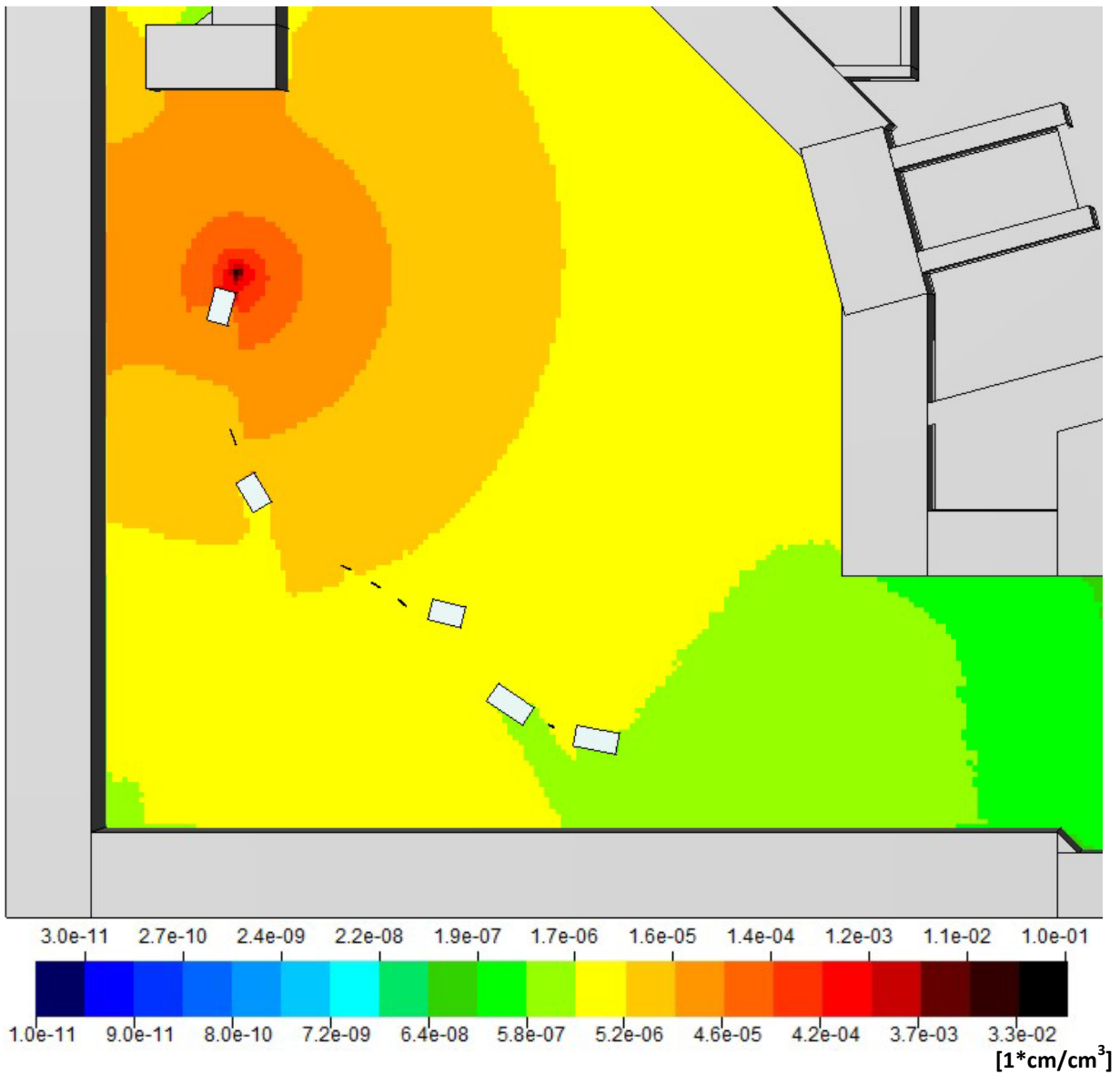


Figure 44: Fluence per primary particle of all particles in the synchrotron hall on beam height, when an ion beam with 400 MeV hits the horizontal beam dump, viewed from above

Most of the particles escaping from the side of the target are able to cross almost the whole hall without obstacles in this simulation as shown in Figure 44, which means a very conservative estimation of activation.

PROTON BEAM 250 MEV

The main 250 MeV proton beam is attenuated very fast inside the heavy tungsten target, with secondary particles escaping in an almost forward direction, pictured in Figure 45.

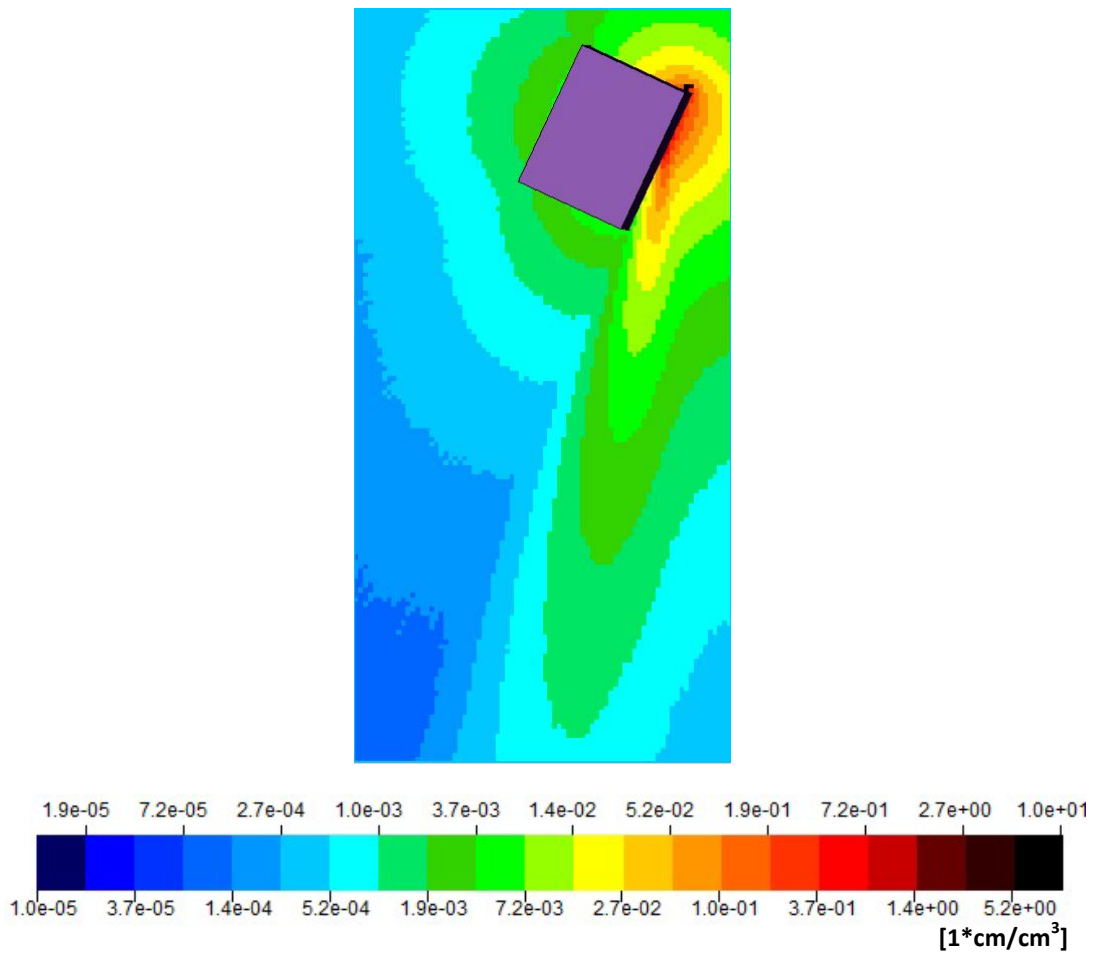


Figure 45: Fluence per primary particle of all particles on beam height when the 250 MeV proton beam hits the 8cm long Tungsten beam dump, viewed from above

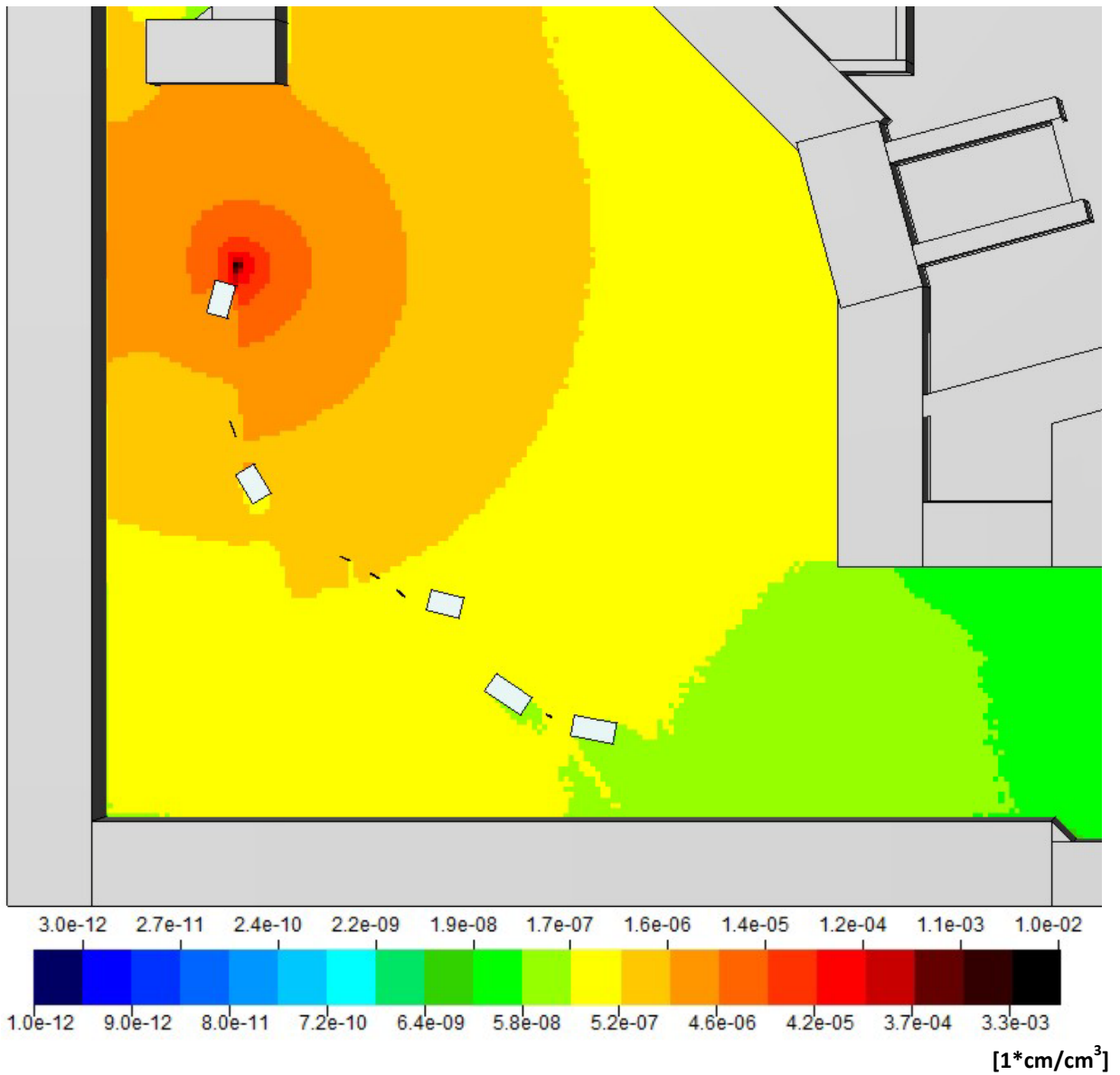


Figure 46: Fluence per primary particle of all particles in the synchrotron hall on beam height, when a proton beam with 250 MeV hits the horizontal beam dump, viewed from above

Figure 46 shows that most of the forward directed secondary particles are stopped at the next dipole. Stronger scattered particles are spreading again across the hall.

SUMMARY TABLES

Estimations for the activity of the air that is to be released, after dilution and at least 10 minutes of cooling, compared to limits defined by Austrian law are given in Table 31, which lists, besides the scheduled intensity per year for each type of beam, the sum values gained by comparing the calculated activity of each calculated isotope with their respective Ci value and summing up all of these comparison values. For an unrestricted release into the environment, this sum value must not exceed 1.

In this scenario, each Ci value of each isotope is not exceeded by their respective activity, which can be regarded in the tables in Appendix C.

The maximum intensities are defined as for the treatment rooms with $2E+10$ protons per second, respectively $1E+9$ ions per second.

Table 31: Sum values of specific activities compared to Ci values after 10 minutes of cooling time. Sum av/Ci compares specific activities generated considering average intensity, Sum max/Ci compares activities generated by consideration of maximum available intensity.

bdh	Intensity/y	Sum av/Ci	Sum max/Ci
p800	2.40E+14	1.66E-03	4.37E+00
i400	1.80E+14	2.72E-03	4.77E-01
p250	1.50E+15	3.68E-03	8.45E-01

At average loss rate, contribution to the overall activity in the air is not very high. Legal limits of activity in the air are exceeded in this simulation if the proton beam hits the target at maximum energy of 800 MeV and intensity for over an hour, which is an absolute worst case scenario, but not intended to happen. It should be considered, that this is a very conservative estimation totally ignoring self shielding of the final design of the machine. A lot of machine parts, beampipe containers and additional smaller magnets will be attenuating the beam much stronger than in this simulation, where almost no obstacles for scattered particles are installed.

ELECTROSTATIC SEPTUM (ESE)

PROTON BEAM 800 MEV

Fluence distribution in Figure 47 shows the main high energy beam being stopped inside the molybdenum foil with secondary particles heading strongly in forward direction. The foil in the simulation is deliberately made much thicker than in reality, to lose as much of the beam as possible on the designated loss point at one shot.

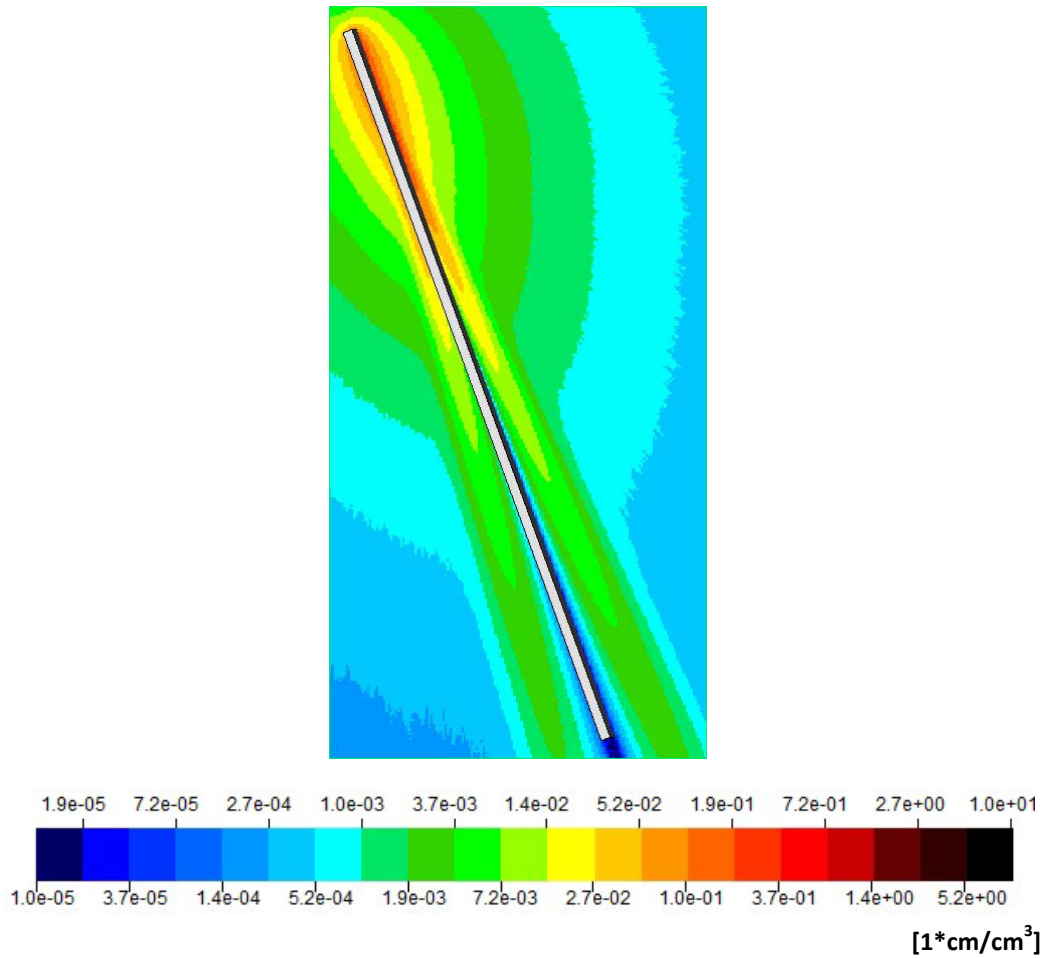


Figure 47: Fluence per primary particle of all particles on beam height when the 800 MeV proton beam hits the molybdenum electromagnetic septum, viewed from above

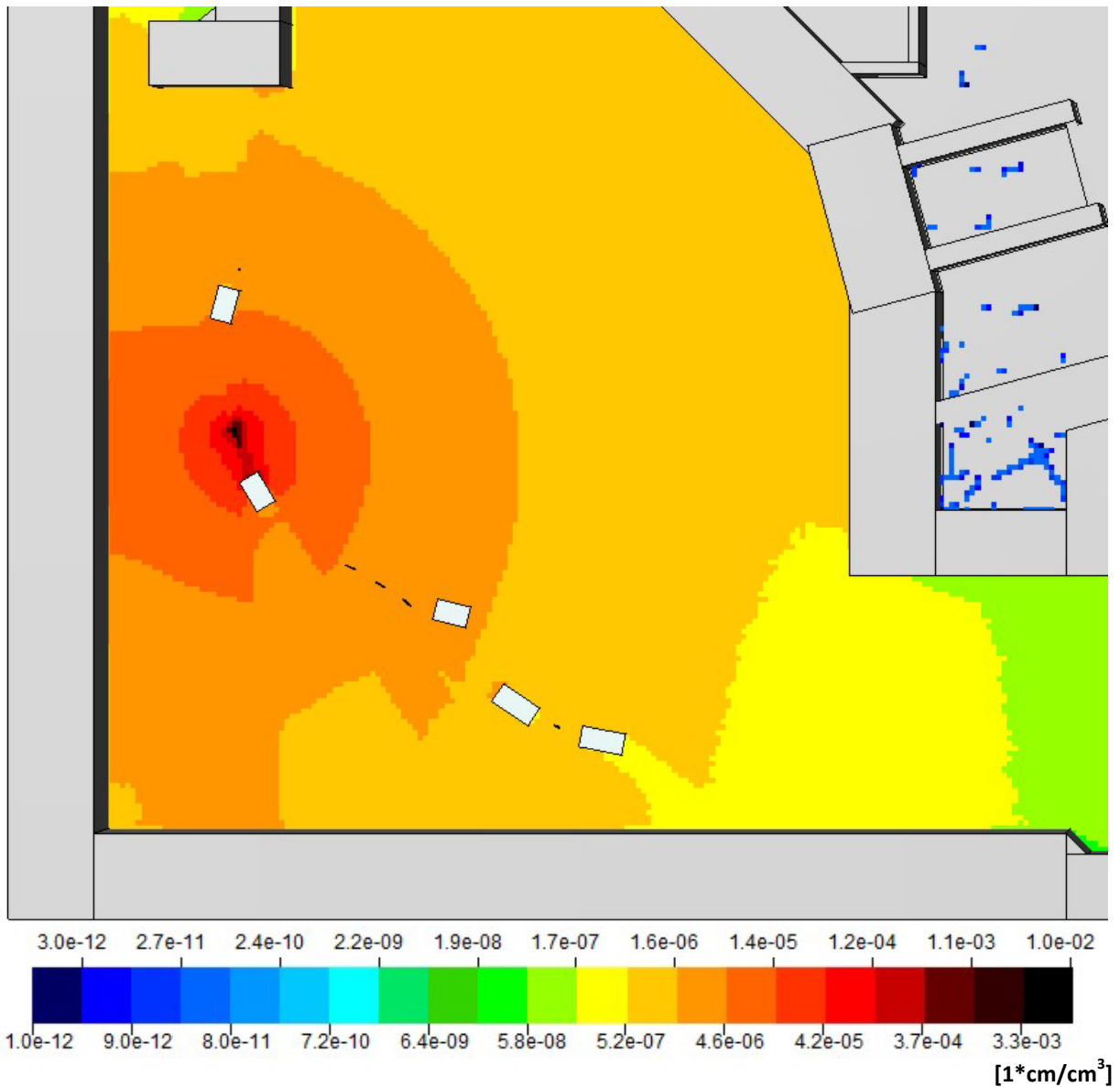


Figure 48: Fluence per primary particle of all particles in the synchrotron hall on beam height, when a proton beam with 800 MeV hits the electromagnetic septum, viewed from above

Most of the particles going away from the target are stopped at the next installed dipole, seen in Figure 48. Using a thicker foil means a higher effect of self shielding, which is more than compensated by the fact that many machine parts in the vicinity, for a example a large titan electrode bar parallel to the foil, which would shield a lot of stray radiation, are missing in this simulation.

ION BEAM 400 MEV

Figure 49 shows the 400 MeV ion beam being attenuated very strongly in the first few centimeters of the heavy molybdenum foil.

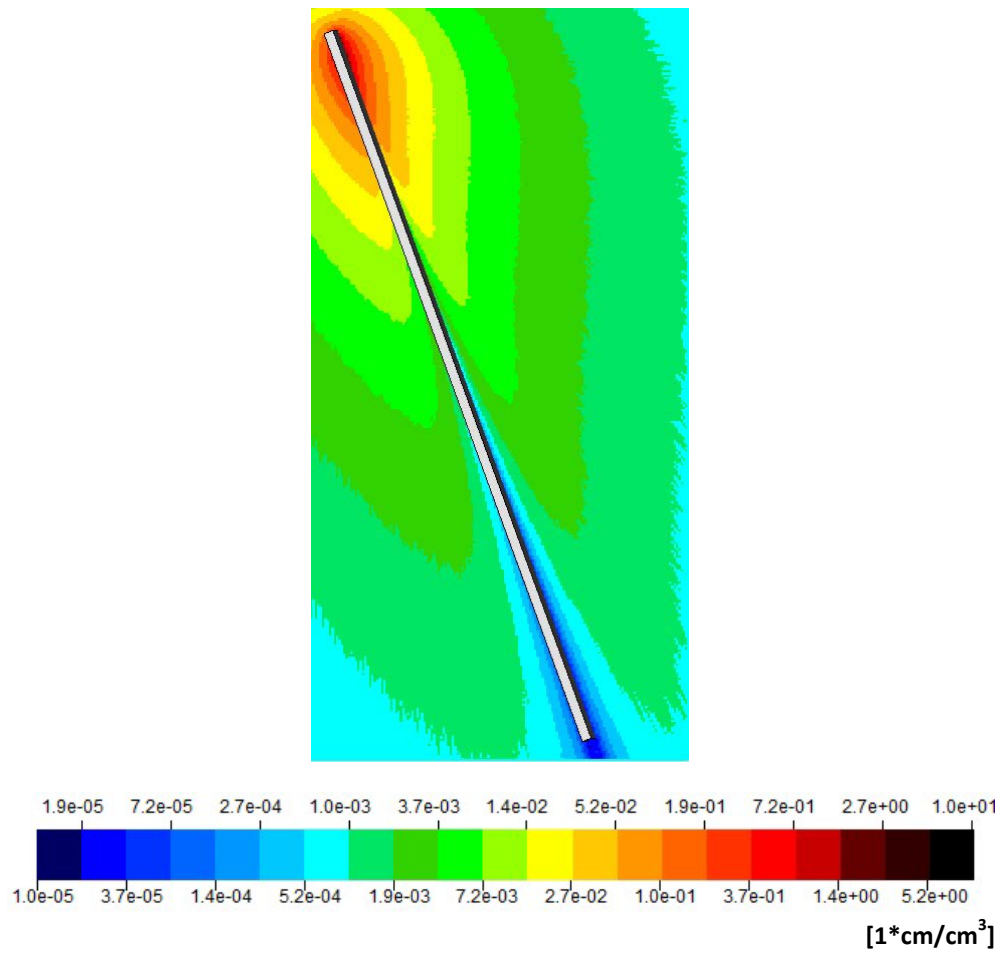


Figure 49: Fluence per primary particle of all particles on beam height when the 400 MeV ion beam hits the molybden electromagnetic septum, viewed from above

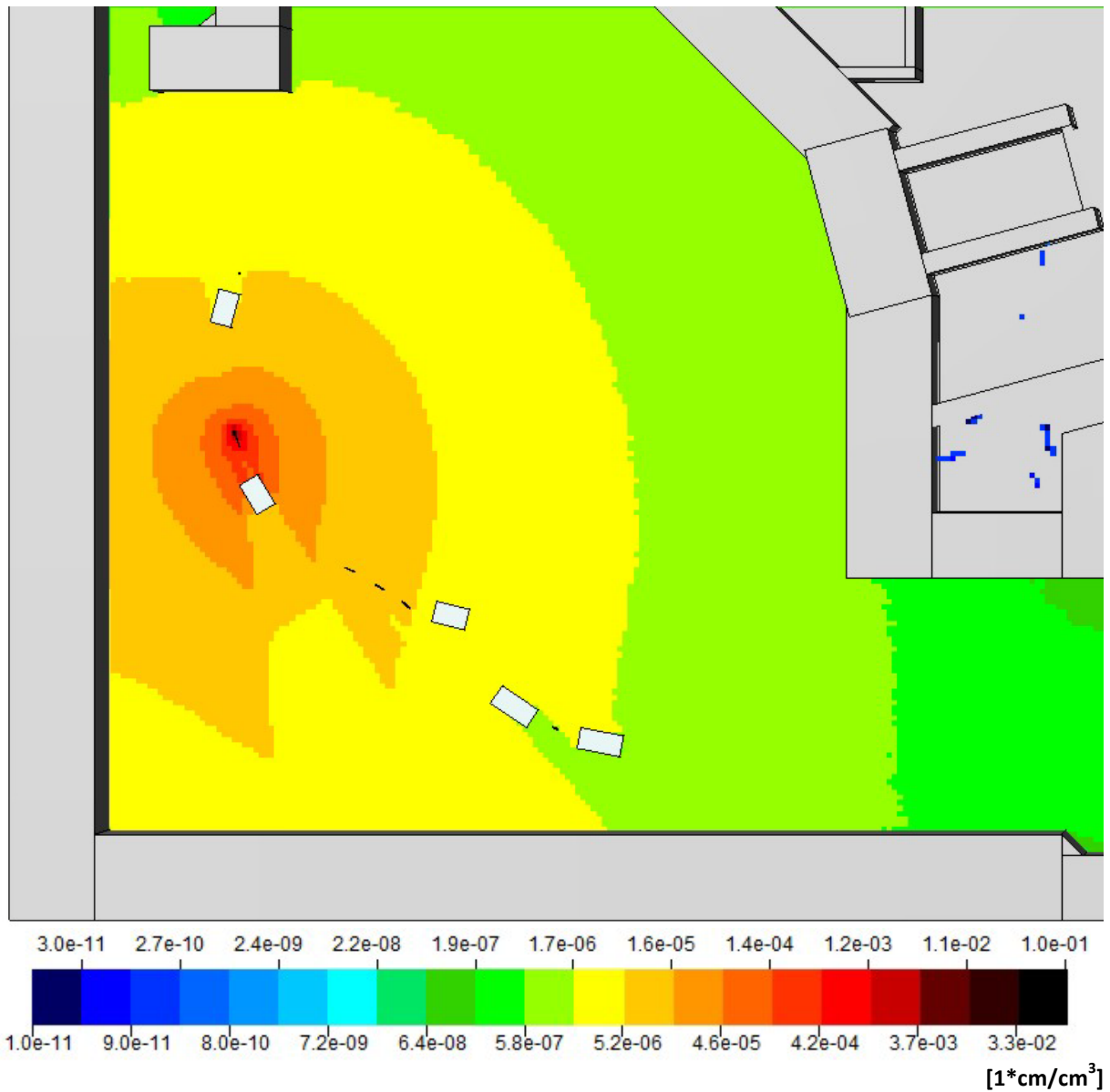


Figure 50: Fluence per primary particle of all particles in the synchrotron hall on beam height, when an ion beam with 400 MeV hits the electromagnetic septum, viewed from above

The uniform distribution of scattered particles seen in Figure 50 finds almost no obstacles when crossing the hall, making for a very conservative estimation.

PROTON BEAM 250 MEV

The 250 MeV proton beam is halted at the very start of the foil as seen in Figure 51, with many secondary particles escaping to both sides, but in almost forward direction.

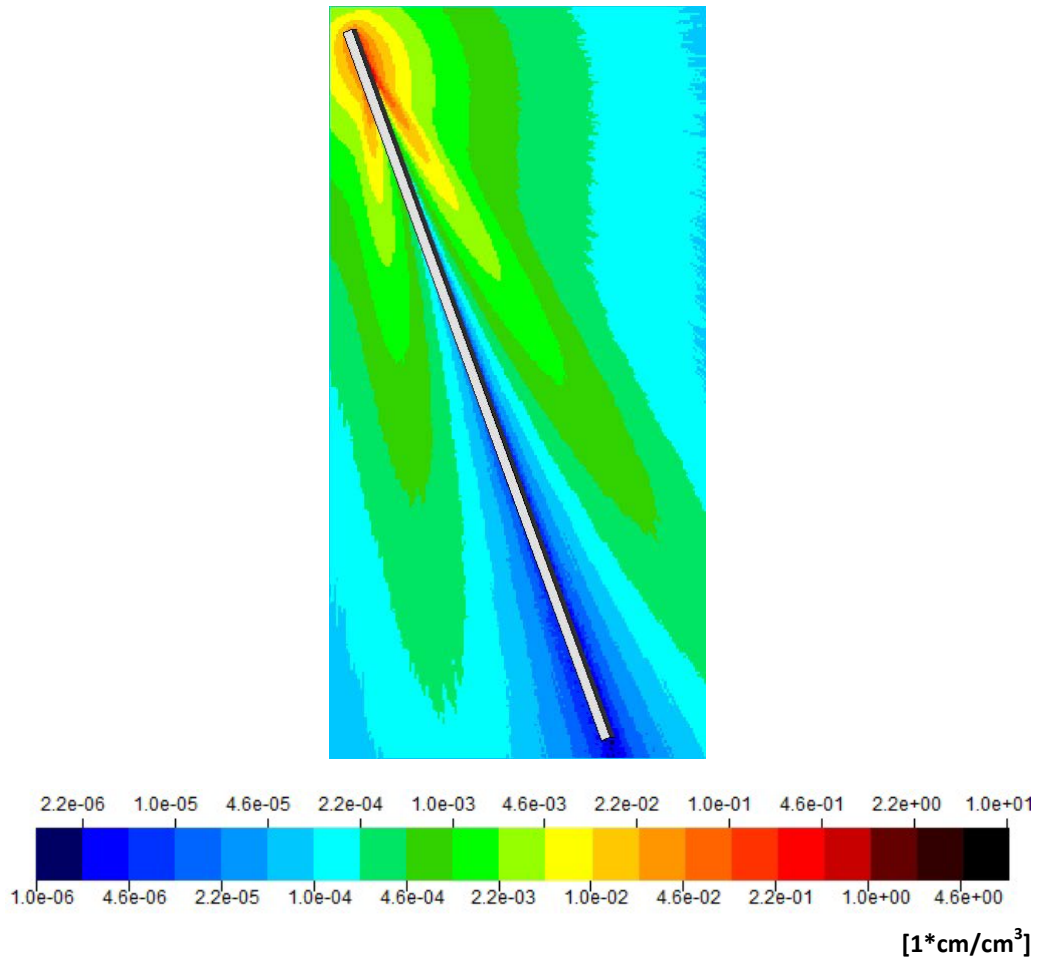


Figure 51: Fluence per primary particle of all particles on beam height when the 250 MeV proton beam hits the molybdenum electromagnetic septum, viewed from above

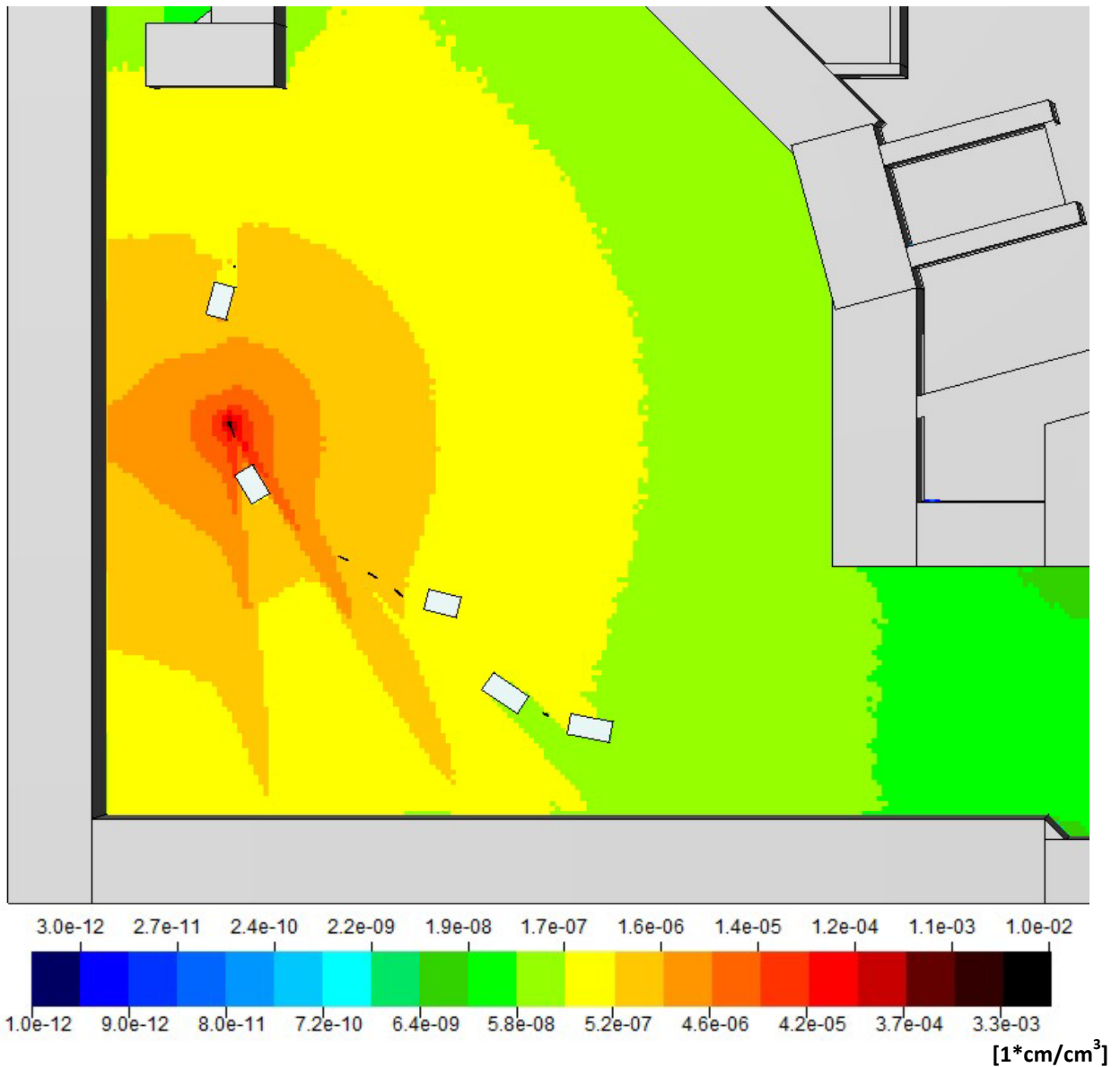


Figure 52: Fluence per primary particle of all particles in the synchrotron hall on beam height, when a proton beam with 250 MeV hits the electromagnetic septum, viewed from above

In this case, the main directions of the scattered secondary particles point slightly around the next big obstacle, displayed in Figure 52, leaving plenty of space to irradiate big parts of the hall, whereas in a more realistic scenario, the particles would be attenuated by various machine parts.

SUMMARY TABLES

Estimations for the activity of the air that is to be released, after dilution and at least 10 minutes of cooling, compared to limits defined by Austrian law are given in Table 32, which lists, besides the scheduled intensity per year for each type of beam, the sum values gained by comparing the calculated activity of each calculated isotope with their respective Ci value and summing up all of these comparison values. For an unrestricted release into the environment, this sum value must not exceed 1.

In this scenario, each Ci value of each isotope is not exceeded by their respective activity, which can be regarded in the tables in Appendix C.

The maximum intensities are defined as for the treatment rooms with $2E+10$ protons per second, respectively $1E+9$ ions per second.

Table 32: Sum values of specific activities compared to Ci values after 10 minutes of cooling time. Sum av/Ci compares specific activities generated considering average intensity, Sum max/Ci compares activities generated by consideration of maximum available intensity.

ese	Intensity/y	Sum av/Ci	Sum max/Ci
p800	2.90E+14	2.53E-03	5.51E+00
i400	3.00E+13	6.76E-04	7.11E-01
p250	2.50E+14	6.59E-04	1.66E+00

At average loss rate, contribution to the overall activity in the air is not very high. Legal limits of activity in the air are exceeded in this simulation if the proton beam hits the target at maximum intensity for over an hour, which is an absolute worst case scenario, but not intended to happen. It should be considered, that this is a very conservative estimation totally ignoring self shielding of the final design of the machine. A lot of machine parts, beampipe containers and additional smaller magnets will be attenuating the beam much stronger than in this simulation, where almost no obstacles for scattered particles are installed.

MAGNETIC SEPTUM (MSE)

PROTON BEAM 800 MEV

Only the part of the copper coil that is directly colliding with the beam is implemented for simulating losses at the magnetic septum displayed in Figure 53, resulting in less attenuation of scattered secondaries.

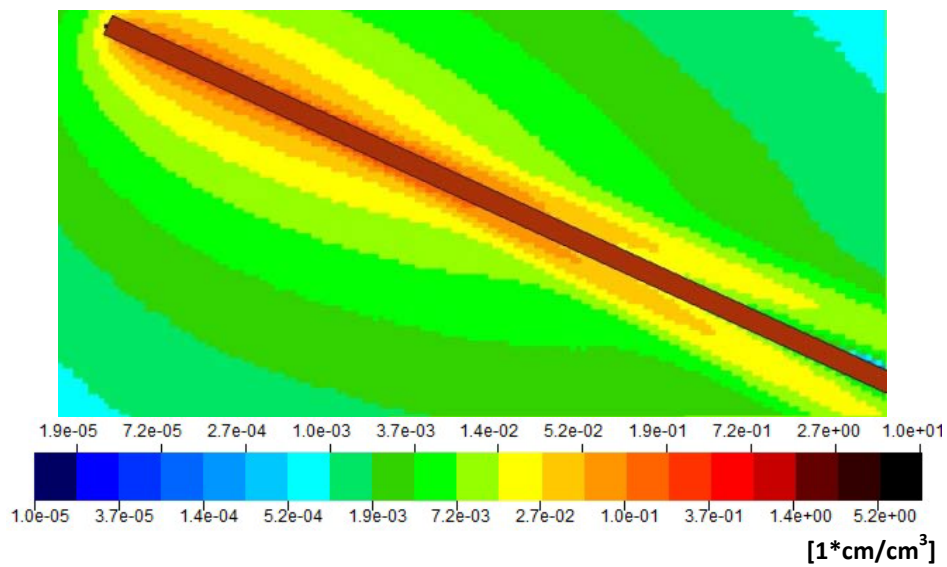


Figure 53: Fluence per primary particle of all particles on beam height when the 800 MeV proton beam hits the copper coil of the magnetic septum, viewed from above

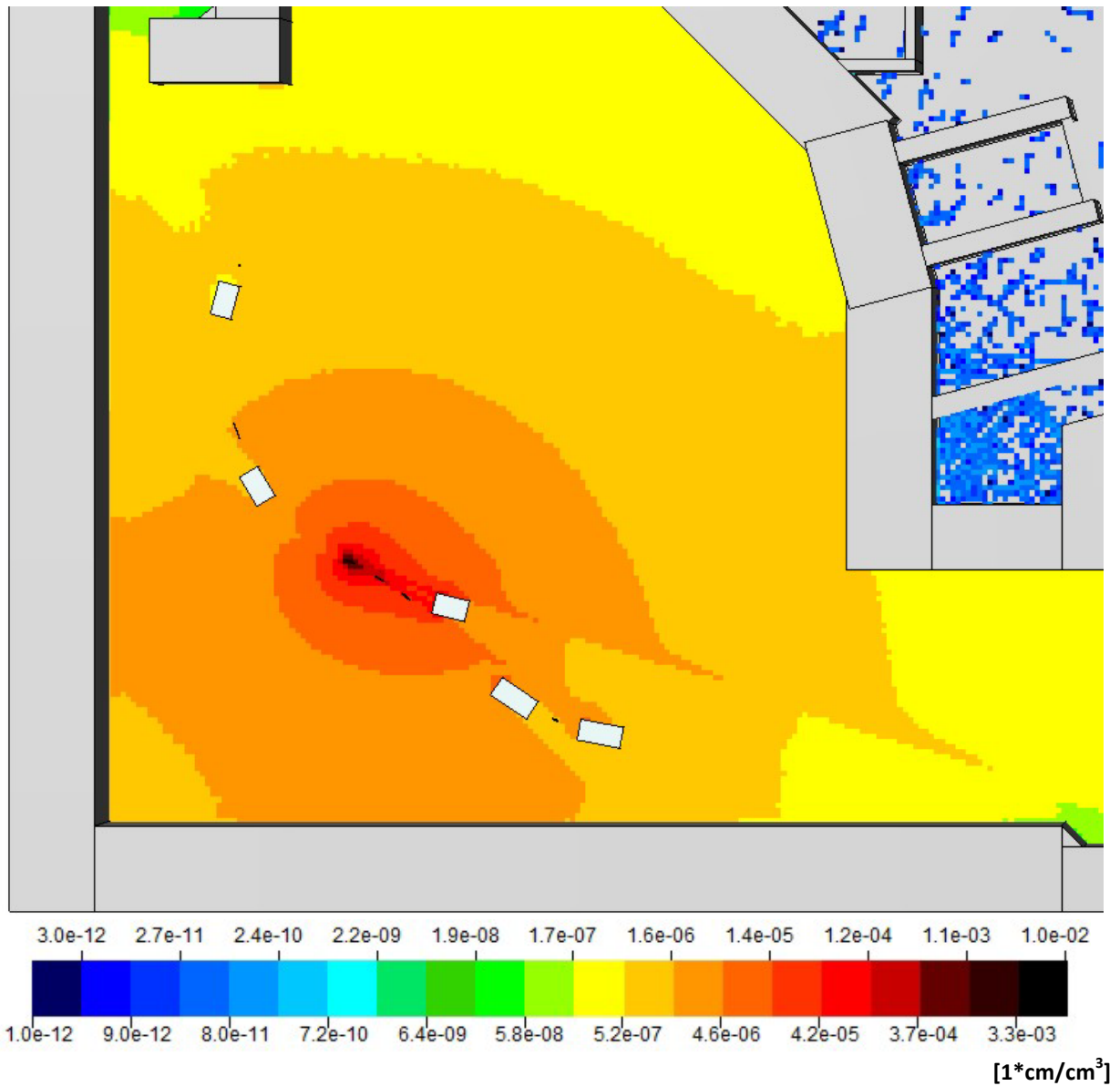


Figure 54: Fluence per primary particle of all particles in the synchrotron hall on beam height, when a proton beam with 800 MeV hits the copper coil of the magnetic septum, viewed from above

Some, but not all of the forward directed secondary particles are halted by the next dipole. In the fluence USBIN at beam height in Figure 54, a comparably large portion of scattered particles cross a large volume of the hall reaching down deep into the High Energy Particle Transfer Line. This also results in the highest air activation rate in the hall considering all simulated loss points. In the final design of the machine, iron yokes together with the rest of the copper coils, which are not implemented in this simulation, will make for a very effective shielding around and along the magnetic septum.

ION BEAM 400 MEV

The 400 MeV ion beam is attenuated very strongly in the first part of the copper target, with secondary particles escaping mostly to the side, as displayed in Figure 55.

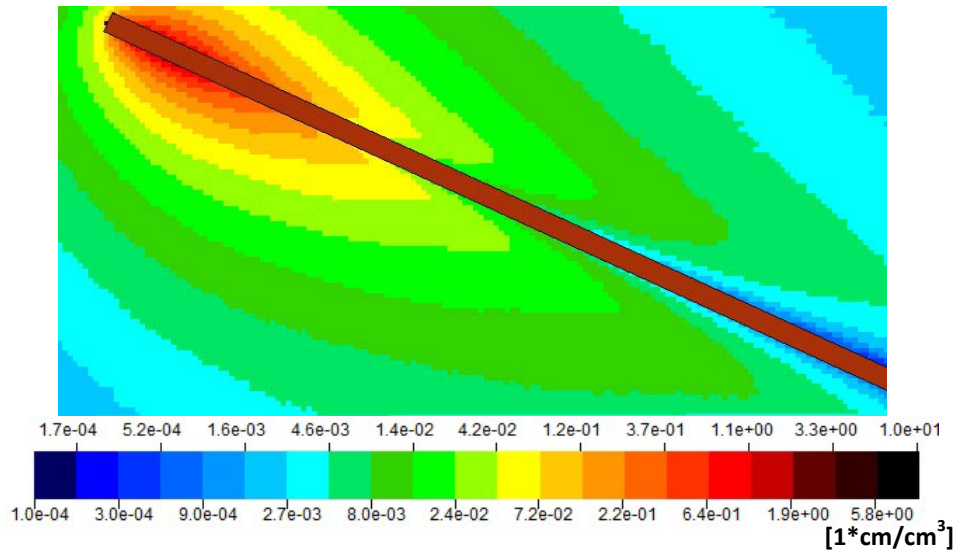


Figure 55: Fluence per primary particle of all particles on beam height when the 400 MeV ion beam hits the copper coil of the magnetic septum, viewed from above

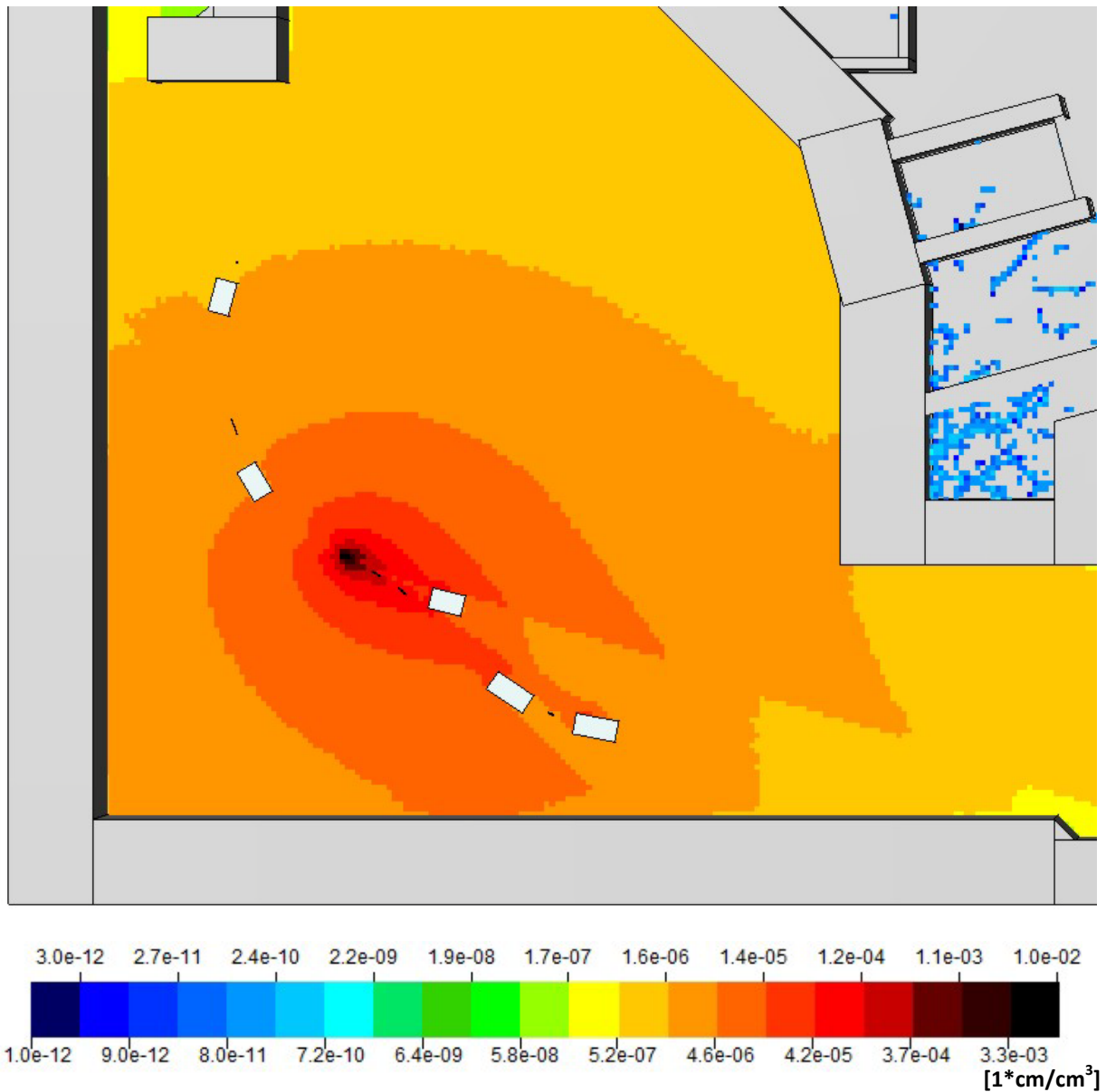


Figure 56: Fluence per primary particle of all particles in the synchrotron hall on beam height, when an ion beam with 400 MeV hits the copper coil of the magnetic septum, viewed from above

As pictured in Figure 56, forward-directed secondary particles are halted after a few meters at the dipole blocks in this simulation, with a host of secondary particles reaching to the sides through the hall.

PROTON BEAM 250 MEV

Figure 57 shows the 250 MeV protons being halted at the very start of the copper target, with secondary particles escaping in forward direction with a slight angle.

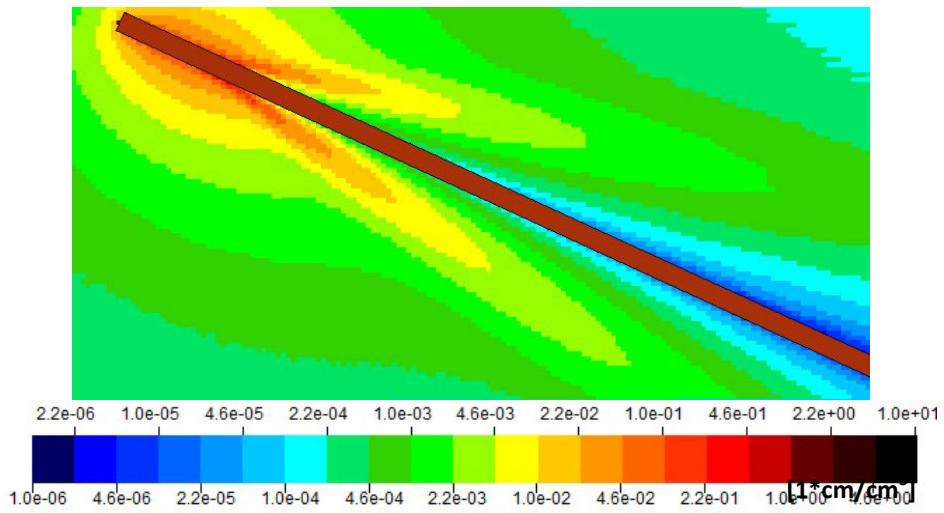


Figure 57: Fluence per primary particle of all particles on beam height when the 250 MeV proton beam hits the copper coil of the magnetic septum, viewed from above

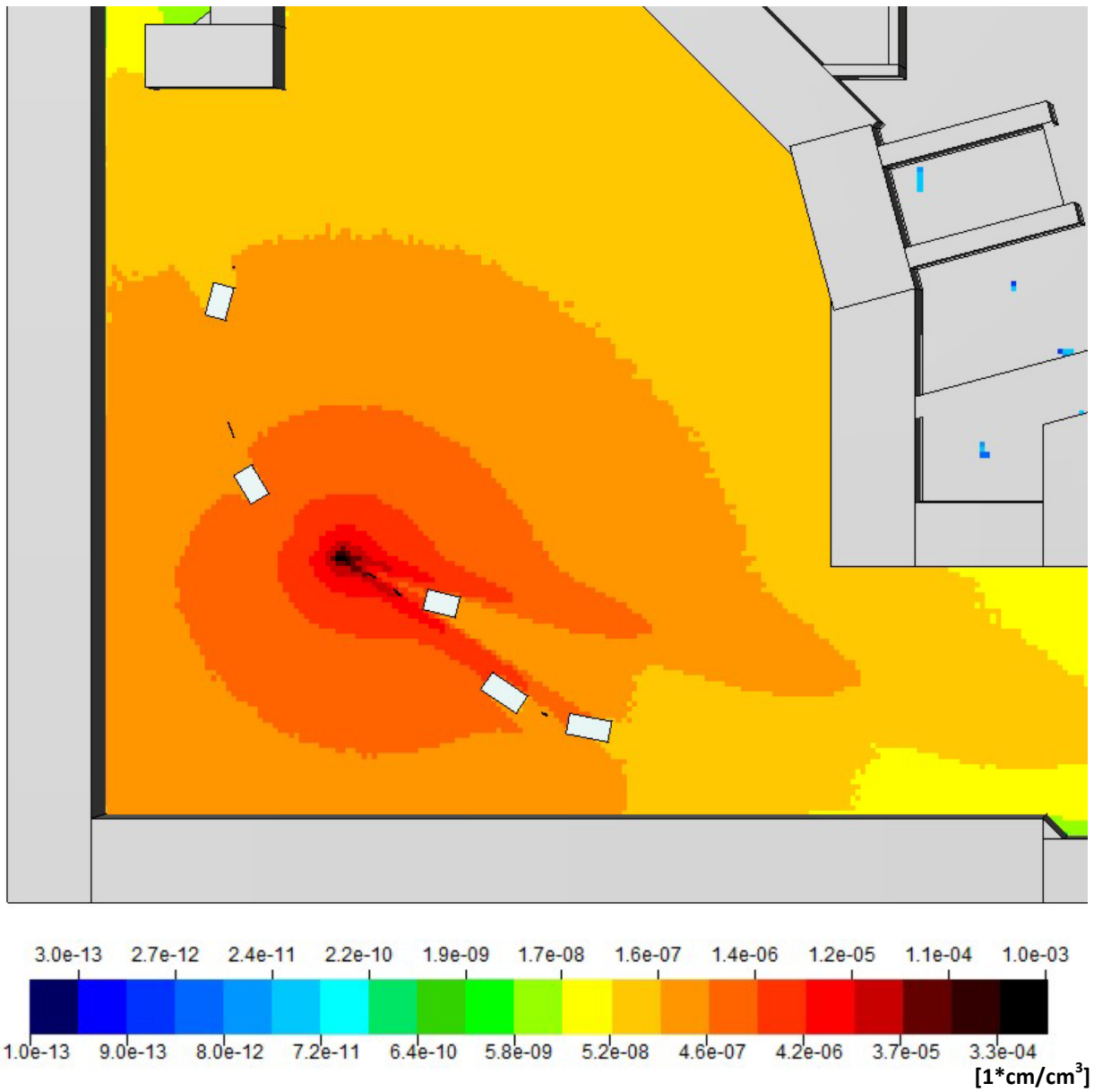


Figure 58: Fluence per primary particle of all particles in the synchrotron hall on beam height, when an proton beam with 250 MeV hits the copper coil of the magnetic septum, viewed from above

The distribution of secondary particles pictured in Figure 58 is slightly directed to the HEBT, allowing the particles to interact with a big volume of air.

SUMMARY TABLES

Estimations for the activity of the air that is to be released, after dilution and at least 10 minutes of cooling, compared to limits defined by Austrian law are given in Table 33, which lists, besides the scheduled intensity per year for each type of beam, the sum values gained by comparing the calculated activity of each calculated isotope with their respective Ci value and summing up all of these comparison values. For an unrestricted release into the environment, this sum value must not exceed 1.

In this scenario, each Ci value of each isotope is not exceeded by their respective activity, which can be regarded in the tables in Appendix C.

The maximum intensities are defined as for the treatment rooms with 2E+10 protons per second, respectively 1E+9 ions per second.

Table 33: Sum values of specific activities compared to Ci values after 10 minutes of cooling time. Sum av/Ci compares specific activities generated considering average intensity, Sum max/Ci compares activities generated by consideration of maximum available intensity.

mse	Intensity/y	Sum av/Ci	Sum max/Ci
p800	2.90E+14	3.07E-03	6.68E+00
i400	3.00E+13	8.26E-04	8.68E-01
p250	2.50E+14	6.96E-04	1.75E+00

At average loss rate, contribution to the overall activity in the air is not very high. Legal limits of activity in the air are exceeded in this simulation if the proton beam hits the target at maximum intensity for over an hour, which is an absolute worst case scenario, but not intended to happen. It should be considered, that this is a very conservative estimation totally ignoring self shielding of the final design of the machine. A lot of machine parts, beampipe containers and additional smaller magnets will be attenuating the beam much stronger than in this simulation, where almost no obstacles for scattered particles are installed.

CHOPPER DUMP (BDC)

PROTON BEAM 800 MEV

Similar to the horizontal beam dump in form and material, but with a few important differences are losses at the chopper dump simulated. The tungsten block is 30 cm long instead of 8 cm, and the beams point of entry is situated roughly 1 cm away from the side, which can be seen in Figure 59.

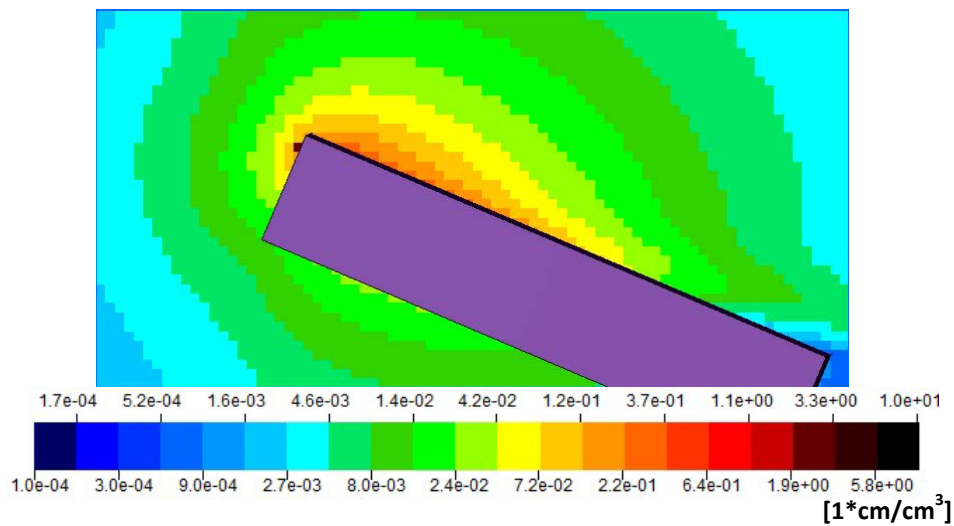


Figure 59: Fluence per primary particle of all particles on beam height when the 800 MeV proton beam hits the 30 cm long Tungsten beam dump, viewed from above

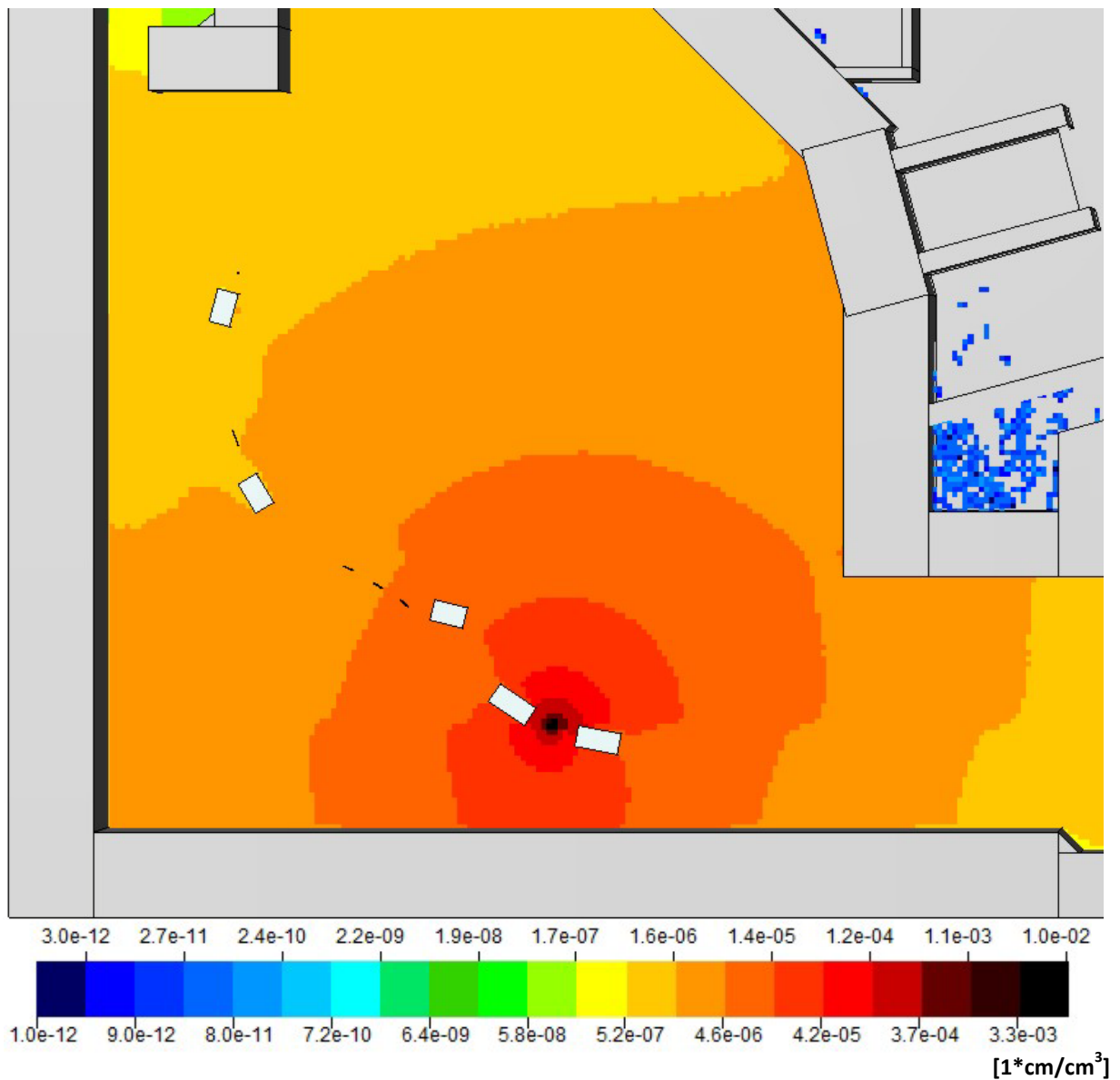


Figure 60: Fluence per primary particle of all particles in the synchrotron hall on beam height, when a proton beam with 800 MeV hits the 30 cm long Tungsten beam dump, viewed from above

Due to the better self shielding of the tungsten dump and of course the two dipoles in the vicinity, secondary particles emerge mostly from the side, pictured in Figure 60.

ION BEAM 400 MEV

The 400 MeV ion beam is fully halted inside the target, as seen in Figure 61.

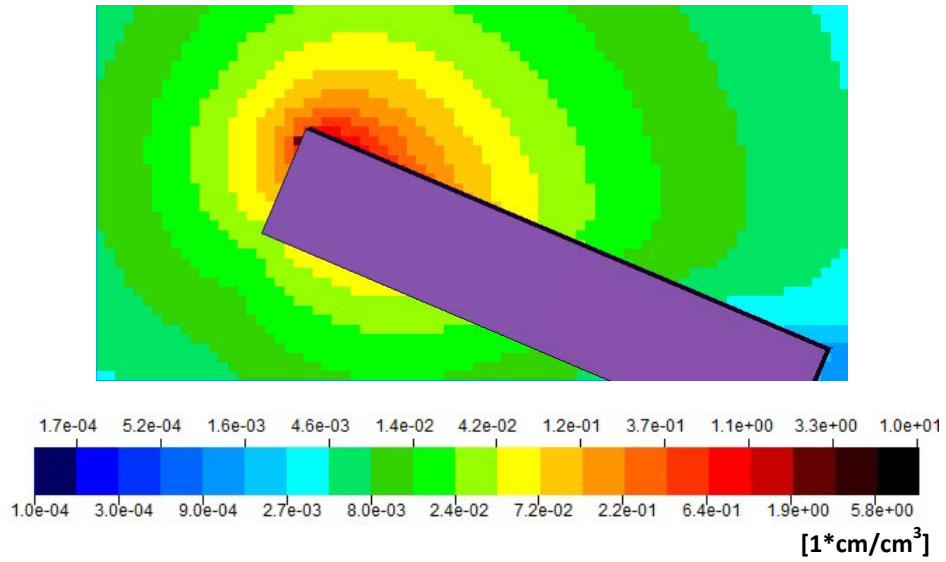


Figure 61: Fluence per primary particle of all particles on beam height when the 400 MeV ion beam hits the 30 cm long Tungsten beam dump, viewed from above

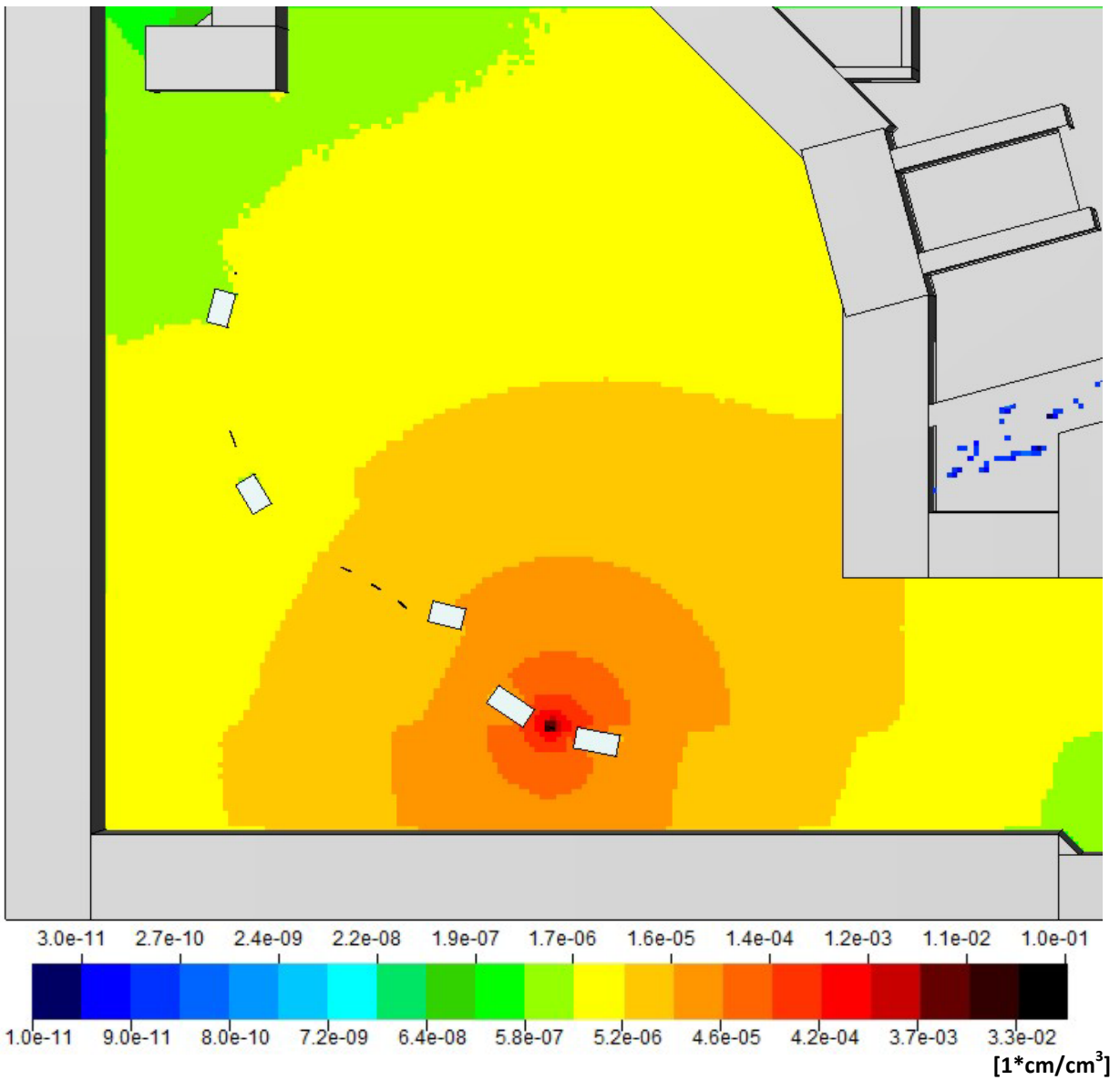


Figure 62: Fluence per primary particle of all particles in the synchrotron hall on beam height, when an ion beam with 400 MeV hits the 30 cm long Tungsten beam dump, viewed from above

The fluence distribution in Figure 62 shows that only secondary particles coming out from the side of the target have a significant influence on overall fluence and therefore activation in this scenario.

PROTON BEAM 250 MEV

The 250 MeV proton beam is almost completely attenuated inside the target, displayed by the fluence USBIN in Figure 63.

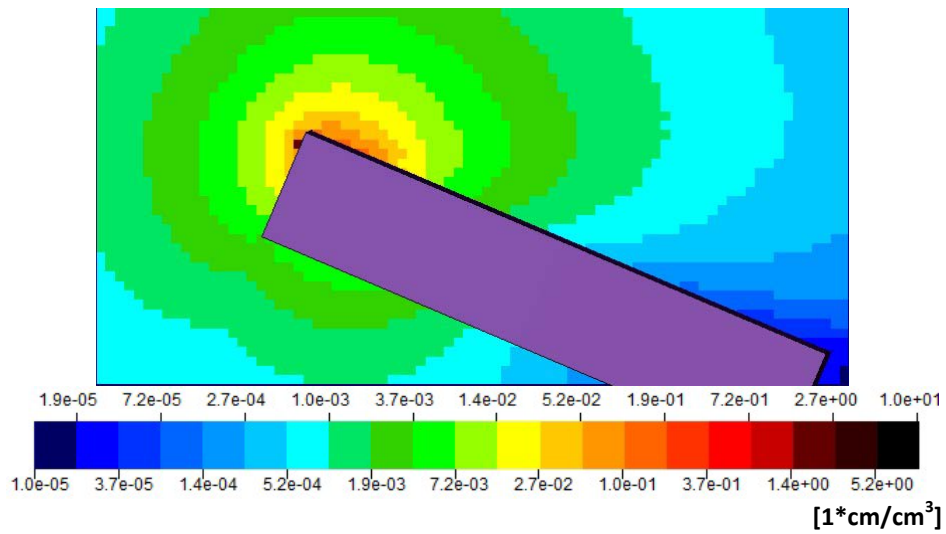


Figure 63: Fluence per primary particle of all particles on beam height when the 250 MeV proton beam hits the 30 cm long Tungsten beam dump, viewed from above

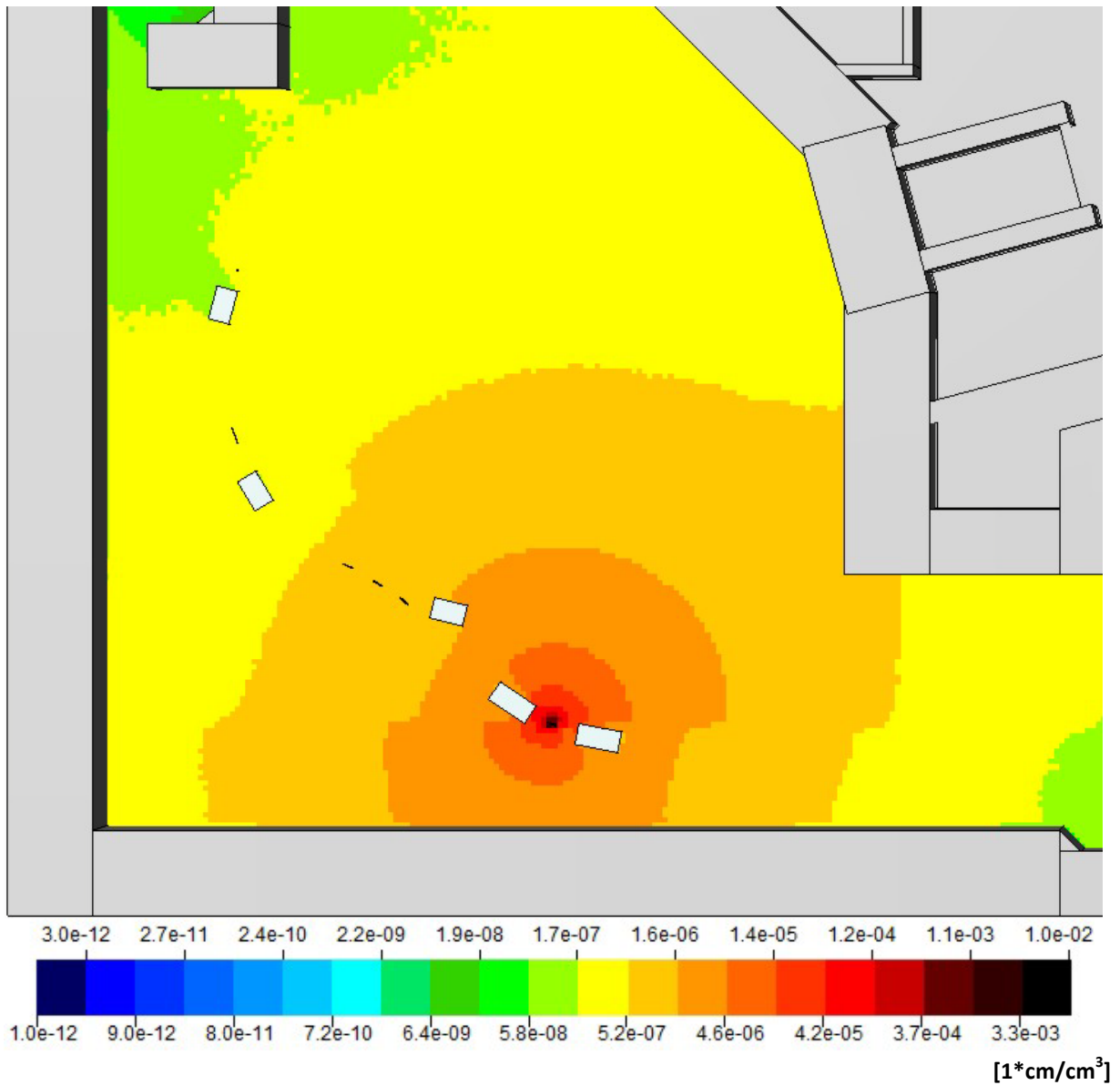


Figure 64: Fluence per primary particle of all particles in the synchrotron hall on beam height, when a proton beam with 250 MeV hits the 30 cm long Tungsten beam dump, viewed from above

Overall fluence in the hall, displayed in Figure 64, is distributed similar to the ion beam scenario, but fluences are lower by a factor of about 10.

SUMMARY TABLES

Estimations for the activity of the air that is to be released, after dilution and at least 10 minutes of cooling, compared to limits defined by Austrian law are given in Table 34, which lists, besides the scheduled intensity per year for each type of beam, the sum values gained by comparing the calculated activity of each calculated isotope with their respective Ci value and summing up all of these comparison values. For an unrestricted release into the environment, this sum value must not exceed 1.

In this scenario, each Ci value of each isotope is not exceeded by their respective activity, which can be regarded in the tables in Appendix C.

The maximum intensities are defined as for the treatment rooms with $2E+10$ protons per second, respectively $1E+9$ ions per second.

At this loss point, no losses are projected at a proton beam energy of 800 MeV.

Table 34: Sum values of specific activities compared to Ci values after 10 minutes of cooling time. Sum av/Ci compares specific activities generated considering average intensity, Sum max/Ci compares activities generated by consideration of maximum available intensity.

chopper	Intensity/y	Sum av/Ci	Sum max/Ci
i400	1.90E+14	3.00E-03	4.98E-01
p250	1.60E+15	1.93E-03	7.60E-01

With no proton beam losses at an energy of 800 MeV, the overall contribution of losses at the chopper dump to the average air activation is quite low.

800 MEV PROTON BEAM

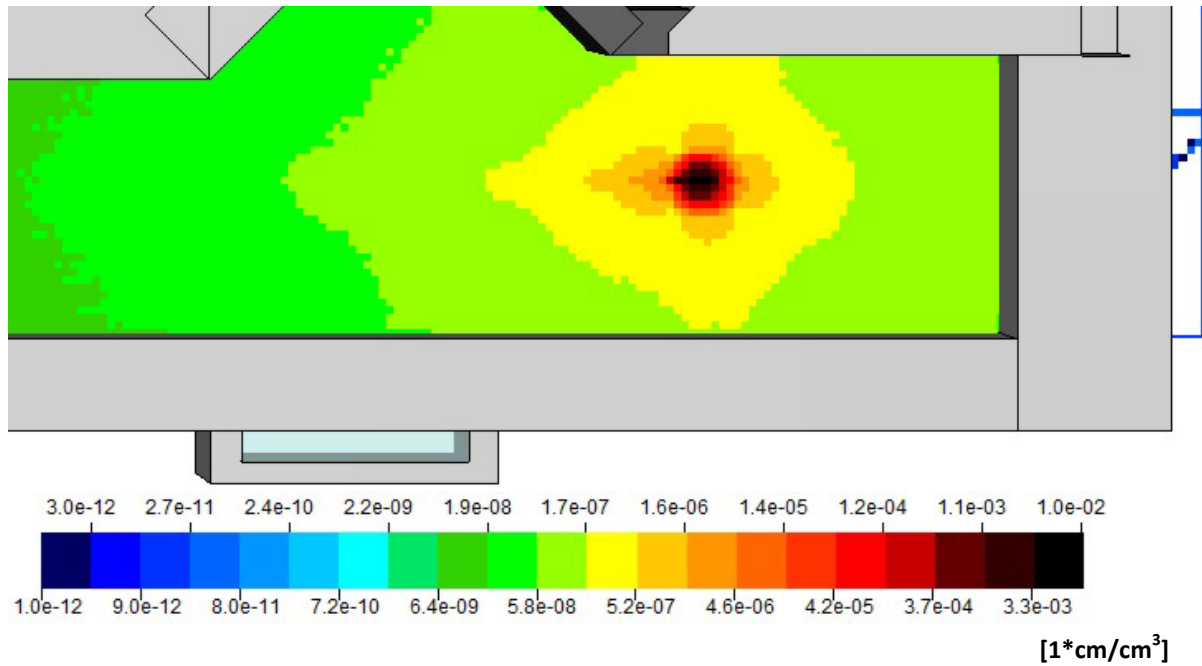


Figure 65: Fluence per primary particle of all particles in the high energy beam transfer line of the synchrotron hall on beam height, when a proton beam with 800 MeV hits the beam dump, viewed from above

Figure 65 displays a fluence USBIN at beam height in the area around the dump, with the beam starting 4 cm in front of the beam hole in the outer concrete shell. The dump itself has been left transparent, in order to view the very efficient attenuation of the 800 MeV proton beam. Most secondary particles are held within the concrete shell of the dump, so that the overall contribution to air activation in the synchrotron hall is quite low.

400 MEV ION BEAM

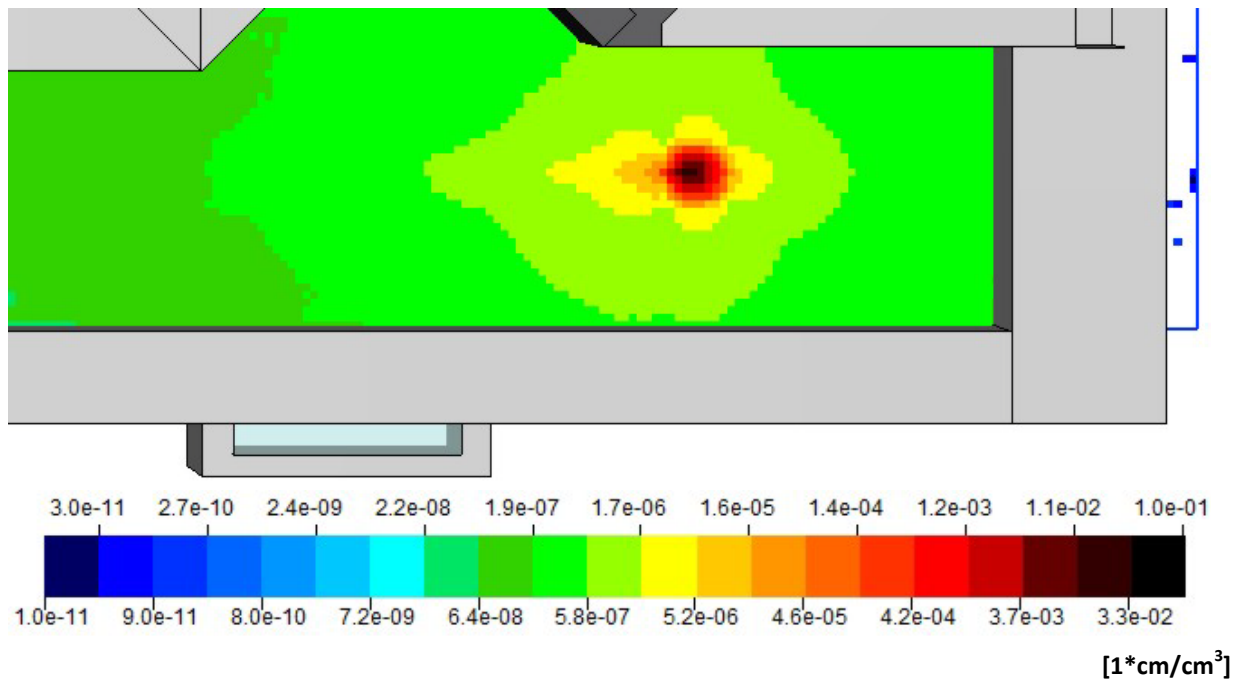


Figure 66: Fluence per primary particle of all particles in the high energy beam transfer line of the synchrotron hall on beam height, when an ion beam with 400 MeV hits the beam dump, viewed from above

Fluence distribution when hitting the beam dump with an ion beam, seen in Figure 66, is also effectively held inside the dump cube.

250 MEV PROTON BEAM

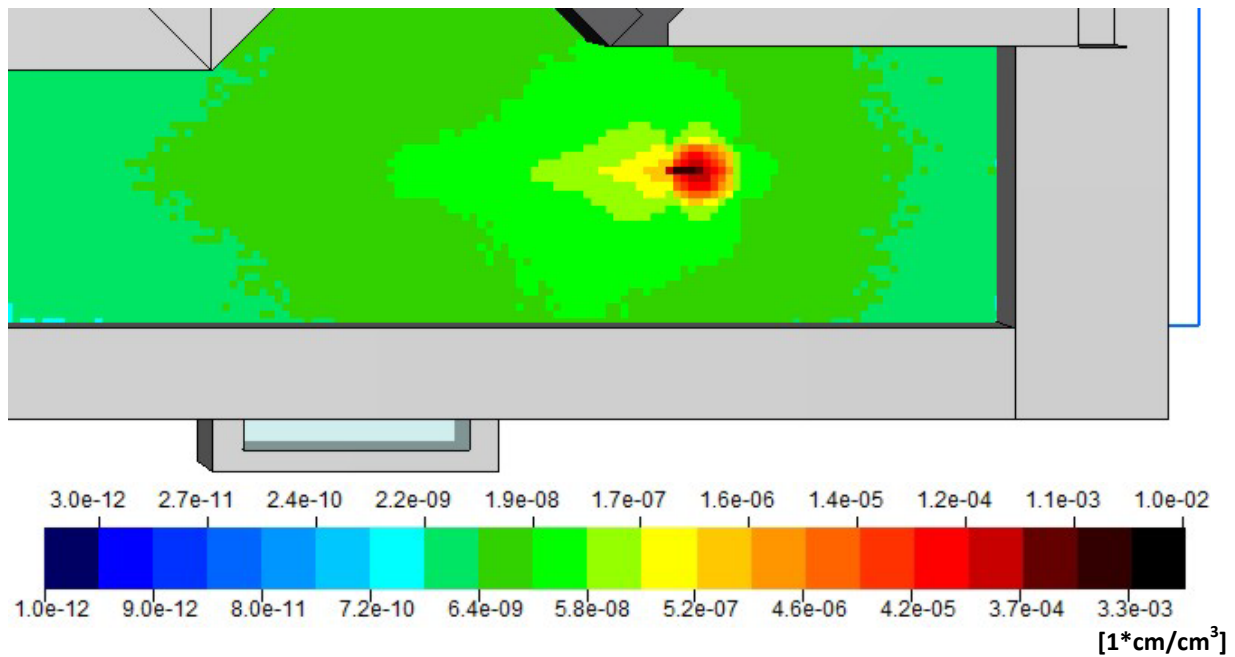


Figure 67: Fluence per primary particle of all particles in the high energy beam transfer line of the synchrotron hall on beam height, when a proton beam with 250 MeV hits the beam dump, viewed from above

Considering that the beam dump is designed to stop a high intensity proton beam at 800 MeV per particle, the attenuation of a 250 MeV proton beam is done with extreme efficiency, as can be seen in Figure 67. Most of the beam is stopped inside the iron part of the dump, as are most of the created secondary particles. Most escaping particles are 180 degree backscattered through the entrance hole in the dump. This entrance hole will be directly connected to the last part of the beam pipe in the machine, so additional shielding will stop many of these secondary particles from activating the air in the hall.

SUMMARY TABLES

Estimations for the activity of the air that is to be released, after dilution and at least 10 minutes of cooling, compared to limits defined by Austrian law are given in Table 35, which lists, besides the scheduled intensity per year for each type of beam, the sum values gained by comparing the calculated activity of each calculated isotope with their respective Ci value and summing up all of these comparison values. For an unrestricted release into the environment, this sum value must not exceed 1.

In this scenario, each Ci value of each isotope is not exceeded by their respective activity, which can be regarded in the tables in Appendix C.

The maximum intensities are defined as for the treatment rooms with $2E+10$ protons per second, respectively $1E+9$ ions per second.

Table 35: Sum values of specific activities compared to Ci values after 10 minutes of cooling time. Sum av/Ci compares specific activities generated considering average intensity, Sum max/Ci compares activities generated by consideration of maximum available intensity.

beam dump	Intensity/y	Sum av/Ci	Sum max/Ci
p800	4.90E+14	6.56E-05	8.44E-02
i400	2.10E+13	8.44E-06	1.27E-02
p250	2.10E+14	6.89E-06	2.07E-02

Since the beam dump has been designed to attenuate all primary radiation, meaning the beam at maximum energy and intensity, as well as much of the radiation coming from secondary particles created in the core of the dump made of iron and concrete, this loss point contributes only a comparably small part to the overall total activation of the air.

SUMMARY OF SYNCHROTRON HALL CALCULATIONS

To illustrate the effect of radiation coming from loss points to the average activation of air released from the synchrotron hall, all comparison values of activities versus Ci values have been added at each beam energy considering 1 hour of irradiation and 10 minutes of cooling time with results displayed in Table 36.

Table 36: Sums of all comparison values of specific activities which were calculated separately at each point with 10 minutes of cooling time at each of the 3 considered beam energies

	Intensity/y	Sum av/Ci
800 MeV proton	1.31E+15	7.33E-03
400 MeV ion	4.51E+14	7.23E-03
250 MeV proton	3.81E+15	6.97E-03

Sum values at different energies are very close, because on one side, the chopper dump is the only loss point where no losses are foreseen at a proton beam energy of 800 MeV, and on the other, the projected losses of a 250 MeV proton beam are almost three times as high as those of the 800 MeV beam, which brings all these values closer together.

Even during average operation with an 800 MeV proton beam, the calculated losses of all points together produce less than 1% of activated air allowed by Ci values. The main portion of activated air released from the facility is produced during patient treatment or experiments in the irradiation rooms.

The beam losses along the high energy beam transfer line (HEBT) are conservatively estimated and defined as follows:

Protons 800 Mev: 1000 times $Int_{max} = 2E13$ particles per year

Protons 250 Mev: 1000 times $Int_{max} = 2E13$ particles per year

Carbon Ions 400 Mev: 2000 times $Int_{max} = 2E12$ particles per year

The effect of these losses concerning the activation of air will be less than 1% compared to the estimated losses in the synchrotron hall, due to their lower intensity, which is a factor 100 smaller than the intensities of the loss points in the synchrotron hall. [5] No simulation was conducted concerning these points along the HEBT. The beam dump at the end of the HEBT is expected to see higher intensities and was therefore included in the simulations.

EFFECTIVE DOSE RATES IN THE SYNCHROTRON HALL CAUSED BY LOSS POINTS

To illustrate the average committed dose rate in the synchrotron hall caused by beam losses at the defined loss points, Figure 68, Figure 69 and Figure 70 show effective dose rates and integral dose developments over time after the end of 1 hour beam operation using a different beam each time, based on the average intensity being lost during a year. Ventilation in the hall is set to one full air exchange per hour, and should also provide for a homogenous distribution in the hall.

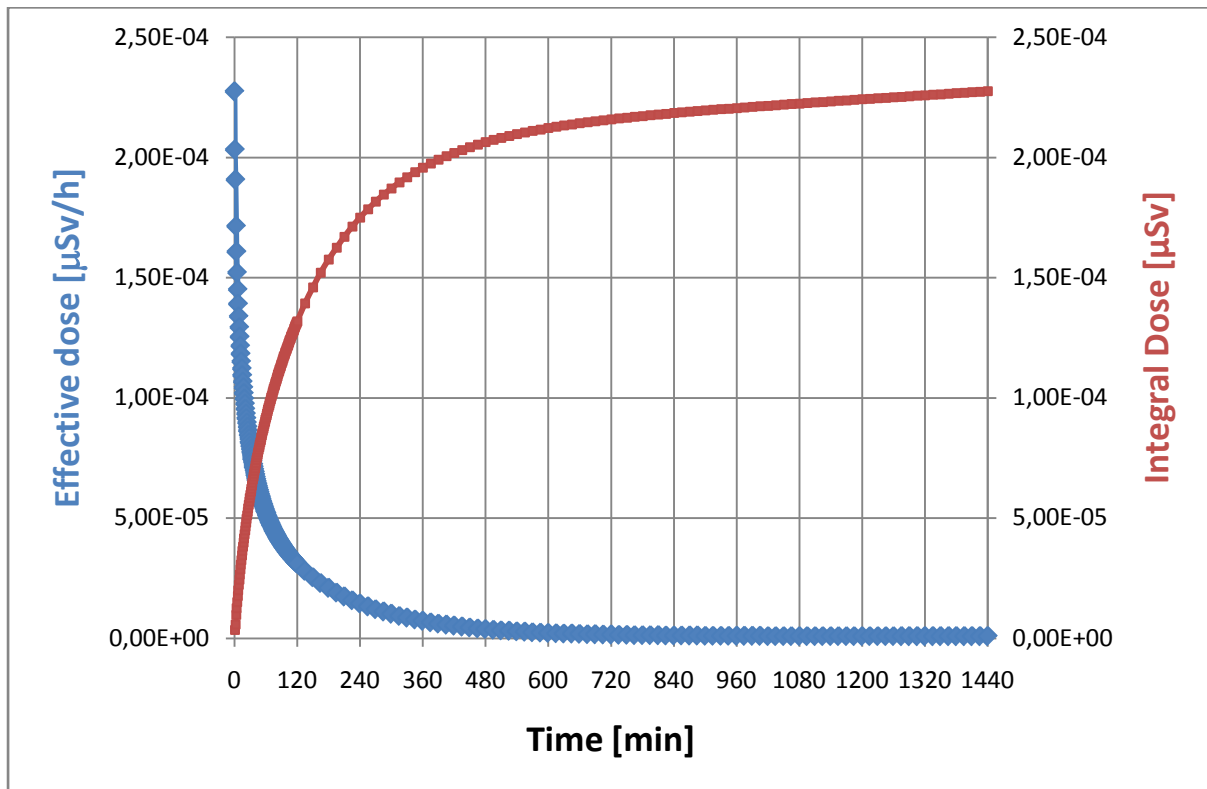


Figure 68: Effective dose rate and integral dose development over time at the end of 1h beam operation with an 800 MeV proton beam, considering defined average losses on all 4 regarded loss points

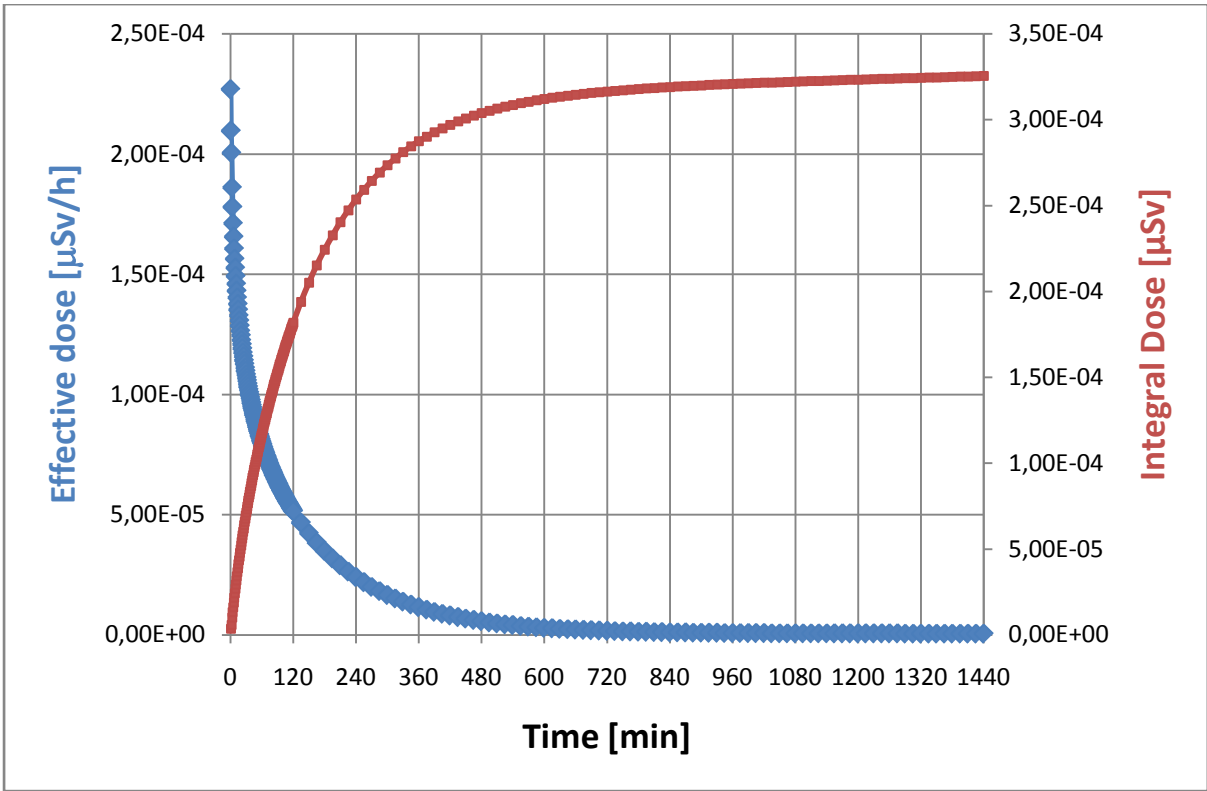


Figure 69: Effective dose rate and integral dose development over time at the end of 1h beam operation with a 400 MeV ion beam, considering defined average losses on all 5 regarded loss points

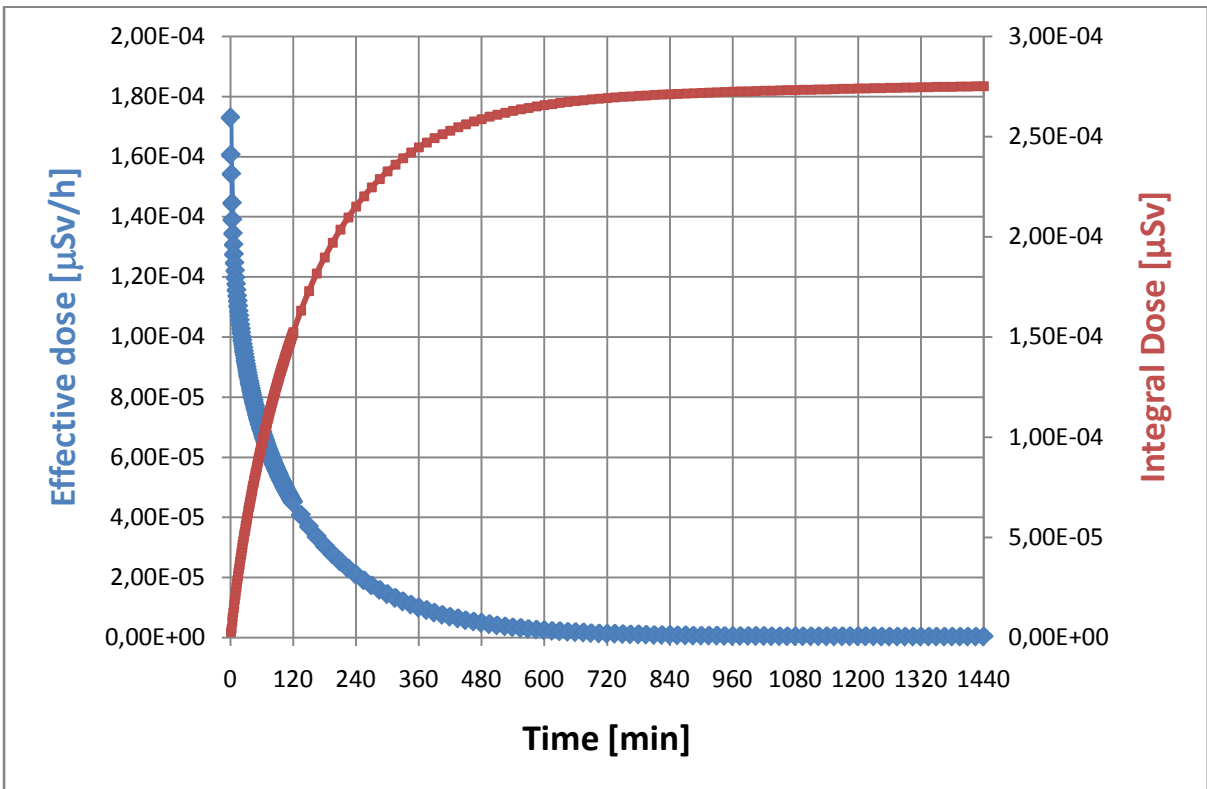


Figure 70: Effective dose rate and integral dose development over time at the end of 1h beam operation with a 250 MeV proton beam, considering defined average losses on all 5 regarded loss points

Figure 68 and Figure 69 showing beam losses at 800 MeV proton and 400 MeV ion operation display very similar values, which mainly comes from the fact that at 800 MeV proton operation, as opposed to 400 MeV ion operation, no losses are foreseen at the chopper dump.

All these values are very conservative because of the neglect of self shielding of the implemented machines during simulations. The main risk of exposure to radiation will come from the irradiated air of the treatment rooms. Before granting access to the synchrotron hall, ventilation should be set to maximum to minimize exposure of personnel.

CONCLUSION

In order to simulate the activation of air in a given volume, 2 different methods are considered. One method comprises the calculation of the fluences of protons, neutrons and pions with FLUKA in order to fold these with the appropriate cross sections for nuclide productions after the simulation is completed. On the other hand, FLUKA is able to calculate nuclide production by itself. The results of both methods are being compared by means of a generic study, to assess advantages and disadvantages of both concerning their suitability to the MedAustron geometry.

The **generic study** comparing the simulation results concerning air activation between two different methods of calculation clearly shows the advantages and disadvantages of each method. These methods are on the one hand a calculation of the fluences of protons, neutrons as well as positive and negative pions in order to fold them with appropriate cross sections for nuclide productions after the simulation is completed, and on the other hand a calculation of nuclide production that is done by FLUKA during the simulation.

The direct simulation of the production of isotopes via FLUKA yields more conservative results of the total activation for proton energies applied at MedAustron.

A detailed view of the 800 MeV proton simulation shows the total activity calculated directly by FLUKA being higher by a factor of about 1.5 compared to the folding method directly after the stop of the beam.

This conservative factor of 1.5 is mainly caused by the circumstance that the specific cross sections for N-13 used by FLUKA differ from the ones used by the `airactiv5-260` routine. The cross sections used with the folding method were evaluated by Huhtinen [7], and resemble experimental values with more accuracy. Cross sections for the production of N-13 by neutrons and protons between 0.25 and 0.8 GeV are significantly overestimated by FLUKA, explaining the difference in yield production between the two methods.

A detailed view of the 400 MeV ion beam simulation shows the total activity of FLUKA results directly after the stop of the beam being higher by a factor of 2.44, which is caused by a combination of using the cross sections of N-13, responsible for the factor of 1.5 discussed with the proton beam simulations, and of course the fact that the ion beam crosses half of the inner air volume of the long cylindrical structure before hitting the target. The folding method used for these simulations does not include cross sections for ion beams, which means that any isotopes produced by the main beam will not show up in the results of the folding method.

The higher activation obtained by the FLUKA results compared to calculations by folding methods at longer cooling times are caused by the fact that FLUKA is creating more long lived radionuclides during the simulation than what the folding methods yield. After about one day of cooldown, only long lived isotopes like H-3 and Be-7 are left to be the main source of radiation and their bigger yield given by FLUKA is responsible for the difference.

For the simulation of air activation caused by proton beams, the folding method utilizing `airactiv5-260` will be used, because the cross sections for the production of N-13 yield results that are closer to experimental data. Also, it proved to be the more efficient and time saving approach in this specific case.

When using an ion beam, the processing of particle fluences with `airactiv5-260` proves difficult, because activation production events caused by the ion particles in the main beam will not be counted towards total activation of the air. Therefore, the activation of air in ion-beam scenarios where the beam is to be expected to traverse a significant length (>1m) of airspace is calculated by using FLUKA itself, namely scoring with the `RESNUCLEi` card and evaluating the yields by using the `usrsuvev` user routine.

The implementation of the detailed **MedAustron** geometry in the simulations for air activation in the treatment rooms and the synchrotron hall yielded realistic but still very conservative estimations.

Regarding comparison values of Ci values against specific activities gained by irradiating a target with the maximum available intensity, considering a direct release after several cooling times but without any dilution, which will not even be possible regarding the design of the MedAustron facility, shows that the concept of diluting and cooling the activated air from the irradiation rooms is a well chosen one which will make an unrestricted release in view of the limits given by Austrian law very feasible.

Considering the foreseen dilution of irradiated air with an air volume of about 14.000 m³ and a cooldown time of 1 hour for each created radioactive isotope on its way to the outside of the facility, and that the calculations for all scenarios were done in a very conservative manner, almost all gained values for unrestricted release still comply to the maximum sum value $\Sigma(\text{activities} / \text{Ci clearance levels})$ of 1 defined by Austrian law, with the sole exception of the case of irradiation of a small lead target with a proton beam with 800 MeV at an intensity of 2E+10 particles per second in irradiation room 1. Although this conservatively estimated case will probably never be part of a realistic long term irradiation scenario, it shows that diligent measuring and logging of all activities released from the treatment rooms is required.

Considering short irradiation procedures during the treatment of patients as well as the effects of ventilation on the decrease of airborne radioactivity, all conservative simulations for the treatment rooms exhibit very low estimated committed dose rates compared to the possible scenarios designed for the experimental-focused IR1. A short waiting time gap between stopping the beam and entering the room should be considered to lower the committed dose rate by means of natural radioactive decay, regarding short lived isotopes, as well as by utilization of ventilation measurements.

Beam loss points defined in the synchrotron hall are considered as very conservative estimations that are totally ignoring self shielding of the final design of the machine. A lot of machine parts, beampipe containers and additional smaller magnets will be attenuating the beam much stronger than it is done in this simulation, where almost no obstacles for scattered particles are installed.

Regarding continuous release of the air, which is activated by the beam losses at either 800 MeV proton, 400 MeV ion or 250 MeV proton operation, into the environment, sum values of comparisons between isotope activation and Ci values at different energies are very close to each other, because on one side, the chopper dump is the only loss point where no losses are foreseen at a proton beam energy of 800 MeV, and on the other, the projected losses of a 250 MeV proton beam are almost three times as high as those of the 800 MeV beam, which brings all these values closer together.

Even during average operation with an 800 MeV proton beam, the calculated losses of all points together produce less than 1% of activated air allowed by Ci values. The main portion of activated air released from the facility is produced during patient treatment or experiments in the irradiation rooms.

Realistic treatment and experimental scenarios that are to be conducted at MedAustron will feature plenty of variation in terms of beam energy with an average energy per particle that will be well below the maximum energies used for the simulations, but reliable information was not available at the time of simulation. This, plus the fact that beam operation inside treatment rooms will rarely take longer than 1 hour, as was assumed in the calculations above, make these estimations, which are based on the available peak of energies and intensities, very conservative.

REFERENCES

- [1] Das Projekt Medaustrom (Designstudie), **T. Auberger, E. Griesmayer**, 2. Auflage 2007, ISBN 978-3-200-00932-5
- [2] The FLUKA code: Description and benchmarking, **G. Battistoni, S. Muraro, P.R. Sala, F. Cerutti, A. Ferrari, S. Roesler, A. Fasso`, J. Ranft**, Proceedings of the Hadronic Shower Simulation Workshop 2006, Fermilab 6--8 September 2006, M. Albrow, R. Raja eds., AIP Conference Proceeding 896, 31-49, (2007)
- [3] FLUKA: a multi-particle transport code, **A. Fasso`, A. Ferrari, J. Ranft, and P.R. Sala**, CERN-2005-10 (2005), INFN/TC_05/11, SLAC-R-773
- [4] Vorhabensbeschreibung B.04-03 – Teilchenbeschleuniger, **CERN – EBG MedAustrom**, Version 1.5E
- [5] **Michael Benedikt** (personal communication)
- [6] EFFECTIVE DOSE TO THE PUBLIC FROM AIR RELEASES AT LHC POINT 7, **M. Brugger, D. Forkel-Wirth, S. Roesler, P. Vojtyla** EDMS No. 493681, CERN-SC-2004-064-RP-TN
- [7] Determination of Cross Sections for Assessments of Air Activation at LHC, **M. Huhtinen**, Internal Report CERN/TIS-RP/TM/96-29 (1997).
- [8] Zahlenwerte und Funktionen aus Naturwissenschaften und Technik - Band 13 Radionuklidproduktion bei mittleren Energien, **A. S. Iljinov et al.**, Landolt-Börnstein, Springer-Verlag (1991).
- [9] <http://www.gesundheitsamt-bw.de/servlet/PB/menu/1141418/index.html> 17.06.2010
- [10] <http://hyperphysics.phy-astr.gsu.edu/Hbase/Nuclear/biohalf.html> 17.06.2010
- [11] <http://emedicine.medscape.com/article/165315-overview> 17.06.2010
- [12] Radiation physics for personnel and environmental protection, **J. Donald Cossairt**, Fermilab report TM-1834 Revision 9B, May 2007
- [13] Radiation Detection and Measurement, Third Edition, **Glenn F. Knoll**, John Wiley & Sons, ISBN-10: 0471073385
- [14] Interactive three dimensional visualization and creation of geometries for Monte Carlo calculations, **Theis C., Buchegger K.H., Brugger M., Forkel-Wirth D., Roesler S., Vincke H.**, Nuclear Instruments and Methods in Physics Research A 562, pp. 827-829 (2006).
- [15] Programmes for the evaluation of the environmental impact, **P. Vojtyla**, <http://rpd.oxfordjournals.org/content/137/1-2/134.full>
- [16] http://www.saphymo.com/pdf/pdf_gb/ASGA%20Environment%2009B.pdf 17.06.2010
- [17] The MORSE Monte Carlo radiation transport system, **M.B. Emmett**, Oak Ridge National Laboratory report, Revision: ORNL-4972/R2 (1984)

[18] "FLAIR: A Powerful But User Friendly Graphical Interface For FLUKA", **V.Vlachoudis**, Proc. Int. Conf. on Mathematics, Computational Methods & Reactor Physics (M&C 2009), Saratoga Springs, New York, 2009, <http://www.fluka.org/flair/index.html>

[19] Allgemeine Strahlenschutzverordnung, **F.Steger, G.Stolba, D. Müller, J.Pritz**, Ausgabe Oktober 2006, ON-V 89, ISBN 3-85402-093-7

[20] <http://www.ebgmedaustrotron.at/index.php> 17.06.2010

APPENDIX

APPENDIX:

PART A: GENERIC STUDY

800 MEV PROTONS

Table 37: Yields of radionuclides scored in the air directly after 1h of irradiation with an 800 MeV proton beam, according to FLUKA ("RESNUC") and the folding method including decay during irradiation ("airactiv"), as well as the ratio between the FLUKA results and the results of the folding method

	Isotope	T 1/2 [s]	Nuc/cm3 RESNUC	rel.error %	Nuc/cm3 airactiv	RESNUC/airactiv [Yield]
3	H	3.89E+08	1.06E-12	0.5	5.61E-13	7.72E-09
6	He	8.07E-01	5.97E-14	1.7		
7	Be	4.60E+06	3.77E-13	0.9	3.54E-13	1.52E-06
8	He	1.19E-01	1.53E-15	9.3		
8	Li	8.38E-01	1.00E-13	1.4		
8	Be	6.71E-17				
8	B	7.70E-01	5.93E-14	1.4		
9	Li	1.78E-01	1.37E-14	3.5		
9	B	8.45E-19				
9	C	1.27E-01	1.01E-14	5.1		
10	Be	4.76E+13	1.37E-13	1.3	1.1E-13	2.10E-13
10	C	1.93E+01	5.58E-14	1.9		
11	Li	8.50E-03	9.95E-17	40.8		
11	Be	1.38E+01	3.32E-15	6.1		
11	C	1.22E+03	5.12E-13	0.4	4.77E-13	8.99E-03
12	Be	2.36E-02	4.15E-16	18.2		
12	B	2.02E-02	7.29E-14	1.4		
12	N	1.10E-02	1.21E-14	4.0		
13	B	1.74E-02	6.35E-15	4.5		
13	N	5.98E+02	1.02E-12	0.6	6.65E-13	2.17E-02
13	O	8.58E-03	1.06E-15	10.8		
14	B	1.38E-02	4.98E-17	53.5		
14	C	1.81E+11	2.52E-11	0.1	2.53E-11	7.75E-11
14	O	7.06E+01	5.63E-14	1.8	5.05E-14	1.98E-01
15	C	2.45E+00	5.31E-16	18.8		
15	O	1.22E+02	5.09E-13	0.6	5.97E-13	1.23E-01
16	C	7.47E-01	1.33E-16	36.0		
16	N	7.13E+00	8.59E-15	4.5		
17	N	4.17E+00	8.96E-16	15.5		
17	F	6.45E+01	6.63E-17	44.3		
18	F	6.59E+03	3.48E-16	19.5	1.58E-15	2.73E-03
19	O	2.69E+01	4.98E-17	72.4	5.3E-17	7.06E-01
20	F	1.10E+01	3.98E-16	15.9		
21	F	4.16E+00	2.65E-16	25.0		
21	Na	2.25E+01	3.32E-17	68.1		

22	F	4.23E+00	4.98E-17	72.4		
22	Na	8.21E+07	3.32E-16	28.0	4.34E-16	2.68E-07
23	Ne	3.72E+01	8.29E-17	37.8	1.46E-16	6.18E-01
23	Mg	1.13E+01	3.32E-17	68.1		
24	Ne	2.03E+02	4.98E-17	53.5	2.88E-17	1.18E-01
24	Na	5.39E+04	3.98E-16	15.3	6.97E-16	4.46E-04
25	Na	5.91E+01	3.48E-16	20.7	2.71E-16	4.23E-01
26	Na	1.07E+00	8.29E-17	47.8		
26	Al	2.33E+13	2.57E-16	18.0	5.81E-16	1.11E-12
26	Si	2.23E+00	1.66E-17	100.0		
27	Mg	5.68E+02	5.31E-16	18.8	4.07E-16	4.76E-02
27	Si	4.16E+00	3.32E-17	68.1		
28	Mg	7.53E+04	1.33E-16	31.0	1.32E-16	3.72E-04
28	Al	1.35E+02	1.81E-15	10.2	1.41E-15	2.08E-01
29	Al	3.94E+02	8.79E-16	12.9	7.58E-16	7.37E-02
29	P	4.14E+00	3.32E-17	68.1		
30	Al	3.60E+00	8.29E-17	37.8		
30	P	1.50E+02	8.13E-16	18.0	4.52E-16	2.00E-01
31	Al	6.44E-01	1.66E-17	100.0		
31	Si	9.44E+03	1.11E-15	5.9	7.78E-16	3.28E-03
31	S	2.57E+00	1.66E-17	100.0		
32	Si	5.42E+09	4.48E-16	25.0	4.08E-16	5.90E-09
32	P	1.23E+06	3.80E-15	7.3	4.73E-15	2.60E-05
33	Si	6.18E+00	1.16E-16	35.4		
33	P	2.19E+06	2.47E-15	9.3	3.23E-15	1.51E-05
34	Si	2.77E+00	1.66E-17	100.0		
34	P	1.24E+01	9.45E-16	10.7		
34	Cl	1.53E+00	2.32E-16	15.6	2.03E-16	2.23E+01
35	P	4.73E+01	2.82E-16	19.0	3.33E-16	7.40E-01
35	S	7.56E+06	3.45E-15	7.0	3.79E-15	4.63E-06
35	Ar	1.78E+00	3.32E-17	68.1		
36	Cl	9.49E+12	7.93E-15	4.2	9.35E-15	3.79E-12
37	S	3.03E+02	4.81E-16	19.9	8.66E-16	1.22E-01
37	Ar	3.03E+06	5.31E-15	6.2	7.65E-15	1.22E-05
38	S	1.02E+04	4.64E-16	14.7	7.89E-16	3.72E-03
38	Cl	2.23E+03	2.72E-15	5.9	6.06E-15	1.70E-02
38	K	4.58E+02	2.49E-17	72.4	1.58E-16	8.29E-02
39	Cl	3.34E+03	9.17E-15	4.4	1.18E-14	1.17E-02
39	Ar	8.48E+09	1.44E-14	2.1	2.32E-14	4.60E-09
40	Cl	8.10E+01	4.64E-16	19.5	4.28E-16	4.94E-01
40	K	4.03E+16	4.31E-16	20.7	3.8E-16	9.93E-16
41	Ar	6.56E+03	5.08E-14	1.5	5.35E-14	6.25E-03

Table 38: Total activity of the air directly after 1h of irradiation with an 800 MeV proton beam, according to FLUKA (“RESNUC”), the folding method including decay during irradiation (“airactiv”) and the reference folding method ignoring decay during irradiation (“airactiv ref.”), as well as the ratio between the FLUKA results and the results of the folding method

Isotope	T 1/2 [s]	Bq/cm3 <i>RESNUC</i>	Bq/cm3 <i>airactiv</i>	Bq/cm3 <i>airactiv ref.</i>	RESNUC/ <i>airactiv</i> [Bq/cmc]	RESNUC/ <i>airref.</i> [Bq/cmc]
3 H	3.89E+08	1.36E-07	7.19E-08	7.20E-08	1.89E+00	1.89E+00
6 He	8.07E-01	1.19E-03				
7 Be	4.60E+06	4.09E-06	3.84E-06	3.84E-06	1.07E+00	1.07E+00
8 He	1.19E-01	3.05E-05				
8 Li	8.38E-01	2.03E-03				
8 Be	6.71E-17	3.55E-03				
8 B	7.70E-01	1.19E-03				
9 Li	1.78E-01	2.75E-04				
9 B	8.45E-19	2.02E-04				
9 C	1.27E-01	2.02E-04				
10 Be	4.76E+13	1.44E-13	1.09E-13	1.15E-13	1.32E+00	1.25E+00
10 C	1.93E+01	1.12E-03				
11 Li	8.50E-03	1.99E-06				
11 Be	1.38E+01	6.71E-05				
11 C	1.22E+03	8.91E-03	8.30E-03	1.95E-02	1.07E+00	4.57E-01
12 Be	2.36E-02	8.29E-06				
12 B	2.02E-02	1.47E-03				
12 N	1.10E-02	2.42E-04				
13 B	1.74E-02	1.27E-04				
13 N	5.98E+02	2.00E-02	1.31E-02	5.55E-02	1.53E+00	3.61E-01
13 O	8.58E-03	2.12E-05				
14 B	1.38E-02	9.95E-07				
14 C	1.81E+11	6.97E-09	6.99E-09	6.99E-09	9.98E-01	9.97E-01
14 O	7.06E+01	1.13E-03	1.01E-03	3.57E-02	1.12E+00	3.16E-02
15 C	2.45E+00	1.06E-05				
15 O	1.22E+02	1.02E-02	1.19E-02	2.44E-01	8.53E-01	4.18E-02
16 C	7.47E-01	2.65E-06				
16 N	7.13E+00	1.75E-04				
17 N	4.17E+00	1.79E-05				
17 F	6.45E+01	1.33E-06				
18 F	6.59E+03	2.20E-06	9.97E-06	1.20E-05	2.20E-01	1.84E-01
19 O	2.69E+01	9.95E-07	1.06E-06	9.83E-05	9.39E-01	1.01E-02
20 F	1.10E+01	7.96E-06				
21 F	4.16E+00	5.31E-06				
21 Na	2.25E+01	6.63E-07				
22 F	4.23E+00	9.95E-07				
22 Na	8.21E+07	2.02E-10	2.64E-10	2.64E-10	7.65E-01	7.64E-01
23 Ne	3.72E+01	1.66E-06	2.92E-06	1.96E-04	5.68E-01	8.47E-03
23 Mg	1.13E+01	6.63E-07				
24 Ne	2.03E+02	9.95E-07	5.76E-07	7.09E-06	1.73E+00	1.40E-01
24 Na	5.39E+04	7.62E-07	6.30E-07	6.46E-07	1.21E+00	1.18E+00

25	Na	5.91E+01	6.97E-06	5.42E-06	2.29E-04	1.29E+00	3.04E-02
26	Na	1.07E+00	1.66E-06				
26	Al	2.33E+13	5.85E-16	1.28E-15	1.24E-15	4.56E-01	4.71E-01
26	Si	2.23E+00	3.32E-07				
27	Mg	5.68E+02	1.05E-05	8.04E-06	3.58E-05	1.30E+00	2.93E-01
27	Si	4.16E+00	6.63E-07				
28	Mg	7.53E+04	8.65E-08	8.61E-08	8.75E-08	1.01E+00	9.89E-01
28	Al	1.35E+02	3.62E-05	2.82E-05	5.23E-04	1.28E+00	6.92E-02
29	Al	3.94E+02	1.76E-05	1.51E-05	9.61E-05	1.16E+00	1.83E-01
29	P	4.14E+00	6.63E-07				
30	Al	3.60E+00	1.66E-06				
30	P	1.50E+02	1.63E-05	9.04E-06	1.50E-04	1.80E+00	1.08E-01
31	Al	6.44E-01	3.32E-07				
31	Si	9.44E+03	5.24E-06	3.62E-06	4.11E-06	1.45E+00	1.27E+00
31	S	2.57E+00	3.32E-07				
32	Si	5.42E+09	4.12E-12	4.22E-12	3.75E-12	9.77E-01	1.10E+00
32	P	1.23E+06	1.54E-07	1.91E-07	1.92E-07	8.05E-01	8.02E-01
33	Si	6.18E+00	2.32E-06				
33	P	2.19E+06	5.89E-08	7.34E-08	7.36E-08	8.03E-01	8.00E-01
34	Si	2.77E+00	3.32E-07				
34	P	1.24E+01	1.92E-05				
34	Cl	1.53E+00	6.15E-06	2.95E-06	6.64E-03	2.08E+00	9.26E-04
35	P	4.73E+01	5.64E-06	6.66E-06	3.51E-04	8.47E-01	1.60E-02
35	S	7.56E+06	2.46E-08	2.50E-08	2.50E-08	9.82E-01	9.83E-01
35	Ar	1.78E+00	6.63E-07				
36	Cl	9.49E+12	4.17E-14	4.91E-14	4.92E-14	8.48E-01	8.48E-01
37	S	3.03E+02	9.62E-06	1.73E-05	1.43E-04	5.55E-01	6.74E-02
37	Ar	3.03E+06	8.74E-08	1.26E-07	1.26E-07	6.93E-01	6.93E-01
38	S	1.02E+04	2.01E-06	3.39E-06	3.85E-06	5.94E-01	5.22E-01
38	Cl	2.23E+03	7.40E-05	8.16E-05	1.35E-04	9.07E-01	5.47E-01
38	K	4.58E+02	4.95E-07	3.15E-06	1.72E-05	1.57E-01	2.88E-02
39	Cl	3.34E+03	9.66E-05	1.24E-04	1.77E-04	7.77E-01	5.47E-01
39	Ar	8.48E+09	1.01E-10	1.36E-10	1.36E-10	7.40E-01	7.39E-01
40	Cl	8.10E+01	9.29E-06	8.56E-06	2.64E-04	1.08E+00	3.52E-02
40	K	4.03E+16	5.34E-19	4.69E-19	4.71E-19	1.14E+00	1.13E+00
41	Ar	6.56E+03	3.22E-04	3.38E-04	4.07E-04	9.52E-01	7.90E-01
	SUM VALUES:		5.28E-02	3.50E-02	3.64E-01	1.51E+00	1.45E-01

Table 39: Total activity of the air after 1h of irradiation with an 800 MeV proton beam and a cooling time of 3600 seconds (1h), according to FLUKA ("RESNUC"), the folding method including decay during irradiation ("airactiv") and the reference folding method ignoring decay during irradiation ("airactiv ref."), as well as the ratio between the FLUKA results and the results of the folding method

Isotope	T 1/2 [s]	Bq/cm3 <i>RESNUC</i>	Bq/cm3 <i>airactiv</i>	Bq/cm3 <i>airactiv ref.</i>	RESNUC/ <i>airactiv</i> [Bq/cm3]	RESNUC/ <i>airref.</i> [Bq/cm3]
3 H	3.89E+08	1.36E-07	7.19E-08	7.20E-08	1.89E+00	1.89E+00
6 He	8.07E-01	0.00E+00				
7 Be	4.60E+06	4.09E-06	3.83E-06	3.84E-06	1.07E+00	1.07E+00
8 He	1.19E-01	0.00E+00				
8 Li	8.38E-01	0.00E+00				
8 Be	6.71E-17	0.00E+00				
8 B	7.70E-01	0.00E+00				
9 Li	1.78E-01	0.00E+00				
9 B	8.45E-19	0.00E+00				
9 C	1.27E-01	0.00E+00				
10 Be	4.76E+13	1.44E-13	1.09E-13	1.15E-13	1.32E+00	1.25E+00
10 C	1.93E+01	5.64E-60				
11 Li	8.50E-03	0.00E+00				
11 Be	1.38E+01	2.26E-83				
11 C	1.22E+03	1.16E-03	1.08E-03	2.53E-03	1.07E+00	4.57E-01
12 Be	2.36E-02	0.00E+00				
12 B	2.02E-02	0.00E+00				
12 N	1.10E-02	0.00E+00				
13 B	1.74E-02	0.00E+00				
13 N	5.98E+02	3.08E-04	2.02E-04	8.55E-04	1.53E+00	3.61E-01
13 O	8.58E-03	0.00E+00				
14 B	1.38E-02	0.00E+00				
14 C	1.81E+11	6.97E-09	6.99E-09	6.99E-09	9.98E-01	9.97E-01
14 O	7.06E+01	5.06E-19	4.53E-19	1.60E-17	1.12E+00	3.16E-02
15 C	2.45E+00	0.00E+00				
15 O	1.22E+02	1.38E-11	1.62E-11	3.30E-10	8.53E-01	4.18E-02
16 C	7.47E-01	0.00E+00				
16 N	7.13E+00	1.77E-156				
17 N	4.17E+00	3.61E-265				
17 F	6.45E+01	2.08E-23				
18 F	6.59E+03	1.50E-06	6.82E-06	8.20E-06	2.20E-01	1.84E-01
19 O	2.69E+01	5.32E-47	5.67E-47	5.26E-45	9.39E-01	1.01E-02
20 F	1.10E+01	2.41E-104				
21 F	4.16E+00	1.24E-266				
21 Na	2.25E+01	4.32E-55				
22 F	4.23E+00	6.34E-263				
22 Na	8.21E+07	2.02E-10	2.64E-10	2.64E-10	7.65E-01	7.64E-01
23 Ne	3.72E+01	1.32E-35	2.32E-35	1.55E-33	5.68E-01	8.47E-03
23 Mg	1.13E+01	1.22E-102				
24 Ne	2.03E+02	4.51E-12	2.61E-12	3.21E-11	1.73E+00	1.40E-01
24 Na	5.39E+04	7.28E-07	6.01E-07	6.17E-07	1.21E+00	1.18E+00

25	Na	5.91E+01	3.21E-24	2.50E-24	1.05E-22	1.29E+00	3.04E-02
26	Na	1.07E+00	0.00E+00				
26	Al	2.33E+13	5.85E-16	1.28E-15	1.24E-15	4.56E-01	4.71E-01
26	Si	2.23E+00	0.00E+00				
27	Mg	5.68E+02	1.29E-07	9.90E-08	4.41E-07	1.30E+00	2.93E-01
27	Si	4.16E+00	2.07E-267				
28	Mg	7.53E+04	8.37E-08	8.33E-08	8.47E-08	1.01E+00	9.89E-01
28	Al	1.35E+02	3.18E-13	2.47E-13	4.59E-12	1.28E+00	6.92E-02
29	Al	3.94E+02	3.10E-08	2.67E-08	1.70E-07	1.16E+00	1.83E-01
29	P	4.14E+00	1.52E-268				
30	Al	3.60E+00	1.55E-307				
30	P	1.50E+02	9.58E-13	5.33E-13	8.87E-12	1.80E+00	1.08E-01
31	Al	6.44E-01	0.00E+00				
31	Si	9.44E+03	4.02E-06	2.78E-06	3.16E-06	1.45E+00	1.27E+00
31	S	2.57E+00	0.00E+00				
32	Si	5.42E+09	4.12E-12	4.22E-12	3.75E-12	9.77E-01	1.10E+00
32	P	1.23E+06	1.53E-07	1.91E-07	1.91E-07	8.05E-01	8.02E-01
33	Si	6.18E+00	1.02E-181				
33	P	2.19E+06	5.89E-08	7.33E-08	7.36E-08	8.03E-01	8.00E-01
34	Si	2.77E+00	0.00E+00				
34	P	1.24E+01	1.26E-92				
34	Cl	1.53E+00	0.00E+00	0.00E+00	0.00E+00		
35	P	4.73E+01	6.91E-29	8.17E-29	4.31E-27	8.47E-01	1.60E-02
35	S	7.56E+06	2.46E-08	2.50E-08	2.50E-08	9.82E-01	9.83E-01
35	Ar	1.78E+00	0.00E+00				
36	Cl	9.49E+12	4.17E-14	4.91E-14	4.92E-14	8.48E-01	8.48E-01
37	S	3.03E+02	2.55E-09	4.59E-09	3.78E-08	5.55E-01	6.74E-02
37	Ar	3.03E+06	8.74E-08	1.26E-07	1.26E-07	6.93E-01	6.93E-01
38	S	1.02E+04	1.58E-06	2.65E-06	3.02E-06	5.94E-01	5.22E-01
38	Cl	2.23E+03	2.42E-05	2.67E-05	4.43E-05	9.07E-01	5.47E-01
38	K	4.58E+02	2.14E-09	1.36E-08	7.42E-08		
39	Cl	3.34E+03	4.57E-05	5.88E-05	8.36E-05	7.77E-01	5.47E-01
39	Ar	8.48E+09	1.01E-10	1.36E-10	1.36E-10	7.40E-01	7.39E-01
40	Cl	8.10E+01	3.88E-19	3.58E-19	1.10E-17	1.08E+00	3.52E-02
40	K	4.03E+16	5.34E-19	4.69E-19	4.71E-19	1.14E+00	1.13E+00
41	Ar	6.56E+03	2.20E-04	2.31E-04	2.78E-04	9.52E-01	7.90E-01
	SUM VALUES:		1.77E-03	1.61E-03	3.81E-03	1.10E+00	4.64E-01

Table 40: Total activity of the air after 1h of irradiation with an 800 MeV proton beam and a cooling time of 86400 seconds (1d), according to FLUKA ("RESNUC"), the folding method including decay during irradiation ("airactiv") and the reference folding method ignoring decay during irradiation ("airactiv ref."), as well as the ratio between the FLUKA results and the results of the folding method

Isotope	T 1/2 [s]	Bq/cm3 <i>RESNUC</i>	Bq/cm3 <i>airactiv</i>	Bq/cm3 <i>airactiv ref.</i>	RESNUC/ <i>airactiv</i> [Bq/cm3]	RESNUC/ <i>airref.</i> [Bq/cm3]
3 H	3.89E+08	1.36E-07	7.19E-08	7.20E-08	1.89E+00	1.89E+00
6 He	8.07E-01	0.00E+00				
7 Be	4.60E+06	4.04E-06	3.79E-06	3.79E-06	1.07E+00	1.07E+00
8 He	1.19E-01	0.00E+00				
8 Li	8.38E-01	0.00E+00				
8 Be	6.71E-17	0.00E+00				
8 B	7.70E-01	0.00E+00				
9 Li	1.78E-01	0.00E+00				
9 B	8.45E-19	0.00E+00				
9 C	1.27E-01	0.00E+00				
10 Be	4.76E+13	1.44E-13	1.09E-13	1.15E-13	1.32E+00	1.25E+00
10 C	1.93E+01	0.00E+00				
11 Li	8.50E-03	0.00E+00				
11 Be	1.38E+01	0.00E+00				
11 C	1.22E+03	4.82E-24	4.49E-24	1.05E-23	1.07E+00	4.57E-01
12 Be	2.36E-02	0.00E+00				
12 B	2.02E-02	0.00E+00				
12 N	1.10E-02	0.00E+00				
13 B	1.74E-02	0.00E+00				
13 N	5.98E+02	6.32E-46	4.14E-46	1.75E-45	1.53E+00	3.61E-01
13 O	8.58E-03	0.00E+00				
14 B	1.38E-02	0.00E+00				
14 C	1.81E+11	6.97E-09	6.99E-09	6.99E-09	9.98E-01	9.97E-01
14 O	7.06E+01	0.00E+00	0.00E+00	0.00E+00		
15 C	2.45E+00	0.00E+00				
15 O	1.22E+02	1.47E-215	1.73E-215	3.53E-214	8.53E-01	4.18E-02
16 C	7.47E-01	0.00E+00				
16 N	7.13E+00	0.00E+00				
17 N	4.17E+00	0.00E+00				
17 F	6.45E+01	0.00E+00				
18 F	6.59E+03	2.47E-10	1.12E-09	1.35E-09	2.20E-01	1.84E-01
19 O	2.69E+01	0.00E+00	0.00E+00	0.00E+00		
20 F	1.10E+01	0.00E+00				
21 F	4.16E+00	0.00E+00				
21 Na	2.25E+01	0.00E+00				
22 F	4.23E+00	0.00E+00				
22 Na	8.21E+07	2.02E-10	2.64E-10	2.64E-10	7.65E-01	7.64E-01
23 Ne	3.72E+01	0.00E+00	0.00E+00	0.00E+00		
23 Mg	1.13E+01	0.00E+00				
24 Ne	2.03E+02	5.60E-135	3.24E-135	3.99E-134	1.73E+00	1.40E-01
24 Na	5.39E+04	2.51E-07	2.07E-07	2.12E-07	1.21E+00	1.18E+00

25	Na	5.91E+01	0.00E+00	0.00E+00	0.00E+00		
26	Na	1.07E+00	0.00E+00				
26	Al	2.33E+13	5.85E-16	1.28E-15	1.24E-15	4.56E-01	4.71E-01
26	Si	2.23E+00	0.00E+00				
27	Mg	5.68E+02	1.55E-51	1.19E-51	5.28E-51	1.30E+00	2.93E-01
27	Si	4.16E+00	0.00E+00				
28	Mg	7.53E+04	3.90E-08	3.89E-08	3.95E-08		
28	Al	1.35E+02	1.53E-198	1.19E-198	2.20E-197	1.28E+00	6.92E-02
29	Al	3.94E+02	1.46E-71	1.26E-71	8.00E-71	1.16E+00	1.83E-01
29	P	4.14E+00	0.00E+00				
30	Al	3.60E+00	0.00E+00				
30	P	1.50E+02	5.03E-179	2.80E-179	4.66E-178	1.80E+00	1.08E-01
31	Al	6.44E-01	0.00E+00				
31	Si	9.44E+03	9.20E-09	6.34E-09	7.22E-09	1.45E+00	1.27E+00
31	S	2.57E+00	0.00E+00				
32	Si	5.42E+09	4.12E-12	4.22E-12	3.75E-12	9.77E-01	1.10E+00
32	P	1.23E+06	1.46E-07	1.82E-07	1.83E-07	8.05E-01	8.02E-01
33	Si	6.18E+00	0.00E+00				
33	P	2.19E+06	5.73E-08	7.14E-08	7.17E-08	8.03E-01	8.00E-01
34	Si	2.77E+00	0.00E+00				
34	P	1.24E+01	0.00E+00				
34	Cl	1.53E+00	0.00E+00	0.00E+00	0.00E+00		
35	P	4.73E+01	0.00E+00	0.00E+00	0.00E+00		
35	S	7.56E+06	2.44E-08	2.48E-08	2.48E-08	9.82E-01	9.83E-01
35	Ar	1.78E+00	0.00E+00				
36	Cl	9.49E+12	4.17E-14	4.91E-14	4.92E-14	8.48E-01	8.48E-01
37	S	3.03E+02	1.40E-91	2.51E-91	2.07E-90	5.55E-01	6.74E-02
37	Ar	3.03E+06	8.57E-08	1.24E-07	1.24E-07	6.93E-01	6.93E-01
38	S	1.02E+04	5.74E-09	9.65E-09	1.10E-08	5.94E-01	5.22E-01
38	Cl	2.23E+03	1.69E-16	1.86E-16	3.08E-16	9.07E-01	5.47E-01
38	K	4.58E+02	8.54E-64	5.43E-63	2.97E-62		
39	Cl	3.34E+03	1.54E-12	1.99E-12	2.82E-12		
39	Ar	8.48E+09	1.01E-10	1.36E-10	1.36E-10	7.40E-01	7.39E-01
40	Cl	8.10E+01	0.00E+00	0.00E+00	0.00E+00		
40	K	4.03E+16	5.34E-19	4.69E-19	4.71E-19	1.14E+00	1.13E+00
41	Ar	6.56E+03	3.49E-08	3.66E-08	4.41E-08	9.52E-01	7.90E-01
	SUM	VALUES:	4.83E-06	4.57E-06	4.59E-06	1.06E+00	1.05E+00

400 MEV CARBON IONS

Table 41: Yields of radionuclides scored in the air directly after 1h of irradiation with a 400 MeV carbon ion beam, according to FLUKA ("RESNUC") and the folding method including decay during irradiation ("airactiv"), as well as the ratio between the FLUKA results and the results of the folding method

Isotope	T 1/2 [s]	Nuc/cm3 RESNUC	rel.error %	Nuc/cm3 airactiv	RESNUC/airactiv [Yield]
3 H	3.89E+08	9.28E-12	0.2	1.72E-12	5.39E+00
6 He	8.07E-01	4.67E-13	1		
7 Be	4.60E+06	4.35E-12	0.3	7.86E-13	5.53E+00
8 He	1.19E-01	1.96E-14	5.2		
8 Li	8.38E-01	7.18E-13	0.9		
8 Be	6.71E-17		0.7		
8 B	7.70E-01	3.87E-13	1.1		
9 Li	1.78E-01	1.00E-13	2.7		
9 B	8.45E-19		2.6		
9 C	1.27E-01	5.49E-14	2.6		
10 Be	4.76E+13	1.19E-12	0.5	6.29E-13	1.90E+00
10 C	1.93E+01	3.43E-13	1.3		
11 Li	8.50E-03	4.71E-16	31.7		
11 Be	1.38E+01	2.20E-14	3.7		
11 C	1.22E+03	3.06E-12	0.4	1.42E-12	2.15E+00
12 Be	2.36E-02	1.52E-15	22.9		
12 B	2.02E-02	4.38E-13	1		
12 N	1.10E-02	5.94E-14	3.5		
13 Be	0.00E+00	5.24E-17	99		
13 B	1.74E-02	5.07E-14	3.5		
13 N	5.98E+02	5.02E-12	0.3	2.65E-12	1.89E+00
13 O	8.58E-03	5.45E-15	12.4		
14 B	1.38E-02	3.14E-16	37.9		
14 C	1.81E+11	1.23E-10	0.1	1.23E-10	1.00E+00
14 O	7.06E+01	2.86E-13	1.2	2.04E-13	1.40E+00
15 C	2.45E+00	5.08E-15	8.7		
15 O	1.22E+02	2.76E-12	0.4	1.93E-12	1.43E+00
16 C	7.47E-01	1.05E-16	69.7		
16 N	7.13E+00	8.05E-14	2.6		
17 N	4.17E+00	5.18E-15	8		
17 F	6.45E+01	5.76E-16	27.4		
18 N	6.24E-01	1.05E-16	69.7		
18 F	6.59E+03	1.83E-15	18.1	9.18E-16	2.00E+00
19 O	2.69E+01	4.19E-16	31.7	1.64E-17	2.55E+01
19 Ne	1.73E+01	5.24E-17	99		
20 O	1.35E+01	2.62E-16	42.2		
20 F	1.10E+01	1.68E-15	15.7		
21 F	4.16E+00	1.15E-15	21.1		
21 Na	2.25E+01	2.09E-16	56.1		
22 F	4.23E+00	4.19E-16	36.4		

22	Na	8.21E+07	1.94E-15	15.2	3.83E-16	5.06E+00
23	F	2.23E+00	2.09E-16	56.1		
23	Ne	3.72E+01	1.10E-15	18.8	7.50E-17	1.47E+01
23	Mg	1.13E+01	1.05E-16	69.7		
24	F	3.40E-01	5.24E-17	99		
24	Ne	2.03E+02	2.62E-16	38.8	1.05E-17	2.49E+01
24	Na	5.39E+04	1.54E-15	10.5	6.44E-16	2.40E+00
25	Na	5.91E+01	1.41E-15	18.9	1.84E-16	7.68E+00
25	Al	7.18E+00	1.57E-16	56.1		
26	Na	1.07E+00	4.19E-16	36.4		
26	Al	2.33E+13	1.23E-15	12.8	5.32E-16	2.31E+00
27	Na	3.01E-01	5.24E-17	99		
27	Mg	5.68E+02	2.57E-15	12.7	3.73E-16	6.88E+00
27	Si	4.16E+00	1.57E-16	56.1		
28	Mg	7.53E+04	6.28E-16	26.9	2.07E-16	3.04E+00
28	Al	1.35E+02	8.69E-15	6.1	1.93E-15	4.50E+00
29	Mg	1.30E+00	5.24E-17	99		
29	Al	3.94E+02	5.24E-15	9.1	9.55E-16	5.48E+00
29	P	4.14E+00	1.05E-16	99		
30	Al	3.60E+00	1.10E-15	18.7		
30	P	1.50E+02	4.14E-15	10.5	3.61E-16	1.15E+01
31	Al	6.44E-01	3.14E-16	37.9		
31	Si	9.44E+03	7.86E-15	7.9	9.19E-16	8.55E+00
32	Al	3.30E-02	1.05E-16	69.7		
32	Si	5.42E+09	3.88E-15	13.1	6.14E-16	6.31E+00
32	P	1.23E+06	2.04E-14	5.2	1.35E-14	1.51E+00
33	Si	6.18E+00	4.19E-16	31.7		
33	P	2.19E+06	1.88E-14	4.1	1.00E-14	1.88E+00
33	Cl	2.51E+00	5.24E-17	99		
34	Si	2.77E+00	4.19E-16	36.4		
34	P	1.24E+01	5.18E-15	10.9		
34	Cl	1.53E+00	1.28E-15	11.3	5.04E-16	2.55E+00
35	P	4.73E+01	2.41E-15	13.7	9.53E-16	2.53E+00
35	S	7.56E+06	2.51E-14	5.4	1.26E-14	2.00E+00
35	Ar	1.78E+00	1.57E-16	56.1		
36	P	5.60E+00	1.57E-16	56.1		
36	Cl	9.49E+12	5.13E-14	3.4	3.81E-14	1.35E+00
37	P	2.31E+00	5.24E-17	99		
37	S	3.03E+02	4.56E-15	12.9	3.26E-15	1.40E+00
37	Ar	3.03E+06	3.15E-14	4	3.66E-14	8.60E-01
38	S	1.02E+04	2.67E-15	12.4	2.41E-15	1.11E+00
38	Cl	2.23E+03	1.99E-14	2.5	2.49E-14	7.98E-01
38	K	4.58E+02	1.31E-16	42.2	9.15E-16	1.43E-01
39	Cl	3.34E+03	6.06E-14	3.1	4.01E-14	1.51E+00
39	Ar	8.48E+09	1.21E-13	1.8	1.22E-13	9.88E-01
40	Cl	8.10E+01	3.98E-15	11.9	4.97E-15	8.01E-01

40	K	4.03E+16	3.56E-15	13	3.78E-15	9.42E-01
41	Ar	6.56E+03	2.62E-13	1.4	2.60E-13	1.01E+00

Table 42: Total activity of the air directly after 1h of irradiation with a 400 MeV carbon ion beam, according to FLUKA ("RESNUC"), the folding method including decay during irradiation ("airactiv") and the reference folding method ignoring decay during irradiation ("airactiv ref."), as well as the ratio between the FLUKA results and the results of the folding method

	Isotope	T 1/2 [s]	Bq/cm3 RESNUC	Bq/cm3 airactiv	Bq/cm3 airactiv ref.	RESNUC/airactiv [Bq/cmc]	RESNUC/airref. [Bq/cmc]
3	H	3.89E+08	1.19E-06	2.20E-07	2.21E-07	5.40E+00	5.39E+00
6	He	8.07E-01	9.38E-03				
7	Be	4.60E+06	4.72E-05	8.52E-06	8.52E-06	5.54E+00	5.54E+00
8	He	1.19E-01	3.94E-04				
8	Li	8.38E-01	1.47E-02				
8	Be	6.71E-17	2.45E-02				
8	B	7.70E-01	7.72E-03				
9	Li	1.78E-01	2.00E-03				
9	B	8.45E-19	1.10E-03				
9	C	1.27E-01	1.10E-03				
10	Be	4.76E+13	1.25E-12	6.22E-13	6.59E-13	2.01E+00	1.90E+00
10	C	1.93E+01	6.87E-03				
11	Li	8.50E-03	8.61E-06				
11	Be	1.38E+01	4.40E-04				
11	C	1.22E+03	5.31E-02	2.47E-02	5.79E-02	2.15E+00	9.17E-01
12	Be	2.36E-02	2.90E-05				
12	B	2.02E-02	8.79E-03				
12	N	1.10E-02	1.19E-03				
13	Be	0.00E+00	0.00E+00				
13	B	1.74E-02	1.01E-03				
13	N	5.98E+02	9.89E-02	5.22E-02	2.21E-01	1.90E+00	4.47E-01
13	O	8.58E-03	1.09E-04				
14	B	1.38E-02	6.45E-06				
14	C	1.81E+11	3.40E-08	3.40E-08	3.40E-08	1.00E+00	1.00E+00
14	O	7.06E+01	5.74E-03	4.08E-03	1.44E-01	1.41E+00	3.98E-02
15	C	2.45E+00	1.00E-04				
15	O	1.22E+02	5.51E-02	3.86E-02	7.88E-01	1.43E+00	6.99E-02
16	C	7.47E-01	2.15E-06				
16	N	7.13E+00	1.62E-03				
17	N	4.17E+00	1.03E-04				
17	F	6.45E+01	1.08E-05				
18	N	6.24E-01	2.15E-06				
18	F	6.59E+03	1.15E-05	5.79E-06	6.96E-06	1.99E+00	1.66E+00
19	O	2.69E+01	8.61E-06	3.28E-07	3.04E-05	2.62E+01	2.83E-01
19	Ne	1.73E+01	1.08E-06				
20	O	1.35E+01	5.38E-06				

20	F	1.10E+01	3.98E-05				
21	F	4.16E+00	2.26E-05				
21	Na	2.25E+01	3.23E-06				
22	F	4.23E+00	8.61E-06				
22	Na	8.21E+07	1.18E-09	2.33E-10	2.33E-10	5.06E+00	5.06E+00
23	F	2.23E+00	3.23E-06				
23	Ne	3.72E+01	2.58E-05	1.50E-06	1.01E-04	1.72E+01	2.57E-01
23	Mg	1.13E+01	2.15E-06				
24	F	3.40E-01	1.08E-06				
24	Ne	2.03E+02	6.45E-06	2.10E-07	2.58E-06	3.07E+01	2.50E+00
24	Na	5.39E+04	3.05E-06	5.82E-07	5.97E-07	5.24E+00	5.10E+00
25	Na	5.91E+01	2.90E-05	3.68E-06	1.55E-04	7.89E+00	1.87E-01
25	Al	7.18E+00	3.23E-06				
26	Na	1.07E+00	8.61E-06				
26	Al	2.33E+13	2.70E-15	1.18E-15	1.14E-15	2.30E+00	2.38E+00
27	Na	3.01E-01	1.08E-06				
27	Mg	5.68E+02	5.10E-05	7.37E-06	3.28E-05	6.92E+00	1.55E+00
27	Si	4.16E+00	3.23E-06				
28	Mg	7.53E+04	4.21E-07	1.35E-07	1.37E-07	3.12E+00	3.07E+00
28	Al	1.35E+02	1.75E-04	3.86E-05	7.16E-04	4.53E+00	2.44E-01
29	Mg	1.30E+00	1.08E-06				
29	Al	3.94E+02	1.02E-04	1.91E-05	1.21E-04	5.35E+00	8.42E-01
29	P	4.14E+00	1.08E-06				
30	Al	3.60E+00	2.26E-05				
30	P	1.50E+02	8.18E-05	7.22E-06	1.20E-04	1.13E+01	6.80E-01
31	Al	6.44E-01	6.45E-06				
31	Si	9.44E+03	3.77E-05	4.27E-06	4.86E-06	8.84E+00	7.77E+00
32	Al	3.30E-02	2.15E-06				
32	Si	5.42E+09	3.66E-11	6.35E-12	5.65E-12	5.77E+00	6.48E+00
32	P	1.23E+06	8.25E-07	5.45E-07	5.47E-07	1.51E+00	1.51E+00
33	Si	6.18E+00	8.61E-06				
33	P	2.19E+06	4.41E-07	2.27E-07	2.28E-07	1.94E+00	1.93E+00
33	Cl	2.51E+00	1.08E-06				
34	Si	2.77E+00	8.61E-06				
34	P	1.24E+01	1.13E-04				
34	Cl	1.53E+00	3.42E-05	7.33E-06	1.65E-02	4.66E+00	2.07E-03
35	P	4.73E+01	4.95E-05	1.91E-05	1.01E-03	2.60E+00	4.92E-02
35	S	7.56E+06	1.82E-07	8.32E-08	8.32E-08	2.19E+00	2.19E+00
35	Ar	1.78E+00	3.23E-06				
36	P	5.60E+00	3.23E-06				
36	Cl	9.49E+12	2.68E-13	2.00E-13	2.00E-13	1.34E+00	1.34E+00
37	P	2.31E+00	1.08E-06				
37	S	3.03E+02	9.14E-05	6.52E-05	5.37E-04	1.40E+00	1.70E-01
37	Ar	3.03E+06	5.15E-07	6.03E-07	6.03E-07	8.53E-01	8.53E-01
38	S	1.02E+04	1.19E-05	1.03E-05	1.18E-05	1.15E+00	1.01E+00
38	Cl	2.23E+03	5.37E-04	3.35E-04	5.56E-04	1.60E+00	9.65E-01

38	K	4.58E+02	2.68E-06	1.82E-05	9.97E-05	1.47E-01	2.69E-02
39	Cl	3.34E+03	6.41E-04	4.22E-04	6.00E-04	1.52E+00	1.07E+00
39	Ar	8.48E+09	8.14E-10	7.17E-10	7.18E-10	1.14E+00	1.13E+00
40	Cl	8.10E+01	8.07E-05	9.94E-05	3.06E-03	8.12E-01	2.63E-02
40	K	4.03E+16	4.47E-18	4.67E-18	4.68E-18	9.57E-01	9.53E-01
41	Ar	6.56E+03	1.65E-03	1.64E-03	1.98E-03	1.01E+00	8.36E-01
SUM VALUES:		2.98E-01	1.22E-01	1.24E+00	2.44E+00	2.44E+00	2.41E-01

Table 43: Total activity of the air after 1h of irradiation with a 400 MeV carbon ion beam and a cooling time of 3600 seconds (1h), according to FLUKA ("RESNUC"), the folding method including decay during irradiation ("airactiv") and the reference folding method ignoring decay during irradiation ("airactiv.ref."), as well as the ratio between the FLUKA results and the results of the folding method

	Isotope	T 1/2 [s]	Bq/cm3 RESNUC	Bq/cm3 airactiv	Bq/cm3 airactiv.ref.	RESNUC/airactiv [Bq/cmc]	RESNUC/airref. [Bq/cmc]
3	H	3.89E+08	1.19E-06	2.20E-07	2.21E-07	5.40E+00	5.39E+00
6	He	8.07E-01	0.00E+00				
7	Be	4.60E+06	4.71E-05	8.51E-06	8.52E-06	5.54E+00	5.54E+00
8	He	1.19E-01	0.00E+00				
8	Li	8.38E-01	0.00E+00				
8	Be	6.71E-17	0.00E+00				
8	B	7.70E-01	0.00E+00				
9	Li	1.78E-01	0.00E+00				
9	B	8.45E-19	0.00E+00				
9	C	1.27E-01	0.00E+00				
10	Be	4.76E+13	1.25E-12	6.22E-13	6.59E-13	2.01E+00	1.90E+00
10	C	1.93E+01	3.47E-59				
11	Li	8.50E-03	0.00E+00				
11	Be	1.38E+01	1.48E-82				
11	C	1.22E+03	6.90E-03	3.21E-03	7.53E-03	2.15E+00	9.17E-01
12	Be	2.36E-02	0.00E+00				
12	B	2.02E-02	0.00E+00				
12	N	1.10E-02	0.00E+00				
13	Be	0.00E+00	0.00E+00				
13	B	1.74E-02	0.00E+00				
13	N	5.98E+02	1.52E-03	8.04E-04	3.41E-03	1.90E+00	4.47E-01
13	O	8.58E-03	0.00E+00				
14	B	1.38E-02	0.00E+00				
14	C	1.81E+11	3.40E-08	3.40E-08	3.40E-08	1.00E+00	1.00E+00
14	O	7.06E+01	2.58E-18	1.83E-18	6.47E-17	1.41E+00	3.98E-02
15	C	2.45E+00	0.00E+00				
15	O	1.22E+02	7.46E-11	5.23E-11	1.07E-09	1.43E+00	6.99E-02
16	C	7.47E-01	0.00E+00				
16	N	7.13E+00	1.64E-155				
17	N	4.17E+00	2.08E-264				
17	F	6.45E+01	1.69E-22				

18	N	6.24E-01	0.00E+00				
18	F	6.59E+03	7.89E-06	3.96E-06	4.76E-06	1.99E+00	1.66E+00
19	O	2.69E+01	4.61E-46	1.76E-47	1.63E-45	2.62E+01	2.83E-01
19	Ne	1.73E+01	3.42E-69				
20	O	1.35E+01	3.28E-86				
20	F	1.10E+01	1.20E-103				
21	F	4.16E+00	5.27E-266				
21	Na	2.25E+01	2.10E-54				
22	F	4.23E+00	5.48E-262				
22	Na	8.21E+07	1.18E-09	2.33E-10	2.33E-10	5.06E+00	5.06E+00
23	F	2.23E+00	0.00E+00				
23	Ne	3.72E+01	2.05E-34	1.19E-35	7.97E-34	1.72E+01	2.57E-01
23	Mg	1.13E+01	3.97E-102				
24	F	3.40E-01	0.00E+00				
24	Ne	2.03E+02	2.92E-11	9.52E-13	1.17E-11	3.07E+01	2.50E+00
24	Na	5.39E+04	2.91E-06	5.55E-07	5.70E-07	5.24E+00	5.10E+00
25	Na	5.91E+01	1.34E-23	1.69E-24	7.15E-23	7.89E+00	1.87E-01
25	Al	7.18E+00	4.34E-157				
26	Na	1.07E+00	0.00E+00				
26	Al	2.33E+13	2.70E-15	1.18E-15	1.14E-15	2.30E+00	2.38E+00
27	Na	3.01E-01	0.00E+00				
27	Mg	5.68E+02	6.28E-07	9.07E-08	4.04E-07	6.92E+00	1.55E+00
27	Si	4.16E+00	1.00E-266				
28	Mg	7.53E+04	4.07E-07	1.31E-07	1.33E-07	3.12E+00	3.07E+00
28	Al	1.35E+02	1.53E-12	3.38E-13	6.28E-12	4.53E+00	2.44E-01
29	Mg	1.30E+00	0.00E+00				
29	Al	3.94E+02	1.80E-07	3.36E-08	2.14E-07	5.35E+00	8.42E-01
29	P	4.14E+00	2.47E-268				
30	Al	3.60E+00	2.11E-306				
30	P	1.50E+02	4.82E-12	4.26E-13	7.08E-12	1.13E+01	6.80E-01
31	Al	6.44E-01	0.00E+00				
31	Si	9.44E+03	2.90E-05	3.28E-06	3.73E-06	8.84E+00	7.77E+00
32	Al	3.30E-02	0.00E+00				
32	Si	5.42E+09	3.66E-11	6.35E-12	5.65E-12	5.77E+00	6.48E+00
32	P	1.23E+06	8.23E-07	5.44E-07	5.46E-07	1.51E+00	1.51E+00
33	Si	6.18E+00	3.78E-181				
33	P	2.19E+06	4.41E-07	2.27E-07	2.28E-07	1.94E+00	1.93E+00
33	Cl	2.51E+00	0.00E+00				
34	Si	2.77E+00	0.00E+00				
34	P	1.24E+01	7.38E-92				
34	Cl	1.53E+00	0.00E+00	0.00E+00	0.00E+00		
35	P	4.73E+01	6.07E-28	2.34E-28	1.23E-26	2.60E+00	4.92E-02
35	S	7.56E+06	1.82E-07	8.32E-08	8.31E-08	2.19E+00	2.19E+00
35	Ar	1.78E+00	0.00E+00				
36	P	5.60E+00	9.76E-200				
36	Cl	9.49E+12	2.68E-13	2.00E-13	2.00E-13	1.34E+00	1.34E+00

37	P	2.31E+00	0.00E+00				
37	S	3.03E+02	2.42E-08	1.73E-08	1.42E-07	1.40E+00	1.70E-01
37	Ar	3.03E+06	5.14E-07	6.03E-07	6.03E-07	8.53E-01	8.53E-01
38	S	1.02E+04	9.31E-06	8.10E-06	9.22E-06	1.15E+00	1.01E+00
38	Cl	2.23E+03	1.76E-04	1.10E-04	1.82E-04	1.60E+00	9.65E-01
38	K	4.58E+02	1.16E-08	7.86E-08	4.30E-07	1.47E-01	2.69E-02
39	Cl	3.34E+03	3.04E-04	2.00E-04	2.84E-04	1.52E+00	1.07E+00
39	Ar	8.48E+09	8.14E-10	7.17E-10	7.18E-10	1.14E+00	1.13E+00
40	Cl	8.10E+01	3.37E-18	4.15E-18	1.28E-16	8.12E-01	2.63E-02
40	K	4.03E+16	4.46E-18	4.67E-18	4.68E-18	9.57E-01	9.53E-01
41	Ar	6.56E+03	1.13E-03	1.12E-03	1.35E-03	1.01E+00	8.36E-01
	SUM VALUES:		1.01E-02	5.47E-03	1.28E-02	1.85E+00	7.93E-01

Table 44: Total activity of the air after 1h of irradiation with a 400 MeV carbon ion beam and a cooling time of 86400 seconds (1d), according to FLUKA ("RESNUC"), the folding method including decay during irradiation ("airactiv") and the reference folding method ignoring decay during irradiation ("airactiv.ref."), as well as the ratio between the FLUKA results and the results of the folding method

	Isotope	T 1/2 [s]	Bq/cm3 RESNUC	Bq/cm3 airactiv	Bq/cm3 airactiv.ref.	RESNUC/airactiv [Bq/cm3]	RESNUC/airref. [Bq/cm3]
3	H	3.89E+08	1.19E-06	2.20E-07	2.21E-07	5.40E+00	5.39E+00
6	He	8.07E-01	0.00E+00				
7	Be	4.60E+06	4.66E-05	8.41E-06	8.41E-06	5.54E+00	5.54E+00
8	He	1.19E-01	0.00E+00				
8	Li	8.38E-01	0.00E+00				
8	Be	6.71E-17	0.00E+00				
8	B	7.70E-01	0.00E+00				
9	Li	1.78E-01	0.00E+00				
9	B	8.45E-19	0.00E+00				
9	C	1.27E-01	0.00E+00				
10	Be	4.76E+13	1.25E-12	6.22E-13	6.59E-13	2.01E+00	1.90E+00
10	C	1.93E+01	0.00E+00				
11	Li	8.50E-03	0.00E+00				
11	Be	1.38E+01	0.00E+00				
11	C	1.22E+03	2.88E-23	1.34E-23	3.14E-23	2.15E+00	9.17E-01
12	Be	2.36E-02	0.00E+00				
12	B	2.02E-02	0.00E+00				
12	N	1.10E-02	0.00E+00				
13	Be	0.00E+00	0.00E+00				
13	B	1.74E-02	0.00E+00				
13	N	5.98E+02	3.12E-45	1.65E-45	6.99E-45	1.90E+00	4.47E-01
13	O	8.58E-03	0.00E+00				
14	B	1.38E-02	0.00E+00				
14	C	1.81E+11	3.40E-08	3.40E-08	3.40E-08	1.00E+00	1.00E+00
14	O	7.06E+01	0.00E+00	0.00E+00	0.00E+00		
15	C	2.45E+00	0.00E+00				

			7.98E-				
15	O	1.22E+02	215	5.59E-215	1.14E-213	1.43E+00	6.99E-02
16	C	7.47E-01	0.00E+00				
16	N	7.13E+00	0.00E+00				
17	N	4.17E+00	0.00E+00				
17	F	6.45E+01	0.00E+00				
18	N	6.24E-01	0.00E+00				
18	F	6.59E+03	1.30E-09	6.51E-10	7.82E-10	1.99E+00	1.66E+00
19	O	2.69E+01	0.00E+00	0.00E+00	0.00E+00		
19	Ne	1.73E+01	0.00E+00				
20	O	1.35E+01	0.00E+00				
20	F	1.10E+01	0.00E+00				
21	F	4.16E+00	0.00E+00				
21	Na	2.25E+01	0.00E+00				
22	F	4.23E+00	0.00E+00				
22	Na	8.21E+07	1.18E-09	2.33E-10	2.33E-10	5.06E+00	5.06E+00
23	F	2.23E+00	0.00E+00				
23	Ne	3.72E+01	0.00E+00	0.00E+00	0.00E+00		
23	Mg	1.13E+01	0.00E+00				
24	F	3.40E-01	0.00E+00				
			3.63E-				
24	Ne	2.03E+02	134	1.18E-135	1.45E-134	3.07E+01	2.50E+00
24	Na	5.39E+04	1.00E-06	1.91E-07	1.96E-07	5.24E+00	5.10E+00
25	Na	5.91E+01	0.00E+00	0.00E+00	0.00E+00		
25	Al	7.18E+00	0.00E+00				
26	Na	1.07E+00	0.00E+00				
26	Al	2.33E+13	2.70E-15	1.18E-15	1.14E-15	2.30E+00	2.38E+00
27	Na	3.01E-01	0.00E+00				
27	Mg	5.68E+02	7.53E-51	1.09E-51	4.84E-51	6.92E+00	1.55E+00
27	Si	4.16E+00	0.00E+00				
28	Mg	7.53E+04	1.90E-07	6.09E-08	6.19E-08	3.12E+00	3.07E+00
			7.36E-				
28	Al	1.35E+02	198	1.63E-198	3.02E-197	4.53E+00	2.44E-01
29	Mg	1.30E+00	0.00E+00				
29	Al	3.94E+02	8.49E-71	1.59E-71	1.01E-70	5.35E+00	8.42E-01
29	P	4.14E+00	0.00E+00				
30	Al	3.60E+00	0.00E+00				
			2.53E-				
30	P	1.50E+02	178	2.24E-179	3.72E-178	1.13E+01	6.80E-01
31	Al	6.44E-01	0.00E+00				
31	Si	9.44E+03	6.62E-08	7.49E-09	8.53E-09	8.84E+00	7.77E+00
32	Al	3.30E-02	0.00E+00				
32	Si	5.42E+09	3.66E-11	6.35E-12	5.65E-12	5.77E+00	6.48E+00
32	P	1.23E+06	7.86E-07	5.19E-07	5.21E-07	1.51E+00	1.51E+00
33	Si	6.18E+00	0.00E+00				
33	P	2.19E+06	4.29E-07	2.21E-07	2.22E-07	1.94E+00	1.93E+00
33	Cl	2.51E+00	0.00E+00				
34	Si	2.77E+00	0.00E+00				

34	P	1.24E+01	0.00E+00				
34	Cl	1.53E+00	0.00E+00	0.00E+00	0.00E+00		
35	P	4.73E+01	0.00E+00	0.00E+00	0.00E+00		
35	S	7.56E+06	1.81E-07	8.26E-08	8.25E-08	2.19E+00	2.19E+00
35	Ar	1.78E+00	0.00E+00				
36	P	5.60E+00	0.00E+00				
36	Cl	9.49E+12	2.68E-13	2.00E-13	2.00E-13	1.34E+00	1.34E+00
37	P	2.31E+00	0.00E+00				
37	S	3.03E+02	1.33E-90	9.46E-91	7.79E-90	1.40E+00	1.70E-01
37	Ar	3.03E+06	5.05E-07	5.92E-07	5.92E-07	8.53E-01	8.53E-01
38	S	1.02E+04	3.39E-08	2.95E-08	3.36E-08	1.15E+00	1.01E+00
38	Cl	2.23E+03	1.22E-15	7.64E-16	1.27E-15	1.60E+00	9.65E-01
38	K	4.58E+02	4.62E-63	3.14E-62	1.72E-61	1.47E-01	2.69E-02
39	Cl	3.34E+03	1.02E-11	6.75E-12	9.59E-12	1.52E+00	1.07E+00
39	Ar	8.48E+09	8.14E-10	7.17E-10	7.18E-10	1.14E+00	1.13E+00
40	Cl	8.10E+01	0.00E+00	0.00E+00	0.00E+00		
40	K	4.03E+16	4.46E-18	4.67E-18	4.68E-18	9.57E-01	9.53E-01
41	Ar	6.56E+03	1.79E-07	1.78E-07	2.15E-07	1.01E+00	8.36E-01
	SUM	VALUES:	5.12E-05	1.05E-05	1.06E-05	4.85E+00	4.83E+00

PART B: MEDAUSTRON TREATMENT ROOMS

IRRADIATION ROOM 1 - 800 MEV PROTONS

Table 45: Yield results (per primary particle per cm³) and relative errors, as well as specific activities (in Bq/m³) for each isotope after several cooling times (in seconds) after irradiation with a total intensity of 2.32E+13 protons, which corresponds to 3.1 air exchanges per hour during continuous irradiation with an 800 MeV proton beam and an intensity of 2E+10 protons per second

Isotope	t 1/2 [s]	yield/pp/cm ³	rel. err.	0s	60s	600s	1191.29s	3600s
H-3	3.89E+08	2.54E-12	0.01%	1.05E-01	1.05E-01	1.05E-01	1.05E-01	1.05E-01
Be-7	4.61E+06	8.55E-13	0.00%	2.99E+00	2.99E+00	2.99E+00	2.99E+00	2.99E+00
Be-10	5.05E+13	4.74E-13	0.01%	1.51E-07	1.51E-07	1.51E-07	1.51E-07	1.51E-07
C-11	1.22E+03	1.13E-12	0.01%	1.49E+04	1.44E+04	1.06E+04	7.70E+03	1.93E+03
C-14	1.81E+11	5.00E-10	0.02%	4.45E-02	4.45E-02	4.45E-02	4.45E-02	4.45E-02
N-13	5.98E+02	1.79E-12	0.01%	4.82E+04	4.50E+04	2.40E+04	1.25E+04	7.42E+02
O-14	7.10E+01	1.14E-13	0.02%	2.58E+04	1.44E+04	7.39E+01	3.08E-01	1.41E-11
O-15	1.22E+02	1.45E-12	0.00%	1.91E+05	1.36E+05	6.36E+03	2.64E+02	2.60E-04
O-19	2.71E+01	1.53E-16	0.00%	9.09E+01	1.96E+01	1.97E-05	1.14E-11	9.32E-39
F-18	6.59E+03	4.21E-15	0.00%	1.03E+01	1.02E+01	9.66E+00	9.11E+00	7.05E+00
Ne-23	2.80E+01	3.94E-16	0.00%	2.27E+02	5.13E+01	8.03E-05	7.41E-11	4.48E-37
Ne-24	2.03E+02	8.23E-17	0.00%	6.53E+00	5.32E+00	8.40E-01	1.23E-01	2.96E-05
Na-22	8.21E+07	1.14E-15	0.00%	2.24E-04	2.24E-04	2.24E-04	2.24E-04	2.23E-04
Na-24	5.40E+04	1.79E-15	0.00%	5.34E-01	5.33E-01	5.30E-01	5.26E-01	5.10E-01
Na-25	6.00E+01	7.03E-16	0.00%	1.89E+02	9.43E+01	1.84E-01	2.81E-04	1.64E-16
Mg-27	5.70E+02	1.02E-15	0.00%	2.88E+01	2.68E+01	1.39E+01	7.02E+00	3.62E-01
Mg-28	7.53E+04	3.03E-16	0.00%	6.48E-02	6.48E-02	6.44E-02	6.41E-02	6.27E-02
Al-26	2.26E+13	1.44E-15	0.00%	1.03E-09	1.03E-09	1.03E-09	1.03E-09	1.03E-09
Al-28	1.34E+02	3.30E-15	0.00%	3.95E+02	2.90E+02	1.79E+01	9.90E-01	3.42E-06
Al-29	3.96E+02	1.83E-15	0.00%	7.44E+01	6.70E+01	2.60E+01	9.74E+00	1.36E-01
Si-31	9.44E+03	1.94E-15	0.00%	3.31E+00	3.29E+00	3.17E+00	3.04E+00	2.54E+00
Si-32	5.46E+09	1.02E-15	0.00%	3.01E-06	3.01E-06	3.01E-06	3.01E-06	3.01E-06
P-30	1.50E+02	1.07E-15	0.00%	1.15E+02	8.71E+01	7.17E+00	5.36E-01	6.80E-06
P-32	1.23E+06	1.10E-14	0.00%	1.43E-01	1.43E-01	1.43E-01	1.43E-01	1.43E-01
P-33	2.19E+06	7.74E-15	0.00%	5.68E-02	5.68E-02	5.68E-02	5.68E-02	5.67E-02
P-35	4.74E+01	8.69E-16	0.00%	2.95E+02	1.23E+02	4.57E-02	1.24E-05	4.05E-21
S-35	7.55E+06	9.91E-15	0.00%	2.11E-02	2.11E-02	2.11E-02	2.11E-02	2.11E-02
S-37	3.04E+02	4.40E-15	0.02%	2.33E+02	2.03E+02	5.93E+01	1.65E+01	6.29E-02
S-38	1.03E+04	2.12E-15	0.00%	3.30E+00	3.29E+00	3.17E+00	3.06E+00	2.59E+00
Cl-34	1.92E+03	4.72E-16	0.00%	3.96E+00	3.87E+00	3.19E+00	2.60E+00	1.08E+00
Cl-36	9.50E+12	2.49E-14	0.01%	4.22E-08	4.22E-08	4.22E-08	4.22E-08	4.22E-08
Cl-38	2.23E+03	1.72E-14	0.01%	1.24E+02	1.22E+02	1.03E+02	8.65E+01	4.06E+01
Cl-39	3.34E+03	3.47E-14	0.01%	1.67E+02	1.65E+02	1.48E+02	1.32E+02	7.93E+01
Cl-40	8.40E+01	3.46E-15	0.02%	6.63E+02	4.04E+02	4.69E+00	4.57E-02	8.32E-11
Ar-37	3.03E+06	4.43E-14	0.01%	2.36E-01	2.36E-01	2.36E-01	2.36E-01	2.36E-01
Ar-39	8.49E+09	1.26E-13	0.02%	2.39E-04	2.39E-04	2.39E-04	2.39E-04	2.39E-04
Ar-41	6.58E+03	1.04E-12	0.02%	2.55E+03	2.53E+03	2.39E+03	2.25E+03	1.74E+03
K-38	4.58E+02	3.09E-16	0.02%	1.09E+01	9.92E+00	4.38E+00	1.87E+00	4.68E-02
K-40	4.04E+16	8.56E-16	0.06%	3.41E-13	3.41E-13	3.41E-13	3.41E-13	3.41E-13

Table 46: Ci values for the isotopes gained by the simulation as well as the comparison of activities after several cooling times (0s, 60s, 600s, 1161.29s, 3600s), after irradiation with a total intensity of 2.32E+13 protons, which corresponds to 3.1 air exchanges per hour during continuous irradiation with an 800 MeV proton beam and an intensity of 2E+10 protons per second, to their respective Ci value. Calculated Ci values not mentioned in Austrian law are underlined in light blue. Sum values of the comparison values after the listed cooling times are listed at the bottom, underlined in dark blue.

Isotope	t 1/2 [s]	Ci	0s	60s	600s	1161.29s	3600s
H-3	3.89E+08	100.0	1.05E-03	1.05E-03	1.05E-03	1.05E-03	1.05E-03
Be-7	4.61E+06	600.0	4.98E-03	4.98E-03	4.98E-03	4.98E-03	4.98E-03
Be-10	5.05E+13	1.0	1.51E-07	1.51E-07	1.51E-07	1.51E-07	1.51E-07
C-11	1.22E+03	600.0	2.48E+01	2.40E+01	1.76E+01	1.28E+01	3.22E+00
C-14	1.81E+11	6.0	7.42E-03	7.42E-03	7.42E-03	7.42E-03	7.42E-03
N-13	5.98E+02	2000.0	2.41E+01	2.25E+01	1.20E+01	6.27E+00	3.71E-01
O-14	7.10E+01	927.1	2.79E+01	1.55E+01	7.97E-02	3.32E-04	1.52E-14
O-15	1.22E+02	1000.0	1.91E+02	1.36E+02	6.36E+00	2.64E-01	2.60E-07
O-19	2.71E+01	1916.0	4.74E-02	1.02E-02	1.03E-08	5.98E-15	4.86E-42
F-18	6.59E+03	500.0	2.06E-02	2.05E-02	1.93E-02	1.82E-02	1.41E-02
Ne-23	2.80E+01	1892.7	1.20E-01	2.71E-02	4.24E-08	3.92E-14	2.37E-40
Ne-24	2.03E+02	896.3	7.29E-03	5.94E-03	9.38E-04	1.38E-04	3.30E-08
Na-22	8.21E+07	1.0	2.24E-04	2.24E-04	2.24E-04	2.24E-04	2.23E-04
Na-24	5.40E+04	90.0	5.93E-03	5.92E-03	5.88E-03	5.84E-03	5.66E-03
Na-25	6.00E+01	28648.2	6.58E-03	3.29E-03	6.43E-06	9.82E-09	5.71E-21
Mg-27	5.70E+02	577.8	4.99E-02	4.64E-02	2.40E-02	1.21E-02	6.26E-04
Mg-28	7.53E+04	20.0	3.24E-03	3.24E-03	3.22E-03	3.21E-03	3.13E-03
Al-26	2.26E+13	0.5	2.05E-09	2.05E-09	2.05E-09	2.05E-09	2.05E-09
Al-28	1.34E+02	537.6	7.35E-01	5.40E-01	3.33E-02	1.84E-03	6.36E-09
Al-29	3.96E+02	232.5	3.20E-01	2.88E-01	1.12E-01	4.19E-02	5.87E-04
Si-31	9.44E+03	300.0	1.10E-02	1.10E-02	1.06E-02	1.01E-02	8.47E-03
Si-32	5.46E+09	0.3	9.41E-06	9.41E-06	9.41E-06	9.41E-06	9.41E-06
P-30	1.50E+02	2727.8	4.21E-02	3.19E-02	2.63E-03	1.96E-04	2.49E-09
P-32	1.23E+06	1.0	1.43E-01	1.43E-01	1.43E-01	1.43E-01	1.43E-01
P-33	2.19E+06	20.0	2.84E-03	2.84E-03	2.84E-03	2.84E-03	2.84E-03
P-35	4.74E+01	12148.0	2.43E-02	1.01E-02	3.76E-06	1.02E-09	3.33E-25
S-35	7.55E+06	20.0	1.06E-03	1.06E-03	1.06E-03	1.06E-03	1.06E-03
S-37	3.04E+02	8682.3	2.69E-02	2.34E-02	6.83E-03	1.90E-03	7.24E-06
S-38	1.03E+04	422.8	7.81E-03	7.78E-03	7.50E-03	7.23E-03	6.14E-03
Cl-34	1.92E+03	16.8	2.35E-01	2.30E-01	1.89E-01	1.55E-01	6.41E-02
Cl-36	9.50E+12	0.1	4.22E-07	4.22E-07	4.22E-07	4.22E-07	4.22E-07
Cl-38	2.23E+03	500.0	2.48E-01	2.43E-01	2.06E-01	1.73E-01	8.11E-02
Cl-39	3.34E+03	600.0	2.79E-01	2.76E-01	2.46E-01	2.19E-01	1.32E-01
Cl-40	8.40E+01	292.7	2.27E+00	1.38E+00	1.60E-02	1.56E-04	2.84E-13
Ar-37	3.03E+06	200000000.0	1.18E-09	1.18E-09	1.18E-09	1.18E-09	1.18E-09
Ar-39	8.49E+09	6000.0	3.98E-08	3.98E-08	3.98E-08	3.98E-08	3.98E-08
Ar-41	6.58E+03	200.0	1.27E+01	1.26E+01	1.19E+01	1.13E+01	8.71E+00
K-38	4.58E+02	4622.1	2.35E-03	2.15E-03	9.48E-04	4.05E-04	1.01E-05
K-40	4.04E+16	0.3	1.09E-12	1.09E-12	1.09E-12	1.09E-12	1.09E-12
Sum:			2.85E+02	2.14E+02	4.91E+01	3.14E+01	1.28E+01

Table 47: Activity of the air after irradiation of a lead target with an 800 MeV proton beam, compared to Ci values, considering a cooling time of 1 hour and thinning the air to a volume of 14.000 m³ at average (5.71E+8 particles per second) and maximum (2E+10 particles per second) intensity

Isotope	Bq (total/y)	av. sp. act.	max. sp. act.	Ci [Bq/m ³]	av./Ci	max./Ci
H-3	4.19E+04	3.42E-04	1.20E-02	100.00	3.42E-06	1.20E-04
Be-7	1.19E+06	9.72E-03	3.41E-01	600.00	1.62E-05	5.68E-04
Be-10	6.04E-02	4.92E-10	1.72E-08	1.00	4.92E-10	1.72E-08
C-11	5.94E+09	6.29E+00	2.20E+02	600.00	1.05E-02	3.67E-01
C-14	1.78E+04	1.45E-04	5.08E-03	6.00	2.42E-05	8.47E-04
N-13	1.92E+10	2.42E+00	8.46E+01	2000.00	1.21E-03	4.23E-02
O-14	1.03E+10	4.59E-14	1.61E-12	927.09	4.95E-17	1.73E-15
O-15	7.62E+10	8.47E-07	2.97E-05	1000.00	8.47E-10	2.97E-08
O-19	3.63E+07	3.03E-41	1.06E-39	1916.02	1.58E-44	5.55E-43
F-18	4.11E+06	2.29E-02	8.03E-01	500.00	4.59E-05	1.61E-03
Ne-23	9.04E+07	1.46E-39	5.11E-38	1892.75	7.70E-43	2.70E-41
Ne-24	2.61E+06	9.64E-08	3.38E-06	896.31	1.08E-10	3.77E-09
Na-22	8.92E+01	7.27E-07	2.55E-05	1.00	7.27E-07	2.55E-05
Na-24	2.13E+05	1.66E-03	5.81E-02	90.00	1.84E-05	6.46E-04
Na-25	7.53E+07	5.32E-19	1.87E-17	28648.19	1.86E-23	6.51E-22
Mg-27	1.15E+07	1.18E-03	4.12E-02	577.79	2.04E-06	7.14E-05
Mg-28	2.59E+04	2.04E-04	7.15E-03	20.00	1.02E-05	3.57E-04
Al-26	4.09E-04	3.34E-12	1.17E-10	0.50	6.68E-12	2.34E-10
Al-28	1.58E+08	1.11E-08	3.90E-07	537.59	2.07E-11	7.25E-10
Al-29	2.97E+07	4.44E-04	1.56E-02	232.45	1.91E-06	6.69E-05
Si-31	1.32E+06	8.27E-03	2.90E-01	300.00	2.76E-05	9.66E-04
Si-32	1.20E+00	9.80E-09	3.43E-07	0.32	3.06E-08	1.07E-06
P-30	4.59E+07	2.21E-08	7.76E-07	2727.82	8.12E-12	2.84E-10
P-32	5.72E+04	4.66E-04	1.63E-02	1.00	4.66E-04	1.63E-02
P-33	2.27E+04	1.85E-04	6.47E-03	20.00	9.23E-06	3.23E-04
P-35	1.18E+08	1.32E-23	4.61E-22	12148.03	1.08E-27	3.80E-26
S-35	8.43E+03	6.87E-05	2.41E-03	20.00	3.44E-06	1.20E-04
S-37	9.31E+07	2.05E-04	7.17E-03	8682.34	2.36E-08	8.26E-07
S-38	1.32E+06	8.44E-03	2.96E-01	422.83	2.00E-05	7.00E-04
Cl-34	1.58E+06	3.51E-03	1.23E-01	16.84	2.09E-04	7.31E-03
Cl-36	1.68E-02	1.37E-10	4.81E-09	0.10	1.37E-09	4.81E-08
Cl-38	4.95E+07	1.32E-01	4.63E+00	500.00	2.64E-04	9.25E-03
Cl-39	6.68E+07	2.58E-01	9.04E+00	600.00	4.30E-04	1.51E-02
Cl-40	2.65E+08	2.71E-13	9.49E-12	292.72	9.25E-16	3.24E-14
Ar-37	9.41E+04	7.66E-04	2.69E-02	20000000.00	3.83E-12	1.34E-10
Ar-39	9.54E+01	7.78E-07	2.72E-05	6000.00	1.30E-10	4.54E-09
Ar-41	1.02E+09	5.67E+00	1.99E+02	200.00	2.83E-02	9.93E-01
K-38	4.33E+06	1.52E-04	5.34E-03	4622.10	3.30E-08	1.16E-06
K-40	1.36E-07	1.11E-15	3.89E-14	0.31	3.55E-15	1.24E-13
Sum:					4.16E-02	1.46E+00

IRRADIATION ROOM 1 - 400 MEV CARBON IONS

Table 48: Yield results (per primary particle per cm³) and relative errors, as well as specific activities (in Bq/m³) for each isotope after several cooling times (in seconds) after irradiation with a total intensity of 1.16E+12 carbon ions, which corresponds to 3.1 air exchanges per hour during continuous irradiation with a 400 MeV ion beam and an intensity of 1E+9 ions per second

Isotope	t 1/2 [s]	yield/pp/cm3	rel. err.	0s	60s	600s	1191.29s	3600s
H-3	3.89E+08	2.54E-12	0.01%	2.80E-02	2.80E-02	2.80E-02	2.80E-02	2.80E-02
Be-7	4.61E+06	8.55E-13	0.00%	3.93E-01	3.93E-01	3.93E-01	3.93E-01	3.93E-01
Be-10	5.05E+13	4.74E-13	0.01%	2.39E-08	2.39E-08	2.39E-08	2.39E-08	2.39E-08
C-11	1.22E+03	1.13E-12	0.01%	1.62E+03	1.57E+03	1.16E+03	8.41E+02	2.11E+02
C-14	1.81E+11	5.00E-10	0.02%	3.28E-03	3.28E-03	3.28E-03	3.28E-03	3.28E-03
N-13	5.98E+02	1.79E-12	0.01%	5.80E+03	5.41E+03	2.89E+03	1.51E+03	8.93E+01
O-14	7.10E+01	1.14E-13	0.02%	1.68E+03	9.33E+02	4.79E+00	2.00E-02	9.14E-13
O-15	1.22E+02	1.45E-12	0.00%	1.46E+04	1.04E+04	4.86E+02	2.02E+01	1.99E-05
O-19	2.71E+01	1.53E-16	0.00%	2.31E+01	4.97E+00	4.99E-06	2.91E-12	2.36E-39
F-18	6.59E+03	4.21E-15	0.00%	2.25E-01	2.24E-01	2.12E-01	2.00E-01	1.54E-01
Ne-23	2.80E+01	3.94E-16	0.00%	3.07E+01	6.95E+00	1.09E-05	1.00E-11	6.07E-38
Ne-24	2.03E+02	8.23E-17	0.00%	3.08E+00	2.51E+00	3.97E-01	5.82E-02	1.40E-05
Na-22	8.21E+07	1.14E-15	0.00%	2.00E-05	2.00E-05	2.00E-05	2.00E-05	2.00E-05
Na-24	5.40E+04	1.79E-15	0.00%	5.21E-02	5.21E-02	5.17E-02	5.13E-02	4.97E-02
Na-25	6.00E+01	7.03E-16	0.00%	3.00E+01	1.50E+01	2.93E-02	4.47E-05	2.60E-17
Mg-27	5.70E+02	1.02E-15	0.00%	2.47E+00	2.29E+00	1.19E+00	6.01E-01	3.10E-02
Mg-28	7.53E+04	3.03E-16	0.00%	1.35E-02	1.35E-02	1.34E-02	1.34E-02	1.31E-02
Al-26	2.26E+13	1.44E-15	0.00%	1.25E-10	1.25E-10	1.25E-10	1.25E-10	1.25E-10
Al-28	1.34E+02	3.30E-15	0.00%	4.48E+01	3.29E+01	2.03E+00	1.12E-01	3.87E-07
Al-29	3.96E+02	1.83E-15	0.00%	9.28E+00	8.35E+00	3.25E+00	1.21E+00	1.70E-02
Si-31	9.44E+03	1.94E-15	0.00%	5.71E-01	5.69E-01	5.47E-01	5.25E-01	4.39E-01
Si-32	5.46E+09	1.02E-15	0.00%	5.44E-07	5.44E-07	5.44E-07	5.44E-07	5.44E-07
P-30	1.50E+02	1.07E-15	0.00%	1.77E+01	1.34E+01	1.11E+00	8.26E-02	1.05E-06
P-32	1.23E+06	1.10E-14	0.00%	1.03E-02	1.03E-02	1.03E-02	1.02E-02	1.02E-02
P-33	2.19E+06	7.74E-15	0.00%	5.41E-03	5.41E-03	5.41E-03	5.41E-03	5.41E-03
P-35	4.74E+01	8.69E-16	0.00%	3.13E+01	1.30E+01	4.85E-03	1.32E-06	4.29E-22
S-35	7.55E+06	9.91E-15	0.00%	2.72E-03	2.72E-03	2.72E-03	2.72E-03	2.72E-03
S-37	3.04E+02	4.40E-15	0.02%	2.14E+01	1.86E+01	5.43E+00	1.51E+00	5.76E-03
S-38	1.03E+04	2.12E-15	0.00%	3.40E-01	3.39E-01	3.27E-01	3.15E-01	2.67E-01
Cl-34	1.92E+03	4.72E-16	0.00%	7.73E-01	7.57E-01	6.23E-01	5.09E-01	2.11E-01
Cl-36	9.50E+12	2.49E-14	0.01%	3.41E-09	3.41E-09	3.41E-09	3.41E-09	3.41E-09
Cl-38	2.23E+03	1.72E-14	0.01%	1.35E+01	1.33E+01	1.12E+01	9.45E+00	4.43E+00
Cl-39	3.34E+03	3.47E-14	0.01%	1.70E+01	1.68E+01	1.50E+01	1.34E+01	8.05E+00
Cl-40	8.40E+01	3.46E-15	0.02%	7.44E+01	4.54E+01	5.27E-01	5.13E-03	9.34E-12
Ar-37	3.03E+06	4.43E-14	0.01%	1.50E-02	1.50E-02	1.50E-02	1.50E-02	1.50E-02
Ar-39	8.49E+09	1.26E-13	0.02%	2.36E-05	2.36E-05	2.36E-05	2.36E-05	2.36E-05
Ar-41	6.58E+03	1.04E-12	0.02%	1.86E+02	1.84E+02	1.74E+02	1.64E+02	1.27E+02
K-38	4.58E+02	3.09E-16	0.02%	1.71E-01	1.56E-01	6.88E-02	2.94E-02	7.35E-04
K-40	4.04E+16	8.56E-16	0.06%	4.45E-14	4.45E-14	4.45E-14	4.45E-14	4.45E-14

Table 49: Ci values for the isotopes gained by the simulation as well as the comparison of activities after several cooling times (0s, 60s, 600s, 1161.29s, 3600s), after irradiation with a total intensity of 1.16E+12 carbon ions, which corresponds to 3.1 air exchanges per hour during continuous irradiation with an 400 MeV ion beam and an intensity of 1E+9 ions per second, to their respective Ci value. Calculated Ci values not mentioned in Austrian law are underlined in light blue. Sum values of the comparison values after the listed cooling times are listed at the bottom, underlined in dark blue.

Isotope	t 1/2 [s]	Ci	0s	60s	600s	1161.29s	3600s
H-3	3.89E+08	100.0	2.80E-04	2.80E-04	2.80E-04	2.80E-04	2.80E-04
Be-7	4.61E+06	600.0	6.55E-04	6.55E-04	6.55E-04	6.55E-04	6.55E-04
Be-10	5.05E+13	1.0	2.39E-08	2.39E-08	2.39E-08	2.39E-08	2.39E-08
C-11	1.22E+03	600.0	2.71E+00	2.62E+00	1.93E+00	1.40E+00	3.52E-01
C-14	1.81E+11	6.0	5.47E-04	5.47E-04	5.47E-04	5.47E-04	5.47E-04
N-13	5.98E+02	2000.0	2.90E+00	2.70E+00	1.45E+00	7.54E-01	4.46E-02
O-14	7.10E+01	927.1	1.81E+00	1.01E+00	5.17E-03	2.16E-05	9.86E-16
O-15	1.22E+02	1000.0	1.46E+01	1.04E+01	4.86E-01	2.02E-02	1.99E-08
O-19	2.71E+01	1916.0	1.20E-02	2.60E-03	2.60E-09	1.52E-15	1.23E-42
F-18	6.59E+03	500.0	4.51E-04	4.48E-04	4.23E-04	3.99E-04	3.09E-04
Ne-23	2.80E+01	1892.7	1.62E-02	3.67E-03	5.75E-09	5.31E-15	3.21E-41
Ne-24	2.03E+02	896.3	3.44E-03	2.80E-03	4.42E-04	6.50E-05	1.56E-08
Na-22	8.21E+07	1.0	2.00E-05	2.00E-05	2.00E-05	2.00E-05	2.00E-05
Na-24	5.40E+04	90.0	5.79E-04	5.78E-04	5.74E-04	5.70E-04	5.53E-04
Na-25	6.00E+01	28648.2	1.05E-03	5.23E-04	1.02E-06	1.56E-09	9.07E-22
Mg-27	5.70E+02	577.8	4.27E-03	3.97E-03	2.06E-03	1.04E-03	5.36E-05
Mg-28	7.53E+04	20.0	6.75E-04	6.74E-04	6.71E-04	6.68E-04	6.53E-04
Al-26	2.26E+13	0.5	2.49E-10	2.49E-10	2.49E-10	2.49E-10	2.49E-10
Al-28	1.34E+02	537.6	8.33E-02	6.11E-02	3.77E-03	2.09E-04	7.20E-10
Al-29	3.96E+02	232.5	3.99E-02	3.59E-02	1.40E-02	5.23E-03	7.32E-05
Si-31	9.44E+03	300.0	1.90E-03	1.90E-03	1.82E-03	1.75E-03	1.46E-03
Si-32	5.46E+09	0.3	1.70E-06	1.70E-06	1.70E-06	1.70E-06	1.70E-06
P-30	1.50E+02	2727.8	6.50E-03	4.92E-03	4.06E-04	3.03E-05	3.85E-10
P-32	1.23E+06	1.0	1.03E-02	1.03E-02	1.03E-02	1.02E-02	1.02E-02
P-33	2.19E+06	20.0	2.71E-04	2.71E-04	2.71E-04	2.71E-04	2.70E-04
P-35	4.74E+01	12148.0	2.58E-03	1.07E-03	3.99E-07	1.09E-10	3.53E-26
S-35	7.55E+06	20.0	1.36E-04	1.36E-04	1.36E-04	1.36E-04	1.36E-04
S-37	3.04E+02	8682.3	2.46E-03	2.15E-03	6.25E-04	1.74E-04	6.63E-07
S-38	1.03E+04	422.8	8.05E-04	8.02E-04	7.73E-04	7.45E-04	6.32E-04
Cl-34	1.92E+03	16.8	4.59E-02	4.49E-02	3.70E-02	3.02E-02	1.25E-02
Cl-36	9.50E+12	0.1	3.41E-08	3.41E-08	3.41E-08	3.41E-08	3.41E-08
Cl-38	2.23E+03	500.0	2.71E-02	2.66E-02	2.25E-02	1.89E-02	8.86E-03
Cl-39	3.34E+03	600.0	2.83E-02	2.80E-02	2.50E-02	2.23E-02	1.34E-02
Cl-40	8.40E+01	292.7	2.54E-01	1.55E-01	1.80E-03	1.75E-05	3.19E-14
Ar-37	3.03E+06	200000000.0	7.49E-11	7.49E-11	7.49E-11	7.49E-11	7.48E-11
Ar-39	8.49E+09	6000.0	3.94E-09	3.94E-09	3.94E-09	3.94E-09	3.94E-09
Ar-41	6.58E+03	200.0	9.28E-01	9.22E-01	8.71E-01	8.21E-01	6.35E-01
K-38	4.58E+02	4622.1	3.69E-05	3.37E-05	1.49E-05	6.37E-06	1.59E-07
K-40	4.04E+16	0.3	1.42E-13	1.42E-13	1.42E-13	1.42E-13	1.42E-13
Sum:			2.35E+01	1.80E+01	4.86E+00	3.09E+00	1.08E+00

Table 50: Activity of the air after irradiation of a lead target with a 400 MeV carbon ion beam, compared to Ci values, considering a cooling time of 1 hour and thinning the air to a volume of 14.000 m³ at average (2.47E+7 particles per second) and maximum (1E+9 particles per second) intensity

Isotope	Bq (total/y)	av. sp. act.	max. sp. act.	Ci [Bq/m ³]	av./Ci	max./Ci
H-3	9.70E+03	7.91E-05	3.20E-03	100.00	7.91E-07	3.20E-05
Be-7	1.36E+05	1.11E-03	4.48E-02	600.00	1.85E-06	7.47E-05
Be-10	8.28E-03	6.75E-11	2.73E-09	1.00	6.75E-11	2.73E-09
C-11	5.62E+08	5.95E-01	2.41E+01	600.00	9.92E-04	4.01E-02
C-14	1.14E+03	9.27E-06	3.75E-04	6.00	1.54E-06	6.24E-05
N-13	2.01E+09	2.52E-01	1.02E+01	2000.00	1.26E-04	5.09E-03
O-14	5.80E+08	2.58E-15	1.04E-13	927.09	2.78E-18	1.12E-16
O-15	5.05E+09	5.62E-08	2.27E-06	1000.00	5.62E-11	2.27E-09
O-19	7.98E+06	6.67E-42	2.70E-40	1916.02	3.48E-45	1.41E-43
F-18	7.80E+04	4.35E-04	1.76E-02	500.00	8.71E-07	3.52E-05
Ne-23	1.06E+07	1.71E-40	6.92E-39	1892.75	9.05E-44	3.66E-42
Ne-24	1.07E+06	3.94E-08	1.59E-06	896.31	4.40E-11	1.78E-09
Na-22	6.91E+00	5.64E-08	2.28E-06	1.00	5.64E-08	2.28E-06
Na-24	1.80E+04	1.40E-04	5.67E-03	90.00	1.56E-06	6.30E-05
Na-25	1.04E+07	7.33E-20	2.96E-18	28648.19	2.56E-24	1.03E-22
Mg-27	8.54E+05	8.74E-05	3.53E-03	577.79	1.51E-07	6.11E-06
Mg-28	4.67E+03	3.68E-05	1.49E-03	20.00	1.84E-06	7.44E-05
Al-26	4.31E-05	3.51E-13	1.42E-11	0.50	7.02E-13	2.84E-11
Al-28	1.55E+07	1.09E-09	4.41E-08	537.59	2.03E-12	8.21E-11
Al-29	3.21E+06	4.80E-05	1.94E-03	232.45	2.06E-07	8.34E-06
Si-31	1.98E+05	1.24E-03	5.00E-02	300.00	4.12E-06	1.67E-04
Si-32	1.88E-01	1.54E-09	6.21E-08	0.32	4.80E-09	1.94E-07
P-30	6.13E+06	2.96E-09	1.20E-07	2727.82	1.08E-12	4.39E-11
P-32	3.55E+03	2.89E-05	1.17E-03	1.00	2.89E-05	1.17E-03
P-33	1.87E+03	1.52E-05	6.17E-04	20.00	7.62E-07	3.08E-05
P-35	1.08E+07	1.21E-24	4.90E-23	12148.03	9.97E-29	4.03E-27
S-35	9.41E+02	7.67E-06	3.10E-04	20.00	3.84E-07	1.55E-05
S-37	7.39E+06	1.62E-05	6.56E-04	8682.34	1.87E-09	7.56E-08
S-38	1.18E+05	7.54E-04	3.05E-02	422.83	1.78E-06	7.21E-05
Cl-34	2.68E+05	5.95E-04	2.40E-02	16.84	3.53E-05	1.43E-03
Cl-36	1.18E-03	9.63E-12	3.89E-10	0.10	9.63E-11	3.89E-09
Cl-38	4.69E+06	1.25E-02	5.05E-01	500.00	2.50E-05	1.01E-03
Cl-39	5.88E+06	2.27E-02	9.18E-01	600.00	3.78E-05	1.53E-03
Cl-40	2.57E+07	2.63E-14	1.07E-12	292.72	9.00E-17	3.64E-15
Ar-37	5.18E+03	4.22E-05	1.71E-03	20000000.00	2.11E-13	8.53E-12
Ar-39	8.17E+00	6.66E-08	2.69E-06	6000.00	1.11E-11	4.49E-10
Ar-41	6.42E+07	3.58E-01	1.45E+01	200.00	1.79E-03	7.24E-02
K-38	5.90E+04	2.07E-06	8.39E-05	4622.10	4.49E-10	1.81E-08
K-40	1.54E-08	1.26E-16	5.07E-15	0.31	4.01E-16	1.62E-14
Sum:					3.05E-03	1.23E-01

IRRADIATION ROOM 1 - 250 MEV PROTONS

Table 51: Yield results (per primary particle per cm³) and relative errors, as well as specific activities (in Bq/m³) for each isotope after several cooling times (in seconds) after irradiation with a total intensity of 2.32E+13 protons, which corresponds to 3.1 air exchanges per hour during continuous irradiation with an 250 MeV proton beam and an intensity of 2E+10 protons per second

Isotope	t 1/2 [s]	yield/pp/cm ³	rel.error	0s	60s	600s	1191.29s	3600s
H-3	3.89E+08	2.54E-12	0.01%	2.29E-02	2.29E-02	2.29E-02	2.29E-02	2.29E-02
Be-7	4.61E+06	8.55E-13	0.00%	2.38E+00	2.38E+00	2.38E+00	2.38E+00	2.38E+00
Be-10	5.05E+13	4.74E-13	0.01%	2.60E-08	2.60E-08	2.60E-08	2.60E-08	2.60E-08
C-11	1.22E+03	1.13E-12	0.01%	1.42E+04	1.37E+04	1.01E+04	7.36E+03	1.85E+03
C-14	1.81E+11	5.00E-10	0.02%	4.05E-03	4.05E-03	4.05E-03	4.05E-03	4.05E-03
N-13	5.98E+02	1.79E-12	0.01%	4.36E+04	4.07E+04	2.18E+04	1.14E+04	6.72E+02
O-14	7.10E+01	1.14E-13	0.02%	3.58E+04	1.99E+04	1.02E+02	4.27E-01	1.95E-11
O-15	1.22E+02	1.45E-12	0.00%	2.03E+05	1.44E+05	6.75E+03	2.80E+02	2.76E-04
O-19	2.71E+01	1.53E-16	0.00%	4.79E+00	1.03E+00	1.04E-06	6.03E-13	4.91E-40
F-18	6.59E+03	4.21E-15	0.00%	1.86E+00	1.84E+00	1.74E+00	1.64E+00	1.27E+00
Ne-23	2.80E+01	3.94E-16	0.00%	2.96E+01	6.69E+00	1.05E-05	9.67E-12	5.84E-38
Ne-24	2.03E+02	8.23E-17	0.00%	4.81E-01	3.92E-01	6.19E-02	9.09E-03	2.18E-06
Na-22	8.21E+07	1.14E-15	0.00%	7.45E-05	7.45E-05	7.45E-05	7.45E-05	7.45E-05
Na-24	5.40E+04	1.79E-15	0.00%	1.63E-01	1.63E-01	1.62E-01	1.61E-01	1.56E-01
Na-25	6.00E+01	7.03E-16	0.00%	3.86E+01	1.93E+01	3.77E-02	5.76E-05	3.35E-17
Mg-27	5.70E+02	1.02E-15	0.00%	9.12E+00	8.48E+00	4.40E+00	2.22E+00	1.15E-01
Mg-28	7.53E+04	3.03E-16	0.00%	4.00E-02	4.00E-02	3.98E-02	3.96E-02	3.87E-02
Al-26	2.26E+13	1.44E-15	0.00%	3.28E-10	3.28E-10	3.28E-10	3.28E-10	3.28E-10
Al-28	1.34E+02	3.30E-15	0.00%	2.18E+02	1.60E+02	9.88E+00	5.46E-01	1.88E-06
Al-29	3.96E+02	1.83E-15	0.00%	3.60E+01	3.24E+01	1.26E+01	4.72E+00	6.61E-02
Si-31	9.44E+03	1.94E-15	0.00%	1.12E+00	1.11E+00	1.07E+00	1.03E+00	8.59E-01
Si-32	5.46E+09	1.02E-15	0.00%	1.23E-06	1.23E-06	1.23E-06	1.23E-06	1.23E-06
P-30	1.50E+02	1.07E-15	0.00%	4.08E+01	3.09E+01	2.55E+00	1.90E-01	2.42E-06
P-32	1.23E+06	1.10E-14	0.00%	1.25E-01	1.25E-01	1.25E-01	1.25E-01	1.25E-01
P-33	2.19E+06	7.74E-15	0.00%	4.18E-02	4.18E-02	4.18E-02	4.18E-02	4.18E-02
P-35	4.74E+01	8.69E-16	0.00%	1.16E+02	4.84E+01	1.80E-02	4.91E-06	1.60E-21
S-35	7.55E+06	9.91E-15	0.00%	1.25E-02	1.25E-02	1.25E-02	1.25E-02	1.25E-02
S-37	3.04E+02	4.40E-15	0.02%	4.87E+01	4.25E+01	1.24E+01	3.44E+00	1.31E-02
S-38	1.03E+04	2.12E-15	0.00%	1.08E+00	1.08E+00	1.04E+00	9.99E-01	8.48E-01
Cl-34	1.92E+03	4.72E-16	0.00%	4.54E+00	4.45E+00	3.66E+00	2.99E+00	1.24E+00
Cl-36	9.50E+12	2.49E-14	0.01%	3.92E-08	3.92E-08	3.92E-08	3.92E-08	3.92E-08
Cl-38	2.23E+03	1.72E-14	0.01%	6.45E+01	6.33E+01	5.35E+01	4.50E+01	2.11E+01
Cl-39	3.34E+03	3.47E-14	0.01%	7.05E+01	6.96E+01	6.22E+01	5.54E+01	3.33E+01
Cl-40	8.40E+01	3.46E-15	0.02%	4.27E+01	2.60E+01	3.02E-01	2.95E-03	5.36E-12
Ar-37	3.03E+06	4.43E-14	0.01%	1.07E-01	1.07E-01	1.07E-01	1.07E-01	1.07E-01
Ar-39	8.49E+09	1.26E-13	0.02%	7.95E-05	7.95E-05	7.95E-05	7.95E-05	7.95E-05
Ar-41	6.58E+03	1.04E-12	0.02%	2.32E+02	2.31E+02	2.18E+02	2.05E+02	1.59E+02
K-38	4.58E+02	3.09E-16	0.02%	2.94E+01	2.69E+01	1.19E+01	5.08E+00	1.27E-01
K-40	4.04E+16	8.56E-16	0.06%	8.37E-13	8.37E-13	8.37E-13	8.37E-13	8.37E-13

Table 52: Ci values for the isotopes gained by the simulation as well as the comparison of activities after several cooling times (0s, 60s, 600s, 1161.29s, 3600s), after irradiation with a total intensity of 2.32E+13 protons, which corresponds to 3.1 air exchanges per hour during continuous irradiation with an 250 MeV proton beam and an intensity of 2E+10 protons per second, to their respective Ci value. Calculated Ci values not mentioned in Austrian law are underlined in light blue. Sum values of the comparison values after the listed cooling times are listed at the bottom, underlined in dark blue.

Isotope	t 1/2 [s]	Ci	0s	60s	600s	1161.29s	3600s
H-3	3.89E+08	100.0	2.29E-04	2.29E-04	2.29E-04	2.29E-04	2.29E-04
Be-7	4.61E+06	600.0	3.97E-03	3.97E-03	3.97E-03	3.97E-03	3.97E-03
Be-10	5.05E+13	1.0	2.60E-08	2.60E-08	2.60E-08	2.60E-08	2.60E-08
C-11	1.22E+03	600.0	2.37E+01	2.29E+01	1.69E+01	1.23E+01	3.08E+00
C-14	1.81E+11	6.0	6.76E-04	6.76E-04	6.76E-04	6.76E-04	6.76E-04
N-13	5.98E+02	2000.0	2.18E+01	2.03E+01	1.09E+01	5.68E+00	3.36E-01
O-14	7.10E+01	927.1	3.86E+01	2.15E+01	1.10E-01	4.61E-04	2.11E-14
O-15	1.22E+02	1000.0	2.03E+02	1.44E+02	6.75E+00	2.80E-01	2.76E-07
O-19	2.71E+01	1916.0	2.50E-03	5.39E-04	5.41E-10	3.15E-16	2.56E-43
F-18	6.59E+03	500.0	3.71E-03	3.69E-03	3.48E-03	3.28E-03	2.54E-03
Ne-23	2.80E+01	1892.7	1.56E-02	3.54E-03	5.53E-09	5.11E-15	3.09E-41
Ne-24	2.03E+02	896.3	5.37E-04	4.37E-04	6.90E-05	1.01E-05	2.43E-09
Na-22	8.21E+07	1.0	7.45E-05	7.45E-05	7.45E-05	7.45E-05	7.45E-05
Na-24	5.40E+04	90.0	1.82E-03	1.81E-03	1.80E-03	1.79E-03	1.73E-03
Na-25	6.00E+01	28648.2	1.35E-03	6.74E-04	1.32E-06	2.01E-09	1.17E-21
Mg-27	5.70E+02	577.8	1.58E-02	1.47E-02	7.61E-03	3.85E-03	1.98E-04
Mg-28	7.53E+04	20.0	2.00E-03	2.00E-03	1.99E-03	1.98E-03	1.93E-03
Al-26	2.26E+13	0.5	6.55E-10	6.55E-10	6.55E-10	6.55E-10	6.55E-10
Al-28	1.34E+02	537.6	4.06E-01	2.98E-01	1.84E-02	1.02E-03	3.51E-09
Al-29	3.96E+02	232.5	1.55E-01	1.40E-01	5.42E-02	2.03E-02	2.84E-04
Si-31	9.44E+03	300.0	3.73E-03	3.71E-03	3.57E-03	3.42E-03	2.86E-03
Si-32	5.46E+09	0.3	3.85E-06	3.85E-06	3.85E-06	3.85E-06	3.85E-06
P-30	1.50E+02	2727.8	1.50E-02	1.13E-02	9.34E-04	6.97E-05	8.86E-10
P-32	1.23E+06	1.0	1.25E-01	1.25E-01	1.25E-01	1.25E-01	1.25E-01
P-33	2.19E+06	20.0	2.09E-03	2.09E-03	2.09E-03	2.09E-03	2.09E-03
P-35	4.74E+01	12148.0	9.59E-03	3.99E-03	1.48E-06	4.04E-10	1.31E-25
S-35	7.55E+06	20.0	6.24E-04	6.24E-04	6.24E-04	6.24E-04	6.24E-04
S-37	3.04E+02	8682.3	5.61E-03	4.89E-03	1.43E-03	3.96E-04	1.51E-06
S-38	1.03E+04	422.8	2.55E-03	2.54E-03	2.45E-03	2.36E-03	2.01E-03
Cl-34	1.92E+03	16.8	2.70E-01	2.64E-01	2.17E-01	1.77E-01	7.36E-02
Cl-36	9.50E+12	0.1	3.92E-07	3.92E-07	3.92E-07	3.92E-07	3.92E-07
Cl-38	2.23E+03	500.0	1.29E-01	1.27E-01	1.07E-01	8.99E-02	4.22E-02
Cl-39	3.34E+03	600.0	1.17E-01	1.16E-01	1.04E-01	9.23E-02	5.56E-02
Cl-40	8.40E+01	292.7	1.46E-01	8.90E-02	1.03E-03	1.01E-05	1.83E-14
Ar-37	3.03E+06	200000000.0	5.37E-10	5.37E-10	5.37E-10	5.37E-10	5.37E-10
Ar-39	8.49E+09	6000.0	1.32E-08	1.32E-08	1.32E-08	1.32E-08	1.32E-08
Ar-41	6.58E+03	200.0	1.16E+00	1.15E+00	1.09E+00	1.03E+00	7.94E-01
K-38	4.58E+02	4622.1	6.36E-03	5.81E-03	2.57E-03	1.10E-03	2.74E-05
K-40	4.04E+16	0.3	2.67E-12	2.67E-12	2.67E-12	2.67E-12	2.67E-12
Sum:			2.90E+02	2.11E+02	3.64E+01	1.98E+01	4.52E+00

Table 53: Activity of the air after irradiation of a lead target with an 250 MeV proton beam, compared to Ci values, considering a cooling time of 1 hour and thinning the air to a volume of 14.000 m³ at average (2.47E+8 particles per second) and maximum (2E+10 particles per second) intensity

Isotope	Bq (total/y)	av. sp. act.	max. sp. act.	Ci [Bq/m ³]	av./Ci	max./Ci
H-3	3.96E+03	3.23E-05	2.61E-03	100.00	3.23E-07	2.61E-05
Be-7	4.12E+05	3.36E-03	2.72E-01	600.00	5.60E-06	4.53E-04
Be-10	4.50E-03	3.67E-11	2.97E-09	1.00	3.67E-11	2.97E-09
C-11	2.46E+09	2.61E+00	2.11E+02	600.00	4.34E-03	3.51E-01
C-14	7.01E+02	5.72E-06	4.62E-04	6.00	9.53E-07	7.70E-05
N-13	7.54E+09	9.47E-01	7.66E+01	2000.00	4.74E-04	3.83E-02
O-14	6.20E+09	2.75E-14	2.23E-12	927.09	2.97E-17	2.40E-15
O-15	3.51E+10	3.90E-07	3.15E-05	1000.00	3.90E-10	3.15E-08
O-19	8.28E+05	6.92E-43	5.60E-41	1916.02	3.61E-46	2.92E-44
F-18	3.21E+05	1.79E-03	1.45E-01	500.00	3.58E-06	2.90E-04
Ne-23	5.11E+06	8.24E-41	6.66E-39	1892.75	4.35E-44	3.52E-42
Ne-24	8.32E+04	3.07E-09	2.49E-07	896.31	3.43E-12	2.77E-10
Na-22	1.29E+01	1.05E-07	8.50E-06	1.00	1.05E-07	8.50E-06
Na-24	2.83E+04	2.20E-04	1.78E-02	90.00	2.44E-06	1.98E-04
Na-25	6.68E+06	4.73E-20	3.82E-18	28648.19	1.65E-24	1.33E-22
Mg-27	1.58E+06	1.62E-04	1.31E-02	577.79	2.80E-07	2.26E-05
Mg-28	6.92E+03	5.46E-05	4.41E-03	20.00	2.73E-06	2.21E-04
Al-26	5.67E-05	4.62E-13	3.74E-11	0.50	9.24E-13	7.47E-11
Al-28	3.77E+07	2.66E-09	2.15E-07	537.59	4.94E-12	4.00E-10
Al-29	6.23E+06	9.32E-05	7.53E-03	232.45	4.01E-07	3.24E-05
Si-31	1.94E+05	1.21E-03	9.80E-02	300.00	4.04E-06	3.27E-04
Si-32	2.13E-01	1.74E-09	1.40E-07	0.32	5.42E-09	4.39E-07
P-30	7.06E+06	3.41E-09	2.75E-07	2727.82	1.25E-12	1.01E-10
P-32	2.16E+04	1.76E-04	1.42E-02	1.00	1.76E-04	1.42E-02
P-33	7.23E+03	5.89E-05	4.76E-03	20.00	2.95E-06	2.38E-04
P-35	2.01E+07	2.25E-24	1.82E-22	12148.03	1.85E-28	1.50E-26
S-35	2.16E+03	1.76E-05	1.42E-03	20.00	8.80E-07	7.12E-05
S-37	8.43E+06	1.85E-05	1.50E-03	8682.34	2.13E-09	1.72E-07
S-38	1.87E+05	1.20E-03	9.67E-02	422.83	2.83E-06	2.29E-04
Cl-34	7.86E+05	1.75E-03	1.41E-01	16.84	1.04E-04	8.39E-03
Cl-36	6.77E-03	5.52E-11	4.46E-09	0.10	5.52E-10	4.46E-08
Cl-38	1.11E+07	2.97E-02	2.40E+00	500.00	5.95E-05	4.81E-03
Cl-39	1.22E+07	4.70E-02	3.80E+00	600.00	7.84E-05	6.34E-03
Cl-40	7.39E+06	7.57E-15	6.12E-13	292.72	2.58E-17	2.09E-15
Ar-37	1.86E+04	1.51E-04	1.22E-02	20000000.00	7.57E-13	6.12E-11
Ar-39	1.37E+01	1.12E-07	9.06E-06	6000.00	1.87E-11	1.51E-09
Ar-41	4.01E+07	2.24E-01	1.81E+01	200.00	1.12E-03	9.05E-02
K-38	5.09E+06	1.79E-04	1.45E-02	4622.10	3.87E-08	3.13E-06
K-40	1.45E-07	1.18E-15	9.54E-14	0.31	3.77E-15	3.05E-13
Sum:					6.38E-03	5.16E-01

IRRADIATION ROOM 2 – 400 MEV CARBON IONS – HORIZONTAL SCENARIO

Table 54: Yield results (per primary particle per cm³) and relative errors, as well as specific activities (in Bq/m³) for each isotope after several cooling times (in seconds) after irradiation with a total intensity of 2.25E+12 carbon ions, which corresponds to 1.6 air exchanges per hour during continuous irradiation with a 400 MeV carbon ion beam and an intensity of 1E+9 ions per second

Isotope	t 1/2 [s]	yield/pp/cm ³	rel. error	0s	60s	600s	2250s	3600s
H-3	3.89E+08	2.54E-12	0.01%	2.72E-03	2.72E-03	2.72E-03	2.72E-03	2.72E-03
Be-7	4.61E+06	8.55E-13	0.00%	7.48E-02	7.48E-02	7.48E-02	7.48E-02	7.48E-02
Be-10	5.05E+13	4.74E-13	0.01%	7.88E-09	7.88E-09	7.88E-09	7.88E-09	7.88E-09
C-11	1.22E+03	1.13E-12	0.01%	5.19E+02	5.02E+02	3.69E+02	1.45E+02	6.75E+01
C-14	1.81E+11	5.00E-10	0.02%	5.70E-04	5.70E-04	5.70E-04	5.70E-04	5.70E-04
N-13	5.98E+02	1.79E-12	0.01%	2.17E+03	2.02E+03	1.08E+03	1.60E+02	3.34E+01
O-14	7.10E+01	1.14E-13	0.02%	1.19E+03	6.65E+02	3.42E+00	3.45E-07	6.51E-13
O-15	1.22E+02	1.45E-12	0.00%	7.18E+03	5.11E+03	2.39E+02	2.07E-02	9.79E-06
O-19	2.71E+01	1.53E-16	0.00%	2.18E-01	4.70E-02	4.72E-08	2.22E-26	2.24E-41
F-18	6.59E+03	4.21E-15	0.00%	5.38E-02	5.34E-02	5.05E-02	4.24E-02	3.68E-02
Ne-23	2.80E+01	3.94E-16	0.00%	1.00E+00	2.27E-01	3.55E-07	6.47E-25	1.98E-39
Ne-24	2.03E+02	8.23E-17	0.00%	1.89E-02	1.54E-02	2.43E-03	8.65E-06	8.57E-08
Na-22	8.21E+07	1.14E-15	0.00%	1.87E-06	1.87E-06	1.87E-06	1.87E-06	1.87E-06
Na-24	5.40E+04	1.79E-15	0.00%	4.77E-03	4.76E-03	4.73E-03	4.63E-03	4.55E-03
Na-25	6.00E+01	7.03E-16	0.00%	1.17E+00	5.86E-01	1.14E-03	6.03E-12	1.02E-18
Mg-27	5.70E+02	1.02E-15	0.00%	2.56E-01	2.38E-01	1.23E-01	1.66E-02	3.21E-03
Mg-28	7.53E+04	3.03E-16	0.00%	1.12E-03	1.12E-03	1.11E-03	1.10E-03	1.08E-03
Al-26	2.26E+13	1.44E-15	0.00%	9.18E-12	9.18E-12	9.18E-12	9.18E-12	9.18E-12
Al-28	1.34E+02	3.30E-15	0.00%	5.77E+00	4.23E+00	2.61E-01	5.27E-05	4.98E-08
Al-29	3.96E+02	1.83E-15	0.00%	9.65E-01	8.69E-01	3.38E-01	1.88E-02	1.77E-03
Si-31	9.44E+03	1.94E-15	0.00%	4.20E-02	4.18E-02	4.02E-02	3.56E-02	3.22E-02
Si-32	5.46E+09	1.02E-15	0.00%	5.00E-08	5.00E-08	5.00E-08	5.00E-08	5.00E-08
P-30	1.50E+02	1.07E-15	0.00%	9.38E-01	7.11E-01	5.86E-02	2.85E-05	5.56E-08
P-32	1.23E+06	1.10E-14	0.00%	4.90E-03	4.90E-03	4.90E-03	4.89E-03	4.89E-03
P-33	2.19E+06	7.74E-15	0.00%	2.16E-03	2.16E-03	2.16E-03	2.16E-03	2.16E-03
P-35	4.74E+01	8.69E-16	0.00%	9.90E+00	4.12E+00	1.53E-03	5.09E-14	1.36E-22
S-35	7.55E+06	9.91E-15	0.00%	8.28E-04	8.28E-04	8.28E-04	8.28E-04	8.28E-04
S-37	3.04E+02	4.40E-15	0.02%	6.27E+00	5.46E+00	1.59E+00	3.68E-02	1.69E-03
S-38	1.03E+04	2.12E-15	0.00%	1.15E-01	1.15E-01	1.11E-01	9.92E-02	9.06E-02
Cl-34	1.92E+03	4.72E-16	0.00%	1.11E-01	1.09E-01	8.96E-02	4.94E-02	3.03E-02
Cl-36	9.50E+12	2.49E-14	0.01%	1.94E-09	1.94E-09	1.94E-09	1.94E-09	1.94E-09
Cl-38	2.23E+03	1.72E-14	0.01%	5.94E+00	5.83E+00	4.93E+00	2.95E+00	1.94E+00
Cl-39	3.34E+03	3.47E-14	0.01%	6.45E+00	6.37E+00	5.70E+00	4.04E+00	3.05E+00
Cl-40	8.40E+01	3.46E-15	0.02%	3.97E+01	2.42E+01	2.81E-01	3.43E-07	4.99E-12
Ar-37	3.03E+06	4.43E-14	0.01%	6.86E-03	6.86E-03	6.85E-03	6.85E-03	6.85E-03
Ar-39	8.49E+09	1.26E-13	0.02%	9.30E-06	9.30E-06	9.30E-06	9.30E-06	9.30E-06
Ar-41	6.58E+03	1.04E-12	0.02%	3.30E+01	3.28E+01	3.09E+01	2.60E+01	2.26E+01
K-38	4.58E+02	3.09E-16	0.02%	8.24E-01	7.52E-01	3.32E-01	2.74E-02	3.55E-03
K-40	4.04E+16	8.56E-16	0.06%	3.90E-14	3.90E-14	3.90E-14	3.90E-14	3.90E-14

Table 55: Ci values for the isotopes gained by the simulation as well as the comparison of activities after several cooling times (0s, 60s, 600s, 2250s, 3600s), after irradiation with a total intensity of 2.25E+12 carbon ions, which corresponds to 1.6 air exchanges per hour during continuous irradiation with an 400 MeV ion beam and an intensity of 1E+9 ions per second, to their respective Ci value. Calculated Ci values not mentioned in Austrian law are underlined in light blue. Sum values of the comparison values after the listed cooling times are listed at the bottom, underlined in dark blue.

Isotope	t 1/2 [s]	Ci	0s	60s	600s	2250s	3600s
H-3	3.89E+08	100.0	2.72E-05	2.72E-05	2.72E-05	2.72E-05	2.72E-05
Be-7	4.61E+06	600.0	1.25E-04	1.25E-04	1.25E-04	1.25E-04	1.25E-04
Be-10	5.05E+13	1.0	7.88E-09	7.88E-09	7.88E-09	7.88E-09	7.88E-09
C-11	1.22E+03	600.0	8.65E-01	8.36E-01	6.16E-01	2.42E-01	1.12E-01
C-14	1.81E+11	6.0	9.51E-05	9.51E-05	9.51E-05	9.51E-05	9.51E-05
N-13	5.98E+02	2000.0	1.09E+00	1.01E+00	5.41E-01	7.99E-02	1.67E-02
O-14	7.10E+01	927.1	1.29E+00	7.18E-01	3.68E-03	3.72E-10	7.03E-16
O-15	1.22E+02	1000.0	7.18E+00	5.11E+00	2.39E-01	2.07E-05	9.79E-09
O-19	2.71E+01	1916.0	1.14E-04	2.45E-05	2.46E-11	1.16E-29	1.17E-44
F-18	6.59E+03	500.0	1.08E-04	1.07E-04	1.01E-04	8.48E-05	7.36E-05
Ne-23	2.80E+01	1892.7	5.30E-04	1.20E-04	1.88E-10	3.42E-28	1.05E-42
Ne-24	2.03E+02	896.3	2.11E-05	1.72E-05	2.72E-06	9.65E-09	9.57E-11
Na-22	8.21E+07	1.0	1.87E-06	1.87E-06	1.87E-06	1.87E-06	1.87E-06
Na-24	5.40E+04	90.0	5.29E-05	5.29E-05	5.25E-05	5.14E-05	5.06E-05
Na-25	6.00E+01	28648.2	4.09E-05	2.05E-05	4.00E-08	2.11E-16	3.55E-23
Mg-27	5.70E+02	577.8	4.43E-04	4.12E-04	2.13E-04	2.87E-05	5.56E-06
Mg-28	7.53E+04	20.0	5.59E-05	5.59E-05	5.56E-05	5.48E-05	5.41E-05
Al-26	2.26E+13	0.5	1.84E-11	1.84E-11	1.84E-11	1.84E-11	1.84E-11
Al-28	1.34E+02	537.6	1.07E-02	7.87E-03	4.86E-04	9.79E-08	9.27E-11
Al-29	3.96E+02	232.5	4.15E-03	3.74E-03	1.45E-03	8.09E-05	7.61E-06
Si-31	9.44E+03	300.0	1.40E-04	1.39E-04	1.34E-04	1.19E-04	1.07E-04
Si-32	5.46E+09	0.3	1.56E-07	1.56E-07	1.56E-07	1.56E-07	1.56E-07
P-30	1.50E+02	2727.8	3.44E-04	2.61E-04	2.15E-05	1.05E-08	2.04E-11
P-32	1.23E+06	1.0	4.90E-03	4.90E-03	4.90E-03	4.89E-03	4.89E-03
P-33	2.19E+06	20.0	1.08E-04	1.08E-04	1.08E-04	1.08E-04	1.08E-04
P-35	4.74E+01	12148.0	8.15E-04	3.39E-04	1.26E-07	4.19E-18	1.12E-26
S-35	7.55E+06	20.0	4.14E-05	4.14E-05	4.14E-05	4.14E-05	4.14E-05
S-37	3.04E+02	8682.3	7.22E-04	6.29E-04	1.83E-04	4.24E-06	1.94E-07
S-38	1.03E+04	422.8	2.73E-04	2.72E-04	2.62E-04	2.35E-04	2.14E-04
Cl-34	1.92E+03	16.8	6.61E-03	6.47E-03	5.32E-03	2.93E-03	1.80E-03
Cl-36	9.50E+12	0.1	1.94E-08	1.94E-08	1.94E-08	1.94E-08	1.94E-08
Cl-38	2.23E+03	500.0	1.19E-02	1.17E-02	9.86E-03	5.91E-03	3.88E-03
Cl-39	3.34E+03	600.0	1.08E-02	1.06E-02	9.49E-03	6.74E-03	5.09E-03
Cl-40	8.40E+01	292.7	1.36E-01	8.27E-02	9.60E-04	1.17E-09	1.70E-14
Ar-37	3.03E+06	200000000.0	3.43E-11	3.43E-11	3.43E-11	3.43E-11	3.42E-11
Ar-39	8.49E+09	6000.0	1.55E-09	1.55E-09	1.55E-09	1.55E-09	1.55E-09
Ar-41	6.58E+03	200.0	1.65E-01	1.64E-01	1.55E-01	1.30E-01	1.13E-01
K-38	4.58E+02	4622.1	1.78E-04	1.63E-04	7.19E-05	5.92E-06	7.68E-07
K-40	4.04E+16	0.3	1.25E-13	1.25E-13	1.25E-13	1.25E-13	1.25E-13
Sum:			1.08E+01	7.97E+00	1.59E+00	4.73E-01	2.58E-01

Table 56: Activity of the air after irradiation of a water target with a 400 MeV carbon ion beam, compared to Ci values, considering a cooling time of 1 hour and thinning the air to a volume of 14.000 m3 at average (1.49E+7 particles per second) and maximum (1E+9 particles per second) intensity

Bq (total/y)	av. sp. act.	max. sp. act.	Ci [Bq/m3]	av./Ci	max./Ci
1.14E+03	9.26E-06	6.21E-04	100.00	9.26E-08	6.21E-06
3.13E+04	2.55E-04	1.71E-02	600.00	4.25E-07	2.85E-05
3.29E-03	2.68E-11	1.80E-09	1.00	2.68E-11	1.80E-09
2.17E+08	2.30E-01	1.54E+01	600.00	3.83E-04	2.57E-02
2.38E+02	1.94E-06	1.30E-04	6.00	3.24E-07	2.17E-05
9.07E+08	1.14E-01	7.64E+00	2000.00	5.69E-05	3.82E-03
4.99E+08	2.22E-15	1.49E-13	927.09	2.39E-18	1.61E-16
3.00E+09	3.34E-08	2.24E-06	1000.00	3.34E-11	2.24E-09
9.11E+04	7.62E-44	5.11E-42	1916.02	3.98E-47	2.67E-45
2.25E+04	1.25E-04	8.41E-03	500.00	2.51E-07	1.68E-05
4.19E+05	6.75E-42	4.53E-40	1892.75	3.57E-45	2.39E-43
7.90E+03	2.92E-10	1.96E-08	896.31	3.26E-13	2.19E-11
7.79E-01	6.35E-09	4.26E-07	1.00	6.35E-09	4.26E-07
1.99E+03	1.55E-05	1.04E-03	90.00	1.72E-07	1.16E-05
4.90E+05	3.46E-21	2.32E-19	28648.19	1.21E-25	8.11E-24
1.07E+05	1.09E-05	7.34E-04	577.79	1.89E-08	1.27E-06
4.67E+02	3.69E-06	2.47E-04	20.00	1.84E-07	1.24E-05
3.84E-06	3.13E-14	2.10E-12	0.50	6.25E-14	4.20E-12
2.41E+06	1.70E-10	1.14E-08	537.59	3.16E-13	2.12E-11
4.03E+05	6.03E-06	4.04E-04	232.45	2.59E-08	1.74E-06
1.75E+04	1.10E-04	7.36E-03	300.00	3.66E-07	2.45E-05
2.09E-02	1.70E-10	1.14E-08	0.32	5.33E-10	3.57E-08
3.92E+05	1.89E-10	1.27E-08	2727.82	6.94E-14	4.65E-12
2.05E+03	1.67E-05	1.12E-03	1.00	1.67E-05	1.12E-03
9.03E+02	7.35E-06	4.93E-04	20.00	3.68E-07	2.47E-05
4.14E+06	4.62E-25	3.10E-23	12148.03	3.81E-29	2.55E-27
3.46E+02	2.82E-06	1.89E-04	20.00	1.41E-07	9.46E-06
2.62E+06	5.75E-06	3.86E-04	8682.34	6.63E-10	4.45E-08
4.82E+04	3.09E-04	2.07E-02	422.83	7.30E-07	4.90E-05
4.65E+04	1.03E-04	6.93E-03	16.84	6.14E-06	4.12E-04
8.09E-04	6.60E-12	4.43E-10	0.10	6.60E-11	4.43E-09
2.48E+06	6.61E-03	4.44E-01	500.00	1.32E-05	8.88E-04
2.70E+06	1.04E-02	6.98E-01	600.00	1.73E-05	1.16E-03
1.66E+07	1.70E-14	1.14E-12	292.72	5.80E-17	3.89E-15
2.86E+03	2.33E-05	1.57E-03	200000000.00	1.17E-13	7.83E-12
3.88E+00	3.17E-08	2.12E-06	6000.00	5.28E-12	3.54E-10
1.38E+07	7.68E-02	5.16E+00	200.00	3.84E-04	2.58E-02
3.44E+05	1.21E-05	8.12E-04	4622.10	2.62E-09	1.76E-07
1.63E-08	1.33E-16	8.91E-15	0.31	4.25E-16	2.85E-14
Sum:				8.81E-04	5.91E-02

IRRADIATION ROOM 2 – 400 MEV CARBON IONS – VERTICAL SCENARIO

Table 57: Yield results (per primary particle per cm³) and relative errors, as well as specific activities (in Bq/m³) for each isotope after several cooling times (in seconds) after irradiation with a total intensity of 2.25E+12 carbon ions, which corresponds to 1.6 air exchanges per hour during continuous irradiation with a 400 MeV carbon ion beam and an intensity of 1E+9 ions per second

Isotope	t 1/2 [s]	yield/pp/cm ³	rel. error	0s	60s	600s	2250s	3600s
H-3	3.89E+08	2.54E-12	0.01%	1.68E-03	1.68E-03	1.68E-03	1.68E-03	1.68E-03
Be-7	4.61E+06	8.55E-13	0.00%	2.49E-02	2.49E-02	2.49E-02	2.48E-02	2.48E-02
Be-10	5.05E+13	4.74E-13	0.01%	4.61E-09	4.61E-09	4.61E-09	4.61E-09	4.61E-09
C-11	1.22E+03	1.13E-12	0.01%	1.77E+02	1.71E+02	1.26E+02	4.95E+01	2.30E+01
C-14	1.81E+11	5.00E-10	0.02%	5.64E-04	5.64E-04	5.64E-04	5.64E-04	5.64E-04
N-13	5.98E+02	1.79E-12	0.01%	8.89E+02	8.30E+02	4.44E+02	6.55E+01	1.37E+01
O-14	7.10E+01	1.14E-13	0.02%	3.95E+02	2.20E+02	1.13E+00	1.14E-07	2.16E-13
O-15	1.22E+02	1.45E-12	0.00%	2.54E+03	1.81E+03	8.45E+01	7.31E-03	3.46E-06
O-19	2.71E+01	1.53E-16	0.00%	5.13E-02	1.11E-02	1.11E-08	5.21E-27	5.26E-42
F-18	6.59E+03	4.21E-15	0.00%	1.47E-02	1.46E-02	1.38E-02	1.16E-02	1.01E-02
Ne-23	2.80E+01	3.94E-16	0.00%	2.41E-01	5.45E-02	8.52E-08	1.55E-25	4.76E-40
Ne-24	2.03E+02	8.23E-17	0.00%	4.50E-03	3.66E-03	5.79E-04	2.06E-06	2.04E-08
Na-22	8.21E+07	1.14E-15	0.00%	4.71E-07	4.71E-07	4.71E-07	4.71E-07	4.71E-07
Na-24	5.40E+04	1.79E-15	0.00%	1.23E-03	1.23E-03	1.22E-03	1.19E-03	1.17E-03
Na-25	6.00E+01	7.03E-16	0.00%	2.86E-01	1.43E-01	2.79E-04	1.47E-12	2.48E-19
Mg-27	5.70E+02	1.02E-15	0.00%	6.35E-02	5.90E-02	3.06E-02	4.11E-03	7.97E-04
Mg-28	7.53E+04	3.03E-16	0.00%	2.90E-04	2.90E-04	2.88E-04	2.84E-04	2.81E-04
Al-26	2.26E+13	1.44E-15	0.00%	2.28E-12	2.28E-12	2.28E-12	2.28E-12	2.28E-12
Al-28	1.34E+02	3.30E-15	0.00%	1.47E+00	1.08E+00	6.68E-02	1.35E-05	1.27E-08
Al-29	3.96E+02	1.83E-15	0.00%	2.46E-01	2.22E-01	8.61E-02	4.80E-03	4.51E-04
Si-31	9.44E+03	1.94E-15	0.00%	1.18E-02	1.18E-02	1.13E-02	1.00E-02	9.07E-03
Si-32	5.46E+09	1.02E-15	0.00%	1.47E-08	1.47E-08	1.47E-08	1.47E-08	1.47E-08
P-30	1.50E+02	1.07E-15	0.00%	2.40E-01	1.82E-01	1.50E-02	7.30E-06	1.42E-08
P-32	1.23E+06	1.10E-14	0.00%	1.49E-03	1.49E-03	1.49E-03	1.49E-03	1.49E-03
P-33	2.19E+06	7.74E-15	0.00%	7.10E-04	7.10E-04	7.10E-04	7.09E-04	7.09E-04
P-35	4.74E+01	8.69E-16	0.00%	3.49E+00	1.45E+00	5.40E-04	1.79E-14	4.78E-23
S-35	7.55E+06	9.91E-15	0.00%	3.12E-04	3.12E-04	3.12E-04	3.12E-04	3.12E-04
S-37	3.04E+02	4.40E-15	0.02%	3.58E+00	3.12E+00	9.09E-01	2.10E-02	9.63E-04
S-38	1.03E+04	2.12E-15	0.00%	3.89E-02	3.88E-02	3.74E-02	3.35E-02	3.06E-02
Cl-34	1.92E+03	4.72E-16	0.00%	3.15E-02	3.08E-02	2.54E-02	1.40E-02	8.59E-03
Cl-36	9.50E+12	2.49E-14	0.01%	6.90E-10	6.90E-10	6.90E-10	6.90E-10	6.90E-10
Cl-38	2.23E+03	1.72E-14	0.01%	2.51E+00	2.46E+00	2.08E+00	1.25E+00	8.20E-01
Cl-39	3.34E+03	3.47E-14	0.01%	2.83E+00	2.79E+00	2.50E+00	1.77E+00	1.34E+00
Cl-40	8.40E+01	3.46E-15	0.02%	2.53E+01	1.54E+01	1.79E-01	2.18E-07	3.17E-12
Ar-37	3.03E+06	4.43E-14	0.01%	3.89E-03	3.89E-03	3.89E-03	3.88E-03	3.88E-03
Ar-39	8.49E+09	1.26E-13	0.02%	6.41E-06	6.41E-06	6.41E-06	6.41E-06	6.41E-06
Ar-41	6.58E+03	1.04E-12	0.02%	3.27E+01	3.25E+01	3.07E+01	2.58E+01	2.24E+01
K-38	4.58E+02	3.09E-16	0.02%	2.54E-01	2.32E-01	1.03E-01	8.45E-03	1.10E-03
K-40	4.04E+16	8.56E-16	0.06%	1.40E-14	1.40E-14	1.40E-14	1.40E-14	1.40E-14

Table 58: Ci values for the isotopes gained by the simulation as well as the comparison of activities after several cooling times (0s, 60s, 600s, 2250s, 3600s), after irradiation with a total intensity of 2.25E+12 carbon ions, which corresponds to 1.6 air exchanges per hour during continuous irradiation with an 400 MeV ion beam and an intensity of 1E+9 ions per second, to their respective Ci value. Calculated Ci values not mentioned in Austrian law are underlined in light blue. Sum values of the comparison values after the listed cooling times are listed at the bottom, underlined in dark blue.

Isotope	t 1/2 [s]	Ci	0s	60s	600s	2250s	3600s
H-3	3.89E+08	100.0	1.68E-05	1.68E-05	1.68E-05	1.68E-05	1.68E-05
Be-7	4.61E+06	600.0	4.14E-05	4.14E-05	4.14E-05	4.14E-05	4.14E-05
Be-10	5.05E+13	1.0	4.61E-09	4.61E-09	4.61E-09	4.61E-09	4.61E-09
C-11	1.22E+03	600.0	2.95E-01	2.86E-01	2.10E-01	8.25E-02	3.84E-02
C-14	1.81E+11	6.0	9.41E-05	9.41E-05	9.41E-05	9.41E-05	9.41E-05
N-13	5.98E+02	2000.0	4.45E-01	4.15E-01	2.22E-01	3.28E-02	6.85E-03
O-14	7.10E+01	927.1	4.26E-01	2.37E-01	1.22E-03	1.23E-10	2.32E-16
O-15	1.22E+02	1000.0	2.54E+00	1.81E+00	8.45E-02	7.31E-06	3.46E-09
O-19	2.71E+01	1916.0	2.68E-05	5.77E-06	5.79E-12	2.72E-30	2.74E-45
F-18	6.59E+03	500.0	2.95E-05	2.93E-05	2.77E-05	2.32E-05	2.02E-05
Ne-23	2.80E+01	1892.7	1.27E-04	2.88E-05	4.50E-11	8.21E-29	2.51E-43
Ne-24	2.03E+02	896.3	5.02E-06	4.09E-06	6.46E-07	2.30E-09	2.27E-11
Na-22	8.21E+07	1.0	4.71E-07	4.71E-07	4.71E-07	4.71E-07	4.71E-07
Na-24	5.40E+04	90.0	1.36E-05	1.36E-05	1.35E-05	1.33E-05	1.30E-05
Na-25	6.00E+01	28648.2	9.98E-06	4.99E-06	9.75E-09	5.13E-17	8.66E-24
Mg-27	5.70E+02	577.8	1.10E-04	1.02E-04	5.30E-05	7.12E-06	1.38E-06
Mg-28	7.53E+04	20.0	1.45E-05	1.45E-05	1.44E-05	1.42E-05	1.40E-05
Al-26	2.26E+13	0.5	4.56E-12	4.56E-12	4.56E-12	4.56E-12	4.56E-12
Al-28	1.34E+02	537.6	2.74E-03	2.01E-03	1.24E-04	2.50E-08	2.37E-11
Al-29	3.96E+02	232.5	1.06E-03	9.53E-04	3.70E-04	2.06E-05	1.94E-06
Si-31	9.44E+03	300.0	3.94E-05	3.92E-05	3.77E-05	3.34E-05	3.02E-05
Si-32	5.46E+09	0.3	4.59E-08	4.59E-08	4.59E-08	4.59E-08	4.59E-08
P-30	1.50E+02	2727.8	8.81E-05	6.67E-05	5.50E-06	2.68E-09	5.22E-12
P-32	1.23E+06	1.0	1.49E-03	1.49E-03	1.49E-03	1.49E-03	1.49E-03
P-33	2.19E+06	20.0	3.55E-05	3.55E-05	3.55E-05	3.55E-05	3.55E-05
P-35	4.74E+01	12148.0	2.87E-04	1.19E-04	4.44E-08	1.47E-18	3.94E-27
S-35	7.55E+06	20.0	1.56E-05	1.56E-05	1.56E-05	1.56E-05	1.56E-05
S-37	3.04E+02	8682.3	4.12E-04	3.59E-04	1.05E-04	2.42E-06	1.11E-07
S-38	1.03E+04	422.8	9.21E-05	9.17E-05	8.85E-05	7.92E-05	7.23E-05
Cl-34	1.92E+03	16.8	1.87E-03	1.83E-03	1.51E-03	8.31E-04	5.10E-04
Cl-36	9.50E+12	0.1	6.90E-09	6.90E-09	6.90E-09	6.90E-09	6.90E-09
Cl-38	2.23E+03	500.0	5.02E-03	4.92E-03	4.16E-03	2.49E-03	1.64E-03
Cl-39	3.34E+03	600.0	4.71E-03	4.66E-03	4.16E-03	2.95E-03	2.23E-03
Cl-40	8.40E+01	292.7	8.63E-02	5.26E-02	6.10E-04	7.46E-10	1.08E-14
Ar-37	3.03E+06	200000000.0	1.94E-11	1.94E-11	1.94E-11	1.94E-11	1.94E-11
Ar-39	8.49E+09	6000.0	1.07E-09	1.07E-09	1.07E-09	1.07E-09	1.07E-09
Ar-41	6.58E+03	200.0	1.64E-01	1.63E-01	1.54E-01	1.29E-01	1.12E-01
K-38	4.58E+02	4622.1	5.50E-05	5.02E-05	2.22E-05	1.83E-06	2.37E-07
K-40	4.04E+16	0.3	4.48E-14	4.48E-14	4.48E-14	4.48E-14	4.48E-14
Sum:			3.97E+00	2.98E+00	6.84E-01	2.53E-01	1.63E-01

Table 59: Activity of the air after irradiation of a water target with a 400 MeV carbon ion beam, compared to Ci values, considering a cooling time of 1 hour and thinning the air to a volume of 14.000 m3 at average (1.49E+7 particles per second) and maximum (1E+9 particles per second) intensity

Isotope	Bq (total/y)	av. sp. act.	max. sp. act.	Ci [Bq/m3]	av./Ci	max./Ci
H-3	7.03E+02	5.73E-06	3.84E-04	100.00	5.73E-08	3.84E-06
Be-7	1.04E+04	8.46E-05	5.68E-03	600.00	1.41E-07	9.46E-06
Be-10	1.92E-03	1.57E-11	1.05E-09	1.00	1.57E-11	1.05E-09
C-11	7.41E+07	7.85E-02	5.27E+00	600.00	1.31E-04	8.78E-03
C-14	2.36E+02	1.92E-06	1.29E-04	6.00	3.20E-07	2.15E-05
N-13	3.72E+08	4.67E-02	3.13E+00	2000.00	2.33E-05	1.57E-03
O-14	1.65E+08	7.34E-16	4.93E-14	927.09	7.92E-19	5.31E-17
O-15	1.06E+09	1.18E-08	7.91E-07	1000.00	1.18E-11	7.91E-10
O-19	2.14E+04	1.79E-44	1.20E-42	1916.02	9.35E-48	6.27E-46
F-18	6.15E+03	3.44E-05	2.30E-03	500.00	6.87E-08	4.61E-06
Ne-23	1.01E+05	1.62E-42	1.09E-40	1892.75	8.56E-46	5.75E-44
Ne-24	1.88E+03	6.95E-11	4.66E-09	896.31	7.75E-14	5.20E-12
Na-22	1.97E-01	1.60E-09	1.08E-07	1.00	1.60E-09	1.08E-07
Na-24	5.13E+02	3.99E-06	2.68E-04	90.00	4.44E-08	2.98E-06
Na-25	1.19E+05	8.45E-22	5.67E-20	28648.19	2.95E-26	1.98E-24
Mg-27	2.65E+04	2.71E-06	1.82E-04	577.79	4.70E-09	3.15E-07
Mg-28	1.21E+02	9.56E-07	6.41E-05	20.00	4.78E-08	3.21E-06
Al-26	9.52E-07	7.76E-15	5.21E-13	0.50	1.55E-14	1.04E-12
Al-28	6.16E+05	4.34E-11	2.91E-09	537.59	8.07E-14	5.42E-12
Al-29	1.03E+05	1.54E-06	1.03E-04	232.45	6.62E-09	4.44E-07
Si-31	4.94E+03	3.09E-05	2.07E-03	300.00	1.03E-07	6.91E-06
Si-32	6.14E-03	5.01E-11	3.36E-09	0.32	1.56E-10	1.05E-08
P-30	1.00E+05	4.85E-11	3.25E-09	2727.82	1.78E-14	1.19E-12
P-32	6.23E+02	5.07E-06	3.40E-04	1.00	5.07E-06	3.40E-04
P-33	2.97E+02	2.42E-06	1.62E-04	20.00	1.21E-07	8.10E-06
P-35	1.46E+06	1.63E-25	1.09E-23	12148.03	1.34E-29	9.00E-28
S-35	1.30E+02	1.06E-06	7.12E-05	20.00	5.31E-08	3.56E-06
S-37	1.49E+06	3.28E-06	2.20E-04	8682.34	3.78E-10	2.54E-08
S-38	1.63E+04	1.04E-04	6.99E-03	422.83	2.46E-07	1.65E-05
Cl-34	1.32E+04	2.93E-05	1.96E-03	16.84	1.74E-06	1.17E-04
Cl-36	2.88E-04	2.35E-12	1.58E-10	0.10	2.35E-11	1.58E-09
Cl-38	1.05E+06	2.79E-03	1.87E-01	500.00	5.59E-06	3.75E-04
Cl-39	1.18E+06	4.56E-03	3.06E-01	600.00	7.60E-06	5.10E-04
Cl-40	1.05E+07	1.08E-14	7.24E-13	292.72	3.69E-17	2.47E-15
Ar-37	1.62E+03	1.32E-05	8.88E-04	200000000.00	6.61E-14	4.44E-12
Ar-39	2.68E+00	2.18E-08	1.47E-06	6000.00	3.64E-12	2.44E-10
Ar-41	1.37E+07	7.63E-02	5.12E+00	200.00	3.81E-04	2.56E-02
K-38	1.06E+05	3.73E-06	2.51E-04	4622.10	8.08E-10	5.42E-08
K-40	5.86E-09	4.77E-17	3.20E-15	0.31	1.53E-16	1.02E-14
Sum:					5.57E-04	3.74E-02

IRRADIATION ROOM 3 – 400 MEV CARBON IONS

Table 60: Yield results (per primary particle per cm³) and relative errors, as well as specific activities (in Bq/m³) for each isotope after several cooling times (in seconds) after irradiation with a total intensity of 1.16E+12 carbon ions, which corresponds to 3.1 air exchanges per hour during continuous irradiation with a 400 MeV ion beam and an intensity of 1E+9 ions per second

Isotope	t 1/2 [s]	yield/pp/cm ³	rel. error	0s	60s	600s	1191.29s	3600s
H-3	3.89E+08	2.54E-12	0.01%	8.97E-03	8.97E-03	8.97E-03	8.97E-03	8.97E-03
Be-7	4.61E+06	8.55E-13	0.00%	2.74E-01	2.74E-01	2.74E-01	2.74E-01	2.74E-01
Be-10	5.05E+13	4.74E-13	0.01%	2.65E-08	2.65E-08	2.65E-08	2.65E-08	2.65E-08
C-11	1.22E+03	1.13E-12	0.01%	1.90E+03	1.84E+03	1.35E+03	9.85E+02	2.47E+02
C-14	1.81E+11	5.00E-10	0.02%	1.33E-03	1.33E-03	1.33E-03	1.33E-03	1.33E-03
N-13	5.98E+02	1.79E-12	0.01%	7.74E+03	7.22E+03	3.86E+03	2.01E+03	1.19E+02
O-14	7.10E+01	1.14E-13	0.02%	4.44E+03	2.47E+03	1.27E+01	5.30E-02	2.42E-12
O-15	1.22E+02	1.45E-12	0.00%	2.61E+04	1.86E+04	8.68E+02	3.60E+01	3.55E-05
O-19	2.71E+01	1.53E-16	0.00%	8.38E-01	1.81E-01	1.81E-07	1.06E-13	8.59E-41
F-18	6.59E+03	4.21E-15	0.00%	2.03E-01	2.02E-01	1.90E-01	1.80E-01	1.39E-01
Ne-23	2.80E+01	3.94E-16	0.00%	3.82E+00	8.66E-01	1.35E-06	1.25E-12	7.56E-39
Ne-24	2.03E+02	8.23E-17	0.00%	7.22E-02	5.88E-02	9.29E-03	1.36E-03	3.27E-07
Na-22	8.21E+07	1.14E-15	0.00%	7.01E-06	7.01E-06	7.01E-06	7.01E-06	7.01E-06
Na-24	5.40E+04	1.79E-15	0.00%	1.79E-02	1.79E-02	1.78E-02	1.76E-02	1.71E-02
Na-25	6.00E+01	7.03E-16	0.00%	4.44E+00	2.22E+00	4.34E-03	6.62E-06	3.85E-18
Mg-27	5.70E+02	1.02E-15	0.00%	9.65E-01	8.97E-01	4.65E-01	2.35E-01	1.21E-02
Mg-28	7.53E+04	3.03E-16	0.00%	4.18E-03	4.18E-03	4.16E-03	4.14E-03	4.04E-03
Al-26	2.26E+13	1.44E-15	0.00%	3.46E-11	3.46E-11	3.46E-11	3.46E-11	3.46E-11
Al-28	1.34E+02	3.30E-15	0.00%	2.16E+01	1.59E+01	9.79E-01	5.42E-02	1.87E-07
Al-29	3.96E+02	1.83E-15	0.00%	3.62E+00	3.26E+00	1.27E+00	4.74E-01	6.64E-03
Si-31	9.44E+03	1.94E-15	0.00%	1.55E-01	1.55E-01	1.49E-01	1.43E-01	1.19E-01
Si-32	5.46E+09	1.02E-15	0.00%	1.84E-07	1.84E-07	1.84E-07	1.84E-07	1.84E-07
P-30	1.50E+02	1.07E-15	0.00%	3.53E+00	2.68E+00	2.21E-01	1.65E-02	2.09E-07
P-32	1.23E+06	1.10E-14	0.00%	1.81E-02	1.81E-02	1.81E-02	1.80E-02	1.80E-02
P-33	2.19E+06	7.74E-15	0.00%	7.89E-03	7.89E-03	7.88E-03	7.88E-03	7.88E-03
P-35	4.74E+01	8.69E-16	0.00%	3.58E+01	1.49E+01	5.54E-03	1.51E-06	4.91E-22
S-35	7.55E+06	9.91E-15	0.00%	2.97E-03	2.97E-03	2.97E-03	2.97E-03	2.97E-03
S-37	3.04E+02	4.40E-15	0.02%	2.09E+01	1.82E+01	5.32E+00	1.48E+00	5.64E-03
S-38	1.03E+04	2.12E-15	0.00%	4.19E-01	4.17E-01	4.03E-01	3.88E-01	3.29E-01
Cl-34	1.92E+03	4.72E-16	0.00%	4.11E-01	4.02E-01	3.31E-01	2.70E-01	1.12E-01
Cl-36	9.50E+12	2.49E-14	0.01%	7.01E-09	7.01E-09	7.01E-09	7.01E-09	7.01E-09
Cl-38	2.23E+03	1.72E-14	0.01%	2.11E+01	2.07E+01	1.75E+01	1.47E+01	6.89E+00
Cl-39	3.34E+03	3.47E-14	0.01%	2.27E+01	2.24E+01	2.00E+01	1.78E+01	1.07E+01
Cl-40	8.40E+01	3.46E-15	0.02%	1.31E+02	8.00E+01	9.29E-01	9.05E-03	1.65E-11
Ar-37	3.03E+06	4.43E-14	0.01%	2.20E-02	2.20E-02	2.20E-02	2.20E-02	2.20E-02
Ar-39	8.49E+09	1.26E-13	0.02%	3.01E-05	3.01E-05	3.01E-05	3.01E-05	3.01E-05
Ar-41	6.58E+03	1.04E-12	0.02%	7.64E+01	7.59E+01	7.17E+01	6.76E+01	5.23E+01
K-38	4.58E+02	3.09E-16	0.02%	3.06E+00	2.79E+00	1.23E+00	5.28E-01	1.32E-02
K-40	4.04E+16	8.56E-16	0.06%	1.46E-13	1.46E-13	1.46E-13	1.46E-13	1.46E-13

Table 61: Ci values for the isotopes gained by the simulation as well as the comparison of activities after several cooling times (0s, 60s, 600s, 1161.29s, 3600s), after irradiation with a total intensity of 1.16E+12 carbon ions, which corresponds to 3.1 air exchanges per hour during continuous irradiation with an 400 MeV ion beam and an intensity of 1E+9 ions per second, to their respective Ci value. Calculated Ci values not mentioned in Austrian law are underlined in light blue. Sum values of the comparison values after the listed cooling times are listed at the bottom, underlined in dark blue.

Isotope	t 1/2 [s]	Ci	0s	60s	600s	1161.29s	3600s
H-3	3.89E+08	100.0	8.97E-05	8.97E-05	8.97E-05	8.97E-05	8.97E-05
Be-7	4.61E+06	600.0	4.57E-04	4.57E-04	4.57E-04	4.57E-04	4.57E-04
Be-10	5.05E+13	1.0	2.65E-08	2.65E-08	2.65E-08	2.65E-08	2.65E-08
C-11	1.22E+03	600.0	3.17E+00	3.06E+00	2.26E+00	1.64E+00	4.12E-01
C-14	1.81E+11	6.0	2.21E-04	2.21E-04	2.21E-04	2.21E-04	2.21E-04
N-13	5.98E+02	2000.0	3.87E+00	3.61E+00	1.93E+00	1.01E+00	5.96E-02
O-14	7.10E+01	927.1	4.79E+00	2.67E+00	1.37E-02	5.71E-05	2.61E-15
O-15	1.22E+02	1000.0	2.61E+01	1.86E+01	8.68E-01	3.60E-02	3.55E-08
O-19	2.71E+01	1916.0	4.37E-04	9.42E-05	9.46E-11	5.51E-17	4.48E-44
F-18	6.59E+03	500.0	4.06E-04	4.03E-04	3.81E-04	3.59E-04	2.78E-04
Ne-23	2.80E+01	1892.7	2.02E-03	4.57E-04	7.16E-10	6.61E-16	3.99E-42
Ne-24	2.03E+02	896.3	8.06E-05	6.57E-05	1.04E-05	1.52E-06	3.65E-10
Na-22	8.21E+07	1.0	7.01E-06	7.01E-06	7.01E-06	7.01E-06	7.01E-06
Na-24	5.40E+04	90.0	1.99E-04	1.99E-04	1.97E-04	1.96E-04	1.90E-04
Na-25	6.00E+01	28648.2	1.55E-04	7.75E-05	1.51E-07	2.31E-10	1.34E-22
Mg-27	5.70E+02	577.8	1.67E-03	1.55E-03	8.05E-04	4.07E-04	2.10E-05
Mg-28	7.53E+04	20.0	2.09E-04	2.09E-04	2.08E-04	2.07E-04	2.02E-04
Al-26	2.26E+13	0.5	6.92E-11	6.92E-11	6.92E-11	6.92E-11	6.92E-11
Al-28	1.34E+02	537.6	4.02E-02	2.95E-02	1.82E-03	1.01E-04	3.48E-10
Al-29	3.96E+02	232.5	1.56E-02	1.40E-02	5.45E-03	2.04E-03	2.85E-05
Si-31	9.44E+03	300.0	5.17E-04	5.15E-04	4.95E-04	4.75E-04	3.97E-04
Si-32	5.46E+09	0.3	5.76E-07	5.76E-07	5.76E-07	5.76E-07	5.76E-07
P-30	1.50E+02	2727.8	1.29E-03	9.81E-04	8.08E-05	6.04E-06	7.67E-11
P-32	1.23E+06	1.0	1.81E-02	1.81E-02	1.81E-02	1.80E-02	1.80E-02
P-33	2.19E+06	20.0	3.94E-04	3.94E-04	3.94E-04	3.94E-04	3.94E-04
P-35	4.74E+01	12148.0	2.95E-03	1.23E-03	4.56E-07	1.24E-10	4.04E-26
S-35	7.55E+06	20.0	1.49E-04	1.49E-04	1.49E-04	1.49E-04	1.49E-04
S-37	3.04E+02	8682.3	2.41E-03	2.10E-03	6.12E-04	1.70E-04	6.49E-07
S-38	1.03E+04	422.8	9.91E-04	9.87E-04	9.52E-04	9.17E-04	7.79E-04
Cl-34	1.92E+03	16.8	2.44E-02	2.39E-02	1.96E-02	1.60E-02	6.65E-03
Cl-36	9.50E+12	0.1	7.01E-08	7.01E-08	7.01E-08	7.01E-08	7.01E-08
Cl-38	2.23E+03	500.0	4.21E-02	4.13E-02	3.50E-02	2.94E-02	1.38E-02
Cl-39	3.34E+03	600.0	3.78E-02	3.74E-02	3.34E-02	2.97E-02	1.79E-02
Cl-40	8.40E+01	292.7	4.48E-01	2.73E-01	3.17E-03	3.09E-05	5.63E-14
Ar-37	3.03E+06	200000000.0	1.10E-10	1.10E-10	1.10E-10	1.10E-10	1.10E-10
Ar-39	8.49E+09	6000.0	5.01E-09	5.01E-09	5.01E-09	5.01E-09	5.01E-09
Ar-41	6.58E+03	200.0	3.82E-01	3.79E-01	3.58E-01	3.38E-01	2.61E-01
K-38	4.58E+02	4622.1	6.61E-04	6.04E-04	2.67E-04	1.14E-04	2.85E-06
K-40	4.04E+16	0.3	4.67E-13	4.67E-13	4.67E-13	4.67E-13	4.67E-13
Sum:			3.89E+01	2.87E+01	5.55E+00	3.12E+00	7.92E-01

Table 62: Activity of the air after irradiation of a water target with a 400 MeV carbon ion beam, compared to Ci values, considering a cooling time of 1 hour and thinning the air to a volume of 14.000 m³ at average (2.47E+7 particles per second) and maximum (1E+9 particles per second) intensity

Isotope	Bq (total/y)	av. sp. act.	max. sp. act.	Ci [Bq/m ³]	av./Ci	max./Ci
H-3	1.04E+03	8.50E-06	5.70E-04	100.00	8.50E-08	5.70E-06
Be-7	3.19E+04	2.60E-04	1.74E-02	600.00	4.33E-07	2.91E-05
Be-10	3.08E-03	2.51E-11	1.68E-09	1.00	2.51E-11	1.68E-09
C-11	2.21E+08	2.34E-01	1.57E+01	600.00	3.90E-04	2.62E-02
C-14	1.54E+02	1.26E-06	8.44E-05	6.00	2.10E-07	1.41E-05
N-13	8.99E+08	1.13E-01	7.58E+00	2000.00	5.64E-05	3.79E-03
O-14	5.16E+08	2.29E-15	1.54E-13	927.09	2.48E-18	1.66E-16
O-15	3.03E+09	3.37E-08	2.26E-06	1000.00	3.37E-11	2.26E-09
O-19	9.73E+04	8.13E-44	5.46E-42	1916.02	4.24E-47	2.85E-45
F-18	2.36E+04	1.32E-04	8.83E-03	500.00	2.63E-07	1.77E-05
Ne-23	4.44E+05	7.16E-42	4.81E-40	1892.75	3.78E-45	2.54E-43
Ne-24	8.39E+03	3.10E-10	2.08E-08	896.31	3.46E-13	2.32E-11
Na-22	8.14E-01	6.64E-09	4.45E-07	1.00	6.64E-09	4.45E-07
Na-24	2.08E+03	1.62E-05	1.09E-03	90.00	1.80E-07	1.21E-05
Na-25	5.16E+05	3.65E-21	2.45E-19	28648.19	1.27E-25	8.54E-24
Mg-27	1.12E+05	1.15E-05	7.69E-04	577.79	1.98E-08	1.33E-06
Mg-28	4.86E+02	3.83E-06	2.57E-04	20.00	1.92E-07	1.29E-05
Al-26	4.02E-06	3.28E-14	2.20E-12	0.50	6.55E-14	4.40E-12
Al-28	2.51E+06	1.77E-10	1.19E-08	537.59	3.29E-13	2.21E-11
Al-29	4.20E+05	6.28E-06	4.22E-04	232.45	2.70E-08	1.81E-06
Si-31	1.80E+04	1.13E-04	7.57E-03	300.00	3.76E-07	2.52E-05
Si-32	2.14E-02	1.75E-10	1.17E-08	0.32	5.46E-10	3.66E-08
P-30	4.10E+05	1.98E-10	1.33E-08	2727.82	7.26E-14	4.87E-12
P-32	2.10E+03	1.71E-05	1.15E-03	1.00	1.71E-05	1.15E-03
P-33	9.16E+02	7.46E-06	5.01E-04	20.00	3.73E-07	2.50E-05
P-35	4.16E+06	4.65E-25	3.12E-23	12148.03	3.83E-29	2.57E-27
S-35	3.45E+02	2.81E-06	1.89E-04	20.00	1.41E-07	9.44E-06
S-37	2.43E+06	5.34E-06	3.58E-04	8682.34	6.15E-10	4.13E-08
S-38	4.87E+04	3.12E-04	2.09E-02	422.83	7.37E-07	4.95E-05
Cl-34	4.77E+04	1.06E-04	7.12E-03	16.84	6.30E-06	4.23E-04
Cl-36	8.14E-04	6.64E-12	4.45E-10	0.10	6.64E-11	4.45E-09
Cl-38	2.45E+06	6.52E-03	4.38E-01	500.00	1.30E-05	8.75E-04
Cl-39	2.64E+06	1.02E-02	6.83E-01	600.00	1.70E-05	1.14E-03
Cl-40	1.52E+07	1.56E-14	1.05E-12	292.72	5.33E-17	3.58E-15
Ar-37	2.56E+03	2.08E-05	1.40E-03	20000000.00	1.04E-13	6.99E-12
Ar-39	3.49E+00	2.85E-08	1.91E-06	6000.00	4.74E-12	3.18E-10
Ar-41	8.87E+06	4.95E-02	3.32E+00	200.00	2.47E-04	1.66E-02
K-38	3.55E+05	1.25E-05	8.38E-04	4622.10	2.70E-09	1.81E-07
K-40	1.70E-08	1.38E-16	9.28E-15	0.31	4.42E-16	2.97E-14
Sum:					7.51E-04	5.04E-02

IRRADIATION ROOM 4 – 250 MEV PROTONS – HORIZONTAL SCENARIO

Table 63: Yield results (per primary particle per cm³) and relative errors, as well as specific activities (in Bq/m³) for each isotope after several cooling times (in seconds) after irradiation with a total intensity of 3.43E+13 protons, which corresponds to 2.1 air exchanges per hour during continuous irradiation with a 250 MeV proton beam and an intensity of 2E+10 protons per second

Isotope	t 1/2 [s]	yield/pp/cm ³	rel. error	0s	60s	600s	1714.29s	3600s
H-3	3.89E+08	2.54E-12	0.01%	2.80E-03	2.80E-03	2.80E-03	2.80E-03	2.80E-03
Be-7	4.61E+06	8.55E-13	0.00%	1.51E-01	1.51E-01	1.51E-01	1.51E-01	1.51E-01
Be-10	5.05E+13	4.74E-13	0.01%	6.78E-09	6.78E-09	6.78E-09	6.78E-09	6.78E-09
C-11	1.22E+03	1.13E-12	0.01%	9.41E+02	9.09E+02	6.69E+02	3.56E+02	1.22E+02
C-14	1.81E+11	5.00E-10	0.02%	3.71E-04	3.71E-04	3.71E-04	3.71E-04	3.71E-04
N-13	5.98E+02	1.79E-12	0.01%	3.24E+03	3.02E+03	1.61E+03	4.43E+02	4.98E+01
O-14	7.10E+01	1.14E-13	0.02%	2.19E+03	1.22E+03	6.26E+00	1.18E-04	1.19E-12
O-15	1.22E+02	1.45E-12	0.00%	1.33E+04	9.44E+03	4.42E+02	7.96E-01	1.81E-05
O-19	2.71E+01	1.53E-16	0.00%	2.70E-01	5.82E-02	5.84E-08	2.45E-20	2.77E-41
F-18	6.59E+03	4.21E-15	0.00%	1.07E-01	1.06E-01	1.01E-01	8.95E-02	7.34E-02
Ne-23	2.80E+01	3.94E-16	0.00%	1.68E+00	3.81E-01	5.95E-07	6.24E-19	3.32E-39
Ne-24	2.03E+02	8.23E-17	0.00%	2.73E-02	2.22E-02	3.51E-03	7.79E-05	1.24E-07
Na-22	8.21E+07	1.14E-15	0.00%	4.31E-06	4.31E-06	4.31E-06	4.31E-06	4.31E-06
Na-24	5.40E+04	1.79E-15	0.00%	9.59E-03	9.59E-03	9.52E-03	9.39E-03	9.16E-03
Na-25	6.00E+01	7.03E-16	0.00%	2.21E+00	1.10E+00	2.15E-03	5.53E-09	1.91E-18
Mg-27	5.70E+02	1.02E-15	0.00%	5.25E-01	4.88E-01	2.53E-01	6.53E-02	6.59E-03
Mg-28	7.53E+04	3.03E-16	0.00%	2.36E-03	2.36E-03	2.35E-03	2.32E-03	2.28E-03
Al-26	2.26E+13	1.44E-15	0.00%	1.88E-11	1.88E-11	1.88E-11	1.88E-11	1.88E-11
Al-28	1.34E+02	3.30E-15	0.00%	1.27E+01	9.32E+00	5.75E-01	1.84E-03	1.10E-07
Al-29	3.96E+02	1.83E-15	0.00%	2.09E+00	1.89E+00	7.33E-01	1.04E-01	3.84E-03
Si-31	9.44E+03	1.94E-15	0.00%	7.05E-02	7.02E-02	6.75E-02	6.22E-02	5.41E-02
Si-32	5.46E+09	1.02E-15	0.00%	8.06E-08	8.06E-08	8.06E-08	8.06E-08	8.06E-08
P-30	1.50E+02	1.07E-15	0.00%	2.33E+00	1.77E+00	1.45E-01	8.43E-04	1.38E-07
P-32	1.23E+06	1.10E-14	0.00%	8.33E-03	8.33E-03	8.33E-03	8.33E-03	8.32E-03
P-33	2.19E+06	7.74E-15	0.00%	3.12E-03	3.12E-03	3.12E-03	3.12E-03	3.12E-03
P-35	4.74E+01	8.69E-16	0.00%	1.05E+01	4.36E+00	1.62E-03	1.36E-10	1.44E-22
S-35	7.55E+06	9.91E-15	0.00%	1.04E-03	1.04E-03	1.04E-03	1.04E-03	1.04E-03
S-37	3.04E+02	4.40E-15	0.02%	5.73E+00	5.00E+00	1.46E+00	1.14E-01	1.54E-03
S-38	1.03E+04	2.12E-15	0.00%	1.08E-01	1.08E-01	1.04E-01	9.66E-02	8.51E-02
Cl-34	1.92E+03	4.72E-16	0.00%	2.72E-01	2.66E-01	2.19E-01	1.47E-01	7.42E-02
Cl-36	9.50E+12	2.49E-14	0.01%	2.95E-09	2.95E-09	2.95E-09	2.95E-09	2.95E-09
Cl-38	2.23E+03	1.72E-14	0.01%	6.78E+00	6.66E+00	5.63E+00	3.98E+00	2.22E+00
Cl-39	3.34E+03	3.47E-14	0.01%	7.34E+00	7.25E+00	6.48E+00	5.14E+00	3.47E+00
Cl-40	8.40E+01	3.46E-15	0.02%	3.14E+01	1.91E+01	2.22E-01	2.26E-05	3.94E-12
Ar-37	3.03E+06	4.43E-14	0.01%	8.72E-03	8.72E-03	8.72E-03	8.71E-03	8.71E-03
Ar-39	8.49E+09	1.26E-13	0.02%	1.01E-05	1.01E-05	1.01E-05	1.01E-05	1.01E-05
Ar-41	6.58E+03	1.04E-12	0.02%	2.14E+01	2.13E+01	2.01E+01	1.79E+01	1.47E+01
K-38	4.58E+02	3.09E-16	0.02%	1.71E+00	1.56E+00	6.88E-01	1.28E-01	7.36E-03
K-40	4.04E+16	8.56E-16	0.06%	5.35E-14	5.35E-14	5.35E-14	5.35E-14	5.35E-14

Table 64: Ci values for the isotopes gained by the simulation as well as the comparison of activities after several cooling times (0s, 60s, 600s, 1714.29s, 3600s), after irradiation with a total intensity of $3.43\text{E}+13$ protons, which corresponds to 2.1 air exchanges per hour during continuous irradiation with a 250 MeV proton beam and an intensity of $2\text{E}+10$ protons per second, to their respective Ci value. Calculated Ci values not mentioned in Austrian law are underlined in light blue. Sum values of the comparison values after the listed cooling times are listed at the bottom, underlined in dark blue.

Isotope	t 1/2 [s]	Ci	0s	60s	600s	1714.29s	3600s
H-3	3.89E+08	100.0	2.80E-05	2.80E-05	2.80E-05	2.80E-05	2.80E-05
Be-7	4.61E+06	600.0	2.52E-04	2.52E-04	2.52E-04	2.52E-04	2.52E-04
Be-10	5.05E+13	1.0	6.78E-09	6.78E-09	6.78E-09	6.78E-09	6.78E-09
C-11	1.22E+03	600.0	1.57E+00	1.52E+00	1.12E+00	5.93E-01	2.04E-01
C-14	1.81E+11	6.0	6.18E-05	6.18E-05	6.18E-05	6.18E-05	6.18E-05
N-13	5.98E+02	2000.0	1.62E+00	1.51E+00	8.07E-01	2.22E-01	2.49E-02
O-14	7.10E+01	927.1	2.36E+00	1.31E+00	6.75E-03	1.27E-07	1.29E-15
O-15	1.22E+02	1000.0	1.33E+01	9.44E+00	4.42E-01	7.96E-04	1.81E-08
O-19	2.71E+01	1916.0	1.41E-04	3.04E-05	3.05E-11	1.28E-23	1.45E-44
F-18	6.59E+03	500.0	2.14E-04	2.13E-04	2.01E-04	1.79E-04	1.47E-04
Ne-23	2.80E+01	1892.7	8.88E-04	2.01E-04	3.15E-10	3.30E-22	1.76E-42
Ne-24	2.03E+02	896.3	3.05E-05	2.48E-05	3.92E-06	8.69E-08	1.38E-10
Na-22	8.21E+07	1.0	4.31E-06	4.31E-06	4.31E-06	4.31E-06	4.31E-06
Na-24	5.40E+04	90.0	1.07E-04	1.07E-04	1.06E-04	1.04E-04	1.02E-04
Na-25	6.00E+01	28648.2	7.70E-05	3.85E-05	7.52E-08	1.93E-13	6.68E-23
Mg-27	5.70E+02	577.8	9.09E-04	8.45E-04	4.38E-04	1.13E-04	1.14E-05
Mg-28	7.53E+04	20.0	1.18E-04	1.18E-04	1.17E-04	1.16E-04	1.14E-04
Al-26	2.26E+13	0.5	3.77E-11	3.77E-11	3.77E-11	3.77E-11	3.77E-11
Al-28	1.34E+02	537.6	2.36E-02	1.73E-02	1.07E-03	3.42E-06	2.04E-10
Al-29	3.96E+02	232.5	9.01E-03	8.11E-03	3.15E-03	4.48E-04	1.65E-05
Si-31	9.44E+03	300.0	2.35E-04	2.34E-04	2.25E-04	2.07E-04	1.80E-04
Si-32	5.46E+09	0.3	2.52E-07	2.52E-07	2.52E-07	2.52E-07	2.52E-07
P-30	1.50E+02	2727.8	8.54E-04	6.47E-04	5.33E-05	3.09E-07	5.06E-11
P-32	1.23E+06	1.0	8.33E-03	8.33E-03	8.33E-03	8.33E-03	8.32E-03
P-33	2.19E+06	20.0	1.56E-04	1.56E-04	1.56E-04	1.56E-04	1.56E-04
P-35	4.74E+01	12148.0	8.63E-04	3.59E-04	1.33E-07	1.12E-14	1.18E-26
S-35	7.55E+06	20.0	5.22E-05	5.22E-05	5.22E-05	5.22E-05	5.22E-05
S-37	3.04E+02	8682.3	6.60E-04	5.75E-04	1.68E-04	1.32E-05	1.78E-07
S-38	1.03E+04	422.8	2.56E-04	2.55E-04	2.46E-04	2.28E-04	2.01E-04
Cl-34	1.92E+03	16.8	1.62E-02	1.58E-02	1.30E-02	8.71E-03	4.41E-03
Cl-36	9.50E+12	0.1	2.95E-08	2.95E-08	2.95E-08	2.95E-08	2.95E-08
Cl-38	2.23E+03	500.0	1.36E-02	1.33E-02	1.13E-02	7.96E-03	4.44E-03
Cl-39	3.34E+03	600.0	1.22E-02	1.21E-02	1.08E-02	8.56E-03	5.79E-03
Cl-40	8.40E+01	292.7	1.07E-01	6.54E-02	7.59E-04	7.71E-08	1.35E-14
Ar-37	3.03E+06	200000000.0	4.36E-11	4.36E-11	4.36E-11	4.36E-11	4.36E-11
Ar-39	8.49E+09	6000.0	1.69E-09	1.69E-09	1.69E-09	1.69E-09	1.69E-09
Ar-41	6.58E+03	200.0	1.07E-01	1.06E-01	1.01E-01	8.94E-02	7.33E-02
K-38	4.58E+02	4622.1	3.69E-04	3.37E-04	1.49E-04	2.76E-05	1.59E-06
K-40	4.04E+16	0.3	1.71E-13	1.71E-13	1.71E-13	1.71E-13	1.71E-13
Sum:			1.91E+01	1.40E+01	2.52E+00	9.41E-01	3.26E-01

Table 65: Activity of the air after irradiation of a water target with a 250 MeV proton beam, compared to Ci values, considering a cooling time of 1 hour and thinning the air to a volume of 14.000 m³ at average (2.12E+8 particles per second) and maximum (2E+10 particles per second) intensity

Isotope	Bq (total/y)	av. sp. act.	max. sp. act.	Ci [Bq/m ³]	av./Ci	max./Ci
H-3	1.08E+03	8.79E-06	8.28E-04	100.00	8.79E-08	8.28E-06
Be-7	5.82E+04	4.74E-04	4.47E-02	600.00	7.91E-07	7.44E-05
Be-10	2.61E-03	2.13E-11	2.00E-09	1.00	2.13E-11	2.00E-09
C-11	3.62E+08	3.84E-01	3.61E+01	600.00	6.39E-04	6.02E-02
C-14	1.43E+02	1.16E-06	1.10E-04	6.00	1.94E-07	1.83E-05
N-13	1.25E+09	1.56E-01	1.47E+01	2000.00	7.82E-05	7.36E-03
O-14	8.43E+08	3.75E-15	3.53E-13	927.09	4.04E-18	3.80E-16
O-15	5.10E+09	5.67E-08	5.34E-06	1000.00	5.67E-11	5.34E-09
O-19	1.04E+05	8.69E-44	8.18E-42	1916.02	4.54E-47	4.27E-45
F-18	4.13E+04	2.30E-04	2.17E-02	500.00	4.61E-07	4.34E-05
Ne-23	6.47E+05	1.04E-41	9.82E-40	1892.75	5.51E-45	5.19E-43
Ne-24	1.05E+04	3.88E-10	3.66E-08	896.31	4.33E-13	4.08E-11
Na-22	1.66E+00	1.35E-08	1.27E-06	1.00	1.35E-08	1.27E-06
Na-24	3.69E+03	2.88E-05	2.71E-03	90.00	3.20E-07	3.01E-05
Na-25	8.49E+05	6.01E-21	5.65E-19	28648.19	2.10E-25	1.97E-23
Mg-27	2.02E+05	2.07E-05	1.95E-03	577.79	3.58E-08	3.37E-06
Mg-28	9.09E+02	7.17E-06	6.75E-04	20.00	3.59E-07	3.38E-05
Al-26	7.25E-06	5.91E-14	5.56E-12	0.50	1.18E-13	1.11E-11
Al-28	4.89E+06	3.44E-10	3.24E-08	537.59	6.41E-13	6.03E-11
Al-29	8.06E+05	1.21E-05	1.13E-03	232.45	5.19E-08	4.88E-06
Si-31	2.71E+04	1.70E-04	1.60E-02	300.00	5.66E-07	5.33E-05
Si-32	3.10E-02	2.53E-10	2.38E-08	0.32	7.91E-10	7.44E-08
P-30	8.97E+05	4.33E-10	4.08E-08	2727.82	1.59E-13	1.49E-11
P-32	3.21E+03	2.61E-05	2.46E-03	1.00	2.61E-05	2.46E-03
P-33	1.20E+03	9.78E-06	9.21E-04	20.00	4.89E-07	4.60E-05
P-35	4.03E+06	4.51E-25	4.24E-23	12148.03	3.71E-29	3.49E-27
S-35	4.02E+02	3.28E-06	3.09E-04	20.00	1.64E-07	1.54E-05
S-37	2.21E+06	4.85E-06	4.56E-04	8682.34	5.58E-10	5.25E-08
S-38	4.17E+04	2.67E-04	2.51E-02	422.83	6.32E-07	5.95E-05
Cl-34	1.05E+05	2.33E-04	2.19E-02	16.84	1.38E-05	1.30E-03
Cl-36	1.14E-03	9.27E-12	8.72E-10	0.10	9.27E-11	8.72E-09
Cl-38	2.61E+06	6.96E-03	6.55E-01	500.00	1.39E-05	1.31E-03
Cl-39	2.82E+06	1.09E-02	1.03E+00	600.00	1.82E-05	1.71E-03
Cl-40	1.21E+07	1.24E-14	1.16E-12	292.72	4.23E-17	3.98E-15
Ar-37	3.36E+03	2.73E-05	2.57E-03	20000000.00	1.37E-13	1.29E-11
Ar-39	3.90E+00	3.18E-08	2.99E-06	6000.00	5.30E-12	4.99E-10
Ar-41	8.25E+06	4.60E-02	4.33E+00	200.00	2.30E-04	2.17E-02
K-38	6.57E+05	2.31E-05	2.17E-03	4622.10	5.00E-09	4.70E-07
K-40	2.06E-08	1.68E-16	1.58E-14	0.31	5.37E-16	5.06E-14
Sum:					1.02E-03	9.64E-02

IRRADIATION ROOM 4 – 250 MEV PROTONS – VERTICAL UP SCENARIO

Table 66: Yield results (per primary particle per cm³) and relative errors, as well as specific activities (in Bq/m³) for each isotope after several cooling times (in seconds) after irradiation with a total intensity of 3.43E+13 protons, which corresponds to 2.1 air exchanges per hour during continuous irradiation with a 250 MeV proton beam and an intensity of 2E+10 protons per second

Isotope	t 1/2 [s]	yield/pp/cm ³	rel. error	0s	60s	600s	1714.29s	3600s
H-3	3.89E+08	2.54E-12	0.01%	2.78E-03	2.78E-03	2.78E-03	2.78E-03	2.78E-03
Be-7	4.61E+06	8.55E-13	0.00%	1.47E-01	1.47E-01	1.47E-01	1.47E-01	1.46E-01
Be-10	5.05E+13	4.74E-13	0.01%	6.83E-09	6.83E-09	6.83E-09	6.83E-09	6.83E-09
C-11	1.22E+03	1.13E-12	0.01%	9.13E+02	8.83E+02	6.50E+02	3.46E+02	1.19E+02
C-14	1.81E+11	5.00E-10	0.02%	3.72E-04	3.72E-04	3.72E-04	3.72E-04	3.72E-04
N-13	5.98E+02	1.79E-12	0.01%	3.16E+03	2.95E+03	1.58E+03	4.34E+02	4.87E+01
O-14	7.10E+01	1.14E-13	0.02%	2.13E+03	1.18E+03	6.07E+00	1.15E-04	1.16E-12
O-15	1.22E+02	1.45E-12	0.00%	1.29E+04	9.17E+03	4.29E+02	7.74E-01	1.76E-05
O-19	2.71E+01	1.53E-16	0.00%	2.60E-01	5.61E-02	5.63E-08	2.36E-20	2.67E-41
F-18	6.59E+03	4.21E-15	0.00%	1.04E-01	1.03E-01	9.72E-02	8.65E-02	7.09E-02
Ne-23	2.80E+01	3.94E-16	0.00%	1.62E+00	3.67E-01	5.74E-07	6.02E-19	3.21E-39
Ne-24	2.03E+02	8.23E-17	0.00%	2.62E-02	2.14E-02	3.38E-03	7.49E-05	1.19E-07
Na-22	8.21E+07	1.14E-15	0.00%	4.17E-06	4.17E-06	4.17E-06	4.17E-06	4.17E-06
Na-24	5.40E+04	1.79E-15	0.00%	9.29E-03	9.28E-03	9.21E-03	9.08E-03	8.87E-03
Na-25	6.00E+01	7.03E-16	0.00%	2.13E+00	1.06E+00	2.08E-03	5.33E-09	1.84E-18
Mg-27	5.70E+02	1.02E-15	0.00%	5.09E-01	4.73E-01	2.45E-01	6.33E-02	6.39E-03
Mg-28	7.53E+04	3.03E-16	0.00%	2.28E-03	2.28E-03	2.27E-03	2.24E-03	2.21E-03
Al-26	2.26E+13	1.44E-15	0.00%	1.82E-11	1.82E-11	1.82E-11	1.82E-11	1.82E-11
Al-28	1.34E+02	3.30E-15	0.00%	1.23E+01	8.99E+00	5.55E-01	1.77E-03	1.06E-07
Al-29	3.96E+02	1.83E-15	0.00%	2.02E+00	1.82E+00	7.08E-01	1.01E-01	3.71E-03
Si-31	9.44E+03	1.94E-15	0.00%	6.82E-02	6.79E-02	6.53E-02	6.02E-02	5.24E-02
Si-32	5.46E+09	1.02E-15	0.00%	7.80E-08	7.80E-08	7.80E-08	7.80E-08	7.80E-08
P-30	1.50E+02	1.07E-15	0.00%	2.25E+00	1.71E+00	1.41E-01	8.14E-04	1.33E-07
P-32	1.23E+06	1.10E-14	0.00%	8.07E-03	8.06E-03	8.06E-03	8.06E-03	8.05E-03
P-33	2.19E+06	7.74E-15	0.00%	3.03E-03	3.03E-03	3.03E-03	3.03E-03	3.03E-03
P-35	4.74E+01	8.69E-16	0.00%	1.03E+01	4.27E+00	1.59E-03	1.33E-10	1.41E-22
S-35	7.55E+06	9.91E-15	0.00%	1.02E-03	1.02E-03	1.02E-03	1.02E-03	1.02E-03
S-37	3.04E+02	4.40E-15	0.02%	5.67E+00	4.94E+00	1.44E+00	1.13E-01	1.53E-03
S-38	1.03E+04	2.12E-15	0.00%	1.06E-01	1.06E-01	1.02E-01	9.45E-02	8.33E-02
Cl-34	1.92E+03	4.72E-16	0.00%	2.64E-01	2.58E-01	2.12E-01	1.42E-01	7.19E-02
Cl-36	9.50E+12	2.49E-14	0.01%	2.88E-09	2.88E-09	2.88E-09	2.88E-09	2.88E-09
Cl-38	2.23E+03	1.72E-14	0.01%	6.67E+00	6.55E+00	5.54E+00	3.92E+00	2.18E+00
Cl-39	3.34E+03	3.47E-14	0.01%	7.20E+00	7.11E+00	6.35E+00	5.04E+00	3.41E+00
Cl-40	8.40E+01	3.46E-15	0.02%	3.20E+01	1.95E+01	2.26E-01	2.30E-05	4.01E-12
Ar-37	3.03E+06	4.43E-14	0.01%	8.56E-03	8.56E-03	8.56E-03	8.56E-03	8.55E-03
Ar-39	8.49E+09	1.26E-13	0.02%	1.01E-05	1.01E-05	1.01E-05	1.01E-05	1.01E-05
Ar-41	6.58E+03	1.04E-12	0.02%	2.15E+01	2.13E+01	2.01E+01	1.79E+01	1.47E+01
K-38	4.58E+02	3.09E-16	0.02%	1.66E+00	1.52E+00	6.70E-01	1.24E-01	7.16E-03
K-40	4.04E+16	8.56E-16	0.06%	5.23E-14	5.23E-14	5.23E-14	5.23E-14	5.23E-14

Table 67: Ci values for the isotopes gained by the simulation as well as the comparison of activities after several cooling times (0s, 60s, 600s, 1714.29s, 3600s), after irradiation with a total intensity of $3.43\text{E}+13$ protons, which corresponds to 2.1 air exchanges per hour during continuous irradiation with a 250 MeV proton beam and an intensity of $2\text{E}+10$ protons per second, to their respective Ci value. Calculated Ci values not mentioned in Austrian law are underlined in light blue. Sum values of the comparison values after the listed cooling times are listed at the bottom, underlined in dark blue.

Isotope	t 1/2 [s]	Ci	0s	60s	600s	1714.29s	3600s
H-3	3.89E+08	100.0	2.78E-05	2.78E-05	2.78E-05	2.78E-05	2.78E-05
Be-7	4.61E+06	600.0	2.44E-04	2.44E-04	2.44E-04	2.44E-04	2.44E-04
Be-10	5.05E+13	1.0	6.83E-09	6.83E-09	6.83E-09	6.83E-09	6.83E-09
C-11	1.22E+03	600.0	1.52E+00	1.47E+00	1.08E+00	5.76E-01	1.98E-01
C-14	1.81E+11	6.0	6.20E-05	6.20E-05	6.20E-05	6.20E-05	6.20E-05
N-13	5.98E+02	2000.0	1.58E+00	1.48E+00	7.89E-01	2.17E-01	2.44E-02
O-14	7.10E+01	927.1	2.29E+00	1.28E+00	6.55E-03	1.24E-07	1.25E-15
O-15	1.22E+02	1000.0	1.29E+01	9.17E+00	4.29E-01	7.74E-04	1.76E-08
O-19	2.71E+01	1916.0	1.36E-04	2.93E-05	2.94E-11	1.23E-23	1.39E-44
F-18	6.59E+03	500.0	2.07E-04	2.06E-04	1.94E-04	1.73E-04	1.42E-04
Ne-23	2.80E+01	1892.7	8.56E-04	1.94E-04	3.03E-10	3.18E-22	1.69E-42
Ne-24	2.03E+02	896.3	2.93E-05	2.39E-05	3.77E-06	8.36E-08	1.33E-10
Na-22	8.21E+07	1.0	4.17E-06	4.17E-06	4.17E-06	4.17E-06	4.17E-06
Na-24	5.40E+04	90.0	1.03E-04	1.03E-04	1.02E-04	1.01E-04	9.85E-05
Na-25	6.00E+01	28648.2	7.42E-05	3.71E-05	7.25E-08	1.86E-13	6.44E-23
Mg-27	5.70E+02	577.8	8.80E-04	8.18E-04	4.24E-04	1.09E-04	1.11E-05
Mg-28	7.53E+04	20.0	1.14E-04	1.14E-04	1.13E-04	1.12E-04	1.10E-04
Al-26	2.26E+13	0.5	3.64E-11	3.64E-11	3.64E-11	3.64E-11	3.64E-11
Al-28	1.34E+02	537.6	2.28E-02	1.67E-02	1.03E-03	3.30E-06	1.97E-10
Al-29	3.96E+02	232.5	8.70E-03	7.83E-03	3.04E-03	4.33E-04	1.60E-05
Si-31	9.44E+03	300.0	2.27E-04	2.26E-04	2.18E-04	2.01E-04	1.75E-04
Si-32	5.46E+09	0.3	2.44E-07	2.44E-07	2.44E-07	2.44E-07	2.44E-07
P-30	1.50E+02	2727.8	8.25E-04	6.25E-04	5.15E-05	2.98E-07	4.89E-11
P-32	1.23E+06	1.0	8.07E-03	8.06E-03	8.06E-03	8.06E-03	8.05E-03
P-33	2.19E+06	20.0	1.52E-04	1.52E-04	1.52E-04	1.52E-04	1.51E-04
P-35	4.74E+01	12148.0	8.46E-04	3.52E-04	1.31E-07	1.10E-14	1.16E-26
S-35	7.55E+06	20.0	5.10E-05	5.10E-05	5.10E-05	5.10E-05	5.09E-05
S-37	3.04E+02	8682.3	6.53E-04	5.69E-04	1.66E-04	1.30E-05	1.76E-07
S-38	1.03E+04	422.8	2.51E-04	2.50E-04	2.41E-04	2.24E-04	1.97E-04
Cl-34	1.92E+03	16.8	1.57E-02	1.53E-02	1.26E-02	8.43E-03	4.27E-03
Cl-36	9.50E+12	0.1	2.88E-08	2.88E-08	2.88E-08	2.88E-08	2.88E-08
Cl-38	2.23E+03	500.0	1.33E-02	1.31E-02	1.11E-02	7.84E-03	4.37E-03
Cl-39	3.34E+03	600.0	1.20E-02	1.18E-02	1.06E-02	8.40E-03	5.68E-03
Cl-40	8.40E+01	292.7	1.09E-01	6.66E-02	7.73E-04	7.85E-08	1.37E-14
Ar-37	3.03E+06	200000000.0	4.28E-11	4.28E-11	4.28E-11	4.28E-11	4.28E-11
Ar-39	8.49E+09	6000.0	1.69E-09	1.69E-09	1.69E-09	1.69E-09	1.69E-09
Ar-41	6.58E+03	200.0	1.07E-01	1.07E-01	1.01E-01	8.96E-02	7.34E-02
K-38	4.58E+02	4622.1	3.59E-04	3.28E-04	1.45E-04	2.68E-05	1.55E-06
K-40	4.04E+16	0.3	1.67E-13	1.67E-13	1.67E-13	1.67E-13	1.67E-13
Sum:			1.86E+01	1.36E+01	2.46E+00	9.18E-01	3.19E-01

Table 68: Activity of the air after irradiation of a water target with a 250 MeV proton beam, compared to Ci values, considering a cooling time of 1 hour and thinning the air to a volume of 14.000 m³ at average (2.12E+8 particles per second) and maximum (2E+10 particles per second) intensity

Isotope	Bq (total/y)	av. sp. act.	max. sp. act.	Ci [Bq/m ³]	av./Ci	max./Ci
H-3	1.07E+03	8.73E-06	8.22E-04	100.00	8.73E-08	8.22E-06
Be-7	5.64E+04	4.60E-04	4.33E-02	600.00	7.66E-07	7.21E-05
Be-10	2.63E-03	2.14E-11	2.02E-09	1.00	2.14E-11	2.02E-09
C-11	3.52E+08	3.73E-01	3.51E+01	600.00	6.21E-04	5.85E-02
C-14	1.43E+02	1.17E-06	1.10E-04	6.00	1.95E-07	1.83E-05
N-13	1.22E+09	1.53E-01	1.44E+01	2000.00	7.65E-05	7.20E-03
O-14	8.18E+08	3.64E-15	3.42E-13	927.09	3.92E-18	3.69E-16
O-15	4.96E+09	5.52E-08	5.19E-06	1000.00	5.52E-11	5.19E-09
O-19	1.00E+05	8.38E-44	7.89E-42	1916.02	4.37E-47	4.12E-45
F-18	3.99E+04	2.23E-04	2.10E-02	500.00	4.45E-07	4.19E-05
Ne-23	6.24E+05	1.01E-41	9.47E-40	1892.75	5.32E-45	5.01E-43
Ne-24	1.01E+04	3.73E-10	3.52E-08	896.31	4.17E-13	3.92E-11
Na-22	1.60E+00	1.31E-08	1.23E-06	1.00	1.31E-08	1.23E-06
Na-24	3.57E+03	2.78E-05	2.62E-03	90.00	3.09E-07	2.91E-05
Na-25	8.19E+05	5.79E-21	5.45E-19	28648.19	2.02E-25	1.90E-23
Mg-27	1.96E+05	2.00E-05	1.89E-03	577.79	3.47E-08	3.27E-06
Mg-28	8.78E+02	6.92E-06	6.52E-04	20.00	3.46E-07	3.26E-05
Al-26	7.00E-06	5.71E-14	5.38E-12	0.50	1.14E-13	1.08E-11
Al-28	4.72E+06	3.32E-10	3.13E-08	537.59	6.18E-13	5.82E-11
Al-29	7.79E+05	1.16E-05	1.10E-03	232.45	5.01E-08	4.71E-06
Si-31	2.63E+04	1.64E-04	1.55E-02	300.00	5.48E-07	5.16E-05
Si-32	3.00E-02	2.45E-10	2.30E-08	0.32	7.65E-10	7.20E-08
P-30	8.66E+05	4.18E-10	3.94E-08	2727.82	1.53E-13	1.44E-11
P-32	3.10E+03	2.53E-05	2.38E-03	1.00	2.53E-05	2.38E-03
P-33	1.17E+03	9.51E-06	8.95E-04	20.00	4.75E-07	4.47E-05
P-35	3.96E+06	4.42E-25	4.16E-23	12148.03	3.64E-29	3.43E-27
S-35	3.92E+02	3.20E-06	3.01E-04	20.00	1.60E-07	1.51E-05
S-37	2.18E+06	4.79E-06	4.51E-04	8682.34	5.52E-10	5.20E-08
S-38	4.08E+04	2.61E-04	2.46E-02	422.83	6.18E-07	5.82E-05
Cl-34	1.01E+05	2.26E-04	2.12E-02	16.84	1.34E-05	1.26E-03
Cl-36	1.11E-03	9.03E-12	8.50E-10	0.10	9.03E-11	8.50E-09
Cl-38	2.57E+06	6.85E-03	6.45E-01	500.00	1.37E-05	1.29E-03
Cl-39	2.77E+06	1.07E-02	1.01E+00	600.00	1.78E-05	1.68E-03
Cl-40	1.23E+07	1.26E-14	1.19E-12	292.72	4.30E-17	4.05E-15
Ar-37	3.30E+03	2.69E-05	2.53E-03	20000000.00	1.34E-13	1.26E-11
Ar-39	3.90E+00	3.18E-08	2.99E-06	6000.00	5.30E-12	4.99E-10
Ar-41	8.26E+06	4.61E-02	4.34E+00	200.00	2.31E-04	2.17E-02
K-38	6.39E+05	2.25E-05	2.11E-03	4622.10	4.86E-09	4.58E-07
K-40	2.01E-08	1.64E-16	1.55E-14	0.31	5.25E-16	4.94E-14
Sum:					1.00E-03	9.43E-02

IRRADIATION ROOM 4 – 250 MEV PROTONS – VERTICAL DOWN SCENARIO

Table 69: Yield results (per primary particle per cm³) and relative errors, as well as specific activities (in Bq/m³) for each isotope after several cooling times (in seconds) after irradiation with a total intensity of 3.43E+13 protons, which corresponds to 2.1 air exchanges per hour during continuous irradiation with a 250 MeV proton beam and an intensity of 2E+10 protons per second

Isotope	t 1/2 [s]	yield/pp/cm ³	rel. error	0s	60s	600s	1714.29s	3600s
H-3	3.89E+08	2.54E-12	0.01%	2.55E-03	2.55E-03	2.55E-03	2.55E-03	2.55E-03
Be-7	4.61E+06	8.55E-13	0.00%	1.42E-01	1.42E-01	1.42E-01	1.42E-01	1.42E-01
Be-10	5.05E+13	4.74E-13	0.01%	5.93E-09	5.93E-09	5.93E-09	5.93E-09	5.93E-09
C-11	1.22E+03	1.13E-12	0.01%	8.80E+02	8.51E+02	6.27E+02	3.33E+02	1.14E+02
C-14	1.81E+11	5.00E-10	0.02%	3.74E-04	3.74E-04	3.74E-04	3.74E-04	3.74E-04
N-13	5.98E+02	1.79E-12	0.01%	3.00E+03	2.80E+03	1.50E+03	4.11E+02	4.62E+01
O-14	7.10E+01	1.14E-13	0.02%	2.08E+03	1.16E+03	5.93E+00	1.12E-04	1.13E-12
O-15	1.22E+02	1.45E-12	0.00%	1.24E+04	8.85E+03	4.14E+02	7.47E-01	1.70E-05
O-19	2.71E+01	1.53E-16	0.00%	2.60E-01	5.59E-02	5.62E-08	2.35E-20	2.66E-41
F-18	6.59E+03	4.21E-15	0.00%	1.02E-01	1.02E-01	9.62E-02	8.56E-02	7.02E-02
Ne-23	2.80E+01	3.94E-16	0.00%	1.61E+00	3.65E-01	5.71E-07	5.99E-19	3.19E-39
Ne-24	2.03E+02	8.23E-17	0.00%	2.61E-02	2.13E-02	3.36E-03	7.46E-05	1.18E-07
Na-22	8.21E+07	1.14E-15	0.00%	4.11E-06	4.11E-06	4.11E-06	4.11E-06	4.11E-06
Na-24	5.40E+04	1.79E-15	0.00%	9.15E-03	9.15E-03	9.08E-03	8.95E-03	8.74E-03
Na-25	6.00E+01	7.03E-16	0.00%	2.11E+00	1.06E+00	2.06E-03	5.29E-09	1.83E-18
Mg-27	5.70E+02	1.02E-15	0.00%	5.00E-01	4.65E-01	2.41E-01	6.22E-02	6.28E-03
Mg-28	7.53E+04	3.03E-16	0.00%	2.24E-03	2.24E-03	2.23E-03	2.21E-03	2.17E-03
Al-26	2.26E+13	1.44E-15	0.00%	1.80E-11	1.80E-11	1.80E-11	1.80E-11	1.80E-11
Al-28	1.34E+02	3.30E-15	0.00%	1.21E+01	8.88E+00	5.48E-01	1.75E-03	1.05E-07
Al-29	3.96E+02	1.83E-15	0.00%	2.00E+00	1.80E+00	6.99E-01	9.94E-02	3.66E-03
Si-31	9.44E+03	1.94E-15	0.00%	6.62E-02	6.59E-02	6.34E-02	5.84E-02	5.08E-02
Si-32	5.46E+09	1.02E-15	0.00%	7.49E-08	7.49E-08	7.49E-08	7.49E-08	7.49E-08
P-30	1.50E+02	1.07E-15	0.00%	2.23E+00	1.69E+00	1.40E-01	8.08E-04	1.32E-07
P-32	1.23E+06	1.10E-14	0.00%	7.72E-03	7.72E-03	7.72E-03	7.71E-03	7.70E-03
P-33	2.19E+06	7.74E-15	0.00%	2.85E-03	2.85E-03	2.85E-03	2.85E-03	2.84E-03
P-35	4.74E+01	8.69E-16	0.00%	9.38E+00	3.90E+00	1.45E-03	1.22E-10	1.29E-22
S-35	7.55E+06	9.91E-15	0.00%	9.44E-04	9.44E-04	9.44E-04	9.44E-04	9.43E-04
S-37	3.04E+02	4.40E-15	0.02%	5.21E+00	4.54E+00	1.32E+00	1.04E-01	1.40E-03
S-38	1.03E+04	2.12E-15	0.00%	9.48E-02	9.44E-02	9.10E-02	8.45E-02	7.44E-02
Cl-34	1.92E+03	4.72E-16	0.00%	2.57E-01	2.52E-01	2.07E-01	1.39E-01	7.02E-02
Cl-36	9.50E+12	2.49E-14	0.01%	2.70E-09	2.70E-09	2.70E-09	2.70E-09	2.70E-09
Cl-38	2.23E+03	1.72E-14	0.01%	6.01E+00	5.90E+00	4.99E+00	3.53E+00	1.97E+00
Cl-39	3.34E+03	3.47E-14	0.01%	6.53E+00	6.44E+00	5.76E+00	4.57E+00	3.09E+00
Cl-40	8.40E+01	3.46E-15	0.02%	2.71E+01	1.65E+01	1.92E-01	1.95E-05	3.41E-12
Ar-37	3.03E+06	4.43E-14	0.01%	8.09E-03	8.09E-03	8.09E-03	8.09E-03	8.08E-03
Ar-39	8.49E+09	1.26E-13	0.02%	9.38E-06	9.38E-06	9.38E-06	9.38E-06	9.38E-06
Ar-41	6.58E+03	1.04E-12	0.02%	2.16E+01	2.14E+01	2.02E+01	1.80E+01	1.48E+01
K-38	4.58E+02	3.09E-16	0.02%	1.63E+00	1.49E+00	6.59E-01	1.22E-01	7.05E-03
K-40	4.04E+16	8.56E-16	0.06%	5.07E-14	5.07E-14	5.07E-14	5.07E-14	5.07E-14

Table 70: Ci values for the isotopes gained by the simulation as well as the comparison of activities after several cooling times (0s, 60s, 600s, 1714.29s, 3600s), after irradiation with a total intensity of $3.43\text{E}+13$ protons, which corresponds to 2.1 air exchanges per hour during continuous irradiation with a 250 MeV proton beam and an intensity of $2\text{E}+10$ protons per second, to their respective Ci value. Calculated Ci values not mentioned in Austrian law are underlined in light blue. Sum values of the comparison values after the listed cooling times are listed at the bottom, underlined in dark blue.

Isotope	t 1/2 [s]	Ci	0s	60s	600s	1714.29s	3600s
H-3	3.89E+08	100.0	2.55E-05	2.55E-05	2.55E-05	2.55E-05	2.55E-05
Be-7	4.61E+06	600.0	2.37E-04	2.37E-04	2.37E-04	2.36E-04	2.36E-04
Be-10	5.05E+13	1.0	5.93E-09	5.93E-09	5.93E-09	5.93E-09	5.93E-09
C-11	1.22E+03	600.0	1.47E+00	1.42E+00	1.04E+00	5.55E-01	1.91E-01
C-14	1.81E+11	6.0	6.23E-05	6.23E-05	6.23E-05	6.23E-05	6.23E-05
N-13	5.98E+02	2000.0	1.50E+00	1.40E+00	7.48E-01	2.06E-01	2.31E-02
O-14	7.10E+01	927.1	2.24E+00	1.25E+00	6.40E-03	1.21E-07	1.22E-15
O-15	1.22E+02	1000.0	1.24E+01	8.85E+00	4.14E-01	7.47E-04	1.70E-08
O-19	2.71E+01	1916.0	1.35E-04	2.92E-05	2.93E-11	1.23E-23	1.39E-44
F-18	6.59E+03	500.0	2.05E-04	2.04E-04	1.92E-04	1.71E-04	1.40E-04
Ne-23	2.80E+01	1892.7	8.52E-04	1.93E-04	3.02E-10	3.16E-22	1.68E-42
Ne-24	2.03E+02	896.3	2.92E-05	2.37E-05	3.75E-06	8.32E-08	1.32E-10
Na-22	8.21E+07	1.0	4.11E-06	4.11E-06	4.11E-06	4.11E-06	4.11E-06
Na-24	5.40E+04	90.0	1.02E-04	1.02E-04	1.01E-04	9.95E-05	9.71E-05
Na-25	6.00E+01	28648.2	7.37E-05	3.68E-05	7.20E-08	1.85E-13	6.39E-23
Mg-27	5.70E+02	577.8	8.66E-04	8.05E-04	4.17E-04	1.08E-04	1.09E-05
Mg-28	7.53E+04	20.0	1.12E-04	1.12E-04	1.12E-04	1.10E-04	1.09E-04
Al-26	2.26E+13	0.5	3.60E-11	3.60E-11	3.60E-11	3.60E-11	3.60E-11
Al-28	1.34E+02	537.6	2.25E-02	1.65E-02	1.02E-03	3.25E-06	1.94E-10
Al-29	3.96E+02	232.5	8.60E-03	7.74E-03	3.01E-03	4.28E-04	1.58E-05
Si-31	9.44E+03	300.0	2.21E-04	2.20E-04	2.11E-04	1.95E-04	1.69E-04
Si-32	5.46E+09	0.3	2.34E-07	2.34E-07	2.34E-07	2.34E-07	2.34E-07
P-30	1.50E+02	2727.8	8.19E-04	6.21E-04	5.11E-05	2.96E-07	4.85E-11
P-32	1.23E+06	1.0	7.72E-03	7.72E-03	7.72E-03	7.71E-03	7.70E-03
P-33	2.19E+06	20.0	1.42E-04	1.42E-04	1.42E-04	1.42E-04	1.42E-04
P-35	4.74E+01	12148.0	7.72E-04	3.21E-04	1.19E-07	1.00E-14	1.06E-26
S-35	7.55E+06	20.0	4.72E-05	4.72E-05	4.72E-05	4.72E-05	4.72E-05
S-37	3.04E+02	8682.3	6.00E-04	5.23E-04	1.52E-04	1.20E-05	1.62E-07
S-38	1.03E+04	422.8	2.24E-04	2.23E-04	2.15E-04	2.00E-04	1.76E-04
Cl-34	1.92E+03	16.8	1.53E-02	1.50E-02	1.23E-02	8.23E-03	4.17E-03
Cl-36	9.50E+12	0.1	2.70E-08	2.70E-08	2.70E-08	2.70E-08	2.70E-08
Cl-38	2.23E+03	500.0	1.20E-02	1.18E-02	9.98E-03	7.06E-03	3.93E-03
Cl-39	3.34E+03	600.0	1.09E-02	1.07E-02	9.60E-03	7.62E-03	5.15E-03
Cl-40	8.40E+01	292.7	9.27E-02	5.65E-02	6.56E-04	6.66E-08	1.16E-14
Ar-37	3.03E+06	200000000.0	4.04E-11	4.04E-11	4.04E-11	4.04E-11	4.04E-11
Ar-39	8.49E+09	6000.0	1.56E-09	1.56E-09	1.56E-09	1.56E-09	1.56E-09
Ar-41	6.58E+03	200.0	1.08E-01	1.07E-01	1.01E-01	9.00E-02	7.38E-02
K-38	4.58E+02	4622.1	3.54E-04	3.23E-04	1.43E-04	2.64E-05	1.52E-06
K-40	4.04E+16	0.3	1.62E-13	1.62E-13	1.62E-13	1.62E-13	1.62E-13
Sum:			1.79E+01	1.32E+01	2.36E+00	8.84E-01	3.10E-01

Table 71: Activity of the air after irradiation of a water target with a 250 MeV proton beam, compared to Ci values, considering a cooling time of 1 hour and thinning the air to a volume of 14.000 m³ at average (2.12E+8 particles per second) and maximum (2E+10 particles per second) intensity

Isotope	Bq (total/y)	av. sp. act.	max. sp. act.	Ci [Bq/m ³]	av./Ci	max./Ci
H-3	9.82E+02	8.01E-06	7.54E-04	100.00	8.01E-08	7.54E-06
Be-7	5.46E+04	4.45E-04	4.19E-02	600.00	7.42E-07	6.99E-05
Be-10	2.28E-03	1.86E-11	1.75E-09	1.00	1.86E-11	1.75E-09
C-11	3.39E+08	3.59E-01	3.38E+01	600.00	5.99E-04	5.63E-02
C-14	1.44E+02	1.17E-06	1.10E-04	6.00	1.95E-07	1.84E-05
N-13	1.16E+09	1.45E-01	1.37E+01	2000.00	7.25E-05	6.83E-03
O-14	7.99E+08	3.55E-15	3.34E-13	927.09	3.83E-18	3.61E-16
O-15	4.79E+09	5.32E-08	5.01E-06	1000.00	5.32E-11	5.01E-09
O-19	9.99E+04	8.35E-44	7.86E-42	1916.02	4.36E-47	4.10E-45
F-18	3.95E+04	2.20E-04	2.07E-02	500.00	4.40E-07	4.15E-05
Ne-23	6.21E+05	1.00E-41	9.42E-40	1892.75	5.29E-45	4.98E-43
Ne-24	1.01E+04	3.72E-10	3.50E-08	896.31	4.15E-13	3.90E-11
Na-22	1.58E+00	1.29E-08	1.21E-06	1.00	1.29E-08	1.21E-06
Na-24	3.52E+03	2.74E-05	2.58E-03	90.00	3.05E-07	2.87E-05
Na-25	8.13E+05	5.75E-21	5.41E-19	28648.19	2.01E-25	1.89E-23
Mg-27	1.93E+05	1.97E-05	1.86E-03	577.79	3.41E-08	3.21E-06
Mg-28	8.64E+02	6.82E-06	6.42E-04	20.00	3.41E-07	3.21E-05
Al-26	6.92E-06	5.65E-14	5.31E-12	0.50	1.13E-13	1.06E-11
Al-28	4.66E+06	3.28E-10	3.09E-08	537.59	6.10E-13	5.75E-11
Al-29	7.69E+05	1.15E-05	1.08E-03	232.45	4.95E-08	4.66E-06
Si-31	2.55E+04	1.60E-04	1.50E-02	300.00	5.32E-07	5.01E-05
Si-32	2.88E-02	2.35E-10	2.21E-08	0.32	7.35E-10	6.92E-08
P-30	8.60E+05	4.15E-10	3.91E-08	2727.82	1.52E-13	1.43E-11
P-32	2.97E+03	2.42E-05	2.28E-03	1.00	2.42E-05	2.28E-03
P-33	1.10E+03	8.93E-06	8.41E-04	20.00	4.46E-07	4.20E-05
P-35	3.61E+06	4.03E-25	3.80E-23	12148.03	3.32E-29	3.13E-27
S-35	3.63E+02	2.96E-06	2.79E-04	20.00	1.48E-07	1.39E-05
S-37	2.00E+06	4.40E-06	4.14E-04	8682.34	5.07E-10	4.77E-08
S-38	3.65E+04	2.34E-04	2.20E-02	422.83	5.53E-07	5.20E-05
Cl-34	9.91E+04	2.20E-04	2.07E-02	16.84	1.31E-05	1.23E-03
Cl-36	1.04E-03	8.48E-12	7.98E-10	0.10	8.48E-11	7.98E-09
Cl-38	2.32E+06	6.17E-03	5.81E-01	500.00	1.23E-05	1.16E-03
Cl-39	2.51E+06	9.70E-03	9.13E-01	600.00	1.62E-05	1.52E-03
Cl-40	1.04E+07	1.07E-14	1.01E-12	292.72	3.65E-17	3.44E-15
Ar-37	3.11E+03	2.54E-05	2.39E-03	20000000.00	1.27E-13	1.19E-11
Ar-39	3.61E+00	2.94E-08	2.77E-06	6000.00	4.91E-12	4.62E-10
Ar-41	8.30E+06	4.63E-02	4.36E+00	200.00	2.32E-04	2.18E-02
K-38	6.29E+05	2.21E-05	2.08E-03	4622.10	4.78E-09	4.50E-07
K-40	1.95E-08	1.59E-16	1.50E-14	0.31	5.08E-16	4.78E-14
Sum:					9.72E-04	9.15E-02

HORIZONTAL BEAM DUMP (BDH) – 800 MEV PROTONS

Table 72: Scored yields of radioactive isotopes and calculated activity of the air after irradiation of the tungsten dump with an 800 MeV proton beam, compared to Ci values, considering a cooling time of 10 minutes at average (7.61E+6 particles per second) and maximum (2E+10 particles per second) intensity

Isotope	yield/pp/cm ³	rel.err.	av.sp.act.	max.sp.act.	Ci [Bq/m ³]	av./Ci	max./Ci
H-3	9.31E-14	0.02%	3.85E-06	1.01E-02	100.00	3.85E-08	1.01E-04
Be-7	1.16E-14	0.03%	4.06E-05	1.07E-01	600.00	6.77E-08	1.78E-04
Be-10	1.98E-14	0.03%	6.33E-12	1.66E-08	1.00	6.33E-12	1.66E-08
C-11	2.11E-14	0.03%	1.98E-01	5.20E+02	600.00	3.30E-04	8.67E-01
C-14	3.54E-11	0.02%	3.16E-06	8.30E-03	6.00	5.26E-07	1.38E-03
N-13	4.88E-14	0.02%	6.56E-01	1.72E+03	2000.00	3.28E-04	8.62E-01
O-14	2.60E-15	0.05%	1.69E-03	4.43E+00	927.09	1.82E-06	4.78E-03
O-15	2.92E-14	0.03%	1.28E-01	3.37E+02	1000.00	1.28E-04	3.37E-01
O-19	3.46E-19	0.02%	4.45E-11	1.17E-07	1916.02	2.32E-14	6.11E-11
F-18	1.48E-17	0.02%	3.40E-05	8.94E-02	500.00	6.80E-08	1.79E-04
Ne-23	1.26E-18	0.02%	2.57E-10	6.75E-07	1892.75	1.36E-13	3.57E-10
Ne-24	2.03E-19	0.02%	2.08E-06	5.45E-03	896.31	2.32E-09	6.09E-06
Na-22	5.21E-18	0.02%	1.02E-09	2.69E-06	1.00	1.02E-09	2.69E-06
Na-24	8.92E-18	0.02%	2.64E-06	6.94E-03	90.00	2.94E-08	7.72E-05
Na-25	2.78E-18	0.02%	7.29E-07	1.92E-03	2.86E+04	2.55E-11	6.69E-08
Mg-27	5.12E-18	0.02%	6.98E-05	1.83E-01	577.79	1.21E-07	3.17E-04
Mg-28	2.53E-18	0.02%	5.39E-07	1.42E-03	20.00	2.69E-08	7.08E-05
Al-26	7.39E-18	0.02%	5.27E-15	1.39E-11	0.50	1.05E-14	2.77E-11
Al-28	2.44E-17	0.02%	1.33E-04	3.48E-01	537.59	2.47E-07	6.48E-04
Al-29	1.21E-17	0.02%	1.72E-04	4.53E-01	232.45	7.41E-07	1.95E-03
Si-31	1.33E-17	0.02%	2.17E-05	5.71E-02	300.00	7.25E-08	1.90E-04
Si-32	8.85E-18	0.02%	2.61E-11	6.87E-08	0.32	8.17E-11	2.15E-07
P-30	5.62E-18	0.02%	3.77E-05	9.91E-02	2727.82	1.38E-08	3.63E-05
P-32	1.83E-16	0.03%	2.39E-06	6.28E-03	1.00	2.39E-06	6.28E-03
P-33	1.50E-16	0.02%	1.10E-06	2.89E-03	20.00	5.51E-08	1.45E-04
P-35	1.52E-17	0.02%	8.00E-07	2.10E-03	1.21E+04	6.58E-11	1.73E-07
S-35	2.13E-16	0.03%	4.54E-07	1.19E-03	20.00	2.27E-08	5.97E-05
S-37	1.77E-16	0.03%	2.39E-03	6.28E+00	8682.34	2.75E-07	7.23E-04
S-38	3.69E-17	0.02%	5.53E-05	1.45E-01	422.83	1.31E-07	3.44E-04
Cl-34	6.43E-18	0.03%	4.35E-05	1.14E-01	16.84	2.58E-06	6.78E-03
Cl-36	6.66E-16	0.02%	1.13E-12	2.97E-09	0.10	1.13E-11	2.97E-08
Cl-38	4.92E-16	0.02%	2.95E-03	7.75E+00	500.00	5.90E-06	1.55E-02
Cl-39	8.47E-16	0.02%	3.61E-03	9.49E+00	600.00	6.02E-06	1.58E-02
Cl-40	2.08E-16	0.02%	2.82E-04	7.42E-01	292.72	9.65E-07	2.54E-03
Ar-37	2.49E-15	0.02%	1.33E-05	3.49E-02	2.00E+08	6.63E-14	1.74E-10
Ar-39	5.95E-15	0.02%	1.13E-08	2.97E-05	6000.00	1.88E-12	4.95E-09
Ar-41	7.42E-14	0.02%	1.71E-01	4.49E+02	200.00	8.53E-04	2.24E+00
K-38	1.08E-17	0.06%	1.53E-04	4.03E-01	4622.10	3.32E-08	8.72E-05
K-40	4.77E-17	0.06%	1.90E-17	5.00E-14	0.31	6.08E-17	1.60E-13
Sum:						1.66E-03	4.37E+00

HORIZONTAL BEAM DUMP (BDH) – 400 MEV CARBON IONS

Table 73: Scored yields of radioactive isotopes and calculated activity of the air after irradiation of the tungsten dump with a 400 MeV carbon ion beam, compared to Ci values, considering a cooling time of 10 minutes at average (5.71E+6 ions per second) and maximum (1E+9 ions per second) intensity

Isotope	yield/pp/cm ³	rel.err.	av.sp.act.	max.sp.act.	Ci [Bq/m ³]	av./Ci	max./Ci
H-3	9.31E-14	0.06%	8.19E-06	1.44E-03	100.00	8.19E-08	1.44E-05
Be-7	1.16E-14	0.06%	5.46E-05	9.57E-03	600.00	9.10E-08	1.59E-05
Be-10	1.98E-14	0.06%	2.02E-11	3.54E-09	1.00	2.02E-11	3.54E-09
C-11	2.11E-14	0.06%	2.96E-01	5.19E+01	600.00	4.94E-04	8.65E-02
C-14	3.54E-11	0.06%	4.72E-06	8.28E-04	6.00	7.87E-07	1.38E-04
N-13	4.88E-14	0.05%	1.40E+00	2.46E+02	2000.00	7.01E-04	1.23E-01
O-14	2.60E-15	0.11%	2.08E-03	3.64E-01	927.09	2.24E-06	3.93E-04
O-15	2.92E-14	0.05%	2.16E-01	3.79E+01	1000.00	2.16E-04	3.79E-02
O-19	3.46E-19	0.12%	9.14E-12	1.60E-09	1916.02	4.77E-15	8.36E-13
F-18	1.48E-17	0.10%	1.81E-05	3.17E-03	500.00	3.62E-08	6.34E-06
Ne-23	1.26E-18	0.10%	7.92E-11	1.39E-08	1892.75	4.19E-14	7.33E-12
Ne-24	2.03E-19	0.11%	5.05E-07	8.84E-05	896.31	5.63E-10	9.86E-08
Na-22	5.21E-18	0.08%	5.54E-10	9.70E-08	1.00	5.54E-10	9.70E-08
Na-24	8.92E-18	0.07%	1.52E-06	2.67E-04	90.00	1.69E-08	2.97E-06
Na-25	2.78E-18	0.09%	2.79E-07	4.90E-05	2.86E+04	9.75E-12	1.71E-09
Mg-27	5.12E-18	0.08%	3.33E-05	5.84E-03	577.79	5.77E-08	1.01E-05
Mg-28	2.53E-18	0.07%	3.82E-07	6.69E-05	20.00	1.91E-08	3.34E-06
Al-26	7.39E-18	0.09%	2.46E-15	4.30E-13	0.50	4.91E-15	8.61E-13
Al-28	2.44E-17	0.08%	8.15E-05	1.43E-02	537.59	1.52E-07	2.66E-05
Al-29	1.21E-17	0.08%	1.04E-04	1.82E-02	232.45	4.47E-07	7.83E-05
Si-31	1.33E-17	0.06%	1.91E-05	3.35E-03	300.00	6.37E-08	1.12E-05
Si-32	8.85E-18	0.06%	2.81E-11	4.93E-09	0.32	8.79E-11	1.54E-08
P-30	5.62E-18	0.09%	1.58E-05	2.77E-03	2727.82	5.79E-09	1.02E-06
P-32	1.83E-16	0.06%	2.93E-06	5.13E-04	1.00	2.93E-06	5.13E-04
P-33	1.50E-16	0.05%	1.69E-06	2.96E-04	20.00	8.45E-08	1.48E-05
P-35	1.52E-17	0.05%	1.49E-06	2.61E-04	1.21E+04	1.23E-10	2.15E-08
S-35	2.13E-16	0.05%	9.39E-07	1.65E-04	20.00	4.70E-08	8.23E-06
S-37	1.77E-16	0.07%	4.40E-03	7.71E-01	8682.34	5.07E-07	8.88E-05
S-38	3.69E-17	0.05%	9.85E-05	1.72E-02	422.83	2.33E-07	4.08E-05
Cl-34	6.43E-18	0.07%	3.81E-05	6.68E-03	16.84	2.26E-06	3.97E-04
Cl-36	6.66E-16	0.05%	1.92E-12	3.37E-10	0.10	1.92E-11	3.37E-09
Cl-38	4.92E-16	0.05%	7.28E-03	1.28E+00	500.00	1.46E-05	2.55E-03
Cl-39	8.47E-16	0.05%	8.96E-03	1.57E+00	600.00	1.49E-05	2.62E-03
Cl-40	2.08E-16	0.05%	8.24E-04	1.44E-01	292.72	2.81E-06	4.93E-04
Ar-37	2.49E-15	0.06%	2.20E-05	3.85E-03	2.00E+08	1.10E-13	1.92E-11
Ar-39	5.95E-15	0.05%	2.93E-08	5.14E-06	6000.00	4.89E-12	8.57E-10
Ar-41	7.42E-14	0.06%	2.54E-01	4.44E+01	200.00	1.27E-03	2.22E-01
K-38	1.08E-17	0.17%	1.49E-04	2.61E-02	4622.10	3.22E-08	5.65E-06
K-40	4.77E-17	0.15%	2.75E-17	4.82E-15	0.31	8.80E-17	1.54E-14
Sum:						2.72E-03	4.77E-01

HORIZONTAL BEAM DUMP (BDH) – 250 MEV PROTONS

Table 74: Scored yields of radioactive isotopes and calculated activity of the air after irradiation of the tungsten dump with a 250 MeV proton beam, compared to Ci values, considering a cooling time of 10 minutes at average (4.76E+7 particles per second) and maximum (2E+10 particles per second) intensity

Isotope	yield/pp/cm ³	rel.err.	av.sp.act.	max.sp.act.	Ci [Bq/m ³]	av./Ci	max./Ci
H-3	9.31E-14	0.04%	4.11E-06	1.73E-03	100.00	4.11E-08	1.73E-05
Be-7	1.16E-14	0.10%	4.27E-05	1.79E-02	600.00	7.11E-08	2.99E-05
Be-10	1.98E-14	0.09%	6.57E-12	2.76E-09	1.00	6.57E-12	2.76E-09
C-11	2.11E-14	0.11%	2.08E-01	8.73E+01	600.00	3.46E-04	1.45E-01
C-14	3.54E-11	0.02%	4.29E-06	1.81E-03	6.00	7.15E-07	3.01E-04
N-13	4.88E-14	0.04%	7.16E-01	3.01E+02	2000.00	3.58E-04	1.51E-01
O-14	2.60E-15	0.16%	3.14E-03	1.32E+00	927.09	3.39E-06	1.42E-03
O-15	2.92E-14	0.07%	1.29E-01	5.43E+01	1000.00	1.29E-04	5.43E-02
O-19	3.46E-19	0.16%	6.61E-13	2.78E-10	1916.02	3.45E-16	1.45E-13
F-18	1.48E-17	0.18%	1.91E-05	8.03E-03	500.00	3.82E-08	1.61E-05
Ne-23	1.26E-18	0.15%	9.88E-12	4.15E-09	1892.75	5.22E-15	2.19E-12
Ne-24	2.03E-19	0.15%	4.97E-08	2.09E-05	896.31	5.55E-11	2.33E-08
Na-22	5.21E-18	0.16%	1.36E-10	5.73E-08	1.00	1.36E-10	5.73E-08
Na-24	8.92E-18	0.11%	4.39E-07	1.84E-04	90.00	4.88E-09	2.05E-06
Na-25	2.78E-18	0.14%	4.51E-08	1.90E-05	2.86E+04	1.57E-12	6.62E-10
Mg-27	5.12E-18	0.13%	6.90E-06	2.90E-03	577.79	1.19E-08	5.02E-06
Mg-28	2.53E-18	0.10%	1.15E-07	4.85E-05	20.00	5.76E-09	2.42E-06
Al-26	7.39E-18	0.14%	4.95E-16	2.08E-13	0.50	9.90E-16	4.16E-13
Al-28	2.44E-17	0.12%	2.16E-05	9.08E-03	537.59	4.02E-08	1.69E-05
Al-29	1.21E-17	0.12%	2.71E-05	1.14E-02	232.45	1.17E-07	4.91E-05
Si-31	1.33E-17	0.09%	6.26E-06	2.63E-03	300.00	2.09E-08	8.78E-06
Si-32	8.85E-18	0.07%	9.57E-12	4.02E-09	0.32	2.99E-11	1.26E-08
P-30	5.62E-18	0.13%	5.70E-06	2.40E-03	2727.82	2.09E-09	8.79E-07
P-32	1.83E-16	0.07%	1.52E-06	6.38E-04	1.00	1.52E-06	6.38E-04
P-33	1.50E-16	0.07%	7.30E-07	3.07E-04	20.00	3.65E-08	1.53E-05
P-35	1.52E-17	0.05%	5.13E-07	2.16E-04	1.21E+04	4.22E-11	1.78E-08
S-35	2.13E-16	0.02%	3.41E-07	1.44E-04	20.00	1.71E-08	7.18E-06
S-37	1.77E-16	0.05%	2.40E-03	1.01E+00	8682.34	2.77E-07	1.16E-04
S-38	3.69E-17	0.08%	3.21E-05	1.35E-02	422.83	7.60E-08	3.19E-05
Cl-34	6.43E-18	0.11%	2.70E-05	1.14E-02	16.84	1.61E-06	6.75E-04
Cl-36	6.66E-16	0.06%	1.01E-12	4.26E-10	0.10	1.01E-11	4.26E-09
Cl-38	4.92E-16	0.02%	2.46E-03	1.04E+00	500.00	4.93E-06	2.07E-03
Cl-39	8.47E-16	0.03%	3.04E-03	1.28E+00	600.00	5.07E-06	2.13E-03
Cl-40	2.08E-16	0.05%	3.08E-04	1.30E-01	292.72	1.05E-06	4.42E-04
Ar-37	2.49E-15	0.02%	1.71E-05	7.18E-03	2.00E+08	8.54E-14	3.59E-11
Ar-39	5.95E-15	0.07%	1.34E-08	5.64E-06	6000.00	2.24E-12	9.40E-10
Ar-41	7.42E-14	0.02%	2.31E-01	9.73E+01	200.00	1.16E-03	4.87E-01
K-38	1.08E-17	0.12%	2.95E-04	1.24E-01	4622.10	6.39E-08	2.69E-05
K-40	4.77E-17	0.19%	4.86E-17	2.04E-14	0.31	1.55E-16	6.53E-14
Sum:						2.01E-03	8.45E-01

ELECTROSTATIC SEPTUM (ESE) – 800 MEV PROTONS

Table 75: Scored yields of radioactive isotopes and calculated activity of the air after irradiation of the molybdenum foil with an 800 MeV proton beam, compared to Ci values, considering a cooling time of 10 minutes at average (9.20E+6 particles per second) and maximum (2E+10 particles per second) intensity

Isotope	yield/pp/cm ³	rel.err.	av.sp.act.	max.sp.act.	Ci [Bq/m ³]	av./Ci	max./Ci
H-3	9.31E-14	0.02%	5.20E-06	1.13E-02	100.00	5.20E-08	1.13E-04
Be-7	1.16E-14	0.02%	1.20E-04	2.60E-01	600.00	1.99E-07	4.34E-04
Be-10	1.98E-14	0.03%	9.46E-12	2.06E-08	1.00	9.46E-12	2.06E-08
C-11	2.11E-14	0.02%	5.54E-01	1.21E+03	600.00	9.24E-04	2.01E+00
C-14	3.54E-11	0.02%	1.78E-06	3.87E-03	6.00	2.96E-07	6.45E-04
N-13	4.88E-14	0.02%	1.47E+00	3.21E+03	2000.00	7.37E-04	1.60E+00
O-14	2.60E-15	0.03%	5.42E-03	1.18E+01	927.09	5.84E-06	1.27E-02
O-15	2.92E-14	0.02%	3.46E-01	7.52E+02	1000.00	3.46E-04	7.52E-01
O-19	3.46E-19	0.02%	1.79E-10	3.89E-07	1916.02	9.33E-14	2.03E-10
F-18	1.48E-17	0.02%	1.27E-04	2.77E-01	500.00	2.55E-07	5.54E-04
Ne-23	1.26E-18	0.02%	1.01E-09	2.20E-06	1892.75	5.35E-13	1.16E-09
Ne-24	2.03E-19	0.02%	8.28E-06	1.80E-02	896.31	9.24E-09	2.01E-05
Na-22	5.21E-18	0.02%	3.72E-09	8.10E-06	1.00	3.72E-09	8.10E-06
Na-24	8.92E-18	0.02%	9.56E-06	2.08E-02	90.00	1.06E-07	2.31E-04
Na-25	2.78E-18	0.02%	2.82E-06	6.12E-03	2.86E+04	9.83E-11	2.14E-07
Mg-27	5.12E-18	0.02%	2.62E-04	5.70E-01	577.79	4.53E-07	9.86E-04
Mg-28	2.53E-18	0.02%	1.89E-06	4.11E-03	20.00	9.44E-08	2.05E-04
Al-26	7.39E-18	0.02%	1.98E-14	4.31E-11	0.50	3.97E-14	8.62E-11
Al-28	2.44E-17	0.02%	4.73E-04	1.03E+00	537.59	8.80E-07	1.91E-03
Al-29	1.21E-17	0.02%	6.23E-04	1.35E+00	232.45	2.68E-06	5.83E-03
Si-31	1.33E-17	0.02%	6.89E-05	1.50E-01	300.00	2.30E-07	5.00E-04
Si-32	8.85E-18	0.02%	7.78E-11	1.69E-07	0.32	2.43E-10	5.29E-07
P-30	5.62E-18	0.02%	1.39E-04	3.03E-01	2727.82	5.11E-08	1.11E-04
P-32	1.83E-16	0.02%	6.78E-06	1.47E-02	1.00	6.78E-06	1.47E-02
P-33	1.50E-16	0.02%	2.81E-06	6.12E-03	20.00	1.41E-07	3.06E-04
P-35	1.52E-17	0.02%	1.87E-06	4.06E-03	1.21E+04	1.54E-10	3.35E-07
S-35	2.13E-16	0.02%	1.03E-06	2.24E-03	20.00	5.16E-08	1.12E-04
S-37	1.77E-16	0.02%	3.18E-03	6.91E+00	8682.34	3.66E-07	7.96E-04
S-38	3.69E-17	0.02%	1.28E-04	2.78E-01	422.83	3.03E-07	6.58E-04
Cl-34	6.43E-18	0.02%	1.40E-04	3.04E-01	16.84	8.30E-06	1.80E-02
Cl-36	6.66E-16	0.02%	2.56E-12	5.57E-09	0.10	2.56E-11	5.57E-08
Cl-38	4.92E-16	0.02%	5.86E-03	1.27E+01	500.00	1.17E-05	2.55E-02
Cl-39	8.47E-16	0.02%	7.06E-03	1.54E+01	600.00	1.18E-05	2.56E-02
Cl-40	2.08E-16	0.02%	3.74E-04	8.14E-01	292.72	1.28E-06	2.78E-03
Ar-37	2.49E-15	0.02%	1.22E-05	2.65E-02	2.00E+08	6.08E-14	1.32E-10
Ar-39	5.95E-15	0.03%	1.54E-08	3.35E-05	6000.00	2.57E-12	5.59E-09
Ar-41	7.42E-14	0.02%	9.48E-02	2.06E+02	200.00	4.74E-04	1.03E+00
K-38	1.08E-17	0.04%	5.20E-04	1.13E+00	4622.10	1.12E-07	2.45E-04
K-40	4.77E-17	0.04%	5.93E-17	1.29E-13	0.31	1.90E-16	4.12E-13
Sum:						2.53E-03	5.51E+00

ELECTROSTATIC SEPTUM (ESE) – 400 MEV CARBON IONS

Table 76: Scored yields of radioactive isotopes and calculated activity of the air after irradiation of the molybdenum foil with a 400 MeV carbon ion beam, compared to Ci values, considering a cooling time of 10 minutes at average (9.51E+5 ions per second) and maximum (1E+9 ions per second) intensity

Isotope	yield/pp/cm ³	rel.err.	av.sp.act.	max.sp.act.	Ci [Bq/m ³]	av./Ci	max./Ci
H-3	9.31E-14	0.05%	1.64E-06	1.72E-03	100.00	1.64E-08	1.72E-05
Be-7	1.16E-14	0.05%	2.77E-05	2.92E-02	600.00	4.62E-08	4.86E-05
Be-10	1.98E-14	0.05%	4.63E-12	4.87E-09	1.00	4.63E-12	4.87E-09
C-11	2.11E-14	0.05%	1.40E-01	1.47E+02	600.00	2.33E-04	2.44E-01
C-14	3.54E-11	0.04%	3.82E-07	4.02E-04	6.00	6.37E-08	6.70E-05
N-13	4.88E-14	0.05%	4.71E-01	4.95E+02	2000.00	2.35E-04	2.47E-01
O-14	2.60E-15	0.05%	1.36E-03	1.43E+00	927.09	1.47E-06	1.55E-03
O-15	2.92E-14	0.05%	9.11E-02	9.58E+01	1000.00	9.11E-05	9.58E-02
O-19	3.46E-19	0.10%	1.06E-11	1.11E-08	1916.02	5.52E-15	5.80E-12
F-18	1.48E-17	0.07%	1.48E-05	1.56E-02	500.00	2.97E-08	3.12E-05
Ne-23	1.26E-18	0.09%	8.18E-11	8.60E-08	1892.75	4.32E-14	4.55E-11
Ne-24	2.03E-19	0.10%	5.53E-07	5.82E-04	896.31	6.17E-10	6.49E-07
Na-22	5.21E-18	0.08%	4.69E-10	4.93E-07	1.00	4.69E-10	4.93E-07
Na-24	8.92E-18	0.08%	1.21E-06	1.27E-03	90.00	1.35E-08	1.41E-05
Na-25	2.78E-18	0.09%	2.70E-07	2.83E-04	2.86E+04	9.41E-12	9.89E-09
Mg-27	5.12E-18	0.08%	2.98E-05	3.13E-02	577.79	5.16E-08	5.43E-05
Mg-28	2.53E-18	0.07%	2.90E-07	3.05E-04	20.00	1.45E-08	1.52E-05
Al-26	7.39E-18	0.08%	2.22E-15	2.33E-12	0.50	4.44E-15	4.67E-12
Al-28	2.44E-17	0.08%	6.61E-05	6.95E-02	537.59	1.23E-07	1.29E-04
Al-29	1.21E-17	0.08%	8.51E-05	8.94E-02	232.45	3.66E-07	3.85E-04
Si-31	1.33E-17	0.06%	1.14E-05	1.20E-02	300.00	3.81E-08	4.00E-05
Si-32	8.85E-18	0.06%	1.51E-11	1.58E-08	0.32	4.71E-11	4.95E-08
P-30	5.62E-18	0.08%	1.47E-05	1.54E-02	2727.82	5.38E-09	5.66E-06
P-32	1.83E-16	0.05%	1.59E-06	1.67E-03	1.00	1.59E-06	1.67E-03
P-33	1.50E-16	0.05%	7.60E-07	7.99E-04	20.00	3.80E-08	3.99E-05
P-35	1.52E-17	0.05%	5.71E-07	6.00E-04	1.21E+04	4.70E-11	4.94E-08
S-35	2.13E-16	0.05%	3.31E-07	3.48E-04	20.00	1.65E-08	1.74E-05
S-37	1.77E-16	0.04%	8.70E-04	9.15E-01	8682.34	1.00E-07	1.05E-04
S-38	3.69E-17	0.05%	3.97E-05	4.17E-02	422.83	9.39E-08	9.87E-05
Cl-34	6.43E-18	0.06%	2.69E-05	2.82E-02	16.84	1.60E-06	1.68E-03
Cl-36	6.66E-16	0.04%	7.55E-13	7.94E-10	0.10	7.55E-12	7.94E-09
Cl-38	4.92E-16	0.04%	2.24E-03	2.35E+00	500.00	4.48E-06	4.71E-03
Cl-39	8.47E-16	0.04%	2.61E-03	2.75E+00	600.00	4.35E-06	4.58E-03
Cl-40	2.08E-16	0.05%	1.77E-04	1.86E-01	292.72	6.03E-07	6.34E-04
Ar-37	2.49E-15	0.04%	3.47E-06	3.65E-03	2.00E+08	1.73E-14	1.82E-11
Ar-39	5.95E-15	0.05%	5.86E-09	6.16E-06	6000.00	9.77E-13	1.03E-09
Ar-41	7.42E-14	0.04%	2.04E-02	2.14E+01	200.00	1.02E-04	1.07E-01
K-38	1.08E-17	0.06%	1.24E-04	1.30E-01	4622.10	2.68E-08	2.82E-05
K-40	4.77E-17	0.05%	1.75E-17	1.84E-14	0.31	5.59E-17	5.88E-14
Sum:						6.76E-04	7.11E-01

ELECTROSTATIC SEPTUM (ESE) – 250 MEV PROTONS

Table 77: Scored yields of radioactive isotopes and calculated activity of the air after irradiation of the molybdenum foil with a 250 MeV proton beam, compared to Ci values, considering a cooling time of 10 minutes at average (7.93E+6 particles per second) and maximum (2E+10 particles per second) intensity

Isotope	yield/pp/cm ³	rel.err.	av.sp.act.	max.sp.act.	Ci [Bq/m ³]	av./Ci	max./Ci
H-3	9.31E-14	0.03%	8.71E-07	2.20E-03	100.00	8.71E-09	2.20E-05
Be-7	1.16E-14	0.03%	3.49E-05	8.79E-02	600.00	5.81E-08	1.47E-04
Be-10	1.98E-14	0.06%	1.53E-12	3.85E-09	1.00	1.53E-12	3.85E-09
C-11	2.11E-14	0.03%	1.53E-01	3.87E+02	600.00	2.56E-04	6.45E-01
C-14	3.54E-11	0.05%	3.50E-07	8.84E-04	6.00	5.84E-08	1.47E-04
N-13	4.88E-14	0.03%	4.10E-01	1.04E+03	2000.00	2.05E-04	5.18E-01
O-14	2.60E-15	0.04%	2.72E-03	6.86E+00	927.09	2.93E-06	7.39E-03
O-15	2.92E-14	0.03%	9.51E-02	2.40E+02	1000.00	9.51E-05	2.40E-01
O-19	3.46E-19	0.07%	3.86E-13	9.74E-10	1916.02	2.01E-16	5.08E-13
F-18	1.48E-17	0.04%	1.61E-05	4.05E-02	500.00	3.21E-08	8.10E-05
Ne-23	1.26E-18	0.05%	6.18E-12	1.56E-08	1892.75	3.27E-15	8.24E-12
Ne-24	2.03E-19	0.06%	3.04E-08	7.66E-05	896.31	3.39E-11	8.54E-08
Na-22	5.21E-18	0.05%	9.10E-11	2.30E-07	1.00	9.10E-11	2.30E-07
Na-24	8.92E-18	0.03%	2.99E-07	7.54E-04	90.00	3.32E-09	8.37E-06
Na-25	2.78E-18	0.04%	2.90E-08	7.31E-05	2.86E+04	1.01E-12	2.55E-09
Mg-27	5.12E-18	0.04%	4.56E-06	1.15E-02	577.79	7.89E-09	1.99E-05
Mg-28	2.53E-18	0.02%	7.76E-08	1.96E-04	20.00	3.88E-09	9.79E-06
Al-26	7.39E-18	0.04%	3.25E-16	8.21E-13	0.50	6.51E-16	1.64E-12
Al-28	2.44E-17	0.03%	1.46E-05	3.68E-02	537.59	2.72E-08	6.85E-05
Al-29	1.21E-17	0.03%	1.82E-05	4.60E-02	232.45	7.85E-08	1.98E-04
Si-31	1.33E-17	0.04%	3.66E-06	9.23E-03	300.00	1.22E-08	3.08E-05
Si-32	8.85E-18	0.03%	5.26E-12	1.33E-08	0.32	1.64E-11	4.15E-08
P-30	5.62E-18	0.03%	4.87E-06	1.23E-02	2727.82	1.79E-09	4.51E-06
P-32	1.83E-16	0.02%	1.09E-06	2.74E-03	1.00	1.09E-06	2.74E-03
P-33	1.50E-16	0.03%	4.21E-07	1.06E-03	20.00	2.10E-08	5.31E-05
P-35	1.52E-17	0.04%	2.19E-07	5.52E-04	1.21E+04	1.80E-11	4.54E-08
S-35	2.13E-16	0.03%	1.56E-07	3.94E-04	20.00	7.81E-09	1.97E-05
S-37	1.77E-16	0.04%	4.48E-04	1.13E+00	8682.34	5.16E-08	1.30E-04
S-38	3.69E-17	0.04%	1.20E-05	3.04E-02	422.83	2.85E-08	7.18E-05
Cl-34	6.43E-18	0.03%	2.44E-05	6.16E-02	16.84	1.45E-06	3.66E-03
Cl-36	6.66E-16	0.03%	5.55E-13	1.40E-09	0.10	5.55E-12	1.40E-08
Cl-38	4.92E-16	0.03%	8.99E-04	2.27E+00	500.00	1.80E-06	4.54E-03
Cl-39	8.47E-16	0.03%	9.77E-04	2.47E+00	600.00	1.63E-06	4.11E-03
Cl-40	2.08E-16	0.05%	6.27E-05	1.58E-01	292.72	2.14E-07	5.40E-04
Ar-37	2.49E-15	0.04%	2.97E-06	7.50E-03	2.00E+08	1.49E-14	3.75E-11
Ar-39	5.95E-15	0.06%	3.26E-09	8.23E-06	6000.00	5.44E-13	1.37E-09
Ar-41	7.42E-14	0.05%	1.86E-02	4.70E+01	200.00	9.32E-05	2.35E-01
K-38	1.08E-17	0.05%	3.05E-04	7.68E-01	4622.10	6.59E-08	1.66E-04
K-40	4.77E-17	0.04%	4.16E-17	1.05E-13	0.31	1.33E-16	3.35E-13
Sum:						6.59E-04	1.66E+00

MAGNETIC SEPTUM (MSE) – 800 MEV PROTONS

Table 78: Scored yields of radioactive isotopes and calculated activity of the air after irradiation of the copper target with an 800 MeV proton beam, compared to Ci values, considering a cooling time of 10 minutes at average (9.20E+6 particles per second) and maximum (2E+10 particles per second) intensity

Isotope	yield/pp/cm ³	rel.err.	av.sp.act.	max.sp.act.	Ci [Bq/m ³]	av./Ci	max./Ci
H-3	9.31E-14	0.01%	5.25E-06	1.14E-02	100.00	5.25E-08	1.14E-04
Be-7	1.16E-14	0.01%	1.65E-04	3.60E-01	600.00	2.76E-07	5.99E-04
Be-10	1.98E-14	0.02%	1.00E-11	2.18E-08	1.00	1.00E-11	2.18E-08
C-11	2.11E-14	0.01%	7.49E-01	1.63E+03	600.00	1.25E-03	2.72E+00
C-14	3.54E-11	0.02%	1.37E-06	2.98E-03	6.00	2.28E-07	4.96E-04
N-13	4.88E-14	0.01%	1.85E+00	4.03E+03	2000.00	9.26E-04	2.01E+00
O-14	2.60E-15	0.03%	7.13E-03	1.55E+01	927.09	7.70E-06	1.67E-02
O-15	2.92E-14	0.01%	4.64E-01	1.01E+03	1000.00	4.64E-04	1.01E+00
O-19	3.46E-19	0.03%	3.22E-10	7.00E-07	1916.02	1.68E-13	3.65E-10
F-18	1.48E-17	0.02%	2.12E-04	4.60E-01	500.00	4.23E-07	9.20E-04
Ne-23	1.26E-18	0.02%	1.76E-09	3.83E-06	1892.75	9.30E-13	2.02E-09
Ne-24	2.03E-19	0.03%	1.47E-05	3.20E-02	896.31	1.64E-08	3.57E-05
Na-22	5.21E-18	0.02%	6.07E-09	1.32E-05	1.00	6.07E-09	1.32E-05
Na-24	8.92E-18	0.02%	1.55E-05	3.37E-02	90.00	1.72E-07	3.75E-04
Na-25	2.78E-18	0.02%	4.79E-06	1.04E-02	2.86E+04	1.67E-10	3.63E-07
Mg-27	5.12E-18	0.02%	4.32E-04	9.39E-01	577.79	7.47E-07	1.62E-03
Mg-28	2.53E-18	0.02%	2.93E-06	6.38E-03	20.00	1.47E-07	3.19E-04
Al-26	7.39E-18	0.02%	3.26E-14	7.09E-11	0.50	6.52E-14	1.42E-10
Al-28	2.44E-17	0.02%	7.42E-04	1.61E+00	537.59	1.38E-06	3.00E-03
Al-29	1.21E-17	0.02%	9.89E-04	2.15E+00	232.45	4.26E-06	9.26E-03
Si-31	1.33E-17	0.02%	1.05E-04	2.28E-01	300.00	3.50E-07	7.60E-04
Si-32	8.85E-18	0.02%	1.15E-10	2.50E-07	0.32	3.59E-10	7.81E-07
P-30	5.62E-18	0.02%	2.25E-04	4.90E-01	2727.82	8.26E-08	1.80E-04
P-32	1.83E-16	0.01%	9.40E-06	2.04E-02	1.00	9.40E-06	2.04E-02
P-33	1.50E-16	0.02%	3.78E-06	8.22E-03	20.00	1.89E-07	4.11E-04
P-35	1.52E-17	0.02%	2.47E-06	5.36E-03	1.21E+04	2.03E-10	4.42E-07
S-35	2.13E-16	0.02%	1.33E-06	2.89E-03	20.00	6.65E-08	1.45E-04
S-37	1.77E-16	0.01%	3.15E-03	6.84E+00	8682.34	3.62E-07	7.88E-04
S-38	3.69E-17	0.02%	1.68E-04	3.66E-01	422.83	3.98E-07	8.65E-04
Cl-34	6.43E-18	0.01%	2.00E-04	4.35E-01	16.84	1.19E-05	2.58E-02
Cl-36	6.66E-16	0.01%	3.24E-12	7.05E-09	0.10	3.24E-11	7.05E-08
Cl-38	4.92E-16	0.02%	7.16E-03	1.56E+01	500.00	1.43E-05	3.12E-02
Cl-39	8.47E-16	0.02%	8.66E-03	1.88E+01	600.00	1.44E-05	3.14E-02
Cl-40	2.08E-16	0.02%	3.61E-04	7.85E-01	292.72	1.23E-06	2.68E-03
Ar-37	2.49E-15	0.01%	1.24E-05	2.69E-02	2.00E+08	6.18E-14	1.34E-10
Ar-39	5.95E-15	0.02%	1.54E-08	3.35E-05	6000.00	2.57E-12	5.59E-09
Ar-41	7.42E-14	0.02%	7.28E-02	1.58E+02	200.00	3.64E-04	7.92E-01
K-38	1.08E-17	0.02%	6.77E-04	1.47E+00	4622.10	1.47E-07	3.19E-04
K-40	4.77E-17	0.04%	7.23E-17	1.57E-13	0.31	2.31E-16	5.03E-13
Sum:						3.07E-03	6.68E+00

MAGNETIC SEPTUM (MSE) – 400 MEV CARBON IONS

Table 79: Scored yields of radioactive isotopes and calculated activity of the air after irradiation of the copper target with a 400 MeV carbon ion beam, compared to Ci values, considering a cooling time of 10 minutes at average (9.51E+5 ions per second) and maximum (1E+9 ions per second) intensity

Isotope	yield/pp/cm ³	rel.err.	av.sp.act.	max.sp.act.	Ci [Bq/m ³]	av./Ci	max./Ci
H-3	9.31E-14	0.03%	1.75E-06	1.84E-03	100.00	1.75E-08	1.84E-05
Be-7	1.16E-14	0.03%	3.74E-05	3.93E-02	600.00	6.23E-08	6.55E-05
Be-10	1.98E-14	0.03%	5.03E-12	5.29E-09	1.00	5.03E-12	5.29E-09
C-11	2.11E-14	0.03%	1.86E-01	1.96E+02	600.00	3.11E-04	3.27E-01
C-14	3.54E-11	0.02%	3.12E-07	3.28E-04	6.00	5.20E-08	5.47E-05
N-13	4.88E-14	0.03%	5.83E-01	6.13E+02	2000.00	2.92E-04	3.07E-01
O-14	2.60E-15	0.04%	1.80E-03	1.89E+00	927.09	1.94E-06	2.04E-03
O-15	2.92E-14	0.03%	1.21E-01	1.27E+02	1000.00	1.21E-04	1.27E-01
O-19	3.46E-19	0.09%	1.95E-11	2.05E-08	1916.02	1.02E-14	1.07E-11
F-18	1.48E-17	0.05%	2.31E-05	2.42E-02	500.00	4.61E-08	4.85E-05
Ne-23	1.26E-18	0.07%	1.46E-10	1.53E-07	1892.75	7.70E-14	8.10E-11
Ne-24	2.03E-19	0.08%	1.01E-06	1.06E-03	896.31	1.12E-09	1.18E-06
Na-22	5.21E-18	0.05%	7.75E-10	8.15E-07	1.00	7.75E-10	8.15E-07
Na-24	8.92E-18	0.05%	1.99E-06	2.09E-03	90.00	2.21E-08	2.33E-05
Na-25	2.78E-18	0.06%	4.69E-07	4.93E-04	2.86E+04	1.64E-11	1.72E-08
Mg-27	5.12E-18	0.05%	5.08E-05	5.34E-02	577.79	8.79E-08	9.24E-05
Mg-28	2.53E-18	0.04%	4.68E-07	4.92E-04	20.00	2.34E-08	2.46E-05
Al-26	7.39E-18	0.05%	3.78E-15	3.97E-12	0.50	7.56E-15	7.95E-12
Al-28	2.44E-17	0.04%	1.09E-04	1.14E-01	537.59	2.02E-07	2.12E-04
Al-29	1.21E-17	0.05%	1.41E-04	1.48E-01	232.45	6.05E-07	6.36E-04
Si-31	1.33E-17	0.04%	1.75E-05	1.84E-02	300.00	5.84E-08	6.14E-05
Si-32	8.85E-18	0.04%	2.24E-11	2.35E-08	0.32	6.99E-11	7.35E-08
P-30	5.62E-18	0.05%	2.44E-05	2.57E-02	2727.82	8.95E-09	9.41E-06
P-32	1.83E-16	0.03%	2.27E-06	2.38E-03	1.00	2.27E-06	2.38E-03
P-33	1.50E-16	0.03%	1.05E-06	1.10E-03	20.00	5.23E-08	5.50E-05
P-35	1.52E-17	0.03%	7.63E-07	8.02E-04	1.21E+04	6.28E-11	6.60E-08
S-35	2.13E-16	0.03%	4.27E-07	4.49E-04	20.00	2.13E-08	2.24E-05
S-37	1.77E-16	0.03%	9.65E-04	1.01E+00	8682.34	1.11E-07	1.17E-04
S-38	3.69E-17	0.03%	5.39E-05	5.67E-02	422.83	1.28E-07	1.34E-04
Cl-34	6.43E-18	0.03%	3.99E-05	4.19E-02	16.84	2.37E-06	2.49E-03
Cl-36	6.66E-16	0.03%	9.86E-13	1.04E-09	0.10	9.86E-12	1.04E-08
Cl-38	4.92E-16	0.03%	2.73E-03	2.87E+00	500.00	5.45E-06	5.73E-03
Cl-39	8.47E-16	0.03%	3.15E-03	3.31E+00	600.00	5.25E-06	5.52E-03
Cl-40	2.08E-16	0.03%	1.87E-04	1.96E-01	292.72	6.38E-07	6.70E-04
Ar-37	2.49E-15	0.02%	3.74E-06	3.93E-03	2.00E+08	1.87E-14	1.97E-11
Ar-39	5.95E-15	0.03%	6.12E-09	6.44E-06	6000.00	1.02E-12	1.07E-09
Ar-41	7.42E-14	0.02%	1.66E-02	1.74E+01	200.00	8.30E-05	8.72E-02
K-38	1.08E-17	0.05%	1.68E-04	1.77E-01	4622.10	3.64E-08	3.83E-05
K-40	4.77E-17	0.05%	2.22E-17	2.33E-14	0.31	7.09E-17	7.46E-14
Sum:						8.26E-04	8.68E-01

MAGNETIC SEPTUM (MSE) – 250 MEV PROTONS

Table 80: Scored yields of radioactive isotopes and calculated activity of the air after irradiation of the copper target with a 250 MeV proton beam, compared to Ci values, considering a cooling time of 10 minutes at average (7.93E+6 particles per second) and maximum (2E+10 particles per second) intensity

Isotope	yield/pp/cm ³	rel.err.	av.sp.act.	max.sp.act.	Ci [Bq/m ³]	av./Ci	max./Ci
H-3	9.31E-14	0.00%	8.19E-07	2.07E-03	100.00	8.19E-09	2.07E-05
Be-7	1.16E-14	0.00%	3.90E-05	9.84E-02	600.00	6.50E-08	1.64E-04
Be-10	1.98E-14	0.00%	1.58E-12	3.99E-09	1.00	1.58E-12	3.99E-09
C-11	2.11E-14	0.00%	1.73E-01	4.36E+02	600.00	2.88E-04	7.27E-01
C-14	3.54E-11	0.00%	2.36E-07	5.95E-04	6.00	3.93E-08	9.92E-05
N-13	4.88E-14	0.00%	4.57E-01	1.15E+03	2000.00	2.28E-04	5.76E-01
O-14	2.60E-15	0.00%	3.12E-03	7.88E+00	927.09	3.37E-06	8.50E-03
O-15	2.92E-14	0.00%	1.06E-01	2.67E+02	1000.00	1.06E-04	2.67E-01
O-19	3.46E-19	0.00%	4.87E-13	1.23E-09	1916.02	2.54E-16	6.41E-13
F-18	1.48E-17	0.00%	1.87E-05	4.72E-02	500.00	3.74E-08	9.43E-05
Ne-23	1.26E-18	0.00%	7.50E-12	1.89E-08	1892.75	3.96E-15	1.00E-11
Ne-24	2.03E-19	0.00%	3.74E-08	9.43E-05	896.31	4.17E-11	1.05E-07
Na-22	5.21E-18	0.00%	1.07E-10	2.69E-07	1.00	1.07E-10	2.69E-07
Na-24	8.92E-18	0.00%	3.39E-07	8.56E-04	90.00	3.77E-09	9.51E-06
Na-25	2.78E-18	0.00%	3.47E-08	8.76E-05	2.86E+04	1.21E-12	3.06E-09
Mg-27	5.12E-18	0.00%	5.35E-06	1.35E-02	577.79	9.27E-09	2.34E-05
Mg-28	2.53E-18	0.00%	8.85E-08	2.23E-04	20.00	4.43E-09	1.12E-05
Al-26	7.39E-18	0.00%	3.83E-16	9.65E-13	0.50	7.65E-16	1.93E-12
Al-28	2.44E-17	0.00%	1.68E-05	4.24E-02	537.59	3.13E-08	7.89E-05
Al-29	1.21E-17	0.00%	2.11E-05	5.31E-02	232.45	9.06E-08	2.29E-04
Si-31	1.33E-17	0.00%	4.24E-06	1.07E-02	300.00	1.41E-08	3.56E-05
Si-32	8.85E-18	0.00%	6.09E-12	1.54E-08	0.32	1.90E-11	4.80E-08
P-30	5.62E-18	0.00%	5.35E-06	1.35E-02	2727.82	1.96E-09	4.95E-06
P-32	1.83E-16	0.00%	1.22E-06	3.08E-03	1.00	1.22E-06	3.08E-03
P-33	1.50E-16	0.00%	4.75E-07	1.20E-03	20.00	2.38E-08	5.99E-05
P-35	1.52E-17	0.00%	2.52E-07	6.35E-04	1.21E+04	2.07E-11	5.22E-08
S-35	2.13E-16	0.00%	1.76E-07	4.43E-04	20.00	8.78E-09	2.21E-05
S-37	1.77E-16	0.00%	4.10E-04	1.04E+00	8682.34	4.73E-08	1.19E-04
S-38	3.69E-17	0.00%	1.44E-05	3.62E-02	422.83	3.40E-08	8.57E-05
Cl-34	6.43E-18	0.00%	2.69E-05	6.79E-02	16.84	1.60E-06	4.03E-03
Cl-36	6.66E-16	0.00%	6.12E-13	1.54E-09	0.10	6.12E-12	1.54E-08
Cl-38	4.92E-16	0.00%	1.01E-03	2.55E+00	500.00	2.02E-06	5.10E-03
Cl-39	8.47E-16	0.00%	1.08E-03	2.71E+00	600.00	1.79E-06	4.52E-03
Cl-40	2.08E-16	0.00%	6.22E-05	1.57E-01	292.72	2.13E-07	5.36E-04
Ar-37	2.49E-15	0.00%	2.81E-06	7.10E-03	2.00E+08	1.41E-14	3.55E-11
Ar-39	5.95E-15	0.00%	3.20E-09	8.08E-06	6000.00	5.34E-13	1.35E-09
Ar-41	7.42E-14	0.00%	1.25E-02	3.16E+01	200.00	6.27E-05	1.58E-01
K-38	1.08E-17	0.00%	3.47E-04	8.77E-01	4622.10	7.52E-08	1.90E-04
K-40	4.77E-17	0.00%	4.78E-17	1.21E-13	0.31	1.53E-16	3.85E-13
Sum:						6.96E-04	1.75E+00

CHOPPER DUMP – 400 MEV CARBON IONS

Table 81: Scored yields of radioactive isotopes and calculated activity of the air after irradiation of the tungsten dump with a 400 MeV carbon ion beam, compared to Ci values, considering a cooling time of 10 minutes at average (6.02E+6 ions per second) and maximum (1E+9 ions per second) intensity

Isotope	yield/pp/cm ³	rel.err.	av.sp.act.	max.sp.act.	Ci [Bq/m ³]	av./Ci	max./Ci
H-3	9.31E-14	0.05%	8.72E-06	1.45E-03	100.00	8.72E-08	1.45E-05
Be-7	1.16E-14	0.04%	5.32E-05	8.83E-03	600.00	8.87E-08	1.47E-05
Be-10	1.98E-14	0.05%	2.14E-11	3.55E-09	1.00	2.14E-11	3.55E-09
C-11	2.11E-14	0.04%	2.94E-01	4.88E+01	600.00	4.90E-04	8.14E-02
C-14	3.54E-11	0.04%	5.66E-06	9.39E-04	6.00	9.43E-07	1.56E-04
N-13	4.88E-14	0.04%	1.45E+00	2.40E+02	2000.00	7.24E-04	1.20E-01
O-14	2.60E-15	0.09%	1.43E-03	2.37E-01	927.09	1.54E-06	2.56E-04
O-15	2.92E-14	0.04%	2.21E-01	3.66E+01	1000.00	2.21E-04	3.66E-02
O-19	3.46E-19	0.14%	1.16E-11	1.93E-09	1916.02	6.06E-15	1.01E-12
F-18	1.48E-17	0.09%	1.57E-05	2.60E-03	500.00	3.14E-08	5.20E-06
Ne-23	1.26E-18	0.11%	9.95E-11	1.65E-08	1892.75	5.25E-14	8.72E-12
Ne-24	2.03E-19	0.12%	6.37E-07	1.06E-04	896.31	7.11E-10	1.18E-07
Na-22	5.21E-18	0.08%	6.79E-10	1.13E-07	1.00	6.79E-10	1.13E-07
Na-24	8.92E-18	0.08%	1.84E-06	3.06E-04	90.00	2.05E-08	3.39E-06
Na-25	2.78E-18	0.10%	3.47E-07	5.76E-05	2.86E+04	1.21E-11	2.01E-09
Mg-27	5.12E-18	0.09%	4.11E-05	6.82E-03	577.79	7.12E-08	1.18E-05
Mg-28	2.53E-18	0.08%	4.59E-07	7.61E-05	20.00	2.29E-08	3.81E-06
Al-26	7.39E-18	0.09%	3.03E-15	5.03E-13	0.50	6.07E-15	1.01E-12
Al-28	2.44E-17	0.08%	9.89E-05	1.64E-02	537.59	1.84E-07	3.05E-05
Al-29	1.21E-17	0.08%	1.26E-04	2.10E-02	232.45	5.43E-07	9.02E-05
Si-31	1.33E-17	0.06%	2.24E-05	3.71E-03	300.00	7.46E-08	1.24E-05
Si-32	8.85E-18	0.06%	3.25E-11	5.40E-09	0.32	1.02E-10	1.69E-08
P-30	5.62E-18	0.08%	1.86E-05	3.10E-03	2727.82	6.84E-09	1.13E-06
P-32	1.83E-16	0.05%	3.28E-06	5.44E-04	1.00	3.28E-06	5.44E-04
P-33	1.50E-16	0.05%	1.91E-06	3.16E-04	20.00	9.53E-08	1.58E-05
P-35	1.52E-17	0.05%	1.67E-06	2.78E-04	1.21E+04	1.38E-10	2.29E-08
S-35	2.13E-16	0.05%	1.03E-06	1.70E-04	20.00	5.13E-08	8.51E-06
S-37	1.77E-16	0.05%	4.75E-03	7.89E-01	8682.34	5.47E-07	9.09E-05
S-38	3.69E-17	0.05%	1.13E-04	1.88E-02	422.83	2.68E-07	4.45E-05
Cl-34	6.43E-18	0.06%	4.12E-05	6.84E-03	16.84	2.45E-06	4.06E-04
Cl-36	6.66E-16	0.04%	2.11E-12	3.50E-10	0.10	2.11E-11	3.50E-09
Cl-38	4.92E-16	0.05%	7.92E-03	1.32E+00	500.00	1.58E-05	2.63E-03
Cl-39	8.47E-16	0.04%	9.73E-03	1.61E+00	600.00	1.62E-05	2.69E-03
Cl-40	2.08E-16	0.04%	8.75E-04	1.45E-01	292.72	2.99E-06	4.96E-04
Ar-37	2.49E-15	0.04%	2.54E-05	4.21E-03	2.00E+08	1.27E-13	2.11E-11
Ar-39	5.95E-15	0.05%	3.07E-08	5.09E-06	6000.00	5.11E-12	8.48E-10
Ar-41	7.42E-14	0.04%	3.04E-01	5.05E+01	200.00	1.52E-03	2.52E-01
K-38	1.08E-17	0.11%	9.28E-05	1.54E-02	4622.10	2.01E-08	3.33E-06
K-40	4.77E-17	0.17%	1.57E-17	2.60E-15	0.31	5.01E-17	8.31E-15
Sum:						3.00E-03	4.98E-01

CHOPPER DUMP – 250 MEV PROTONS

Table 82 Table 83: Scored yields of radioactive isotopes and calculated activity of the air after irradiation of the tungsten dump with a 250 MeV proton beam, compared to Ci values, considering a cooling time of 10 minutes at average (5.07E+7 particles per second) and maximum (2E+10 particles per second) intensity

Isotope	yield/pp/cm ³	rel.err.	av.sp.act.	max.sp.act.	Ci [Bq/m ³]	av./Ci	max./Ci
H-3	9.31E-14	0.03%	4.08E-06	1.61E-03	100.00	4.08E-08	1.61E-05
Be-7	1.16E-14	0.06%	2.61E-05	1.03E-02	600.00	4.36E-08	1.72E-05
Be-10	1.98E-14	0.09%	6.86E-12	2.70E-09	1.00	6.86E-12	2.70E-09
C-11	2.11E-14	0.06%	1.34E-01	5.30E+01	600.00	2.24E-04	8.83E-02
C-14	3.54E-11	0.03%	4.85E-06	1.91E-03	6.00	8.09E-07	3.19E-04
N-13	4.88E-14	0.04%	5.68E-01	2.24E+02	2000.00	2.84E-04	1.12E-01
O-14	2.60E-15	0.10%	1.44E-03	5.70E-01	927.09	1.56E-06	6.14E-04
O-15	2.92E-14	0.07%	9.05E-02	3.57E+01	1000.00	9.05E-05	3.57E-02
O-19	3.46E-19	0.17%	6.81E-13	2.68E-10	1916.02	3.55E-16	1.40E-13
F-18	1.48E-17	0.10%	8.81E-06	3.47E-03	500.00	1.76E-08	6.94E-06
Ne-23	1.26E-18	0.10%	9.57E-12	3.77E-09	1892.75	5.06E-15	1.99E-12
Ne-24	2.03E-19	0.12%	4.93E-08	1.94E-05	896.31	5.50E-11	2.17E-08
Na-22	5.21E-18	0.07%	1.23E-10	4.85E-08	1.00	1.23E-10	4.85E-08
Na-24	8.92E-18	0.07%	3.87E-07	1.53E-04	90.00	4.30E-09	1.70E-06
Na-25	2.78E-18	0.07%	4.23E-08	1.67E-05	2.86E+04	1.48E-12	5.82E-10
Mg-27	5.12E-18	0.05%	6.33E-06	2.49E-03	577.79	1.09E-08	4.32E-06
Mg-28	2.53E-18	0.07%	1.02E-07	4.01E-05	20.00	5.08E-09	2.00E-06
Al-26	7.39E-18	0.05%	4.55E-16	1.79E-13	0.50	9.09E-16	3.58E-13
Al-28	2.44E-17	0.05%	1.93E-05	7.61E-03	537.59	3.59E-08	1.42E-05
Al-29	1.21E-17	0.05%	2.42E-05	9.54E-03	232.45	1.04E-07	4.11E-05
Si-31	1.33E-17	0.07%	5.99E-06	2.36E-03	300.00	2.00E-08	7.87E-06
Si-32	8.85E-18	0.05%	9.30E-12	3.66E-09	0.32	2.91E-11	1.15E-08
P-30	5.62E-18	0.13%	3.90E-06	1.54E-03	2727.82	1.43E-09	5.64E-07
P-32	1.83E-16	0.10%	1.22E-06	4.80E-04	1.00	1.22E-06	4.80E-04
P-33	1.50E-16	0.08%	6.71E-07	2.64E-04	20.00	3.35E-08	1.32E-05
P-35	1.52E-17	0.05%	5.23E-07	2.06E-04	1.21E+04	4.30E-11	1.70E-08
S-35	2.13E-16	0.03%	3.29E-07	1.30E-04	20.00	1.64E-08	6.48E-06
S-37	1.77E-16	0.05%	2.44E-03	9.61E-01	8682.34	2.81E-07	1.11E-04
S-38	3.69E-17	0.06%	3.54E-05	1.39E-02	422.83	8.36E-08	3.30E-05
Cl-34	6.43E-18	0.19%	1.71E-05	6.75E-03	16.84	1.02E-06	4.01E-04
Cl-36	6.66E-16	0.07%	8.84E-13	3.48E-10	0.10	8.84E-12	3.48E-09
Cl-38	4.92E-16	0.05%	2.52E-03	9.95E-01	500.00	5.05E-06	1.99E-03
Cl-39	8.47E-16	0.06%	3.13E-03	1.23E+00	600.00	5.21E-06	2.06E-03
Cl-40	2.08E-16	0.07%	3.21E-04	1.27E-01	292.72	1.10E-06	4.33E-04
Ar-37	2.49E-15	0.03%	1.84E-05	7.25E-03	2.00E+08	9.20E-14	3.63E-11
Ar-39	5.95E-15	0.08%	1.30E-08	5.14E-06	6000.00	2.17E-12	8.57E-10
Ar-41	7.42E-14	0.03%	2.62E-01	1.03E+02	200.00	1.31E-03	5.17E-01
K-38	1.08E-17	0.14%	1.28E-04	5.04E-02	4622.10	2.76E-08	1.09E-05
K-40	4.77E-17	0.10%	2.12E-17	8.37E-15	0.31	6.78E-17	2.67E-14
Sum:						1.93E-03	7.60E-01

BEAM DUMP (HEBT) – 800 MEV PROTONS

Table 84: Scored yields of radioactive isotopes and calculated activity of the air after irradiation of the HEBT beam dump with an 800 MeV proton beam, compared to Ci values, considering a cooling time of 10 minutes at average ($1.55E+7$ particles per second) and maximum ($2E+10$ particles per second) intensity

Isotope	yield/pp/cm ³	rel.err.	av.sp.act.	max.sp.act.	Ci [Bq/m ³]	av./Ci	max./Ci
H-3	9.31E-14	0.17%	1.03E-07	1.33E-04	100.00	1.03E-09	1.33E-06
Be-7	1.16E-14	0.09%	2.02E-06	2.60E-03	600.00	3.37E-09	4.34E-06
Be-10	1.98E-14	0.18%	2.99E-13	3.85E-10	1.00	2.99E-13	3.85E-10
C-11	2.11E-14	0.11%	9.31E-03	1.20E+01	600.00	1.55E-05	2.00E-02
C-14	3.54E-11	0.10%	1.03E-07	1.33E-04	6.00	1.72E-08	2.22E-05
N-13	4.88E-14	0.11%	2.88E-02	3.71E+01	2000.00	1.44E-05	1.86E-02
O-14	2.60E-15	0.33%	4.27E-05	5.49E-02	927.09	4.60E-08	5.92E-05
O-15	2.92E-14	0.10%	5.76E-03	7.42E+00	1000.00	5.76E-06	7.42E-03
O-19	3.46E-19	0.02%	7.91E-12	1.02E-08	1916.02	4.13E-15	5.31E-12
F-18	1.48E-17	0.04%	4.02E-06	5.18E-03	500.00	8.05E-09	1.04E-05
Ne-23	1.26E-18	0.03%	3.38E-11	4.35E-08	1892.75	1.78E-14	2.30E-11
Ne-24	2.03E-19	0.02%	3.42E-07	4.41E-04	896.31	3.82E-10	4.92E-07
Na-22	5.21E-18	0.04%	1.06E-10	1.37E-07	1.00	1.06E-10	1.37E-07
Na-24	8.92E-18	0.04%	2.57E-07	3.31E-04	90.00	2.86E-09	3.68E-06
Na-25	2.78E-18	0.04%	8.09E-08	1.04E-04	2.86E+04	2.82E-12	3.63E-09
Mg-27	5.12E-18	0.05%	6.54E-06	8.42E-03	577.79	1.13E-08	1.46E-05
Mg-28	2.53E-18	0.07%	3.77E-08	4.86E-05	20.00	1.89E-09	2.43E-06
Al-26	7.39E-18	0.05%	4.82E-16	6.21E-13	0.50	9.64E-16	1.24E-12
Al-28	2.44E-17	0.06%	9.75E-06	1.26E-02	537.59	1.81E-08	2.33E-05
Al-29	1.21E-17	0.06%	1.37E-05	1.76E-02	232.45	5.88E-08	7.57E-05
Si-31	1.33E-17	0.06%	1.84E-06	2.37E-03	300.00	6.13E-09	7.89E-06
Si-32	8.85E-18	0.08%	2.02E-12	2.60E-09	0.32	6.31E-12	8.13E-09
P-30	5.62E-18	0.05%	3.25E-06	4.18E-03	2727.82	1.19E-09	1.53E-06
P-32	1.83E-16	0.12%	1.40E-07	1.80E-04	1.00	1.40E-07	1.80E-04
P-33	1.50E-16	0.13%	6.84E-08	8.80E-05	20.00	3.42E-09	4.40E-06
P-35	1.52E-17	0.12%	5.46E-08	7.02E-05	1.21E+04	4.49E-12	5.78E-09
S-35	2.13E-16	0.11%	2.74E-08	3.52E-05	20.00	1.37E-09	1.76E-06
S-37	1.77E-16	0.16%	5.65E-05	7.27E-02	8682.34	6.50E-09	8.37E-06
S-38	3.69E-17	0.12%	4.07E-06	5.24E-03	422.83	9.62E-09	1.24E-05
Cl-34	6.43E-18	0.11%	2.21E-06	2.84E-03	16.84	1.31E-07	1.69E-04
Cl-36	6.66E-16	0.15%	5.82E-14	7.49E-11	0.10	5.82E-13	7.49E-10
Cl-38	4.92E-16	0.14%	1.79E-04	2.30E-01	500.00	3.57E-07	4.60E-04
Cl-39	8.47E-16	0.12%	2.11E-04	2.71E-01	600.00	3.51E-07	4.52E-04
Cl-40	2.08E-16	0.18%	1.07E-05	1.38E-02	292.72	3.67E-08	4.72E-05
Ar-37	2.49E-15	0.09%	4.92E-07	6.33E-04	2.00E+08	2.46E-15	3.16E-12
Ar-39	5.95E-15	0.26%	3.08E-10	3.96E-07	6000.00	5.13E-14	6.60E-11
Ar-41	7.42E-14	0.10%	5.73E-03	7.38E+00	200.00	2.87E-05	3.69E-02
K-38	1.08E-17	0.72%	1.76E-06	2.26E-03	4622.10	3.81E-10	4.90E-07
K-40	4.77E-17	1.18%	1.91E-19	2.46E-16	0.31	6.12E-19	7.88E-16
Sum:						6.56E-05	8.44E-02

BEAM DUMP (HEBT) – 400 MEV CARBON IONS

Table 85: Scored yields of radioactive isotopes and calculated activity of the air after irradiation of the HEBT beam dump with a 400 MeV carbon ion beam, compared to Ci values, considering a cooling time of 10 minutes at average (6.66E+5 ions per second) and maximum (1E+9 ions per second) intensity

Isotope	yield/pp/cm ³	rel.err.	av.sp.act.	max.sp.act.	Ci [Bq/m ³]	av./Ci	max./Ci
H-3	9.31E-14	0.13%	1.26E-08	1.89E-05	100.00	1.26E-10	1.89E-07
Be-7	1.16E-14	0.12%	1.33E-07	2.00E-04	600.00	2.22E-10	3.33E-07
Be-10	1.98E-14	0.14%	3.80E-14	5.71E-11	1.00	3.80E-14	5.71E-11
C-11	2.11E-14	0.11%	7.68E-04	1.15E+00	600.00	1.28E-06	1.92E-03
C-14	3.54E-11	0.07%	1.83E-08	2.74E-05	6.00	3.04E-09	4.57E-06
N-13	4.88E-14	0.11%	2.99E-03	4.49E+00	2000.00	1.49E-06	2.24E-03
O-14	2.60E-15	0.35%	2.80E-06	4.21E-03	927.09	3.03E-09	4.54E-06
O-15	2.92E-14	0.11%	5.07E-04	7.62E-01	1000.00	5.07E-07	7.62E-04
O-19	3.46E-19	0.29%	5.39E-14	8.10E-11	1916.02	2.81E-17	4.23E-14
F-18	1.48E-17	0.19%	5.23E-08	7.85E-05	500.00	1.05E-10	1.57E-07
Ne-23	1.26E-18	0.23%	4.53E-13	6.81E-10	1892.75	2.39E-16	3.60E-13
Ne-24	2.03E-19	0.26%	2.93E-09	4.41E-06	896.31	3.27E-12	4.92E-09
Na-22	5.21E-18	0.15%	2.97E-12	4.46E-09	1.00	2.97E-12	4.46E-09
Na-24	8.92E-18	0.15%	7.78E-09	1.17E-05	90.00	8.64E-11	1.30E-07
Na-25	2.78E-18	0.20%	1.56E-09	2.34E-06	2.86E+04	5.44E-14	8.17E-11
Mg-27	5.12E-18	0.17%	1.81E-07	2.72E-04	577.79	3.14E-10	4.71E-07
Mg-28	2.53E-18	0.14%	1.90E-09	2.85E-06	20.00	9.50E-11	1.43E-07
Al-26	7.39E-18	0.18%	1.34E-17	2.01E-14	0.50	2.67E-17	4.01E-14
Al-28	2.44E-17	0.15%	4.23E-07	6.35E-04	537.59	7.87E-10	1.18E-06
Al-29	1.21E-17	0.15%	5.42E-07	8.14E-04	232.45	2.33E-09	3.50E-06
Si-31	1.33E-17	0.12%	8.64E-08	1.30E-04	300.00	2.88E-10	4.32E-07
Si-32	8.85E-18	0.12%	1.19E-13	1.79E-10	0.32	3.72E-13	5.59E-10
P-30	5.62E-18	0.15%	7.63E-08	1.15E-04	2727.82	2.80E-11	4.20E-08
P-32	1.83E-16	0.11%	1.16E-08	1.75E-05	1.00	1.16E-08	1.75E-05
P-33	1.50E-16	0.12%	6.27E-09	9.42E-06	20.00	3.14E-10	4.71E-07
P-35	1.52E-17	0.12%	5.02E-09	7.53E-06	1.21E+04	4.13E-13	6.20E-10
S-35	2.13E-16	0.10%	2.71E-09	4.06E-06	20.00	1.35E-10	2.03E-07
S-37	1.77E-16	0.15%	7.04E-06	1.06E-02	8682.34	8.10E-10	1.22E-06
S-38	3.69E-17	0.12%	3.79E-07	5.69E-04	422.83	8.96E-10	1.35E-06
Cl-34	6.43E-18	0.09%	1.46E-07	2.19E-04	16.84	8.68E-09	1.30E-05
Cl-36	6.66E-16	0.13%	5.85E-15	8.79E-12	0.10	5.85E-14	8.79E-11
Cl-38	4.92E-16	0.12%	1.93E-05	2.91E-02	500.00	3.87E-08	5.81E-05
Cl-39	8.47E-16	0.11%	2.22E-05	3.33E-02	600.00	3.69E-08	5.55E-05
Cl-40	2.08E-16	0.12%	1.47E-06	2.21E-03	292.72	5.03E-09	7.56E-06
Ar-37	2.49E-15	0.06%	7.69E-08	1.15E-04	2.00E+08	3.85E-16	5.77E-13
Ar-39	5.95E-15	0.21%	4.30E-11	6.46E-08	6000.00	7.17E-15	1.08E-11
Ar-41	7.42E-14	0.07%	1.01E-03	1.51E+00	200.00	5.04E-06	7.57E-03
K-38	1.08E-17	1.03%	1.01E-07	1.52E-04	4622.10	2.20E-11	3.30E-08
K-40	4.77E-17	0.89%	1.98E-20	2.98E-17	0.31	6.34E-20	9.52E-17
Sum:						8.44E-06	1.27E-02

BEAM DUMP (HEBT) – 250 MEV PROTONS

Table 86: Scored yields of radioactive isotopes and calculated activity of the air after irradiation of the HEBT beam dump with a 250 MeV proton beam, compared to Ci values, considering a cooling time of 10 minutes at average ($6.66E+6$ particles per second) and maximum ($2E+10$ particles per second) intensity

Isotope	yield/pp/cm ³	rel.err.	av.sp.act.	max.sp.act.	Ci [Bq/m ³]	av./Ci	max./Ci
H-3	9.31E-14	0.43%	5.03E-09	1.51E-05	100.00	5.03E-11	1.51E-07
Be-7	1.16E-14	0.02%	3.37E-07	1.01E-03	600.00	5.61E-10	1.69E-06
Be-10	1.98E-14	0.50%	8.11E-15	2.43E-11	1.00	8.11E-15	2.43E-11
C-11	2.11E-14	0.04%	1.45E-03	4.36E+00	600.00	2.42E-06	7.27E-03
C-14	3.54E-11	0.22%	6.29E-09	1.89E-05	6.00	1.05E-09	3.15E-06
N-13	4.88E-14	0.05%	3.27E-03	9.82E+00	2000.00	1.64E-06	4.91E-03
O-14	2.60E-15	0.08%	1.39E-05	4.16E-02	927.09	1.49E-08	4.49E-05
O-15	2.92E-14	0.03%	9.72E-04	2.92E+00	1000.00	9.72E-07	2.92E-03
O-19	3.46E-19	0.00%	1.46E-13	4.40E-10	1916.02	7.64E-17	2.29E-13
F-18	1.48E-17	0.03%	2.41E-07	7.25E-04	500.00	4.82E-10	1.45E-06
Ne-23	1.26E-18	0.00%	1.48E-12	4.44E-09	1892.75	7.82E-16	2.35E-12
Ne-24	2.03E-19	0.00%	8.72E-09	2.62E-05	896.31	9.73E-12	2.92E-08
Na-22	5.21E-18	0.01%	1.05E-11	3.16E-08	1.00	1.05E-11	3.16E-08
Na-24	8.92E-18	0.01%	2.30E-08	6.90E-05	90.00	2.55E-10	7.67E-07
Na-25	2.78E-18	0.01%	5.33E-09	1.60E-05	2.86E+04	1.86E-13	5.58E-10
Mg-27	5.12E-18	0.01%	6.21E-07	1.87E-03	577.79	1.08E-09	3.23E-06
Mg-28	2.53E-18	0.01%	5.65E-09	1.70E-05	20.00	2.82E-10	8.48E-07
Al-26	7.39E-18	0.01%	4.63E-17	1.39E-13	0.50	9.26E-17	2.78E-13
Al-28	2.44E-17	0.01%	1.40E-06	4.20E-03	537.59	2.60E-09	7.81E-06
Al-29	1.21E-17	0.01%	1.78E-06	5.35E-03	232.45	7.67E-09	2.30E-05
Si-31	1.33E-17	0.02%	1.54E-07	4.64E-04	300.00	5.15E-10	1.55E-06
Si-32	8.85E-18	0.03%	1.79E-13	5.37E-10	0.32	5.59E-13	1.68E-09
P-30	5.62E-18	0.01%	3.59E-07	1.08E-03	2727.82	1.32E-10	3.95E-07
P-32	1.83E-16	0.05%	1.80E-08	5.42E-05	1.00	1.80E-08	5.42E-05
P-33	1.50E-16	0.07%	6.26E-09	1.88E-05	20.00	3.13E-10	9.41E-07
P-35	1.52E-17	0.09%	2.89E-09	8.67E-06	1.21E+04	2.38E-13	7.14E-10
S-35	2.13E-16	0.07%	1.96E-09	5.89E-06	20.00	9.80E-11	2.94E-07
S-37	1.77E-16	1.08%	2.74E-06	8.23E-03	8682.34	3.15E-10	9.48E-07
S-38	3.69E-17	0.13%	1.72E-07	5.16E-04	422.83	4.06E-10	1.22E-06
Cl-34	6.43E-18	0.02%	5.16E-07	1.55E-03	16.84	3.06E-08	9.20E-05
Cl-36	6.66E-16	0.06%	5.89E-15	1.77E-11	0.10	5.89E-14	1.77E-10
Cl-38	4.92E-16	0.09%	9.23E-06	2.77E-02	500.00	1.85E-08	5.54E-05
Cl-39	8.47E-16	0.12%	1.08E-05	3.25E-02	600.00	1.80E-08	5.42E-05
Cl-40	2.08E-16	0.68%	2.30E-07	6.92E-04	292.72	7.87E-10	2.36E-06
Ar-37	2.49E-15	0.13%	3.56E-08	1.07E-04	2.00E+08	1.78E-16	5.35E-13
Ar-39	5.95E-15	0.44%	1.76E-11	5.29E-08	6000.00	2.94E-15	8.82E-12
Ar-41	7.42E-14	0.22%	3.48E-04	1.05E+00	200.00	1.74E-06	5.23E-03
K-38	1.08E-17	0.01%	1.60E-06	4.81E-03	4622.10	3.47E-10	1.04E-06
K-40	4.77E-17	0.23%	1.09E-19	3.27E-16	0.31	3.48E-19	1.05E-15
Sum:						6.89E-06	2.07E-02

Curriculum Vitae

• Contact

- Matthias Karacson
- Schützengasse 1/10/50
- A-2700 Wiener Neustadt
- Austria
- Email: m.karacson@gmx.at
- Phone Nr.: 0043 676 7365292
- Born: November 9th 1980 in Wiener Neustadt

• Education

- University of Technology Vienna (2000 - 2010)
Field of studies: Technical Physics
- Secondary school (1991 - 1999): AHS Bundesgymnasium Zehnergasse Wiener Neustadt, graduation with Matura
- Primary school (1987 - 1991): Volksschule Santa Christiana Wiener Neustadt

• Publications

- September 2005: Co-author of Poster-presentation at the Conference of the Austrian Physical Society „CERN-IH LINAC verification via CERN-DYNAC source code“

• Work experiences

- Austrian Research Centers Seibersdorf Health Physics Division:
 - Health Physics Studies July 2001
 - Dosimetry (Measurements and Evaluations for Project ITRAP) July 2002
 - Laser Safety (resulting in 2 academically credited project works) July and August 2005
- Technical studentship at CERN (resulting in a diploma thesis about air activation at the MedAustron facility) June 2009 – July 2010
- 12 months of alternative national service at the volunteer fire department Wiener Neustadt from October 1999 to October 2000 including volunteer firefighter training